THE LOWER AND MIDDLE ORDOVICIAN PLATFORM CARBONATES OF THE MINGAN ISLANDS, QUEBEC: STRATIGRAPHY, SEDIMENTOLOGY, PALEOKARST, AND LIMESTONE DIAGENESIS

ANDRE DESROCHERS

NOTICE

AVIS

The quality of this microform is heavily dependent upon the quality of the original thesis submitted for microfilming. Every effort has been made to ensure the highest quality of reproduction possible.

If pages are missing, contact the university which granted the degree.

Some pages may have indistinct print especially if the original pages were typed with a poor typewriter ribbon or if the university sent us an inferior photocopy.

La qualité de cette microforme dépend grandement de la qualité de la thèse soumise au microfilmage. Nous avons tout fait pour assurer une qualité supérieure de reproduction.

S'il manque des pages, veuillez communiquer avec l'université qui a conféré le grade.

La qualité d'impression de certaines pages peut laisser à désirer, surtout si les pages originales ont été dactylographiées à l'aide d'un ruban usé ou si l'université nous a fait parvenir une photocopie de qualité inférieure.

Canada

THE LOWER AND MIDDLE ORDOVICIAN PLATFORM CARBONATES

OF THE MINGAN ISLANDS, QUEBEC: STRATIGRAPHY,

SEDIMENTOLOGY, PALEOKARST, AND LIMESTONE DIAGENESIS

BY

© Andre Desrochers, M.Sc.

A thesis submitted to the school of Graduate

Studies in partial fulfillment of the

requirements for the degree of

Doctor of Philosophy

Department of Earth Sciences

Memorial University of Newfoundland

October 1985

St. John's

Newfoundland

Canadä

"La Côte-Nord est fille de feu,

c'est le rebord granitique

du noyau continental américain,

tandis que la Minganie est fille de l'eau

les îles qui la composent

sont des fragments,

des miettes d'une terre ancienne

lentement déposée

au fond des mers ordoviciennes."

Marie-Victorin,

Flore de l'Anticosti - Minganie.

ABSTRACT

An undeformed sequence of Lower and Middle Ordovician shallow-water carbonates is exposed on the Mingan Islands located along the Quebec North Shore of the Gulf of St. Lawrence. This sequence comprises dolostones of the Romaine Formation and limestones of the Mingan Formation. The late Canadian to earliest Whiterockian Romaine Formation is subdivided into three formal members: Sauvage Member, Sainte-Genevieve Member and Grande Ile Member. The Chazyan Mingan Formation is subdivided into four formal members: Corbeau Member, Perroquet Member, Fantome Member and Grande Pointe Member.

The Romaine Formation represents a shallowing-upward sequence comprising a thin basal assemblage of trangressive sandstones, a middle assemblage of subtidal carbonates and an upper assemblage of cyclic peritidal carbonates. Romaine sediments were pervasively dolomitized in shallow subsurface environments (possibly in mixing zones) before the end of post-Romaine karst erosion.

The Mingan Formation is a complex environmental mosaic of peritidal and subtidal limestones with a basal trangressive sandstone overlain by tidal flat siliciclastics. Sedimentation changed abruptly with deposition of peritidal and subtidal limestones prior to a period of subaerial exposure resulting in the formation of a karst surface with substantial relief. Resubmergence of this irregular rocky coastline with scattered beachrocks, resulted in a complex facies mosiac with sand shoals forming in underlying paleokarst depressions as tidal deltas 1-10 km wide.

Three superimposed calcarenite cycles are present in the Mingan sand

shoal complex. These sand shoals were periodically exposed and subject to karstification in response to minor fluctuations in sea level. The amount of sea level fall was minor and deeper inter-shoal areas were not affected by subaerial exposure but were sites of more restricted deposition.

Mingan reef limestones are of three types: biostromes, bioherms which grew in tranquil settings, and bioherm complexes which grew under more turbulent conditions. Reef organisms include lithistid sponges, bryozoans, tabulate corals and solenoporacean algae which occur in a variety of different biotic assemblages. These builders are in part inherited from older bioherms and in part newly involved taxa. Mingan bioherms are typically small mound-shaped structures composed of abundant skeletons and rich in lime mud. Stromatoporoids are conspicuously absent as builders in the Mingan bioherms in contrast to the classic Chazy reefs of Vermont and New York.

Three different types of paleokarst surfaces are present in the Mingan sequence: 1) an extensive karst plain, represented by the post-Romaine unconformity; 2) an irregular karst, represented by the intra-Mingan paleokarst and 3) local karst surfaces capping calcarenite cycles.

Alteration of the Mingan limestones resulted from three distinct phases of diagenesis: marine, near-surface and deep burial; near-surface is the most important, especially beneath subaerial exposure surfaces. Vadose cement is not present in spite of extensive evidence of subaerial exposure. Crystal debris, similar to "vadose silt" and formed by the internal erosion of contemporaneous phreatic cements, was subsequently deposited as geopetal internal sediment.

RESUME

Une séquence de carbonates, d'âge Ordovicien Inférieur et Moyen,
est bien exposé dans l'archipel de Mingan, situé le long de la moyenne
Côte-Nord du Golfe St-Laurent au Québec. Cette séquence comprend les
dolomies de la Formation de Romaine et les calcaires de la Formation de
Mingan. La Formation de Romaine, allant du Canadien inférieur au tout
début du Whiterock, est subdivisée en trois membres formels: les
membres du Sauvage, de Sainte-Geneviève et de la Grande Ile. La
Formation de Mingan, d'âge Chazy, est subdivisée en quatre membres
formels: les Membres du Corbeau, du Perroquet, du Fantôme et de la
Grande Pointe.

La Formation de Romaine représente une séquence du type
"shallowing-upward" comprenant un grès de base, un assemblage médian de
calcaires infralittoraux et un assemblage supérieur de calcaires périlit-
toraux cycliques. Ces sédiments calcaires, cependant, ont été complè-
tement dolomitisés avant la fin de la période d'érosion et de karstifi-
cation observée au sommet de la Formation de Romaine.

Un grès de base et d'autres sédiments siliciclastiques sont
présents à la base de la Formation de Mingan. La sédimentation silici-
clastique, cependant, s'est brusquement arrêtée avec la déposition de
calcaires périlittoraux et infralittoraux et ceci avant une période
d'exposition subaérienne où s'est développée une surface karstique avec
un relief important. Suite à une transgression marine, cette surface
irrégulière a permis la formation de zones littorales rocheuses espacées
localement par des dépôts de plage indurée. De plus, un assemblage

complexe de sédiments calcaires s'est déposé dans des milieux infralittoraux dont des haut-fonds sablonneaux formant des deltas de marée, large de 1 à 10 km, au-dessus des dépressions paléokarstiques.

Trois cycles calcarénitiques superposés sont présents à l'intérieur du complexe de haut-fonds sablonneux de la Formation de Mingan. Ces haut-fonds ont été périodiquement exposés et karstifiés en réponse à des fluctuations mineures du niveau marin. Les régions relativement plus profondes entourant ces haut-fonds n'ont pas été exposées mais sont devenues des milieux où la déposition était plus restreinte.

Les calcaires récifaux de la Formation de Mingan sont groupés en trois types: biostromes, biohermes lesquels se sont développés en milieux peu agités et les complexes à biohermes lesquels se sont développés dans des conditions plus turbulentes. Les biohermes forment de petits monticules à boue calcaire contenant de nombreux organismes constructeurs. Les principaux constructeurs sont des éponges lithistides, des bryozoaires, des coraux tabulés et des algues solénoporacées. Ces organismes sont en partie issus de biohermes plus anciens et en partie de nouveaux taxa. Les stromatoporoides sont remarquablement absents comme constructeurs dans les biohermes de la Formation de Mingan contrairement à ceux du Vermont et de New York, également d'âge Chazy.

Trois différents types de surface paléokarstiques sont présents dans la séquence: 1) une plaine karstique représentée par la discordance post-Romaine; 2) un karst irrégulier représenté par la discordance intra-Mingan et 3) des surfaces karstiques locales surmontant les cycles calcarénitiques.

L'altération des calcaires de la Formation de Mingan sont le résultat de trois phases distinctes de diagénèse: marine, météorique de surface et enfouissement; celle d'origine météorique fut la plus intense, spécialement sous les surfaces d'exposition subaérienne. Les ciments vadoses sont absents en dépit de nombreuses évidences d'exposition. Des débris cristallins, identiques aux "vadose silt" et formés par l'érosion pénécontemporaine de ciments phréatiques, ont été déposés comme sédiments internes géotropes.

ACKNOWLEDGMENTS

TABLE OF CONTENTS

CHAPTER 6 - PALEOKARST UNCONFORMITIES

CHAPTER 7 – SHALLOWING-UPWARD CALCARENITE CYCLES

CHAPTER 8 – LIMESTONE DIAGENESIS

LIST OF FIGURES

- xiii -

LIST OF TABLES

LIST OF PLATES

CHAPTER 1

INTRODUCTION

The Mingan Islands are located along the middle North Shore ("moyenne Cote-Nord") of the Gulf of St. Lawrence, directly north of Anticosti Island (fig. 1-1). These islands are inhabited and will eventually be integrated within a national marine park operated by Parks Canada. Only three small communities, all accessible by the highway 138, are present along the adjacent shore: Longue-Pointe de Mingan, Mingan, and Havre Saint-Pierre.

The Mingan Islands are oriented east-west and extend 85 km along the shore. They consist of approximately 30 major islands with several smaller islands and keys. The total surface of these islands represents only 97 km^2, but more than 200 km of superb coastal exposures are present in the study area. The largest islands are Grande Ile (25 km^2), Ile a la Chasse (16 km^2), and Ile du Havre (9 km^2).

The locality names used in the present study are those recently approved by the "Commission de toponymie du Quebec" (Gauthier Larouche, 1981). Numerous English and French variations to these locality names have been used in the previous studies (Richardson, 1856; Twenhofel, 1938) and topographic maps from the Canada Department of Energy, Mines, and Resources. These variations are summarized in appendix A.

Figure 1.1- Location map of the Mingan Islands, Quebec. Locality names
follow the Commission de toponymie du Quebec (Gauthier Larouche,
1981). 1: Ile aux Perroquets, 2: Ile de la Maison, 3: Ile du Wreck,
4: l'Ilot, 5: Ile Nue de Mingan, 6: Ile du Havre de Mingan, 7: Ile a
Bouleaux de Terre, 8: Ile a Bouleaux du Large, 9: Grande Ile, 10:
Ile de la Grosse Romaine, 11: Ile Quarry, 12: Ile de la Petite
Romaine, 13: Ile Niapiskau, 14: Pointe aux Morts, 15: Ile du
Fantome, 16: Ile a Firmin, 17: Ile du Havre, 18: Ile a Calculot, 19:
Ile aux Goelands, 20: Petite Ile au Marteau, 21: Grosse Ile au
Marteau, 22: Grande Pointe, 23: Pointe Enragee, 24: Ile de la Fausse
Passe, 25: Ile Saint-Charles, 26: Baie Puffin, 27: Ile a Calculot
des Betchouanes, 28: Ile Innu, 29: Ile a la Chasse, 30: Pointe de la
Perdrix, 31: Mont Sainte-Genevieve, 32: Pointe du Sauvage, 33: Ile
Sainte-Genevieve.

QUÉBEC

Longue Pointe

Mingan

6

10   12

7

8

5

1   5
2
3   4

9

11   13

14   Havre Saint Pierre

15
16   17
18   19   20

21

22

23   24

25

26

27   28   29

30

32

31

33

N

Anticosti

0   5   10   15KM

Mingan
Islands

Gulf
of
St-Lawrence
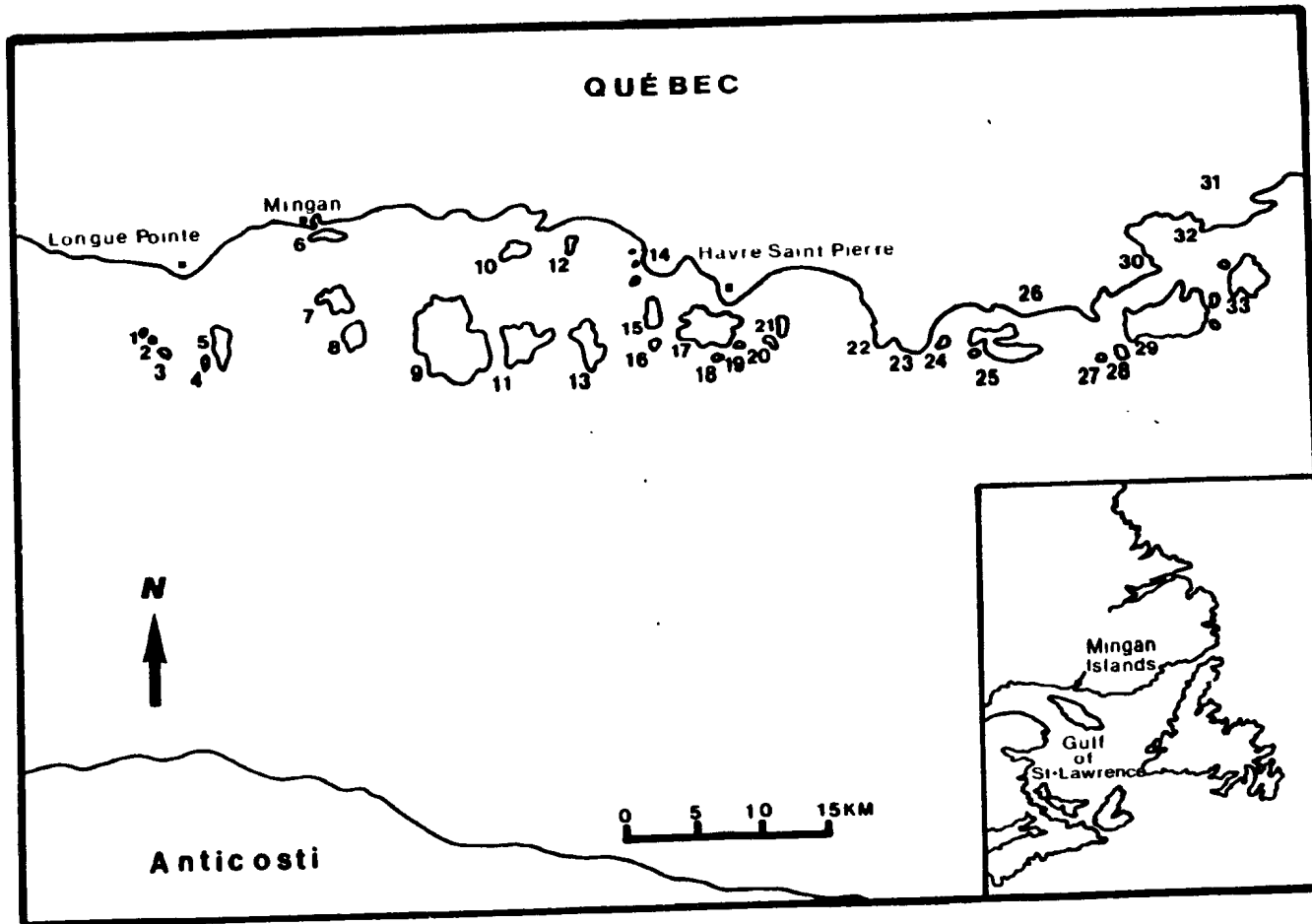
PURPOSE

The Lower and Middle Ordovician Romaine and Mingan Formations
represent an undeformed sequence of shallow-water carbonates, exposed in
the Mingan Islands. These carbonates exhibit similarities with other
platformal sequences, deposited around the perimeter of the North
American craton, yet have a distinctive and unique character. All these
sequences, including the Mingan Islands, were deposited in extensive,
epeiric platforms associated with a passive continental margin during
the Lower Ordovician. A subduction zone, related to the Middle
Ordovician Taconic Orogenesis, significantly affected the eastern
continental margin from Alabama to Greenland. At that time, carbonate
platforms developed adjacent to pericratonic foreland basins.

The first important stratigraphic study of the Mingan Islands was
published in 1938 by Twenhofel. Since that time, the Mingan Islands have
received little attention. As such, this study provides an important
link to the understanding of the overall geology and paleogeography of
eastern Canada.

The dolostones of the Romaine Formation and limestones of the Mingan
Formation are exposed in extensive coastal exposures along the Mingan
Islands. These islands are one of few localities where a carbonate
sequence may be studied in three dimensions. As a result special
emphasis is placed on both vertical and horizontal facies changes.

The geologic history, especially paleokarst unconformities, in the
rocks of the Mingan Islands is a result of the interaction between local
tectonics and eustatic sea level fluctuations. Since there are few
detailed sedimentological studies of regional unconformities in platform
carbonates, the results of this study will be important in understanding

- 4 -

the formation and evolution of such unconformities in general.
Diagenesis is also important in deciphering the effects of meteoric
diagenetic processes which were probably different during the Ordovician
than today, in particular because of the lack of significant land
plants.

The specific purposes of this study are: 1) to establish a formal,
stratigraphic framework for the sequence; 2) to interpret, in detail,
the sedimentary environments and propose depositional models; 3) to
document the various types of reef limestones in the Mingan Formation;
4) to describe the paleokarst unconformities in the sequence and analyze
their sequential development; 5) to study calcarenite cycles in the
Mingan Formation; and 6) to examine the limestone diagenesis, and in
particular the different stages of cementation, in the Mingan Formation.

METHODS

During the course of three seasons of field work in the Mingan
Islands (1982-84), more than forty stratigraphic sections were measured
and described (fig. 1-2). Each section was subdivided into lithofacies
on the basis of sedimentological characteristics (lithology, texture,
structure). Some lithofacies have been further subdivided based on their
microscopic attributes in thin-sections, on polished slabs and in peels.
Some exposures were also mapped in detail, especially those associated
with paleokarst unconformities.

Extensive field sampling of all carbonate lithofacies was carried
out, and a total of 720 samples collected. Large samples (20-50 cm in
size) from the Mingan reef limestones were slabbed and polished in order
to determine interrelationships between reef builders and matrix. In

addition, selected reef fossils were collected and sent for taxonomic identification; these include bryozoans (Dr. R. Cuffey), sponges (Dr. K. Rigby), and stromatoporoids (Dr. C. Stearn).

In total, 560 thin-sections of standard 30 μm thickness were examined. All thin-sections were stained with Alizarin red-S to evaluate the distribution of calcite and dolomite and with potassium ferricyanide to test for ferroan carbonate (Dickson, 1966). The carbonate textural classification used in the present study is that of Dunham (1962) for limestones and that of Gregg and Sibley (1984), which is a modified version of Friedman's (1965) textural classification, for doiostones and dolomitized limestones.

The luminescence characteristics of the major components (skeletal debris, cements, ooids) in the Mingan limestones were studied with a Nuclide Luminoscope. About 75 uncovered, unstained, and polished thin-sections were examined. Working conditions were kept as constant as possible and were: 16-17 KV beam energy, 0.6 ma beam current, 35-45 millitor pressure and 1 cm diameter beam. Photographs were taken with Ektachrome 400 slide film in both transmitted and luminescent light using a Leitz system camera (Wild Photomakroskop M400).

Some petrographic problems associated with grain microfabrics, especially the recognition of microdolomite inclusions in calcite cements, were resolved with the aid of the scanning electron microscope. The SEM observations were performed on both thin-sections and small sample chips that were highly polished and etched with 1% formic acid for approximately 30 seconds. The etching creates a microrelief where the microdolomites stands out in positive relief with respect to the adjacent calcite.

PREVIOUS WORK

The Ordovician sequence of the Mingan Islands has been the subject
of few geological studies. The earliest investigations were combined
with those on Anticosti Island (Richardson, 1856; Logan, 1863;
Schuchert and Twenhofel, 1910). Richardson (1856) provided the first
brief description of the Mingan sequence and also collected fossils
which were later described by Billings (1865). Of particular interest
was Billing's description of two new sponge genera (Archaeoscyphia, and
Eospongia) from specimens collected in the Mingan Islands. Logan (1863)
in his classic study, "Geology of Canada", described two sections from
the islands at Grande Pointe and at Grande Ile. He called what is now
the lower Romaine Formation the Calciferous Formation, and what is now
the upper Romaine Formation and the Mingan Formation the Chazy
Formation, and finally the uppermost strata of the Mingan Formation he
called the Birdseye or Black River Formation.

Schuchert and Twenhofel (1910) presented the Mingan sections as part
of the Mingan-Anticosti sequence. They subdivided the Romaine and Mingan
Formations into a number of lithological units and correlated them with
the Beekmantown and Chazy Series of the Champlain Valley and New York
State. In the uppermost strata of the Mingan Formation (Zone 5), they
recognized a "white limestone" characterized by a problematic molluscan
fauna tentatively assigned to a Black River age. Twenhofel (1926, 1931)
discussed the stratigraphy (western part) and geomorphology of the
Mingan Islands. Twenhofel (1938) subsequently published a synthesis of
his work on the islands, including systematic paleontology and many
section descriptions. He correlated the Romaine Formation with the upper
part of the Beekmantown Group, and the Mingan Formation with the Chazy

Group of the Lake Champlain area. Foerste (in Twenhofel, 1938) observed that none of the cephalopods of Schuchert and Twenhofel's zone 5 suggested a Black River age.

After Twenhofel's studies, relatively little was published on the geology of the Mingan Islands. Cooper (1956) revised and added to the brachiopod list of Twenhofel (1938). Waddington (1950) evaluated the extent and composition of the carbonates for their use as industrial minerals. Shaw (1980) examined the relationships between lithofacies and trilobite biofacies of the Mingan Formation and compared them with coeval fauna of New York (Chazy Group), Newfoundland (Cobbs Arm Formation), and the Northwest Territories (Esbataottine Formation). The Mingan trilobite fauna is essentially similar to that found in other shelf facies around the perimeter of North America during the Middle Ordovician. Furthermore, Shaw described a marked unconformity within the Mingan Formation that he interpreted as an ancient "ravinement" (i.e. a surface resulting from rapid marine transgression in the absence of abundant sediment). Nowlan (1981) presented preliminary data on the stratigraphy and conodont fauna of the Mingan sequence. He suggested that much of the Romaine Formation is of late Canadian age whereas the Mingan Formation is of Chazyan age. He also reported the first Whiterockian conodonts at the top of the Romaine Formation in the western Mingan Islands.

In addition to these studies, mapping projects of the adjacent Precambrian terranes by the Quebec Department of Energy and Resources also covered the Mingan Islands, but their stratigraphy is only discussed briefly (Longley, 1950; Depatie, 1967; Sharma and Franconi, 1975). Preliminary reports of this Ph.D. thesis are also found in Desrochers (1984, 1985).

- 8 -

CHAPTER 2

STRATIGRAPHY

INTRODUCTION

Schuchert and Twenhofel(1910) introduced the formation names Romaine (from an island of the same name at the mouth of the Romaine River) and Mingan (after the Mingan Islands). The Mingan Islands are the type ocality of both formations, however, there is no stratotype. Furthermore, Twenhofel's (1938) stratigraphy is considered unsatisfactory, especially as his individual zones or units exhibit significant lithological variations. The purpose of this chapter is to revise the stratigraphy following the current rules of the North American Stratigraphic Code (1983).

The well-established Romaine and Mingan Formations are maintained, but, seven new members (provisional) are introduced. Most of these members are only mappable locally and therefore are not convenient considered as formations. The Romaine and Mingan Formations consist of a composite-stratotype comprising a type section and supplementary reference sections. A type section or reference section is assigned to each member in order to demonstrate their distribution. This procedure is more convenient for describing stratigraphic units that are characterized by rapid facies changes and sedimentological breaks.

Rocks assigned to the Romaine and Mingan Formations are essentially undeformed strata (150 m thick) that overlie the Precambrian unconformably and dip gently ($1-2°$) to the south (fig. 2-1). The Romaine

Figure 2.1- Geological map of the Mingan Islands and adjacent shore of
the Gulf of St. Lawrence showing the distribution of the Romaine a
Mingan Formations. The Romaine Formation is exposed on the inner
islands, the north side of most of the outer islands, and the
adjacent mainland. The Mingan Formation occurs on most of the oute
islands and at Grande Pointe. The Ordovician strata have a regiona
strike oriented east-west and dip gently toward the south.

ORDOVICIAN - MINGAN ISLANDS
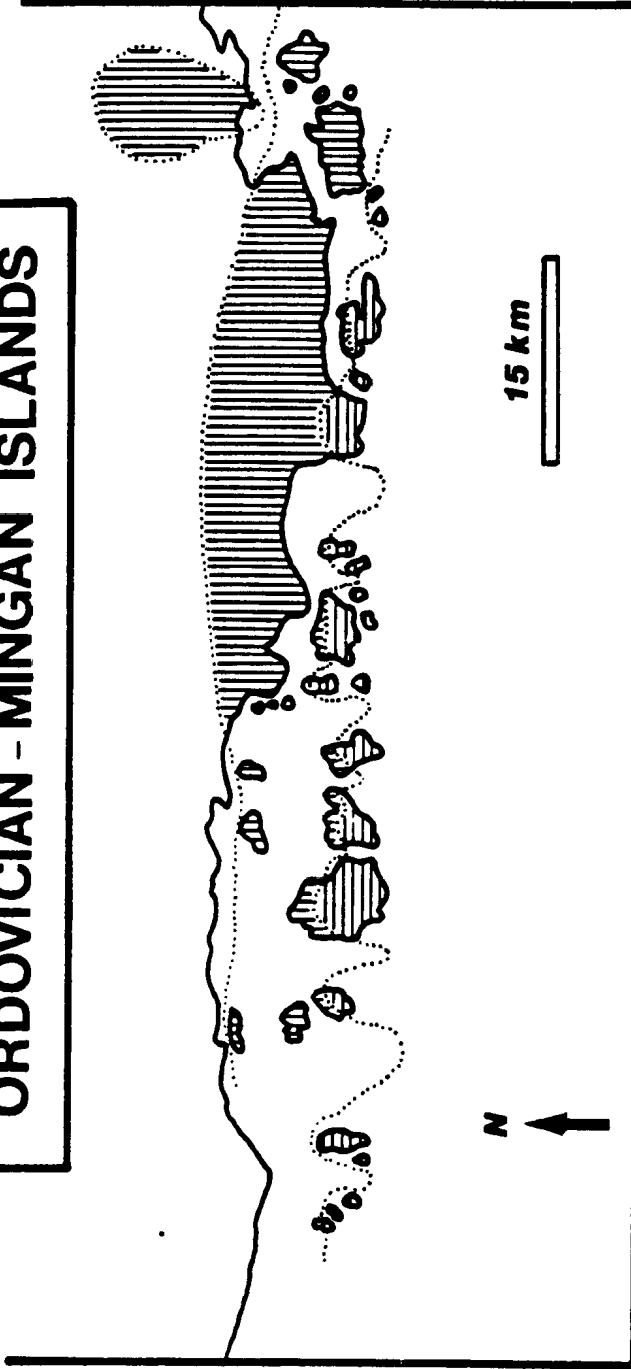
Mingan Formation

Romaine Formation

15 km

N

Formation consists only of dolostone lithofacies while the Mingan

Formation is composed mainly of limestone lithofacies. Both formations,

however, have a basal siliciclastic unit. Information concerning the

distribution of these stratigraphic units is summarized in figures 2-2

and 2-3. Furthermore, detailed descriptions of the reference and type

sections are given in Appendix B.

ROMAINE FORMATION

The Romaine Formation is exposed at numerous localities on the inner

islands, the north side of the outer islands, and the adjacent shore of

the Gulf of St. Lawrence (fig. 2-1). The formation is divided into three

formal members, in ascending order: Sauvage, Sainte-Genevieve and Grande

Ile Members. The Sauvage Member is a thin unit of arkosic sandstones.

The Sainte-Genevieve Member is composed of medium to coarse crystalline,

sucrosic dolostones while rocks of the Grande Ile Member are generally

more finely crystalline dolostones or dolomicrites with minor shale

interbeds. This textural contrast in dolostones of the Romaine Formation

has also been noticed by earlier workers (Schuchert and Twenhofel,

1910).

The base of the Romaine Formation is defined as the contact with the

underlying Precambrian crystalline basement and its top as the

unconformable contact (paleokarst unconformity) with the overlying

siliciclastic Corbeau Member of the Mingan Formation.

The composite-stratotype of the Romaine Formation consists of a type

section on Ile Sainte-Genevieve (fig. 1-2, section 33) and two

supplementary reference sections at Pointe du Sauvage (fig. 1-2, section

32) and on Grande Ile (fig. 1-2, section 9).

Figure 2.2- Generalized stratigraphic section of the Romaine and Min
Formations in the Mingan Islands. See figure 1.2 for symbols.

STRATIGRAPHY

Lower Ordovician — Middle Ordovician

Upper Canadian — Chazyan — Whiter.

Romaine Fm — Mingan Fm

GRANDE POINTE MEMBER

FANTOME MEMBER

PERROQUET MEMBER

CORBEAU MEMBER

GRANDE ILE MEMBER

STE-GENEVIEVE MEMBER

SAUVAGE MEMBER

Precambrian

20 m
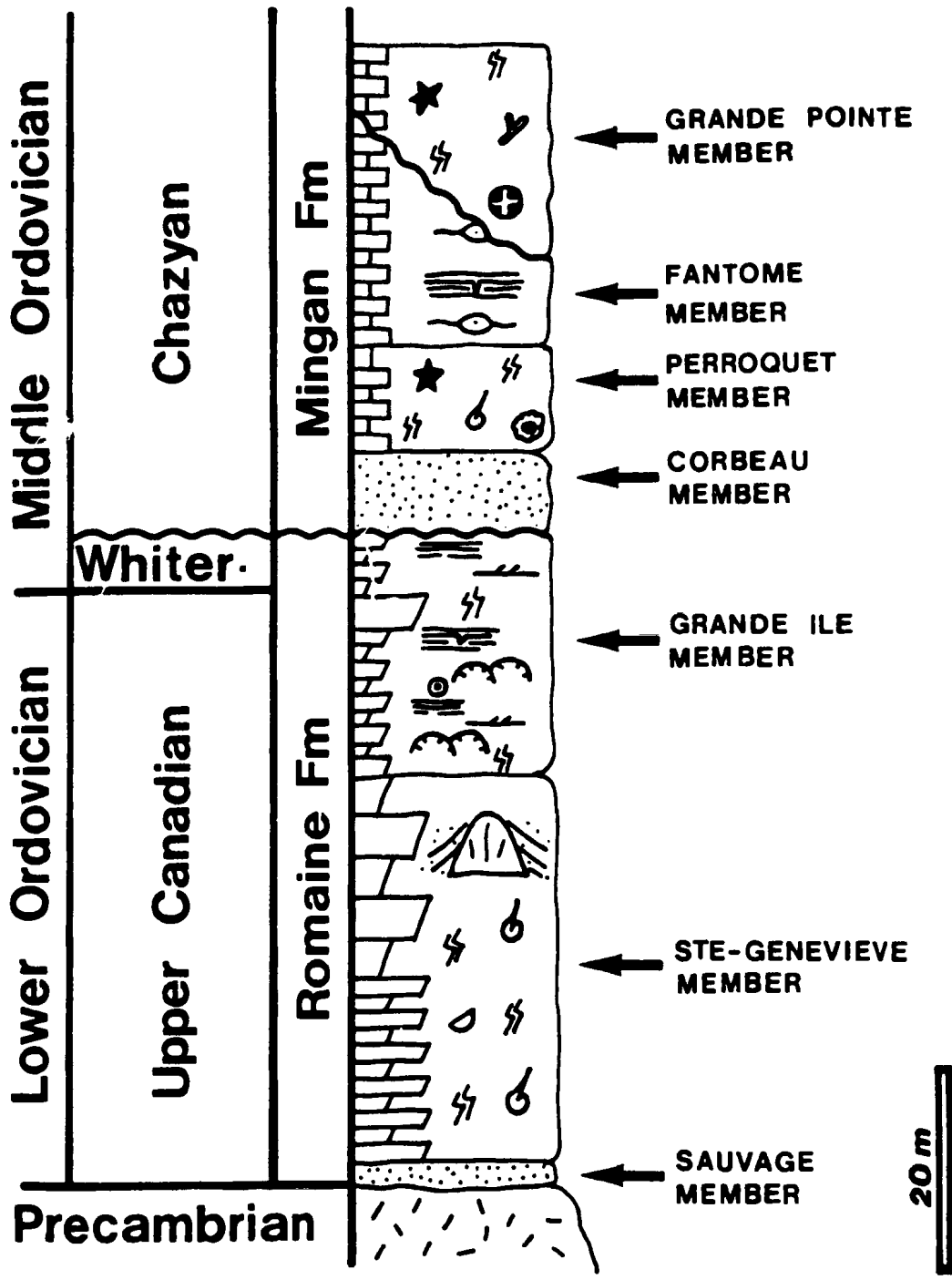
Figure 2.3- Generalized cross-section parallel to the regional stri[
illustrating the distribution of the stratigraphic units within
Romaine and Mingan Formations. Letters correspond to the differ
members; Rs: Sauvage Member, Rsg: Sainte-Genevieve Member, Rgi:
Grande Ile Member, Mc: Corbeau Member, Mf: Fantome Member, Mp:
Perroquet Member, Mgp: Grande Pointe Member. Numbers correspond
the type and reference sections; 1: Pointe du Sauvage, 2: Ile
Sainte-Genevieve, 3: Grande Ile, 4: Ile du Havre (Cap du Corbea
5: Ile aux Perroquets, 6: Ile du Fantome, 7: Grande Pointe. See
figure 1.2 for symbols.

W

Mingan Fm

Mp

M_f

?

M_gp

M_c

M_f

PK

PK

E

5

3

6

4

7

2

1

Romaine Fm

R_gi

R_sg

R_s

Pc

20 m

15 Km
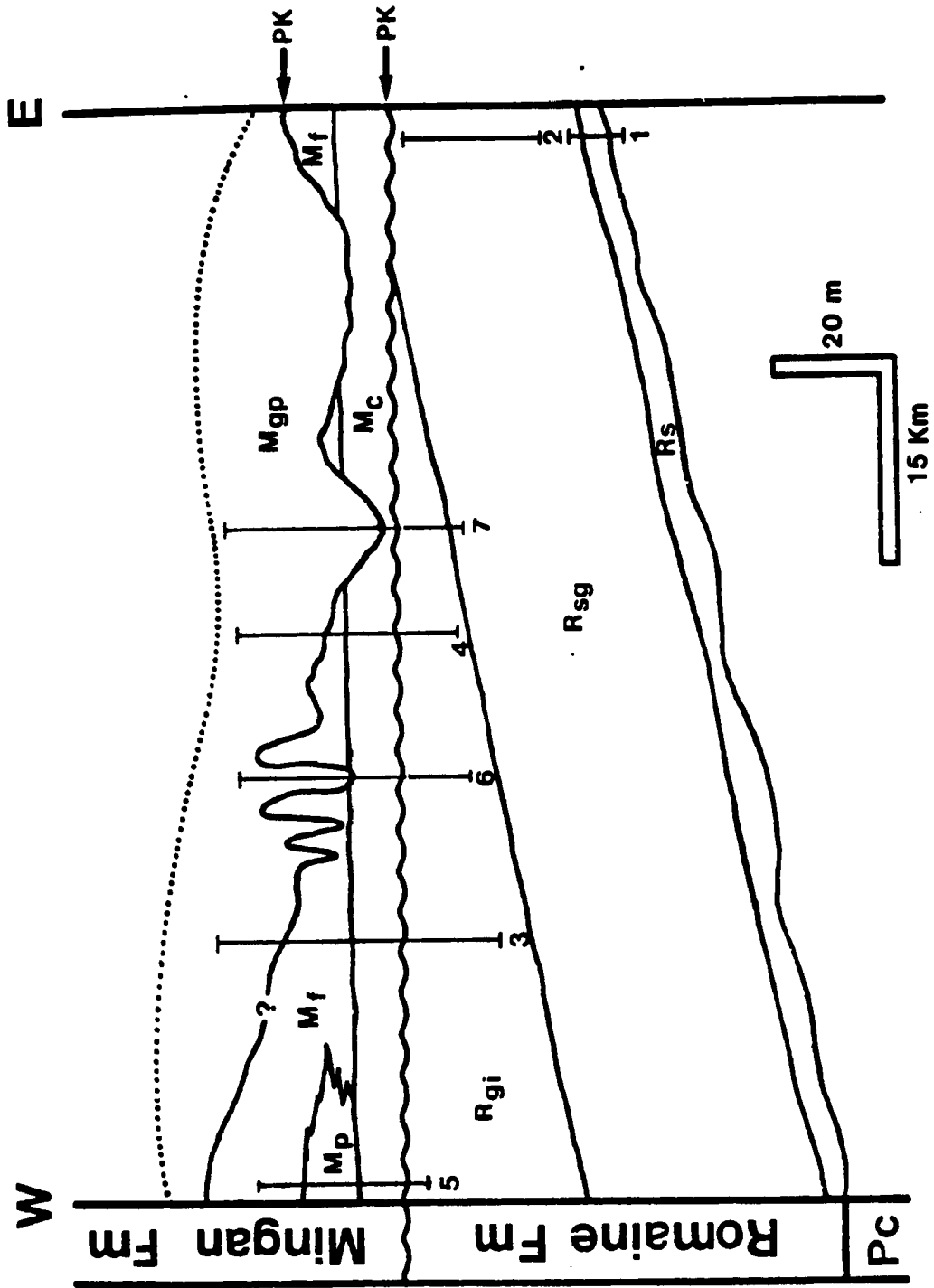
Sauvage Member (new member)

Reference section location- Pointe du Sauvage on the east side of Baie Saint-Laurent; grid reference NTS 12L/6, UD 920689; coastal exposures of wave-cut platforms (fig. 2-3, section 1).

Lithology- Massive, white, medium- to coarse-grained sandstone characterized by an arkosic composition and large scale cross-bedding.

Distribution- This member is present only on Pointe du Sauvage and remains unexposed elsewhere on the mainland due to the presence of thick Pleistocene deposits.

Thickness- ?-3 m

Definition of the boundaries- The lower boundary is the unconformable contact with the Precambrian basement. The upper boundary is conformable and gradational with the overlying Sainte-Genevieve Member. The sandstones of the Sauvage Member become gradually more dolomitic upward. An arbitrary contact is placed at that point where the proportion of dolomite exceeds the proportion of sandstone. This boundary is well exposed on Pointe du Sauvage.

Fauna- The fossil assemblage is restricted to inarticulate brachiopods and gastropods. The vertical trace fossil Skolithos is also present.

Remarks- Despite limited exposure in the study area, sandstones at the base of the Romaine Formation have a regional extent and occur in the subsurface beneath Anticosti Island (Roliff, 1968; A. Desrochers, pers. obsv.).

Sainte-Genevieve Member (new member)

Type section location- West side of Ile Sainte-Genevieve; grid

reference NTS 12L/6 and 12L/7, UD 952672; coastal exposures of vertical cliffs (fig. 2-3, section 2)

Lithology- This member consists of dark-brown, sucrosic dolostones. The lower two thirds are thin-bedded and characterized by a distinctive burrow-mottled texture. Intraclast-rich layers with ripple laminations are frequently intercalated. In contrast, the upper third is massive, thick bedded, and contains pervasively dolomitized thrombolite mounds. These thrombolites mounds may laterally grade into burrow-mottled dolostones. Intraformational breccias are present locally.

Distribution- The Sainte-Genevieve member occurs in the inner island and at several localities on the adjacent mainland (e.g. Pointe aux Morts, Baie Puffin, Tete de la Perdrix, Pointe du Sauvage). This member is laterally traced throughout the study area and best exposed on the eastern islands.

Thickness- Ca. 50 m

Definition of the boundaries- The lower boundary is conformable and gradual with the underlying sandstones of the Sauvage Member. The upper boundary is placed at the first appearance of dolomicrite in the sequence which is coincident with the base of the Grande Ile Member. This boundary in the study area is unexposed but appears, at least at the Grande Pointe section where only 1-2 m is covered, to be sharp and conformable. The same upper boundary in the eastern islands (i.e. east of Ile Saint-Charles) however, corresponds to the contact with the Mingan Formation because the dolomites of the overlying Grande Ile Member have been removed by erosion.

Historical background- This member corresponds to Schuchert and Twenhofel's (1910, p.686) division A1 and Twenhofel's units 2 to 8

(1938, p.24).

Fauna- A relatively diverse fauna is present and includes:
trilobites (mainly bathyurid and pliomerid forms), articulate
brachiopods, low and high-spired gastropods, lithistid sponges, and
echinoderms. These megafossils are generally poorly preserved due to
pervasive dolomitization or partial replacement by chert. Graptolites
are found locally in the Sainte-Genevieve Member.

Remarks- The member thickness is difficult to evaluate in the
eastern islands due to limited exposure. A drilling program was carried
out at Pointe aux Morts by the Quebec Fer et Titane Inc. and cores, up
to 30 m long, were recovered (Bergeron, 1980). These cores consist of
typical "Sainte-Genevieve" lithofacies; however, the underlying
sandstones of the Sauvage Member have not been reached.

Grande Ile Member (new member)

Reference section location- Northwest side of Grande Ile; grid
reference NTS 12L/4, UD 355661; coastal exposures of vertical cliffs
and wave-cut platforms (fig. 2-3, section 3).

Lithology- This member is composed mainly of medium-bedded, light
brown dolomicrites which exhibit a cyclic arrangement of lithofacies.
Each lithofacies cycle represents a progressive shoaling of
depositional paleoenvironments and records shallow subtidal to
supratidal conditions (discussed in detail in chapter 3). The major
lithofacies include: dololaminites, ripple-laminated dolomicrites,
stromatolite dolomicrites, burrowed dolomicrites, and ooid dolostones.

Distribution- The member is exposed on the north side of the outer

islands but is absent east of Ile Saint-Charles.

Thickness- 0-25 m

Definition of the boundaries- The lower boundary is defined by the
appearance of dolomicrites as discussed above. The upper boundary is
sharp and erosional with the overlying siliciclastics of the Corbeau
Member, the basal member of the Mingan Formation.

Historical background- Schuchert and Twenhofel's zones A1, B, and C
(1910, p.687) and Twenhofel's units 9 to 11 (1938, p.23) are considered
equivalent to the Grande Ile Member.

Fauna- The member is generally characterized by a low diversity
fauna (gastropods, ostracods). A more diverse fauna, however, is
present in burrowed dolomicrites forming the base of some
shallowing-upward cycles and includes articulate brachiopods,
trilobites, mollusks, and echinoderm fragments.

Remarks- Burrow-mottled, sucrosic dolostones similar to those in
the Sainte-Genevieve Member are present in the upper part of the Grande
Ile Member. These dolostones form a massive unit (about 5 m thick)
which is well exposed on Ile Niapiskau, Ile Quarry, Grande Ile, and Ile
a Bouleaux de Terre (fig. 2-2).

The Romaine-Mingan contact is widely exposed in the study area and
appears in most outcrops as a disconformity in which the bedding planes
above and below the marked break are essentially parallel. The same
contact at the regional scale, however, is clearly angular as
demonstrated by several key beds in the upper part of the Romaine
Formation that have been systematically truncated and do not extend
more to the east. This relationship is illustrated in figure 2.3.

MINGAN FOPMATION

The Mingan Formation is exposed in the outer islands and at Grande Pointe (fig. 2-1). The formation consists of the basal Corbeau Member (siliciclastics) which underlies one of the following limestone members; Perroquet, Fantome, or Grande Pointe (figs. 2.2 and 2.3). The base of the Mingan Formation is defined as the contact with the underlying dolomites of the Romaine Formation. The top of the formation is unexposed as it lies offshore beneath the Gulf of St. Lawrence. A maximum thickness of 50 m is measured on the islands. The lower 30 m is accessible and well exposed along the coastal exposures while the upper 20 m is present only in a few poor exposures inland on the islands. The composite-stratotype of the formation consists of a type section on Ile du Fantome (fig. 1-2. section 15) and three supplementary reference sections, located at Cap du Corbeau on Ile du Havre (fig. 1-2, section 17, Ile du Perroquet (fig. 1-2, section 1), and Grande Pointe (fig. 1-2, section 22). The type section located on Ile du Fantome displays all the members, except the Perroquet Member.

Of particular importance is the presence of a paleokarst unconformity within the Mingan Formation which is thought to control the distribution of its members (fig. 2-3).

Corbeau Member (new member)

Reference section location- Cap du Corbeau on the northeast side of Ile du Havre; grid reference NTS 12/L4, UD 576637; coastal exposures of vertical cliffs (fig. 2-3, section 4).

Lithology- Major lithofacies include silty dololaminites, laminated shales, laminated sandstones, cross-bedded sandstones, and

channelized sandstones. These lithofacies form sequences characterized by an overall fining-upward texture. Rare limestone lenses with skeletal debris are present.

Distribution- This member occurs on the north side of the outer islands (except on Ile a Bouleaux de Terre) and at Grande Pointe.

Thickness- Ca. 5 m

Definition of the boundaries- The lower boundary is placed at the contact with underlying dolomites of the Romaine Formation. The upper boundary is defined at the top of silty dololaminite beds, if present, where the contact is conformable with the overlying limestones of the Perroquet or Fantome Members. In some cases (e.g. Grosse Ile au Marteau, Grande Pointe, and Ile Saint-Charles), this boundary is erosional and coincident with the intra-Mingan paleokarst unconformity.

Historical background- The member is equivalent with Schuchert and Twenhofel's zones A1 and A2 (1910, p.689) and Twenhofel's units 12 and 13 (1938, p.23).

Fauna: The restricted fauna consists of inarticulate brachiopods and small articulate brachiopods (mainly rhynchonellids) and occurs only in sandstone lithofacies. The vertical trace fossils Skolithos and Diplocraterion are common in sandstones.

Remarks- The thickness of this member is fairly constant across the study area and ranges from 4.0 to 6.0 m. A section on Ile Innu, however, is only 1.5 m thick and probably reflects local erosional relief over the underlying Romaine Formation. Irregular thicknesses (0.5- 3.0 m) are also measured on Grosse Ile au Marteau and at Grande Pointe where the upper boundary of this member is erosional (i.e. intra-Mingan paleokarst unconformity).

Perroquet Member (new member)

Reference section location- Ile aux Perroquets and adjacent Ile de la Maison; grid reference NTS 12L/1, UD 139637; coastal exposures of vertical cliffs and wave-cut platforms (fig. 2-3, section 5).

Lithology- The member consists mainly of medium-grey, burrowed, skeletal wackestones and packstones characterized by thin and uneven beds. Other intercalated lithofacies are skeletal grainstones with rare, but large cross-beds and massive reef limestones which form a biostromal unit (lithistid sponge-bryozoan-tabulate coral rudstone)

Distribution- The member is restricted to the westernmost islands as it occurs on Ile Nue de Mingan, Ile de la Maison and Ile aux Perroquets. The Perroquet Member grades laterally and upward into the limestones of the Fantome Member.

Thickness- Ca. 8 m.

Definition of the boundaries- The lower boundary is defined at the junction between silty dololaminite beds and skeletal wackstones/packstones. The upper contact is placed at the first appearance of fenestral lime mudstones or associated lithofacies of the Fantome Member. Both boundaries are sharp and apparently conformable.

Historical background- The member corresponds to Schuchert and Twenhofel's zone A3 (1910, p.690) and to Twenhofel's unit 14 (1938, p.23).

Fauna- The fossil assemblage is abundant and diverse and includes: articulate brachiopods, trilobites, lithistid sponges, bryozoans, tabulate corals, echinoderm fragments, low and high-spired gastropods, orthocone and cyrtocone cephalopods, calcareous algae, and ostracods. The most common trace fossils are Chondrites, Palaeophycus, and

<u>Planolites</u>. Other trace fossils are also present but remain
unidentified at this stage.

Fantome Member (new member)

<u>Type section location</u>- West side of Ile du Fantome; grid reference
NTS 12L/4, UD 508640; vertical coastal cliffs (fig. 2-3, section 6).

<u>Lithology</u>- The member is mainly medium-bedded, brown-grey,
fenestral lime mudstone. Other associated lithofacies are
cryptalgalaminites, intraclast grainstones, gastropod packstones, and
rare skeletal wackestones.

<u>Distribution</u>- The member is traceable laterally over the study area
except where the intra-Mingan paleokarst unconformity eroded deeply
into the sequence (e.g. Ile Saint-Charles, Grande Pointe, Grosse Ile au
Marteau). In general, this member is exposed on all outer islands and
at Pointe Enragee.

<u>Thickness</u>- 0 - 25 m

<u>Definition of the boundaries</u>- The lower boundary is sharp and
apparently conformable with the underlying Perroquet Member in the
westernmost islands or Corbeau Member in the remaining of the study
area. The upper boundary is sharp and unconformable with the overlying
limestones of the Grande Pointe Member and corresponds to the
intra-Mingan paleokarst unconformity.

<u>Historical background</u>- Schuchert and Twenhofel's zone A4 (1910,
p.691) and parts of Twenhofel's units 14 to 16 (1938, p.23) are
considered equivalent to the present member.

<u>Fauna</u>- The fauna is characterized by a low-diversity fossil
assemblage but may be locally abundant and includes: leperditiid

ostracods, low and high-spired gastropods, and rare orthocone cephalopods. Furthermore, trilobites (only bathyurids) and articulate brachiopods are sometimes present. The lower part of this member is frequently marked by gastropod-rich beds (10-20 cm thick).

Remarks- The erosional style of the intra-Mingan paleokarst unconformity is quite variable and may range from a slight to marked angular unconformity to a disconformity.

Grande Pointe Member (new member)

Reference section location- Grande Pointe on the east side of Baie Placide-Vigneault; grid reference NTS 12L/3, FD 675039; coastal exposures of vertical cliffs (fig. 2-3, section 7).

Lithology- This member consists of a heterogenous package of lithofacies which are in order of importance: skeletal wackestones and packstones, skeletal-ooid grainstones, intraclastic grainstones, and reef limestones. Nodular lime mudstones and brachiopod coquinas are sometimes present near the base of the member. The reef limestones are found either as isolated mounds or as mound complexes which were build by a consortium of lithistid sponges, bryozoans, and tabulate corals.

Distribution- The member is laterally continuous and exposed on the outer islands.

Thickness- Up to 25 m

Definition of the boundaries: The lower boundary is sharp and unconformable with the underlying Fantome Member as defined by the intra-Mingan paleokarst unconformity. The upper boundary is unexposed and occurs beneath the adjacent Gulf of St. Lawrence.

Historical background- The member is equivalent to Schuchert and

Twenhofel's zones A3 and A5 (1910, p.690-692) and parts of Twenhofel's units 14 to 16 (1938, p.23-24).

Fauna- The fossil assemblage is characterized by a highly diverse and abundant fauna which is similar in composition to the fauna in the Perroquet Member.

AGE OF THE UNITS

Lower and Middle Ordovician biostratigraphy, including the equivalence between North American and British series and correlation with the Mingan sequence, is summarized in fig. 2-4.

Romaine Formation

Sandstones of the Sauvage Member, the basal member of the Romaine Formation, yield elements of the Mid-Continent conodont fauna D (Nowlan, 1981). Abundant drepanodan, scolopodan elements of conodont fauna E, including Oepikus communis, are found as low as 15 m above the base of the formation. The Mid-Continent conodont fauna D and E are indicative of a late Canadian age (Barnes et al., 1981). The top of the formation has yielded conodonts of Whiterockian age (zone 1-2), however, these are restricted to the westernmost islands. Brachiopods, found in this part of the formation, are characteristic of the Orthidiella zone and confirm this age (T. Bolton, pers. comm., 1982). The section loss due to the paleokarst unconformity at the top of the Romaine Formation increases eastward as older beds are progressively truncated and explains the absence of Whiterockian conodonts in the eastern islands.

Figure 2.4- Lower and Middle Ordovician chronostratigraphic units in North America; mid-continent conodont faunal units of Sweet et al. (1971); Lower Ordovician and lower Middle Ordovician graptolite zones of Berry (1960) and upper Middle Ordovician graptolite zones of Riva (1969, 1974); Canadian and Whiterockian shelly faunal unit of Ross (1949) and post-Whiterockian shelly faunal zones of Ludvigsen (1979); Lower and Middle Ordovician chronostratigraphic units in Great Britain; stratigraphic range of the Romaine and Mingan Formations.

| NORTH AMERICAN | | | | | BRITISH |
SERIES	STAGES	CONODONT FAUNAS	GRAPTOLITE ZONES	SHELLY FAUNAS & ZONES	SERIES
		8	Diplograptus multidens		
	BLACK RIVERAN	7		Ceraurus gabrielsi	CARADO CIAN
	?	6	Nemagraptus gracilis	Bathyurus ulu	
CHAMPLAI NIAN	CHAZYAN			C. nahanniensis	LLANDEI LIAN
		5	Glyptograptus teretiusculus	Bathyurus granulosus	
				Bathyurus nevadensis	
		4	Paraglossograptus tentaculatus	Anomalorthis N	LLANVIR NIAN
	WHITE ROCKIAN	3		M	
		2		Orthidiella L	
		1		K	
			Isograptus victoriae	J	
CANADIAN		E	Didymograptus protobifidus	Hesperonomia H,I	ARENIGIAN
		D	Tetragrap. fruticosus		
		C	Tetragraptus approximatus	G	

MINGAN ISLANDS

↓

eroded

~ ? ~

MINGAN FM

ROMAINE FM

Pc
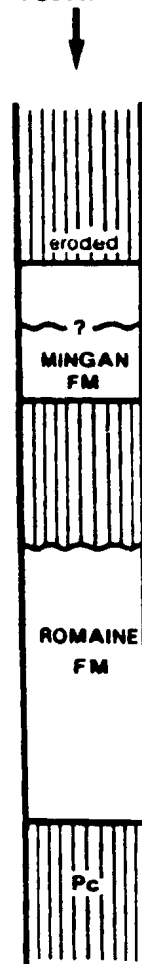
In the Sainte-Genevieve Member, the graptolites _Phyllograptus typus_, _Tetragraptus quadribrachiatus_, and _Dichograptus_ ? sp. are found locally in thin-bedded burrow-mottled dolostones and suggest an early to mid Arenig age for these beds (H.S. Williams, pers.comm. 1983). In addition to graptolites, bathyurid and pliomerid trilobites from the same beds are similar to trilobites in the Catoche Formation of Western Newfoundland (D.Boyce, pers.comm. 1983). The Catoche Formation has been correlated with the zone H of Utah and Nevada and assigned a probable early Arenig age (Fortey, 1979).

On the basis of conodont and other associated faunas, the major part of the Romaine Formation is assigned a late Canadian (early to late Arenig) age. Only the uppermost strata of the Grande Ile Member appear to be early Whiterockian (latest Arenig) in age.

Mingan Formation

Sandstones of the Corbeau Member yield the conodont _Phragmodus flexodus_ which is indicative of a Chazyan age (Mid-Continent fauna 5/6). The Peroquet, Fantome, and Grande Ile Members contain a similar conodont fauna which is dominated by the genera _Panderodus_, _Phragmodus_, _Plectodina_, _Belodina_, _Erismodus_, _Ptiloconus_. All these genera also suggest a Chazyan age. The upper part of the Mingan Formation is characterized by elements of the _Polyplacognathus friendsvillensis_ - _P. swetti_ transition which gives a mid to late Chazyan upper age for the formation (Nowlan, 1981).

In addition to the conodont fauna, the shelly faunas also confirm a Chazyan age for the Mingan Formation. Trilobites and brachiopods show similarities, at least at the generic level, with other Chazyan shelf

sequences such as the Chazy Group of the Lake Champlain in New York and Vermont (Shaw, 1968, 1980), the Chazy Group of the St-Lawrence Lowlands (Hofmann, 1963), the Lenoir Formation of the Southern Appalachians (Cooper, 1956), and the Esbataottine Formation of the MacKenzie Mountains (Ludvigsen, 1978; Shaw, 1980). Furthermore, the bryozoan fauna of the Grande Pointe Member, the uppermost member of the Mingan Formation, may be correlated with the bryozoan fauna of the upper Crown Point and Valcour Formations which are the two upper formations of the Chazy Group in Lake Champlain (R. Cuffey; pers. comm. 1984).

The paleokarst unconformity within the Mingan Formation represents a sedimentological break which occurred during the Chazyan time. The conodont fauna exhibits no marked changes in composition across the unconformity; however, conodont zones or subzones in the Chazyan stage have not been yet defined in detail (Sweet et al., 1971; Sweet, 1984).

Summary

1) The Romaine and Mingan Formations are divided into members on the basis of the lithological composition and erosional breaks in the sequence.

2) The Romaine Formation (late Canadian-early Whiterockian) is subdivided into three members: 1) Sauvage Member, represented by sandstones, 2) Sainte-Genevieve Member, represented by sucrosic dolostones, and 3) Grande Ile Member, represented by dolomicrites.

3) The Mingan Formation (Chazyan) is subdivided into four members; a basal siliciclastic member (Corbeau Member) underlying three limestone members (Perroquet, Fantome, and Grande Pointe Members).

4) Two major erosional breaks are present in the sequence; 1) a paleokarst unconformity at the top of the Romaine Formation where most of the Whiterockian stage is missing, and 2) a paleokarst unconformity within the Mingan Formation which occurred during the Chazyan time.

CHAPTER 3

ROMAINE LITHOFACIES

The Romaine Formation is composed of sediments deposited in a
shallow epeiric sea which rimmed the North American continent during
Early Ordovician time. In spite of the fact that these lithofacies are
pervasively dolomitized, well-preserved megascopic details permit the
recognition of eight discrete lithofacies (for summary see table 3-1).
They are grouped into three assemblages of genetically-related
lithofacies: 1) a lower assemblage of transgressive sandstones; 2) a
middle assemblage of subtidal, open marine carbonates; and 3) an upper
assemblage of peritidal carbonates (fig. 3-1). The lower, middle, and
upper assemblages correspond respectively to the previously defined
Sauvage, Sainte-Genevieve, and Grande Ile Members of the Romaine
Formation. The vertical succession of assemblages represents an overall
shallowing-upward sequence following initial marine transgression. A
simple depositional model is derived from the shallowing-upward sequence
and consists of the following onshore-offshore environmental profile:
tidal flat, lagoon, on-shelf bioherm complex, and offshore shelf.

Similar lithofacies are widespread in age-equivalent cratonic shelf
sequences of North America. They have been recognized in the St-George
Group of Western Newfoundland (Pratt, 1979; Pratt and James, in press),
in the Beekmantown Group of the Central Appalachians (Mazzullo and
Friedman, 1975), in the Knox Group of the Southern Appalachians
(Thompson, 1975; Churnet et al., 1982), in the Ellenburger Group of

TABLE 3-1. CHARACTERISTICS AND DEPOSITIONAL ENVIRONMENTS OF THE ROMAINE FORMATION

LITHOFACIES	LITHOLOGICAL CHARACTERISTICS	INFERRED ENVIRONMENTS
A- Arkosic sandstones	Trough cross-bedding; texturally mature; arkosic composition; restricted marine fauna; <u>Skolithos</u> burrows; lower lithofacies assemblage	Nearshore sand bars
B- Dololaminites	Planar to wavy laminations; mud cracks; tepee structures; local flat-pebble conglomerates; evaporite pseudomorphs; peritidal cycles (upper part) of the upper lithofacies assemblage	Supratidal mud flats
C- Ripple-laminated dolomicrites	Ripple cross-laminations; parallel, wavy, and lenticular bedding; ubiquitous mud cracks; peritidal cycles (central part) of the upper lithofacies assemblage	Intertidal "mixed" sand and mud flats
D- Stromatolite dolomicrites	LLH stromatolites; mud-cracked tops; local columnar stromatolite mounds, peritidal cycles (central part) of the upper lithofacies assemblage	Intertidal stromatolites
E- Burrowed dolomicrites	Moderate to strong bioturbation; restricted marine fauna; infaunal trace fossils; peritidal cycles (lower part) of the upper lithofacies assemblage	Subtidal lagoons
F- Ooid dolostones	Massive to ripple-laminated units; well-sorted ooids; radial cortical layers; local intraclast-rich layer; peritidal cycles (lower part) of the upper lithofacies assemblage	Nearshore ooid sand bars
G- Thrombolite Mounds	Isolated and coalescent metre-size thrombolite heads; common associated flanking beds; diverse but poorly preserved fauna; middle lithofacies assemblage (upper part)	Subtidal patch reefs
H- Burrow-mottled dolostones	Strong bioturbation; storm-generated layers; diverse fauna; infaunal trace fossils; middle lithofacies assemblage	Subtidal, open marine shelf

Figure 3.1— Generalized stratigraphic section of the Romaine Formation
which is subdivided into three lithofacies assemblages: 1) a lower
assemblage, composed of arkosic sandstones; 2) a middle assemblage,
composed of burrow-mottled dolostones and thrombolite mounds and 3)
an upper assemblage, composed of various dolomicritic lithofacies
except in the upper part where burrow-mottled dolostones are
present. These assemblages respectively correspond to the Sauvage,
Sainte-Genevieve, and Grande Ile Members of the Romaine Formation.
See figure 1.2 for symbols.

ROMAINE FORMATION

Grande Ile Mb

Sainte-Genevieve Mb

Sauvage Mb

Pc
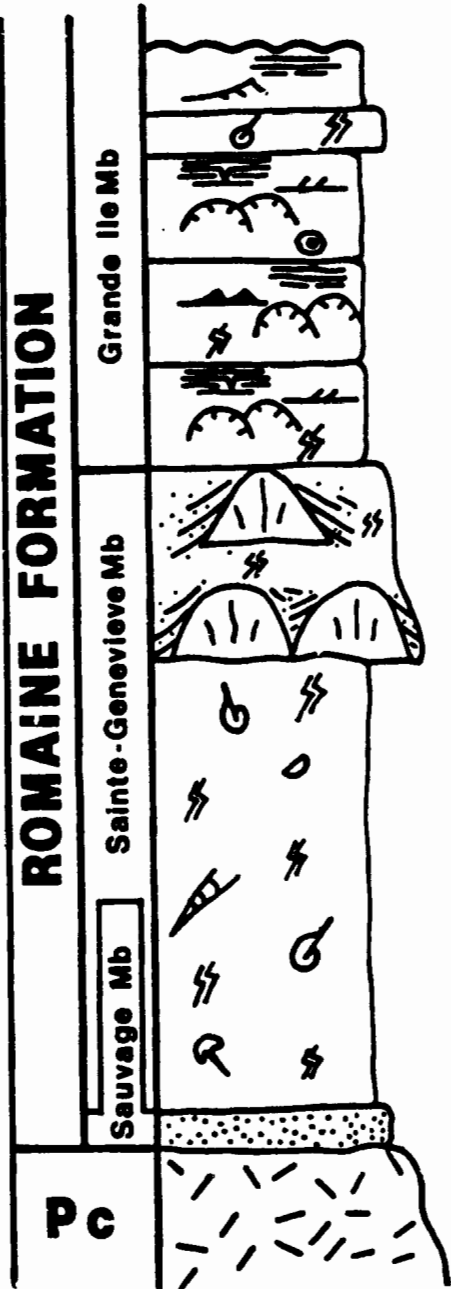
LITHOFACIES
ASSEMBLAGES

CYCLIC
PERITIDAL
CARBONATES

THROMBOLITE
MOUND
COMPLEXES

SUBTIDAL
CARBONATES

BASAL
SANDSTONES

UPPER

MIDDLE

LOWER

10 m

Texas (Loucks and Anderson, 1980), in the Goodwin Limestones of the Antelope Valley, Nevada (Ross, 1976), in the Prairie du Chien Group of the Upper Mississippi Valley (Davis, 1975), and in the Eleanor Bay Formation of the central Arctic Islands (Thorsteinsson and Kerr, 1968; Kerr, 1974).

LITHOFACIES DESCRIPTION AND INTERPRETATION

Lithofacies A: Arkosic sandstones

Description: This lithofacies directly overlies Precambrian basement and forms the basal unit of the Romaine Formation (fig. 3-1). This unit, up to 3.0 m thick, consists of light gray, medium to coarse-grained, trough cross-bedded arkosic sandstones (plate 3-1; A and B). The cross-beds are strongly oriented towards the craton (vector mean of $010°$, n=6). A restricted fauna is composed of inarticulate brachiopods and gastropods. Vertical burrows (Skolithos) are also present. In thin-section, the sandstones are dominated by quartz with up to 30% feldspar. Particles range from 0.5 to 1.5 mm in size but are well sorted within an individual layer (plate 3-1; C). The quartz is typically more rounded than the feldspar which appears more weathered and locally replaced by calcite. Plagioclase is the most abundant feldspar while orthoclase and microcline are less common. Quartz and feldspar overgrowth forms most of the cement with subordinate blocky calcite.

Interpretation: The textural maturity, trough cross-bedding, and associated fauna suggest that these sandstones were deposited in shallow subtidal environments under relatively agitated conditions. They are interpreted as nearshore sand bars actively migrating landward and

PLATE 3-1

LITHOFACIES A - ARKOSIC SANDSTONES

A. Field photograph showing the contact between Precambrian gneiss
    (Pc) and basal arkosic sandstones (ss) of the Romaine Formation at
    Pointe du Sauvage. Nature of the contact is sharp and unconformable
    and indicated by a black line.

B. Polished slab of arkosic sandstones with cross-laminations. Pointe
    du Sauvage.

C. Thin-section photomicrograph under cross-polarized light of arkosic
    sandstones characterized by sub-spherical and relatively well-sorted
    particles. Note the presence of plagioclase feldspar. Scale bar is
    1.0 mm.
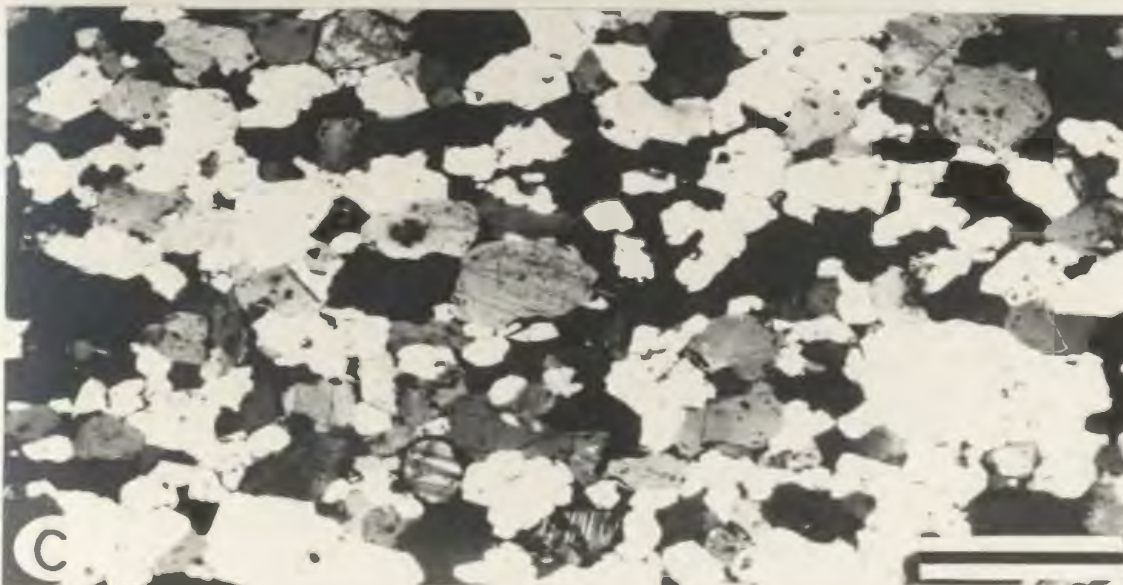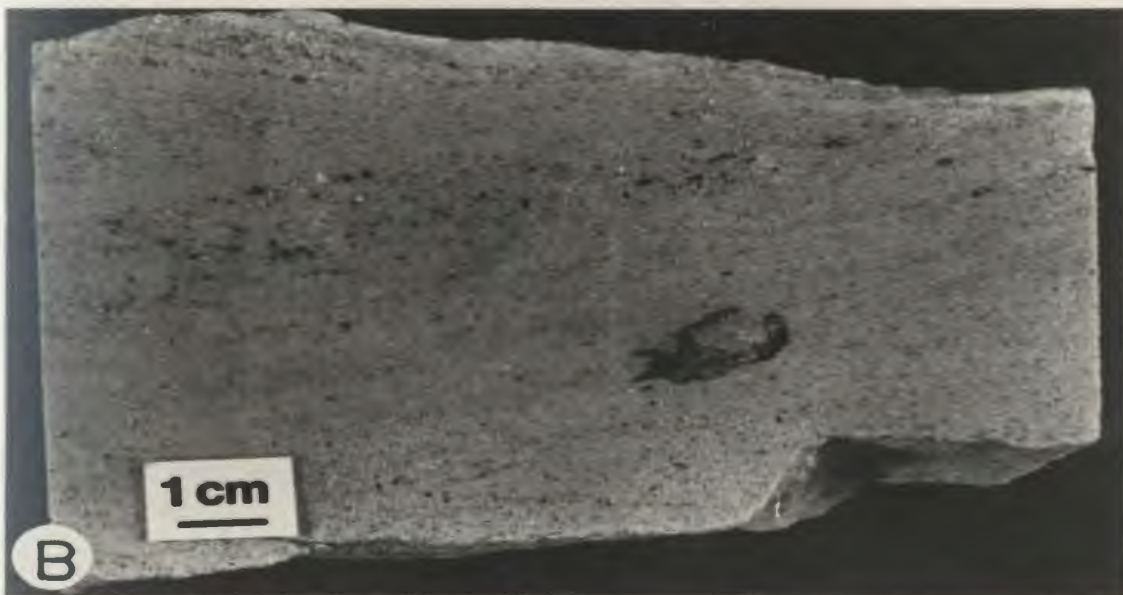
reworking a thin blanket of unconsolidated material (regolith and/or alluvium sediments) derived from the Precambrian basement. Skolithos and other vertical trace fossils are also indicative of such energetic conditions and are best developed in well-sorted shifting particle substrates (Seilacher, 1967; Frey and Pemberton, 1984). The high content of feldspar probably reflects a local source with little sediment transport from the adjacent low-lying rivers draining the Precambrian Shield. Similar, but thicker mature sandstones are usually found at the base of other cratonic Sauk sequences in North America; for instance the Potsdam sandstones in the St. Lawrence Valley (Hofmann, 1972) or the Bradore Formation in Labrador (Hiscott et al. 1984).

Lithofacies B: Dololaminite

Description: Most of this lithofacies is composed of planar laminated dolomicrites which are characterized by common mud cracks, intraclast-rich layers, flat-pebble conglomerates, and tepee structures (plate 3-2). The term "dolomicrite" is used here to describe finely crystalline dolostones with crystal size less than 20 μm . The planar laminations are sometimes wavy and may laterally grade into small isolated hemispheroidal stromatolites. Thin lenses (3 to 10 cm thick) of ripple-laminated dolomicrite are commonly observed. The ubiquitous evidences of evaporite precipitation consists of: 1) casts of lath-shaped aggregates (anhydrite precursor ?) (plate 3-2; F); 2) casts of cube-shaped aggregates (halite precursor ?) (plate 3-2; E); and 3) isolated to coalescent silicified nodules with crystalline form relicts of anhydrite (plate 3-2; E). The dololaminites are present in the upper assemblage, usually capping metre-scale peritidal cycles (fig. 3-1).

PLATE 3-2

LITHOFACIES B: DOLOLAMINITE

A. Field photograph (cross-section view) of dololaminite illustrating wavy to planar laminations and capping a peritidal cycle. Note the presence of mud-cracks which disrupt laminae at the top of the dololaminite unit. Ile du Havre NW.

B. Field photograph (bedding plane view) of mud-cracked dololaminite. Ile Saint-Charles NE.

C. Thin-section microphotograph (plane polarized light) illustrating the finely crystalline nature of the dolomite and well preserved laminae. Scale bar is 1.0 mm.

D. Polished slab of flat-pebble conglomerate associated with dololaminite units. Clasts are composed of rounded fragments of dololaminite with distinct laminae and are locally imbricated.

E. Field photograph (bedding plane view) of isolated silicified nodu within a dololaminite unit which may exhibit relic evaporite crys molds. Scale bar is 2 cm.

F. Field photograph (bedding plane view) showing lath-shaped aggrega of a possible anhydrite precursor. Indivudual laths are 5-10 cm long.
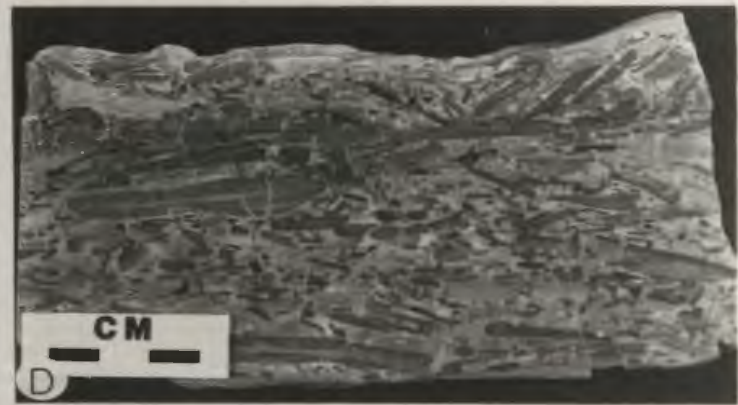
They occur in units ranging from 0.1 to 1.0 m in thickness.

Interpretation: This lithofacies represents sediments deposited on supratidal "sabkha" carbonate mud flats. The mm-scale planar laminations, commonly called cryptalgalaminites (Aitken, 1967), probably result from alternating layers of algal mats and fine-grained sediments deposited during episodic flood events (Hardie, 1977; Shinn, 1983). These sediments were subject to periodic exposure as evidenced by the presence of mud cracks which may laterally override to form small pseudo-anticlines or tepee structures. Tepee structures are commonly found in marine, coastal sequences influenced by arid to semi-arid climatic conditions (Asseretto and Kendall, 1977). The intraclast-rich layers and flat-pebble conglomerates are interpreted to result from erosion and redeposition of early lithified tidal flat sediments during storms. The excellent preservation of the sedimentary fabrics is similar to the fine grained dolomitic sediments observed in modern carbonate tidal flats such as in the sabkhas on the Persian Gulf (Morrow, 1982). Pervasive dolomitization contrasts with sporadic supratidal dolomites found in humid, Bahamas-type tidal flats (Shinn et al., 1965). The presence of evaporite relics is also indicative of an arid climatic setting.

Lithofacies C: Ripple-laminated dolomicrite

Description: This lithofacies is distinguished by parallel, wavy and lenticular bedded dolomicrites which exhibit internal ripple cross-laminations (plate 3-3; A and B). These beds (3 to 10 cm thick) are outlined by sharp bases and by ripple-form tops and are interbedded with structureless dolomicrites. In thin-section, (plate 3-3; C), the

PLATE 3-3

LITHOFACIES C: RIPPLE-LAMINATED DOLOMICRITE

A. Polished slab (cross-section view) of lithofacies C showing
    ripple-laminated interbeds (dark area) and structureless dolomicrite
    interbeds (light area). Note the soft sediment deformation "en
    echelon" at the base of some laminated interbeds. Ile du Havre NW.

B. Polished slab (cross-section view) of a laminated interbed with
    internal ripple cross-laminations. Grande Ile N.

C. Thin-section photomicrograph (plane polarized light) illustrating
    the contact between laminated interbed (bottom) and structureless
    dolomicrite interbed (top). Note in the laminated interbed the
    coarser grained texture of dolomite crystals and the presence of
    silt- to sand-sized dolomicrite intraclasts and quartz particles.
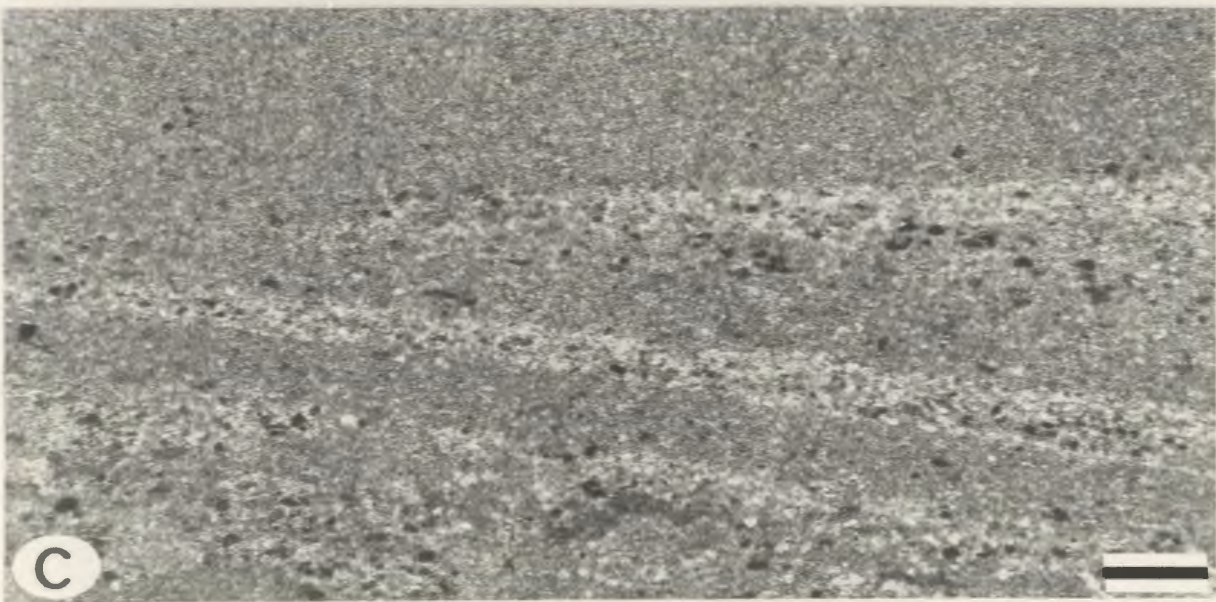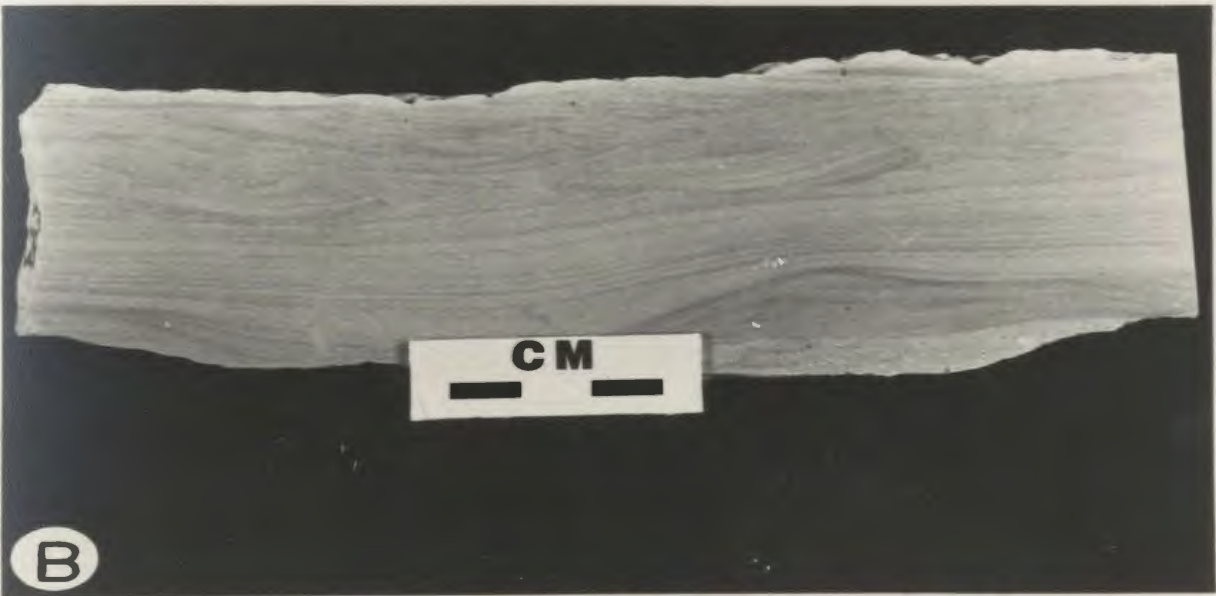
structureless dolomicrite interbeds consist of a mosaic of anhedral
crystals, less than 10 μm in size, with irregular intercrystalline
boundaries (xenotopic-A textural category of Gregg and Sibley, 1984).
The ripple-laminated beds are composed of slightly coarser-grained
dolomicrites with common rhombic crystal forms (Idiotopic-S textural
category of Gregg and Sibley, 1984) and of rare silt to sand-sized
dolomicritic intraclasts and quartz particles. Other observed features
are soft sediment structures, slight bioturbation (mainly vertical
burrows), and rare mud cracks. This lithofacies occurs with other cyclic
peritidal lithofacies (fig. 3-1) and forms units that range from 0.3 to
1.5 m in thickness.

Interpretation: This lithofacies is interpreted as sediments
deposited on a carbonate "mixed" sand and mud intertidal flat
environment. The variety of bedding and sedimentary structures, more
commonly observed in siliciclastic tidal flats (Reineck, 1975; Weimer et
al., 1982), is a function of variation in the availability of mud and
sand particles and in the energy of tidal and wave currents on the tidal
flats. The continuous shifting substrate inhibits the growth of algal
mats similar to those inferred in the dololaminites (lithofacies B). The
inferred environment is also supported by the absence of marine fauna,
rare mud cracks, fabric preservation type of dolomites
(penecontemporaneous), and association with peritidal lithofacies.
Similar lithofacies deposited in a carbonate "mixed" tidal flat regime,
have been recently reported from the rock record (Ashton, 1981; Demicco,
1983).

Lithofacies D: Stromatolite dolomicrite

Description: This lithofacies consists of pervasively dolomitized stromatolites which can be grouped into two categories; 1) closely-spaced hemispheroidal to low domal LLH forms ranging from 10 to 20 cm in height and from 40 to 60 cm in diameter (plate 3-4; A and B); and 2) small coalescent digitate heads forming circular mounds ranging from 3.0 to 5.0 m in diameter and up to 1.0 m in height (plate 3-4; C and D). The LLH stromatolite tops are sometimes desiccation-cracked. The stromatolite microfabrics are well preserved by a dense mosaic of xenotopic dolomicrites. The microfabrics exhibit mm-scale laminations of structureless dolomicrite laminae and/or closely-packed peloid laminae arranged in a laminated manner with common irregular and lamincid fenestrae. The stromatolites are sometimes thinly interbedded with sand to gravel-sized intraclasts of dolomicrite. They occur in units up to 0.8 m thick that make up part of the central portion of the meter-scale peritidal cycles in the upper lithofacies assemblage (fig. 3-1).

Interpretation: Based on the morphology of modern stromatolites (Hoffman, 1976), the hemispheroidal stromatolites represent domed algal mats which can only colonize relatively stable substrates and areas protected from erosive current scours in the intertidal zone. The larger digitate to columnar mounds probably formed in response to higher sedimentation rates in subtidal or low intertidal environments as well as in tidal ponds. An overall intertidal regime is suggested by mud cracks, fenestrate pores, and the vertical association with other peritidal lithofacies. The occurrence of modern stromatolites in Shark Bay, Western Australia (Logan et al., 1970; 1974) is generally ascribed to hypersaline conditions that successfully restrict browsing organisms

PLATE 3-4

LITHOFACIES D: STROMATOLITE

A. Field photograph (bedding plane view) of closely-spaced
   hemisperoidal or LLH (terminology of Logan et al., 1964)
   stromatolites. Ile du Havre W. Hammer is 30 cm.

B. Polished slab (cross-section view) of LLH stromatolites showing the
   internal cryptalgal laminations. Note the presence of small vertica
   fractures (top right) due to the formation of mud cracks on the
   stromatolite. Ile Du Havre W.

C. Field photograph (bedding plane view) of small coalescent
   stromatolite heads forming circular mounds. Ile a Bouleuax de Terre
   S.

D. Polished slab (cross-section view) of small branching columrar
   stromatolites found in stromatolite mounds. Grande Ile NE.

such as gastropods. The presence of stromatolites in the upper

lithofacies assemblage cannot be used alone as an indicator of

hypersaline and/or intertidal conditions. Pratt (1982a) points out that

stromatolites, especially during the Early Paleozoic, were ubiquitous in

most marine environments. Substrate competition from various metazoans,

together with reduced rates of sedimentation, were more likely

responsible for such environmental distributions.

Lithofacies E : Burrowed dolomicrite

Description: The rocks of this lithofacies are characterized by

moderate to intense burrowing which is outlined by contrasts in colour

and microfabric between the burrow-fills and the adjacent matrix (plate

3-5; A). The darker brown coloured Palaeophycus-like burrows are

commonly unbranched, display indistinct margins, and are evenly spaced

both horizontally and vertically. In thin-section (plate 3-5; B), the

burrow-fills and their adjacent matrix are usually composed of a mosaic

of xenotopic dolomicrites; however, matrix dolomicrites have a greater

intercrystalline porosity which is infilled by ferroan dolomite and/or

blocky calcite cements. The burrowed dolomicrites make up the basal part

of some upper assemblage cycles (fig. 3-1). They occur in units ranging

from 0.4 to 3.0 m in thickness. The fauna is restricted to gastropods

but brachiopods and trilobites are sometimes found near the base of the

unit (plate 3-5; C).

Interpretation: This lithofacies represents dolomitized lime muds

deposited in quiet shallow subtidal environments which formed a belt

seaward of the tidal flats. The relatively limited fauna is highly

suggestive of a semi-restricted or lagoonal setting. In addition, the

PLATE 3-5

LITHOFACIES E: BURROWED DOLOMICRITE

A. Polished slab (cross-section view) of lithofacies E showing a well-developed network of unbranched burrows (dark area). Burrows are evenly spaced but display indistinct margins. Ile du Havre NW.

B. Thin-section photomicrograph (plane polarized light) of dark-coloured burrows and adjacent matrix. Note that dolomite crystals of the matrix are slightly coarser and more porous (intercrystalline pores) than in burrows. Scale bar is 1.0 mm

C. Polished slab (vertical view) of lithofacies E with abundant gastropods from the base of the unit. Note the vuggy porosity. Grande Ile N.

diagnostic features commonly associated with intertidal- supratidal
environments (mud cracks, laminations, fenestrae. algal structures) are
missing. These muddy sediments were homogenized by the bioturbation.
Similar burrowed muddy deposits are found seaward of modern tidal flats
in Western Andros Islands, Bahamas (Hardie and Garret, 1977) and in the
Central Persian Gulf (Purser and Evans, 1973).

Lithofacies F: Ooid dolostone

Description: This lithofacies consists of dolomitized ooid
grainstones forming massive to ripple cross-laminated units (plate 3-6;
A). The ooids are well-sorted and range from 0.4mm to 0.6 mm in diameter
(plate 3-6; B). They can make up to 50% of the rock volume. Rounded
pebble-sized intraclasts of dolomicrite are usually present near the
basal part of the ooid units. Soft sediment deformations locally form a
complex sedimentary boudinage. In thin-section (plate 3-6; C), ooids are
composed of a dense mosaic of medium crystalline dolomite crystals that
range from 30 to 100 μm in size. Fabric preservation of the ooid
microstructures varies from well-preserved radial cortical layers to
faint cortex and nucleus outlines in pervasively dolomitized ooids.
Ooids in rare chert nodules exhibit well-preserved cortical layers with
both radial and concentric microstructures. Intergranular pores are
partially filled by more or less ferroan dolomite and/or blocky calcite
cements. The present intergranular and oomoldic porosities may locally
reach 10% of the total volume. In the study area, the ooid units are
used as key markers because they can be traced laterally up to 20 km
between the western Ile du Havre and Ile a Bouleaux de Terre. These
units, up to 1.5 m thick, occur in the basal part of some peritidal

PLATE 3-6

LITHOFACIES F: OOID DOLOSTONE

Photomicrographs - Plane polarized light

A. Field photograph (cross-section view) of an ooid dolostone unit with small-scale cross-bedding. Ile du Havre W.

B. Unpolished slab (vertical view) of lithofacies F showing well-sorted ooids averaging 0.5 mm in diameter. Interparticle porosity in this sample may reach 20%. Microscopic detail in (C). Scale in cm. Ile Niapiskau NE.

C. Thin-section photomicrograph of ooid dolostone showing well-sorted ooids. Detail in (D). Scale bar is 1.0 mm.

D. Thin-section photomicrograph of ooids with still recognizable cortex and nucleus (dark center). Scale bar is 1.0 mm.
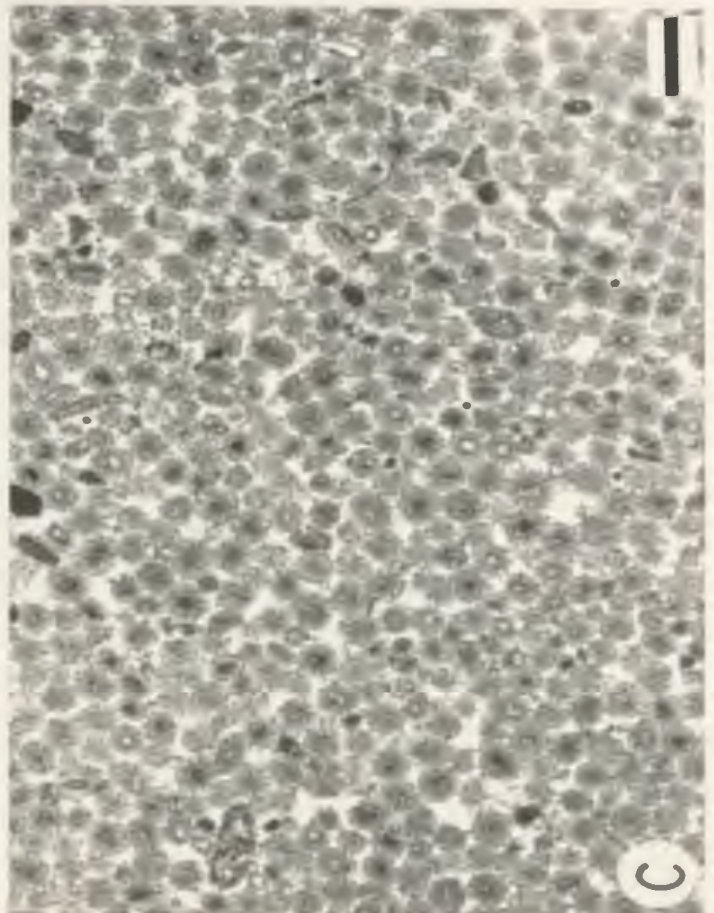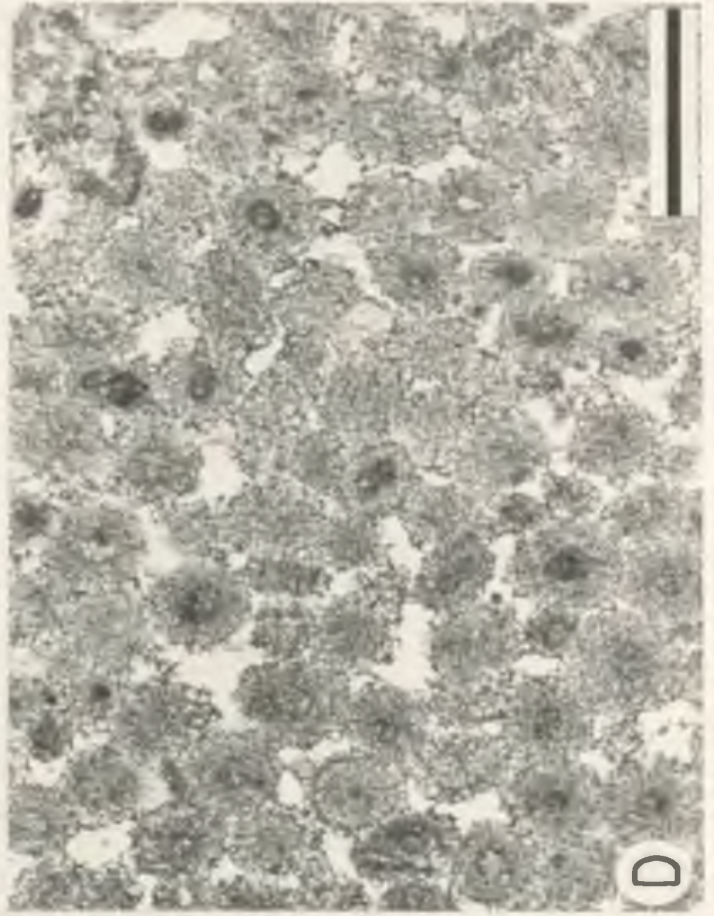
cycles in the upper lithofacies assemblage (fig. 3-1).

Interpretation: The dolomitized ooid grainstones are interpreted as
sediments deposited in shallow environments under moderate to relatively
high energy conditions. Ooids were kept in constant motion as indicated
by cross-laminations that were generated by migrating ripples over sand
flat deposits. Their vertical association with intertidal and supratidal
sediments argue in favor of a nearshore setting adjacent to a tidal flat
similar to the ooid sand bars in the Persian Gulf (Loreau and Purser,
1973) or in Shark Bay, Western Australia (Logan, 1974) rather than a
bank margin setting such as the Bahamian ooid sand shoals (Hine et al.,
1981; Halley et al., 1983). Scattered ooid occurrences in intertidal
deposits (lithofacies C and D) also support the inferred environment.
These latter ooids were probably transported on the adjacent tidal flats
during episodic storms.

Lithofacies G: Burrow-mottled dolostone

Description: Most of this lithofacies is characterized by a
burrow-mottled texture which displays colour and microfabric contrasts
between the burrows and the adjacent matrix. Unlike burrowed dolomicrite
(lithofacies E), this lithofacies is characterized by a diverse fauna,
more compacted burrows, and coarser-crystalline dolomite crystals. The
burrows define an irregular to dendritic network of infaunal trace
fossils in which Palaeophycus and Chondrites can sometimes be identified
(plate 3-7; A, B and C). In general, the burrows are dark brown in
colour and stand out in relief. The more recessively weathering matrix
is lighter brown coloured. The fauna is relatively diverse and includes
gastropods, cephalopods, trilobites, lithistid sponges and other

- 55 -

PLATE 3-7

LITHOFACIES G: BURROW-MOTTLED DOLOSTONE

A. Field photograph of the dendritic network of infaunal trace fossils of lithofacies G standing out in relief on the bedding plane. Ile a la Chasse E. Lens cap is 50 mm in diameter.

B. Close-up of (B) showing the dendritic burrow network and the more recessively weathered matrix (bedding plane view). Ile a la Chasse E. Lens cap is 50 mm in diameter.

C. Polished slab (cross-section view) of burrow-mottled dolostone. Note that the burrows are slightly compacted and light in colour whereas the matrix is dark. Ile Sainte-Genevieve N.

D. Polished slab (cross-section view) of a "storm" layer forming a lenticular bed within lithofacies G. Note the presence of intraclasts at the bottom and laminations at the top. Ile Sainte-Genevieve N.
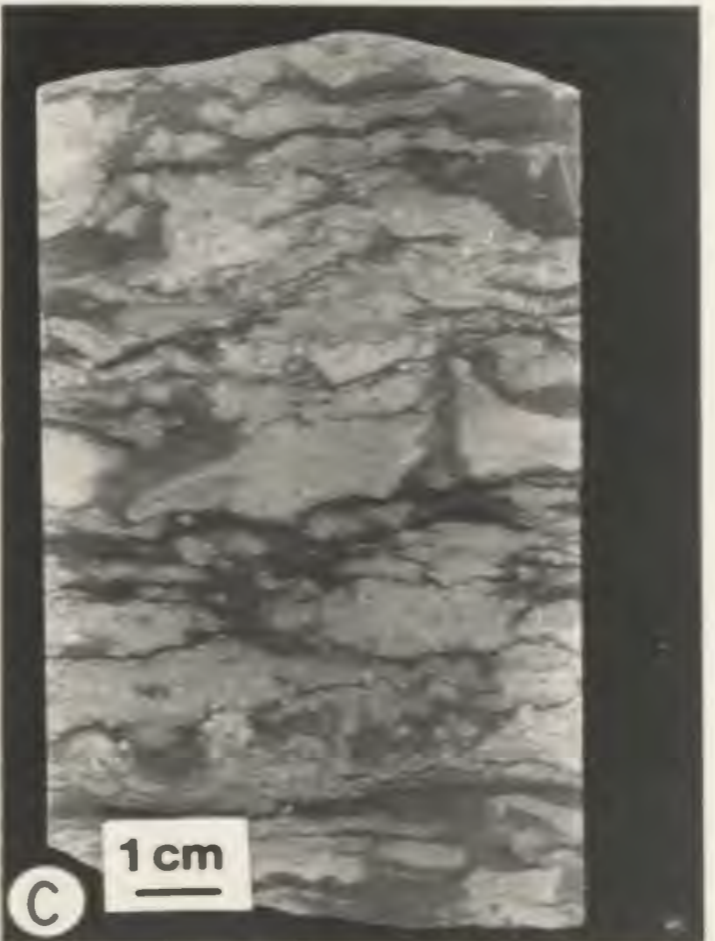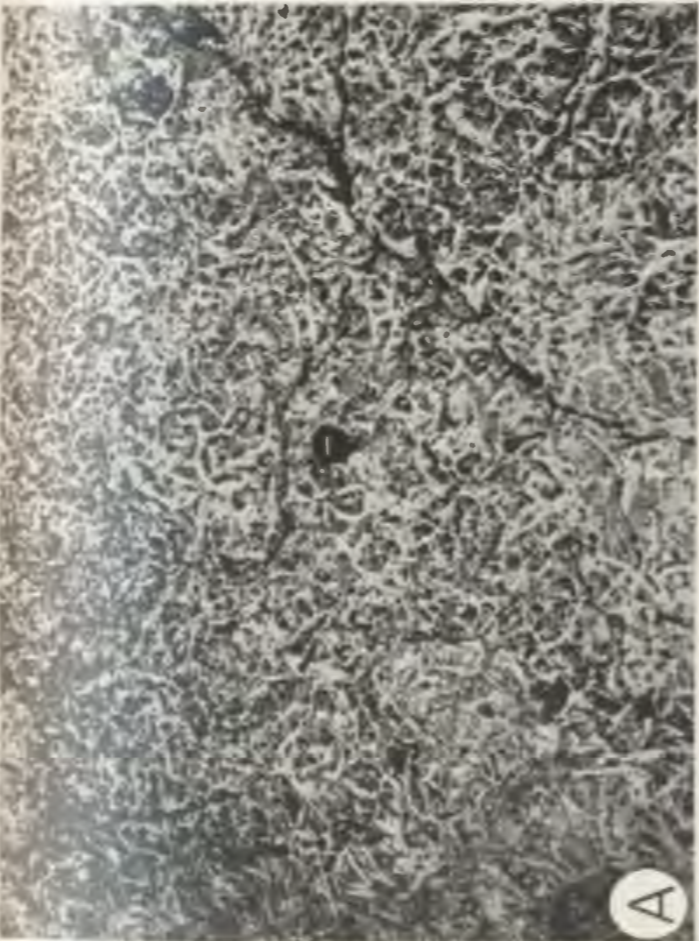
unidentifiable invertebrates; their microscopic fabrics, however, are often obliterated by dolomitization. Graptolites are locally present. In thin-section (plate 3-8; A), the dolostones consist of an aggregation of "sucrosic" dolomite with individual crystals ranging from 50 to 200 μm in size. The burrows (plate 3-8; B) are composed of a dense mosaic of subhedral dolomite crystals (idiotopic-S texture of Gregg and Sibley, 1984) while the matrix (plate 3-8; C) consists of a porous mosaic of euhedral dolomite crystals with intercrystalline areas partially filled with ferroan dolomite and/or blocky spar cement (idiotopic-E texture of Gregg and Sibley, 1984).

This lithofacies is commonly punctuated by several lenticular beds (3 to 20 cm thick). Beds are marked by irregular scoured bases and consist of a basal intraclast-rich layer and an upper laminated layer (plate 3-7; D). The bed tops are slightly burrowed and grade up into the burrow- mottled dolostones. Burrow-mottled dolostones occur as a thin- to medium-bedded unit (25-30 m, thick) in the lower part of the middle lithofacies assemblage and as a massive, thick-bedded unit (5-6 m, thick) at the top of the upper lithofacies assemblage.

Interpretation: The burrow-mottled dolostones are interpreted as dolomitized wackestones and packstones deposited in open marine subtidal environments below the normal fairweather wave base. The presence of a diverse fauna, absence of sedimentary structures indicative of wave or current activity, and intense bioturbation all support the inferred environment. These muddy sediments, however, are periodically affected by storms lowering wave base and reworking sediments on the sea floor. The fining-upward nature of these deposits with a basal scour are similar to other storm-generated sequences observed in the rock record

PLATE 3-8

LITHOFACIES G: BURROW-MOTTLED DOLOSTONE

Photomicrographs - plane polarized light

A. Thin-section photomicrograph of burrow-mottled dolostone showing the coarsely-crystalline nature of dolomite crystals. Note the burrow (b) and matrix (m). Detail in (B and C). Scale bar is 1.0 mm.

B. Thin-section photomicrograph of the burrow shown in (A). Note the dense mosaic of euhedral dolomite crystals which show darker inclusion-rich cores. Scale bar is 1.0 mm.

C. Thin-section photomicrograph of the matrix shown in (A). Note the mosaic of euhedral dolomite crystals (inclusion-rich cores) with intercrystalline pores.
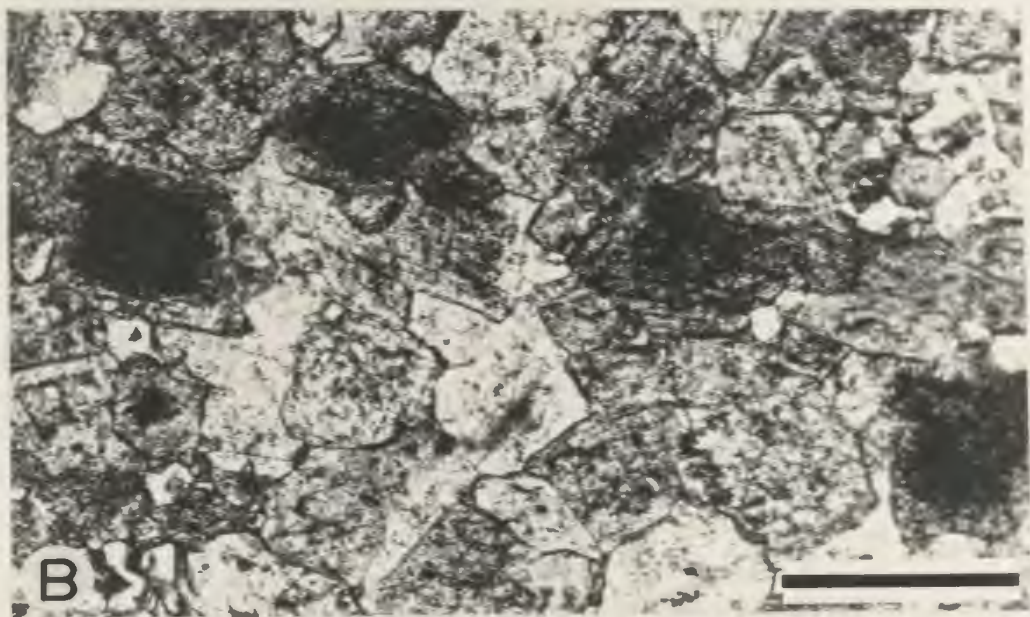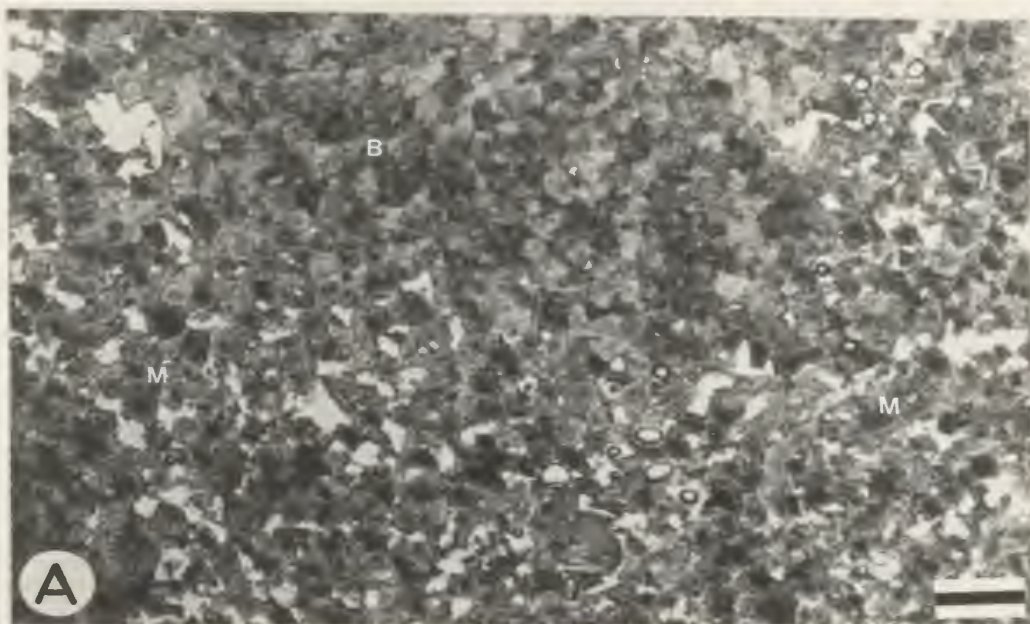
(Jones and Dixon, 1976; Kreisa, 1981).The modern open shelf environments
are generally characterized by a diverse biota and predominance of muddy
sedimentary textures (Enos and Perkins, 1977; Wilson and Jordan, 1983).

Lithofacies H: Thrombolite mounds

Description: This lithofacies consists of stratigraphically
superimposed thrombolite mounds and associated flanking beds (plate 3-9;
A) forming the upper part of the middle lithofacies assemblage (fig.
3-1). The term "thrombolite" is used here to define cryptalgal
structures related to stromatolites but lacking laminations and
characterized by a macroscopic clotted fabric (Aitken, 1967). Pratt and
James (1982) point out that thrombolites essentially refer to the
cryptalgal structures which form the mound framework. The mounds are
circular in plan and may reach up to 4.0 m in height and 50.0 m in
diameter but most are smaller. Each mound is composed of coalescent
metre-sized thrombolite heads which are characterized by a macroscopic,
clotted appearance exhibiting a cerebroid pattern in plan (plate 3-9; B)
and a digitate branching pattern in cross-section (plate 3-9; C). The
fauna is poorly preserved in the sucrosic dolomites but gastropods,
cephalopods, sponges, trilobites, and brachiopods are commonly
identified in both mounds and flanking beds. Lithistid sponges are
sometimes found in growth position within the mounds. Locally, isolated
thrombolite heads are surrounded by burrow-mottled dolostones
(lithofacies G) but do not aggregate to form mounds (plate 3-9; D).

The thrombolite microfabrics are obliterated and replaced by
subhedral to euhedral sucrosic dolomites with crystal size ranging from
100 to 300 µm. The thrombolites consist of a dense mosaic of subhedral

PLATE 3-9

LITHOFACIES H: THROMBOLITE MOUNDS

A. Field photograph (plan view) of a thrombolite mound. Note the sharp contact between the mound (t) and the lighter coloured flanking beds (f). Ile a la Chasse NW. Hammer is 30 cm.

B. Field photograph (bedding plane view) of thrombolite mound (center and bottom) and adjacent flanking beds (top). Mound is composed of coalescent, metre-sized thrombolites heads (h) exhibiting a macroscopic, clotted appearance characterized by a cerebroid pattern. Ile a la Chasse NW. Hammer is 30 cm.

C. Polished slab (cross-section view) of a thrombolite head exhibiting a macroscopic clotted appearance characterized by a branching digitate pattern. Ile a la Chasse NW.

D. Field photograph (cross-section view) of an isolated thrombolite head (h) and flanking burrow-mottled dolostone (b). Baie Puffin E. Hammer is 30 cm.

dolomite whereas the interframe areas are composed of a loosely-packed mosaic of coarser-grained euhedral dolomites (up to 500 μm) with intercrystalline pores partially filled with ferroan dolomite and/or blocky spar cement. The frame and interframe areas respectively correspond to idiotopic-S and idiotopic-E dolomite textures of Gregg and Sibley's classification (1984).

The thrombolite mounds are surrounded and underlain by well-bedded intraclast dolostones (plates 3-9; A & 3-10; A). These dolostones are characterized by rounded intraclasts ranging from 1 to 10 cm in size, ripple laminations, and rare trough cross-beds. Coarsely crystalline dolomites (up to 500 μm) with idiotopic-S texture (Gregg and Sibley, 1984) are usually observed in petrographic examination. The intraclasts are generally seen as faint patches. The intraclast dolostones laterally become more burrowed and grade laterally into thick-bedded, burrow-mottled dolostones (lithofacies G).

Interpretation: In this lithofacies, individual thrombolite mounds represent small cryptalgal-dominated mounds which aggregate together to form extensive on-shelf complexes as indicated by their lateral stratigraphic continuity in the study area. In addition, lithistid sponges are locally present in the thrombolite mounds but their role as potential framebuilders remains unknown. Most of the mounds are surrounded by bioclastic haloes or channels indicating subtidal conditions above the normal wave base. The common occurrence of these mounds clearly indicates that they were able to resist and baffle offshore wave energy. Their synoptic relief above the sea floor, however, was less than a metre as indicated by the bedding attitude of the flanking beds. Other Lower Ordovician thrombolite mounds have been

PLATE 3-10

LITHOFACIES H: THROMBOLITE MOUNDS
DOLOMITE CRYSTALS - POST-ROMAINE PALEOKARST

A. Thin-section photomicrograph (plane polarized light) from a chert nodule in dolostone flanking thrombolite mounds and showing abundant intraclasts. Scale bar is 1.0 mm.

B. Thin-section photomicrograph under cross-polarized light of sucrosic dolomite crystals truncated by the post-Romaine paleokarst unconformity (top) on Ile Innu. Scale bar is 1.0 mm.

C. Thin-section photomicrograph under cross-polarized light of a Trypanites boring truncating finely-crytalline dolomite crystals at the top of the Romaine Formation. Note the infill by siliciclastic material and some lithoclasts of dolomicrite. Ile Saint-Charles NW. Scale bar is 1.0 mm.
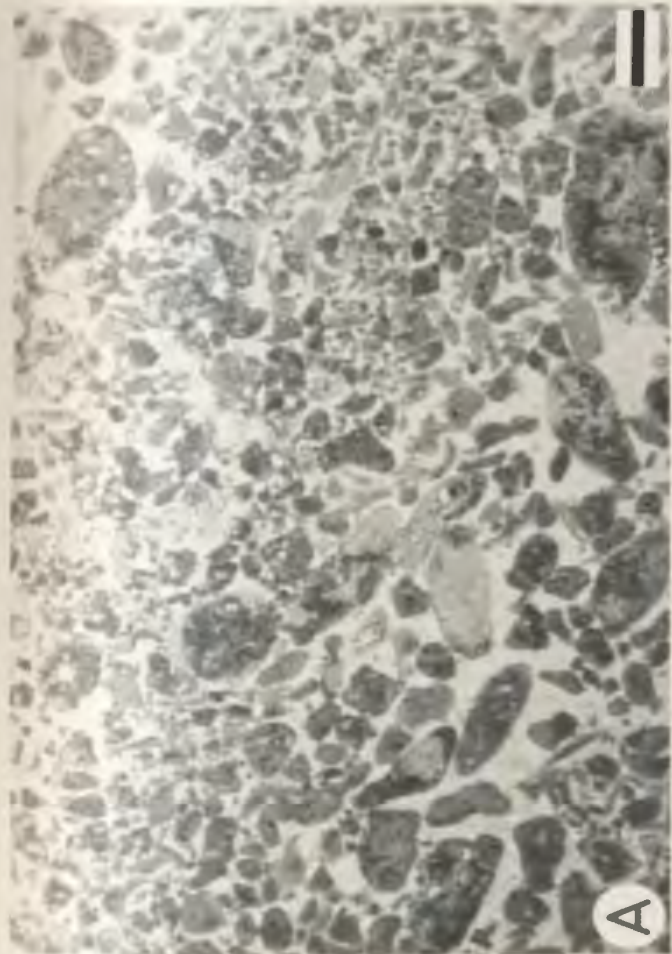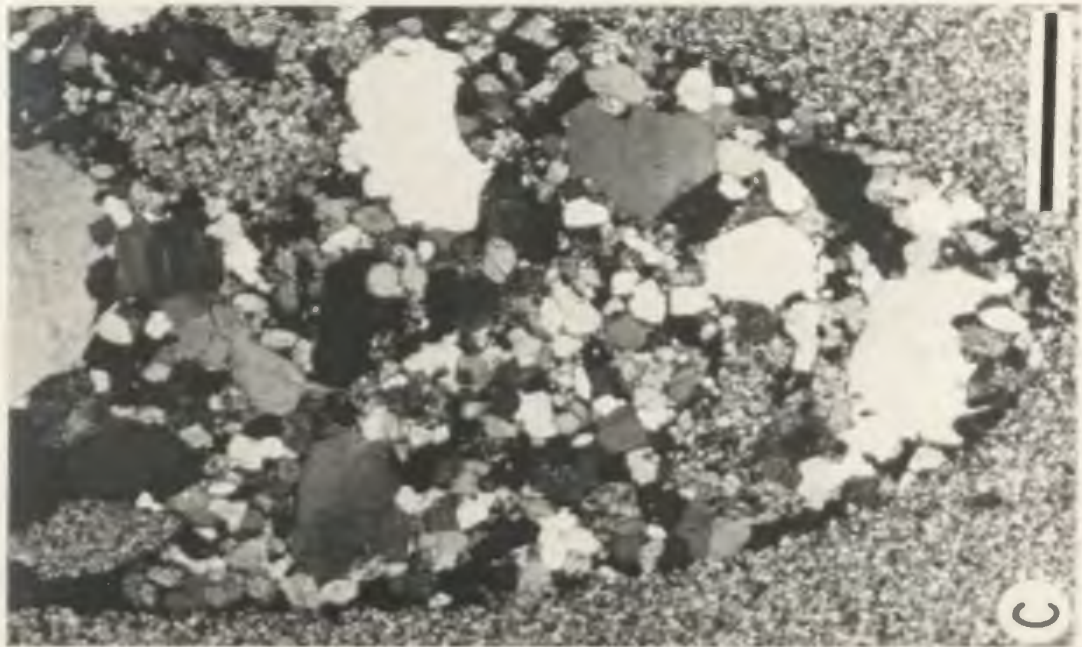
reported from the southwestern United States (Church, 1974; Toomey and Nitecki, 1979) and western Newfoundland (Pratt and James, 1982). They differ only from the Romaine mounds in terms of their associated fauna (sponges, calcified algae, corals, problematic metazoans) which played major constructional roles in several of these mounds. On the other hand, their preservation is such that they are usually unrecognizable and may explain the apparent absence of associated fauna in the Romaine mounds.

LITHOFACIES DISTRIBUTION

The Romaine lithofacies are grouped into three vertical, genetically-related assemblages (figs 3-1 and 3-2): 1) a lower assemblage of trangressive siliciclastics (lithofacies A), 2) a middle assemblage of subtidal carbonates (lithofacies G and H), and 3) an upper assemblage of cyclic peritidal carbonates (lithofacies B, C, D, E, and F). The lower and middle assemblages correspond to the Sainte-Genevieve Member while the upper assemblage represents the Grande Ile Member. The Romaine Formation is capped by a paleokarst unconformity.

The lower assemblage is only observed at Pointe du Sauvage in the Eastern Mingan Islands. The assemblage consists of an arkosic sandstone unit (lithofacies A) which directly overlies Precambrian basement. The sandstone unit reaches 3.0 m in thickness. An irregular basement topography probably played a significant role in the lateral distribution of the lower assemblage but this is difficult to evaluate on the basis of such limited exposure.

The middle assemblage is well-exposed in the Eastern Mingan Islands and ranges from 40 to 45 m in thickness. The lower 25-30 m is composed mainly of thin to medium-bedded burrow-mottled dolostones (lithofacies

Figure 3.2- Schematic stratigraphic cross-section showing the
distribution of the lithofacies assemblages in the Romaine
Formation. Note that the formation is capped by a paleokarst
unconformity. Numbers correspond to measured sections in figure 1-2
and illustrate the excellent stratigraphic control on the
distribution of these lithofacies assemblages.
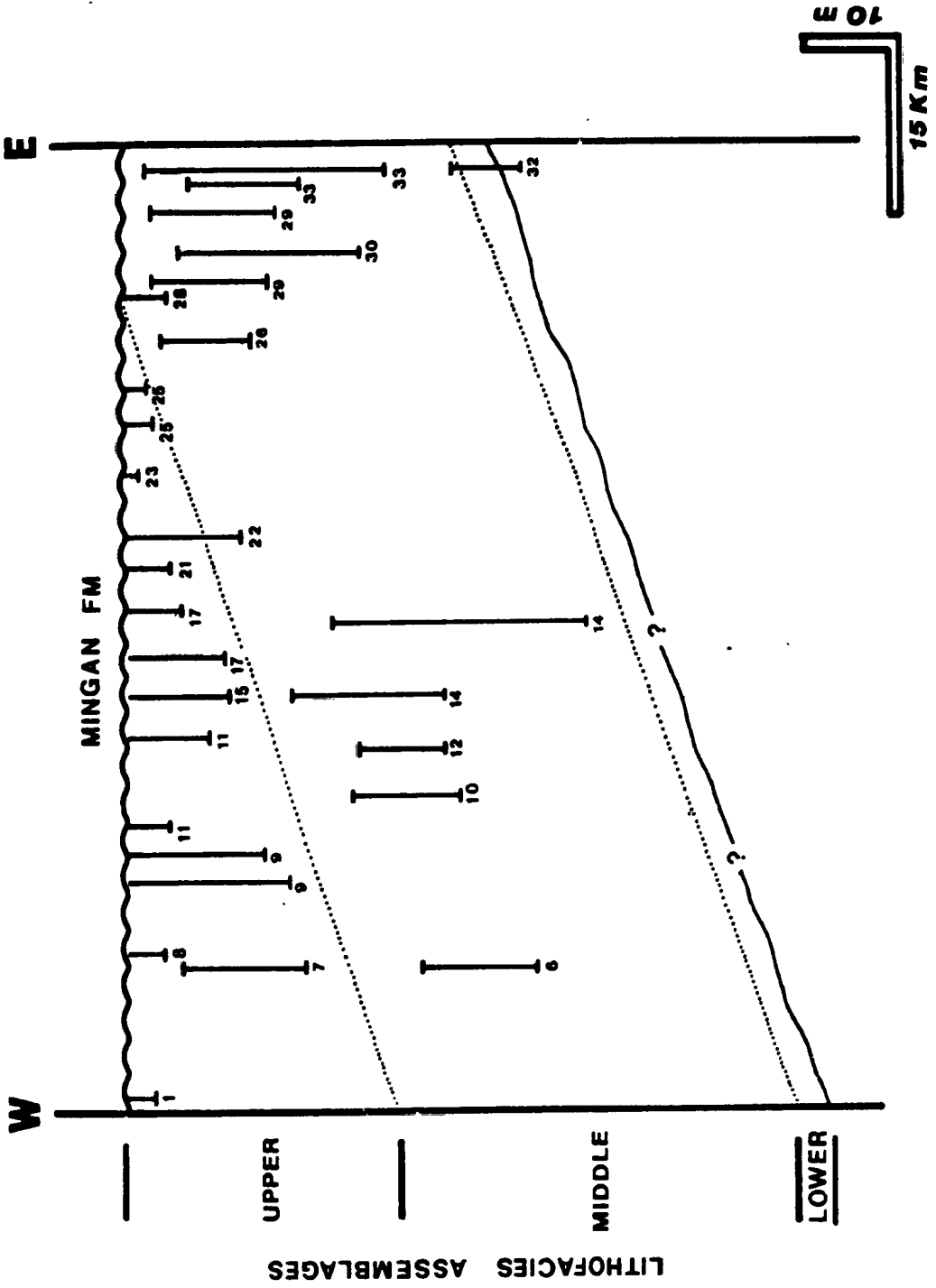
G). The thrombolite mounds and associated lithologies (lithofacies H) form most of the upper part of this assemblage (15-20 m). The thrombolite mounds occur as isolated buildups and closely-spaced buildup complexes which form stratigraphically superimposed units (2.0 to 6.0 m thick).

The upper assemblage is approximately 30 metres thick and is characterized by a cyclic repetition of peritidal lithofacies. Two distinct styles of idealized cycles are recognized but only differ in their basal lithofacies (fig. 3-3). The basal lithofacies consists of either burrowed dolomicrites (lithofacies E) or ooid dolostones (lithofacies F). They grade up into stromatolite dolomicrites (lithofacies D) and ripple-laminated dolomicrites (lithofacies C). The cycles are commonly capped by dololaminites (lithofacies B). The cycles have sharp bases sometimes overlain by intraformational conglomerates. The lithofacies contacts, however, are gradual within each cycle. Most of the upper assemblage cycles range from 2.0 to 5.0 m in thickness. In the Western Mingan Islands where coastal exposure is excellent, these metre-scale cycles have been successfully traced over 20 km with only minor changes in their thickness or in their internal lithofacies organization.

The Romaine Formation is capped by a marked unconformity which has been widely recognized over platform carbonates at or near the Lower-Middle Ordovician contact in North America (Barnes et al., 1981; Ross et al., 1982), and as a result, most of the Whiterock time interval is missing in the study area (Nowlan, 1981). The paleokarst unconformity truncates older beds toward the east where the Mingan Formation directly overlies the middle lithofacies assemblage on Ile

Figure 3.3- Schematic description of idealized peritidal cycles in the upper lithofacies assemblage. Cycles are similar but the subtidal segment may have two possible alternatives, either a muddy, burrowed unit or a grainy, oolitic unit. See figure 1.3 for symbols.

PERITIDAL CYCLES

MUDDY SUBTIDAL UNIT

GRAINY SUBTIDAL UNIT

2-5 m

-72-

Dololaminite

SUPRATIDAL

Ripple-laminated Dolomicrite

INTERTIDAL

Stromatolite

Bioturbated Dolomicrite

SUBTIDAL

Ooid Dolostone
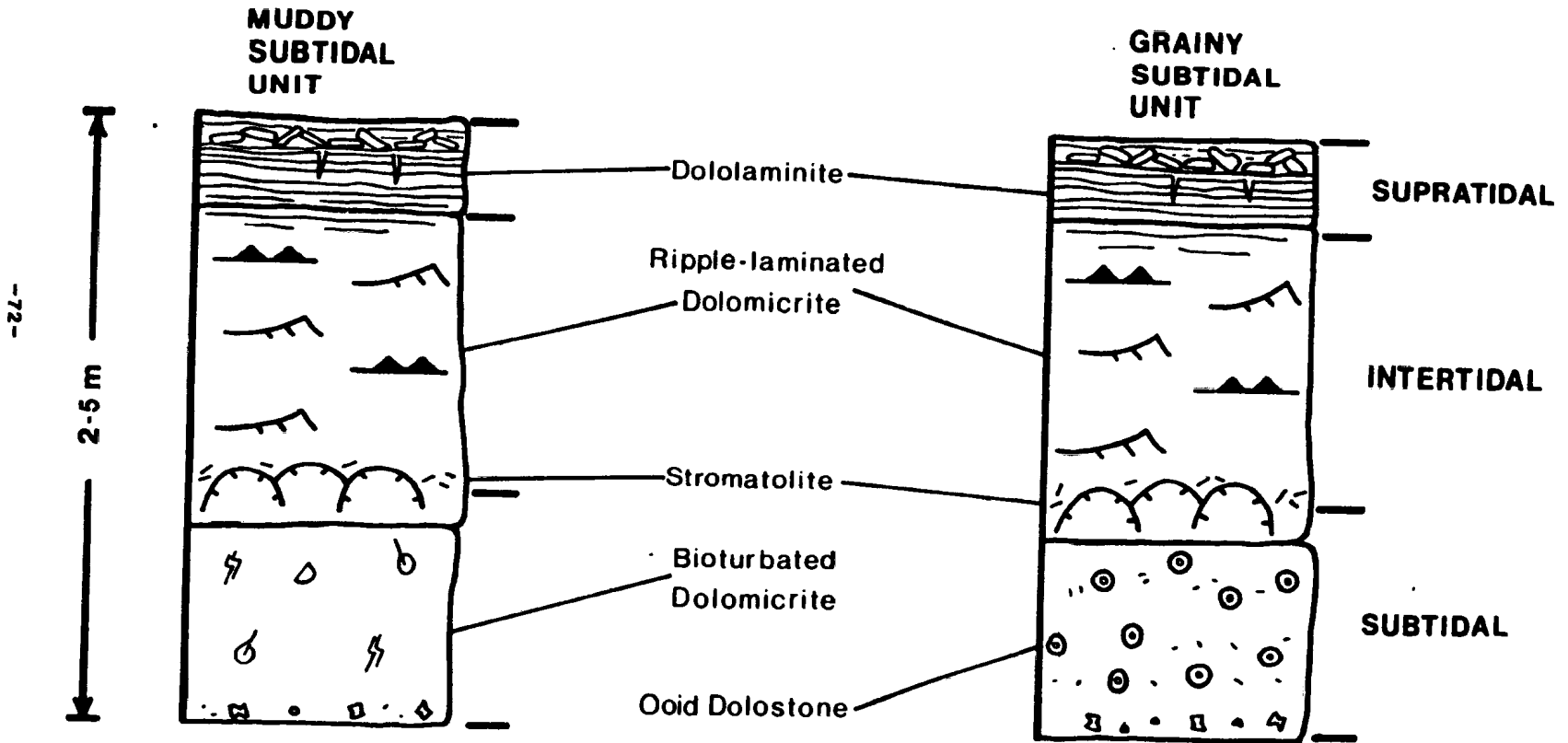
Innu. The absence of the upper assemblage in the eastern islands is regarded as an erosional feature and not a lateral facies change because: 1)younger conodont fauna are restricted to the westernmost islands (G. Nowlan, per. comm. 1983); 2) laterally persistent cycles of the upper assemblage are systematically truncated by the unconformity; 3) extensive superficial karst erosion. The Romaine unconformity is associated with the widespread Valhallan-Whiterock eustatic event interpreted by Fortey (1980, 1984) as a worldwide drop in sea level. In this area, however, Taconic orogenic events have overprinted its development. Like the Knox-Beekmantown unconformity in southern and central Appalachians (Shanmugam and Lash 1982), the Romaine unconformity is probably controlled by the crustal flexure, uplift and leaching of the carbonate shelf sequence in response to overthrust loading on the ancient continental margin or to downwarping of the shelf margin as it approached the subduction zone (Jacobi 1981, Quinlan and Beaumont, 1984). Detailed descriptions and interpretations are beyond the scope of this chapter and are further discussed in chapter 6.

DEPOSITIONAL MODEL

The Romaine Formation records a complete transgressive-regressive cycle which is largely represented by an asymmetrical, shallowing-upward sequence, the transgressive phase being limited to a thin, basal unit of sandstones. Walter's rule of succession of facies has been successfully used by most workers for environmental interpretation of stratigraphic units lacking major depositional breaks. The rule basically states that "only those facies and facies-areas can be superimposed, primarily, that can be observed beside each other at the present time" (from Blatt et

al, 1980, p. 620). In application of Walter's rule, the vertical
succession of Romaine lithofacies assemblages displays an overall
shallowing-upward trend that can be translated into a paleoenvironmental
profile. Four discrete depositional environments are recognized along an
idealized onshore-offshore profile (fig. 3-4): tidal flat, subtidal
lagoon, bioherm complex, and deep shelf. Tidal flat and lagoonal
sediments, deposited contemporaneously with other subtidal carbonates,
may have been present in more western localities but their presence can
be only inferred because these sections since have been removed by
erosion. The lower lithofacies assemblage is not included in the
paleoenvironmental profile because it represents sediments deposited
during the initial marine trangression but these are briefly discussed
here.

Trangressive sediments

The trangressive sediments represent nearshore sand bars actively
migrating toward the craton in response to a marine transgression which
is thought to be largely eustatic in origin during early Late Canadian
(early-mid Arenig) time (Fortey, 1984; Barnes, 1984). The sediments
contrast with other, but older and thicker, siliciclastics found at the
base of the Sauk cratonic sequence (Sloss, 1963) which exhibit a more
complex mosaic of fluvial, marginal and nearshore environments (Driese
et al., 1981; Hiscott et al., 1984). According to Hiscott et al. (1984),
most of these basal Cambrian sandstone units suggest that a thick
blanket of alluvium derived from the erosion of the cratonic interior
rimmed the craton, or at least its margin, prior to the Sauk
transgression. If present in the study area, the alluvium or other
sediments such as *in situ* residual soils overlying the Precambrian

Figure 3.4— Schematic paleoenvironmental profile based on the vertical succession of lithofacies in the Romaine Formation. All environments in this profile, however, were contemporaneous only during the Sainte-Genevieve-Catoche time (see later regional paleogeography). At that time, peritidal sedimentation was probably restricted to areas north of the Mingan Islands. It is only later that peritidal sediments eventually prograded over the study area. By that time (i.e. Grande Ile-Aguathuna time), peritidal sedimentation extended across the platform. Not illustrated on this figure is strandline ooid sands that formed along more exposed portions of the coastline.

Paleoenvironmental Profile

TIDAL
FLAT

LAGOON

BIOHERM
COMPLEX

DEEPER
SHELF

SL

NORMAL
WAVE BASE

STUDY AREA

-76-
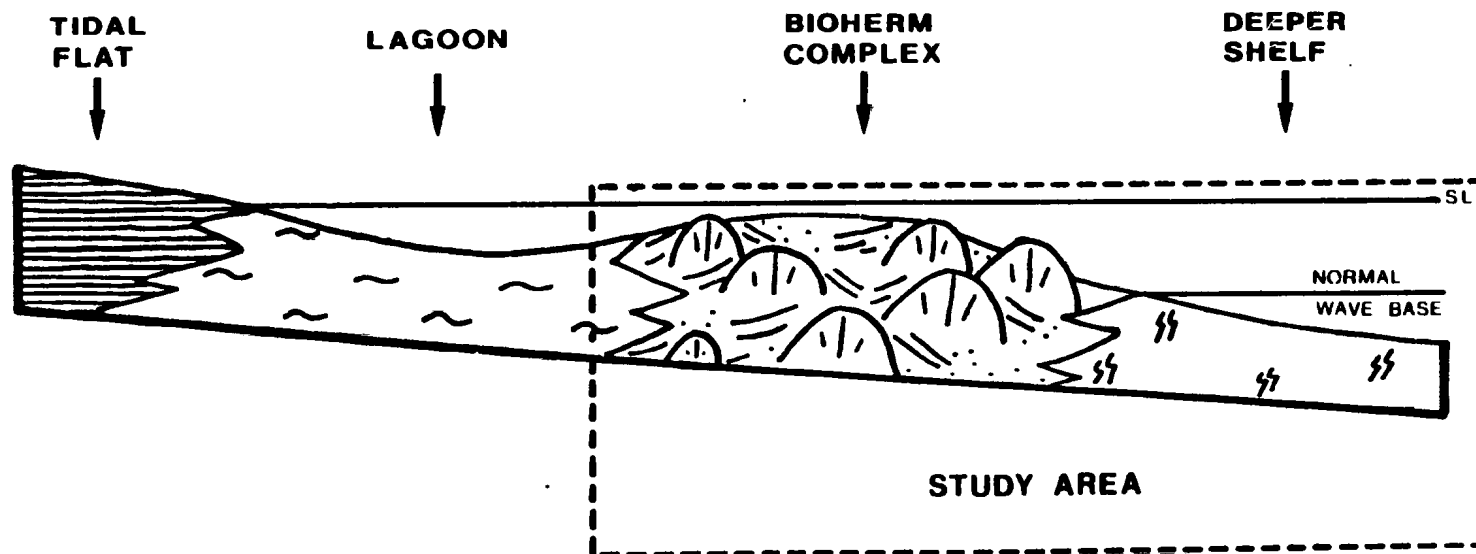
basement were reworked by the marine transgression leaving no
depositional record. In marginal environments such as barrier islands,
back-barrier sediments are commonly destroyed by exposure to erosion and
wave reworking on the shoreface during continuous sea level rise
(Rampino and Sanders,1980). The thin trangressive unit may also reflect
low-lying areas of the cratonic interior where rivers with gentle
gradients could barely deliver terrigenous material. As a result of the
trangression, the terrigenous sediments were probably trapped in a
nearshore position, thus limiting the amount of sediment available for
the open marine setting.

Tidal flats

The tidal flats are represented by different subenvironments which
are characterized by diagnostic sedimentary features of the
intertidal-supratidal regime. The supratidal zone consists of
desiccation-cracked mud flat deposits (lithofacies B) in which planar
laminations are commonly interpreted to be the result of alternating
algal mat growth and deposition of marine sediments transported by
storms or spring tides. The intertidal sediments are composed of
carbonate sands and suspended muds (lithofacies C) and exhibit a wide
spectrum of sedimentary structures in response to wave and current
activity. These structures are more commonly observed in siliciclastic
tidal flats such as the modern North Sea tidal flats in Germany
(Reineck, 1975) but could reflect limited burrowing and/or browsing
activity in the intertidal zone during the Early Paleozoic (Hofmann,
1969; Garret, 1970). In addition, laterally-linked hemispheroidal
stromatolites (lithofacies D) colonized more stable areas of the

intertidal flat while columnar stromatolitic mounds proliferated in
tidal ponds or in the adjacent subtidal zone in response to higher
sedimentation rates (Hoffman, 1976). The tidal flat sediments were
dolomitized soon after their deposition as indicated by the preservation
fabric type of dolomite commonly observed in intertidal and supratidal
areas of modern carbonate tidal flats (Morrow, 1982). Evaporite minerals
were also formed in the tidal flat sediments. This suggests a
depositional setting similar to the modern hypersaline tidal flats or
sabkhas in the Persian Gulf (Purser, 1973; Shinn, 1983).

Subtidal lagoons

The lagoonal deposits consist mainly of muddy sediments (lithofacies
E) forming a belt seaward of ne tidal flats and acting as sediment
source for them. These fine-grained sediments (peloidal muds) were
extensively reworked by bioturbation. In the lagoons, poor water
circulation resulted in "restricted" environmental conditions as
indicated by the low-diversity biota including mainly gastropods. Ooid
sands (lithofacies E) were also formed in more agitated areas of the
lagoon, close to the tidal flats. Coastal ooid occurrences such as in
Shark Bay, Western Australia (Davies, 1970) or in the Persian Gulf
(Loreau and Purser, 1973) are envisaged as modern analogs.

The lagoonal sediments are vertically associated with tidal flat
sediments, both forming the metre-scale peritidal cycles in the upper
lithofacies assemblage. These subtidal cycles are interpreted as
shallowing-upward cycles which most workers attribute to repeated
submergence and lateral migration of tidal facies over subtidal facies
(Wilson, 1975; James, 1984a). No consensus has been reached regarding

mechanisms that could generate such small-scale cyclicity. A two-end
member model with either autocyclic or allocyclic controls is currently
used to explain their formation (summary in Wilkinson, 1982). The two
different styles of peritidal cycles depend on the presence of coastal
ooid sands when tidal flat facies prograde over subtidal facies.

Bioherm complexes

Cryptalgal-dominated (thrombolites) patch reefs (lithofacies G)
represent wave-agitated reef mounds developed on the open shelf. In
general, these patch reefs are closely-spaced, forming complexes which
could baffle offshore waves and currents and form an effective barrier
for the shelf lagoons. The patch reefs are commonly surrounded by
well-winnowed sands composed of reef-derived clasts and skeletal debris.
In spite of their great lateral extent, thrombolite bioherm complexes
are not indicative of a platform margin setting. An on-shelf setting was
probably privileged for reef development in the early Ordovician time
when large skeletal metazoans were absent. James (1981) also points out
that the thrombolitic algal mounds mainly grew on the interior part of
early Paleozoic carbonate platforms while platform margin buildups are
dominated by calcified algae (Girvanella, Epiphyton, Renalcis)

Deep shelf

The deeper shelf deposits (lithofacies H) are located seaward of the
patch reef belt and consist of fine-grained sediments deposited below
the normal wave base but disturbed only episodically by storm waves. The
normal wave base varies in modern shelfs, but normally lies in the 5-15
m range (Walker, 1984). The fauna with several stenohaline taxa

indicates open marine conditions. In addition, the occurrence of graptolites suggests minor topographic or depositional barrier on the shelf and good water circulation with the open ocean. Similar deposits are localized in deeper areas (few tens of metre) of modern carbonate shelfs such as the Hawk Channel in Florida (Enos, 1977) or the Great Pearl Bank, in the Persian Gulf (Wagner and Togt, 1973).

MECHANISMS OF DOLOMITIZATION

It is now well known that dolomites form in many environments and under a wide variety of conditions and, as a result, several dolomitization models have been proposed (Chilingar et al., 1979; Morrow, 1982; Land, 1985). On the basis of the stratigraphic and depositional framework which has been previously discussed, three aspects are important concerning the selection of dolomitization models for the Romaine Formation: 1) textural variation (dolomicrites vs sucrosic dolomites); 2) stratigraphic distribution (cyclic peritidal vs subtidal lithofacies); and 3) pre-Chazyan age. Of particular importance to the timing of dolomitization is that sucrosic dolomite crystals are truncated by Trypanites borings at the top of the Romaine Formation (plate 3-10; C and D). More important is that these crystals are also truncated by the paleokarst unconformity capping the formation (plate 3-10; B). This indicates that dolomitization of the Romaine Formation occurred before the erosion was finished. In dolomicrites, observations are not conclusive due to the fine-grained texture of these dolomites. Nevertheless, dolomicrite clasts, found with patchy chert pebble conglomerates overlying the paleokarst unconformity (see chapter 6), provide evidence for their pre-Chazyan age. Furthermore, dolomitization

must have occurred in the shallow subsurface under the influence of near surface processes rather than burial ones.

Finely crystalline dolostones

The finely crystalline dolostones or dolomicrites are composed of xenotopic dolomite crystals ranging from 5 to 10 μm in size with a maximum of 30 μm. These dolomicrites occur only in peritidal lithofacies which exhibit typical shallowing-upward cycles (James, 1984a). They represent penecontemporaneous dolomitization of calcareous sediments in the upper intertidal to supratidal environments, very similar to the recent sabkhas of the Persian Gulf. An early diagenetic origin for the dolomicrites is suggested by the following: 1) preservation of microcrystalline textures; 2) sedimentary structures and fabrics indicative of peritidal sedimentation; 3) presence of cryptalgal laminae (dololaminites); 4) association with shallowing-upward cycles; and 5) probable former presence of evaporites.

Dolomite in recent sabkhas is pervasive in upper intertidal and supratidal environments and associated with carbonate mud, algal mats, and gypsum (Bush, 1973; De Groot, 1973). In addition, dolomitization of the underlying intertidal and subtidal sediments occurs to a depth of 2 to 3 m beneath the sabkha surface as dense Mg^2 bearing hypersaline floodwater brines sink downward and flow seaward by seepage. It is believed that extensive carbonate sediment wedges were dolomitized as tidal flats prograded during Lower Ordovician time. Dolomicrites in the Romaine Formation, however, differ from their modern peritidal counterparts with respect to their crystal size and nearly stoichiometric composition (based on microprobe analysis) when compared

- 81 -

to the smaller crystal size (1-5 μm) and calcium-rich composition in modern sabkhas. Similar differences in ancient peritidal sequences, together with low concentrations in both trace elements (Sr, Na) and heavy isotopes have been ascribed to neomorphism or stabilization of calcium-rich phase in the presence of fresh water (Churnet and Misra, 1981; Land, 1985). Shallow coastal freshwater aquifers which accompanied the seaward progradation of tidal flats are more likely responsible for this stabilization. Dolomicrites in the Romaine Formation may have formed in a similar manner but their chemical and isotopic composition remains to be tested.

Medium to coarsely grained dolostones

The medium to coarsely grained dolostones or sucrosic dolomites consist of subhedral to euhedral, iron-poor dolomite crystals ranging from 50 to 300 μm in size. They generally occur in subtidal sediments of the middle lithofacies assemblage and in a thin unit (5-6 m thick) at the top of the upper lithofacies assemblage. The sucrosic dolomites probably formed in a marine-fresh water mixing zone by early diagenetic replacement of limestones that were originally deposited in subtidal marine environments. This is suggested by: 1) absence of sedimentary structures and fabrics indicative of widespread penecontemporaneous dolomitization; 2) stratigraphic distribution of sucrosic dolomites; 3) depositional model; 4) shallow burial origin; 5) crystals with cloudy centers and clear rims which are thought to result from diagenetic pore fluids that evolved during dolomitization from a state of near calcite saturation to a state of calcite undersaturation due to progressive influence of mixed-water diagenesis (Sibley, 1980); and 6) comparison

- 82 -

with ancient examples of mixing zone dolomites (Dunhan and Olson, 1980; Churnet et al, 1982).

Salinity and Mg/Ca solution ratio are commonly regarded as two important parameters controlling dolomitization (Folk and Land, 1975). In the mixing zone model, chemistry clearly favors dolomitization which proceeds through slow solution of calcite and precipitation of dolomite (Badiozamani, 1973; Plummer, 1975). Deposition on a slowly subsiding shelf during the Romaine time allowed this mixing zone to be maintained over long periods. It is unclear if dolomitization was due to coastal aquifers associated with peritidal depositional environments which became exposed and subsequently migrated southward during regional regression or was due to a regionally extensive aquifer with a hydrostatic head located to the north in Precambrian terranes. The application of the mixing model to the sucrosic dolomites in the Romaine Formation requires the presence of an aquifer of regional extent recharged from the exterior because the availibility of freshwater may be low in an arid, or at least semi-arid, sabkha setting. Continental-derived waters are known to extend considerable distance offshore (up to 120 km) beneath the west coast of the modern Florida shelf (Hanshaw et al., 1971).

There is no evidence of dolomitization through burial processes. Coarsely crystalline, iron-rich dolomite, however, occurs as intercrystalline, vug, and fracture void-filling cements, alone or with ferroan calcite. These cements are ubiquitous throughout the Romaine Formation (also present in the Mingan Formation as the last stage cements) and commonly fill large fractures which often truncate other types of dolomite. They represent the last stage of cementation and more

likely formed during subsequent burial in a deeper subsurface setting, and therefore are not relevant to the present discussion.

The proposed mechanisms of dolomitization are not without problems, but at this stage they best explain: 1) petrographic differences between dolomites; 2) apparent paleogeographic control on dolomite distribution; and 3) early diagenetic origin in shallow subsurface. These mechanisms raise questions. Were the subtidal sediments dolomitized at the same time ? Were earlier dolomite phases formed and did they act as potential nucleation sites for subsequent dolomite phase ? If these earlier phases were present, are they recognizable or simply overprinted by pervasive sucrosic dolomites ? If the climatic conditions were arid or semi-arid, is it possible that groundwater brines rather than freshwater were mixed with seawater to produce dolomitization in the mixing zone; as suggested by Morrow (1978) ? These questions obviously need further investigations which should combine stratigraphic and petrographic observations with geochemical data (i.e. major elemental composition, degree of crystal disorder, cathodoluminescence, trace elements, and stable isotopes).

DISCUSSION

Origin of the Romaine Formation

The late Canadian to earliest Whiterockian Romaine Formation is characterized by a large-scale shallowing- upward sequence overlying a thin transgressive lag (i.e. lower lithofacies assemblage). This asymmetrical sequence consists of a lower unit dominated by subtidal carbonates and an upper unit with several metre-scale shallowing- upward sequences. Neritic sedimentary sequences are thought to result from fluctuations in the rate and direction of relative sea level changes

which are basically controlled by the interplay of eustatic sea level changes, tectonic changes, and sediment supply (Kendall and Schlager, 1981). These controls are now briefly discussed prior to a comparison of the Romaine sequence with some conceptual models (James, 1984a; Read et al., 1984) which may explain such large-scale asymmetrical units.

A major trangressive-regressive pulse has been suggested for the late Canadian-early Whiterockian time interval. This pulse is believed to have been eustatic in origin because major transgressive and regressive facies changes occurred at the same time in different areas around the margin of the North American craton (Barnes, 1984) as well as over other cratons (Fortey, 1984).

The rate of tectonic subsidence along a passive margin (Steckler and Watts, 1982; Perrodon, 1983), would probably be nearly constant for most, if not all, of the time interval concerned. As discussed earlier, the platform uplift and erosion in the early stages of the Taconic Orogeny post-dated deposition of the sequence in the study area.

Finally, carbonate accumulation based on Holocene environments is able to match or outpace any known relative rates of sea-level rise (Schlager, 1981; Kendall and Schlager,1981). Schlager (1981), however, points out that reduction of the benthic potential growth and/or rapid pulses of relative sea level rise may inhibit, or at least retard, sedimentation in carbonate platforms. In fact, the rock record displays several examples of carbonate platforms that could not keep pace with the rising sea level.

James (1984a, fig. 19) recently proposed a depositional model for large-scale shallowing-upward sequences developed under slow platform subsidence and an uniform rise and fall in eustatic sea level. The final

result is an asymmetrical sequence that is striking similar to the Romaine sequence with a lower half of subtidal sediments and an uppeᴸ half of thin shallowing-upward sequences. In general, the lower half is produced when the rapid rate of sea level rise and tectonic subsidence maintain subtidal conditions over most of the platform while the upper half is formed when the rate of sea level rise slows and eventually falls but on-going subsidence only permits the development of thin shallowing-upward sequences.

Most likely, the sediment supply also assisted the progressive "buildup" of the carbonate platform. Kendall and Schlager (1981) suggested that carbonate platforms display three responses to a relatively rapid sea level rise: 1) start-up phase, when carbonate production is retarded during early flooding; 2) catch-up phase, when carbonate production exceeds sea level rise and the platform builds to sea level; and 3) keep-up phase, when carbonate production matches or exceeds sea level rise. After a rapid sea level rise, the recovery of a carbonate platform could produce a sequence similar to the large-scale asymmetrical sequence predicted by James (1984a). Carbonate production contributed to the formation of the shallowing-upward Romaine sequence, however the dominant factor here is believed to have been an eustatic sea level cycle which similarly affected other contemporaneous cratonic sequences.

Read et al. (1984) also presented a model in which high order eustatic sea level fluctuations (i.e. Vail's 4th-6th order cycles) superimposed on constant sea level rise could generate large-scale asymmetrical sequences. In Read's model, the thin shallowing-upward sequences are only formed when the high order cycles in sea level have

low amplitudes allowing enough time for the tidal flats to prograde over subtidal areas. If the amplitude of sea level oscillations increases, the tidal flats are stranded and seaward displacement of the shoreline outpaced the progradation rate of the tidal flat, and as a result only stacked thin subtidal sequences are deposited. Each subtidal sequence is bounded by well-defined unconformities and are sometimes capped by biostromal units. According to this model, large-scale asymmetrical sequence such as the early Canadian Chepultepec Formation in Virginia (Bova, 1983) are caused by temporal changes in the amplitude of high order cycles in sea level. This model, however, is more unlikely for the Romaine sequence because its lower part consists of conformable, non-cyclic subtidal sediments rather than stacked thin subtidal sequences separated by unconformities. Based upon the work of Hine and Steinmetz (1984) on the Cay Sal Bank in the Bahamas, multiple high order cycles superimposed on the rising portion of a lower order cycle in sea level may retard, if not inhibit, the vertical platform growth. It may eventually result in progressive drowning of the platform below the euphotic zone.

Shallowing-upward depositional sequences are common throughout the geological record (Aitken, 1966, Wilson, 1975). Their recognition, if local tectonic movements are insignificant, is important because they may help to subdivide thick, ancient shelf sequences, and facilitate the correlation of synchronous and worldwide depositional sequences (for example see Ross and Ross, 1985 or Johnson et al, 1985).

Shallow subsurface dolomitization

As discussed earlier, sucrosic dolomites in the Romaine Formation

probably formed in the mixing zone between sea water and continental water. A more important finding of this study is that these dolomites developed under shallow subsurface conditions as indicated by dolomite crystals truncated by the paleokarst unconformity. A uniformitarian approach is inadequate to explain the formation of such early diagenetic dolomites because modern, shallow subsurface sites of dolomitization are rare.

Dolomitization processes under the influence of fresh groundwater are known to operate on a large scale in the deep confined Tertiary carbonate aquifer (100-2000 m) of Florida (Hanshaw et al., 1971). This, however, contrasts with the patchy dolomitization found in shallow subsurface, mixing zones of Holocene and late Pleistocene limestones where only few examples are known (Land, 1973; Margaritz et al, 1980). The rare occurrence and limited extent of these modern mixing zone dolomites are commonly cited as major problems to this model, especially when applied to ancient dolomite sequences. Land (1985) suggested that the variations in the position of the mixing zones throughout the Pleistocene have apparently not been conducive to extensive dolomitization due to repeated sea level changes. In fact, longer duration of sea level stands may be responsible for more widespread dolomitization in slightly older rocks during the Pliocene and early Pleistocene beneath the Caribbean platform and islands, (Sibley, 1980; Pierson, 1982).

A possible explanation for the pervasive dolomitization of subtidal limestones in the Romaine Formation is that permanent dolomitization "cells" formed under the influence of long-standing mixing zones.

Regional stratigraphy and paleogeography

As mentionned earlier,the Romaine sequence represents sediments deposited in epeiric seas that rimmed the North American continent during the Early Ordovician. This discussion, however, is restricted to Eastern Canada and more specifically, to the cratonic segment delimited by the St. Lawrence Promontory (see map of Williams, 1978) which geographically comprises western Newfoundland and the northern Gulf of St. Lawrence. The St. Lawrence Promontory is interpreted as an extensive continental landmass, several hundreds of kilometres wide, projected toward the ancient Iapatus Ocean and reflecting the irregular shape of a rifted continental margin (Thomas, 1977; 1983).

During the late Canadian-earliest Whiterockian time interval, the "St. Lawrence" platform was characterized by two distinct periods of sedimentation; an early subtidal phase followed by a peritidal phase (fig.3-5). The subtidal phase corresponds to the Sainte-Genevieve Member of the Romaine Formation and the Catoche Formation in western Newfoundland (Pratt, 1979, James and Stevens, 1982). The peritidal phase is correlated with the Grande Ile Member of the Romaine Formation and the Aguathuna Formation in western Newfoundland. Both depositional phases have been also observed in cores beneath Anticosti Island (Roliff, 1968; Desrochers, pers. obs.) where the Romaine Formation directly overlies the Precambrian basement.

Prior to the subtidal phase, the carbonate platform was limited to the outer part of the St. Lawrence Promontory in Western Newfoundland (Barnes, 1984, fig. 6). Following the early Canadian eustatic rise, quiet subtidal conditions disturbed only by storm events prevailed over most of the St. Lawrence Promontory. The inner part of the promontory

Figure 3.5– Correlation chart of the stratigraphic units under discussion and the conodont faunas of Sweet et al (1971). Autochthonous units are represented by shelf deposits of the Romaine Formation in Mingan Islands and the St. George Group in western Newfoundland whereas the Cow Head Group is allochthonous and represents deep water facies. In Mingan Islands, the autochthonous shelf deposits consist of pervasively dolomitized subtidal limestones of the Sainte-Genevieve Member and overlying, cyclic peritidal dolostones of the Grande Ile Member. Equivalent units in western Newfoundland are the subtidal limestones of the Catoche Formation and cyclic peritidal dolostones and limestones of the Aguathuna Formation respectively.

LOWER ORDOVICIAN		MIDDLE ORD.		
CANADIAN		WHITEROCK		
D	E	1	2	3
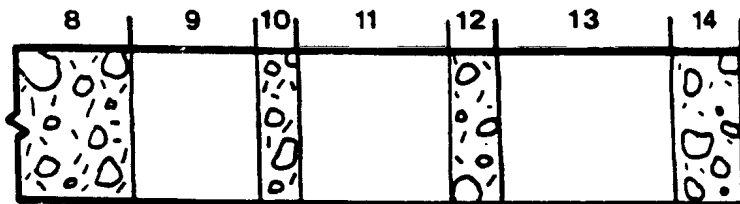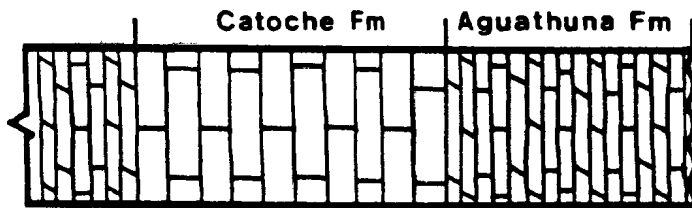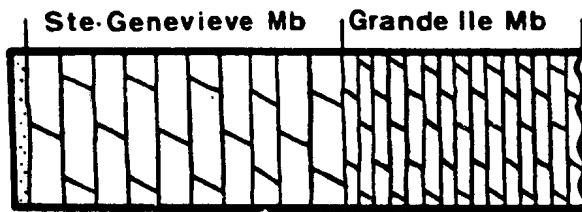
was rapidly flooded leaving a thin transgressive record over the Precambrian basement. Contemporaneous buildups or agitated shoals near the platform margin were probably absent as indicated by the starved sedimentation in slope and basin deposits (beds 9 and 11 in fig. 3.5) of the allochthonous Cow Head Group in western Newfoundland (James and Stevens, 1982). Absence of a significant topographic barrier allowed the deep incursion of extra-cratonic fauna onto the platform such as graptolites and oceanic trilobites (Fortey, 1984). The progressive shoaling of the platform near the wave base stimulate the growth of thrombolite patch reefs which formed widespread on-shelf complexes. Peritidal sedimentation was rare or absent and tidal flats must have been stranded and limited to areas north of the Mingan Islands.

During the second phase (latest Canadian-early Whiterockian time), the "St.-Lawrence" platform experienced widespread peritidal sedimentation. Two distinct styles of peritidal sedimentation occur in well-defined areas in the platform. The platform interior (i.e. Mingan Islands) is characterized by laterally persistant and remarkly uniform peritidal cycles which are interpreted as prograding coastal tidal flat wedges. In the platform exterior (i.e. western Newfoundland), the peritidal cycles are laterally-discontinuous and individual lithologies cannot be correlated between sections only a few kilometres apart (Pratt, 1979; Pratt and James, in press). These cycles are explained by an "island" tidal flat model where small supratidal islands and intertidal banks accreted and migrated over subtidal areas. The peritidal phase occurred after the platform built to sea level, when carbonate production could match or exceed the sea level rise. This period of sediment oversupply is also reflected in the contemporaneous

slope and basin deposits of the Cow Head Group (James and Stevens, 1982) where both resedimented sands and breccias are common (beds 12 and 13 in fig. 3-5).

Regional paleogeography and dolomitization

Changes observed in the regional dolomitization pattern are consistent with the inferred paleogeography of the "St. Lawrence" platform.

The nature and timing of dolomitization in western Newfoundland have been recently studied by Haywick (1984). He found several varieties of dolomites and dolostones commonly interbedded with limestones. Major types of dolostones include dololaminites and coarser grained pervasive dolostones that are respectively interpreted as resulting from penecontemporaneous dolomitization of intertidal-supratidal sediments and from early replacement of limestones in a mixing-zone environment. Dolomitization, however, is more complex, with other early diagenetic dolomite phases in the lime mud matrix or ichnofossils of dolomitic limestones as well as late diagenetic phases associated with sphalerite mineralization in the Daniel's Harbour area of western Newfoundland.

The "Grande Ile-Aguathuna" phase, characterized by cyclic peritidal sedimentation, is generally composed of dolomicritic lithofacies in the Mingan Islands and by interbedded dololaminites and limestones in western Newfoundland (fig. 3-5). As discussed earlier, the regional paleogeography of the "St. Lawrence" platform at this time was a broad coastal tidal flat adjacent to a marine environment dotted with island-tidal flats. With the eventual progradation of these tidal flats, extensive penecontemporaneous dolomitization occurred in upper

- 93 -

intertidal-supratidal environments (this study; Haywick, 1984). The island-tidal flat model better explains the spatial distribution of the dolomites and dolostones in western Newfoundland where they are characterized by lateral discontinuity. The progradation of these island tidal flats resulted in the formation of dololaminites capping cyclic peritidal cycles. Furthermore, these islands could have served as local recharge areas for fresh water which when mixed with sea water would have resulted in the alteration to limestones of medium to coarse-grained dolostones. In an island setting, local aquifers with different chemistries would not have been necessarily conducive to dolomitization and may explain common occurrences of interbedded dololaminites and limestones. In contrast, widespread and continuous progradation of coastal tidal flats in the Mingan area at this time resulted in the complete dolomitization of peritidal sediments that are laterally extensive. Such a relation between dolomitization and paleogeography was probably not unique to the St. Lawrence platform at that time. A similar depositional model has been suggested to explain the spatial and time distribution of dolomites in the carbonate sediments of the upper Knox Group in the Southern Appalachians (Churnet et al. 1982).

During the "Sainte-Genevieve-Catoche" phase, sediments were deposited mainly under subtidal conditions and consist of pervasive dolostones in the Mingan Islands and mostly of limestones in western Newfoundland (fig. 3-5). The absence of peritidal sedimentation is also reflected by the absence of penecontemporaneous dolomites associated with tidal flats. Indeed coarser grained dolostones were formed in shallow subsurface by the early replacement of these sediments due to

mixing of marine pore water with fresh water. Regional, fresh-phreatic groundwater aquifers have been invoked for the formation of sucrosic dolostones in the Romaine Formation. These groundwaters were recharged laterally to the north and flowed in a southward direction. Their limited extent to the south beneath the "St. Lawrence" platform may explain the absence of such dolomitization in equivalent subtidal limestones in the subsurface of Anticosti Island or in the Catoche Formation with the exception of the northern part of western Newfoundland where pervasive dolostones are present.

SUMMARY

1) Eight discrete lithofacies can be recognized in the Romaine Formation and occur in stratigraphic units that are laterally continuous across the study area (up to 20 km), if not affected by the post-Romaine paleokarst unconformity. These lithofacies, similar to those previously reported from other contemporaneous Sauk sequences, represent sediments deposited in inner and middle shelf environments. Of particular interest to the Romaine sequence, middle shelf sedimentation was characterized by the extensive development of thrombolitic patch reefs. These reef complexes, however, were located in the platform interior at least several hundreds of kilometres away from the platform margin dominated by different buildups composed of calcified algae. Inner shelf lithofacies (dololaminites, stromatolites) are typical of peritidal carbonate sedimentation with the exception of the ripple-laminated dolomicrites representing "mixed" sand and mud intertidal flat sediments. Such sediments are more commonly observed in siliciclastic

tidal flat systems.

2) The depositional sequence of the Romaine Formation represents a
"classic" shallowing-upward sequence which formed under slow platform
subsidence (stable platform margin) and possibly an uniform rise and
fall in eustatic sea level during the late Early Ordovician time. The
sequence is subdivided into three assemblages: 1) a thin, lower
assemblage of trangressive sandstones; 2) a middle assemblage of open
marine, subtidal carbonates and 3) an upper assemblage of cyclic
peritidal carbonates.

3) The vertical succession of Romaine lithofacies suggests that four
distinct sedimentary belts were laterally adjacent during the deposition
of the Romaine Formation and include, along an onshore-offshore profile:
tidal flats, lagoon, bioherm complex and deeper shelf.

4) Romaine lithofacies assemblages can be correlated over 500 km
across the Gulf of St. Lawrence with equivalent units in western
Newfoundland. Sedimentation regimes across the platform changed through
time from dominantly subtidal to peritidal deposition. During the
subtidal phase, extensive mudbanks and thrombolite patch reefs developed
on the platform with possibly stranded tidal flats located north of the
Mingan Islands. As time passed, a broad coastal tidal flat in the Mingan
Islands developed adjacent to a marine environment dotted with
.island-tidal flats, and as a result cyclic peritidal sedimentation
prevailed across the platform.

5) Two textural varieties of dolomite can be recognized in the Romaine Formation: finely crystalline dolostones associated with cyclic peritidal carbonates and sucrosic dolostones associated with subtidal carbonates. Dolomitization in cyclic peritidal carbonates was contemporaneous with their deposition in sabkha-like environments. On the other hand, sucrosic dolomite probably formed in the mixing zone by replacement of limestones that were originally deposited in subtidal marine environments. This type of dolomitization occurred under shallow subsurface conditions before the final development of the post-Romaine paleokarst unconformity.

CHAPTER 4

MINGAN LITHOFACIES

In the study area, the Romaine Formation (late Canadian-earliest Whiterock) is unconformably overlain by the Mingan Formation (Chazyan) which contains a wide spectrum of both siliciclastic and carbonate shelf sediments deposited during trangression of early Middle Ordovician seas. The Mingan Formation consists of three discrete sedimentary packages (fig. 4-1): 1) a lower lithofacies assemblage, composed of peritidal siliciclastics; 2) a middle lithofacies assemblage, composed of peritidal and subtidal limestones; and 3) an upper lithofacies assemblage, composed of subtidal limestones. The Mingan Formation is a classic siliciclastic-carbonate trangressive sequence with a basal siliciclastic unit but with numerous second-order superimposed trangressions and regressions. Furthermore, a paleokarst unconformity (termed "intra-Mingan") is observed within the Mingan Formation and usually separates the middle, locally the lower, assemblage from the upper assemblage. Of particular importance is the erosional relief related to this unconformity which controls the lithofacies distribution in the overlying upper assemblage. The Mingan sequence is similar to other basal Middle Ordovician platform sequences in eastern North America (Klappa et al., 1980,; Read, 1980; Ruppel and Walker, 1984) yet has a distinctive and unique character.

Figure 4.1- Generalized stratigraphic column of the Mingan Formation, showing the distribution of members and lithofacies assemblages. The Mingan Formation is subdivided into three distinct sedimentary packages: 1) a lower assemblage of peritidal siliciclastic lithofacies; 2) a middle assemblage of peritidal and subtidal limestone assemblages and 3) an upper assemblage of subtidal limestone lithofacies. Note the presence of two paleokarst unconformities (PK). See figure 1-2 for symbols.

LITHOFACIES
ASSEMBLAGES

MINGAN FM

Grande Pointe Mb

Fantome Mb

Perroquet Mb

Corbeau Mb

ROMAINE FM

SUBTIDAL
LIMESTONES — UPPER

PERITIDAL
LIMESTONES

MIDDLE

SUBTIDAL
LIMESTONES

PERITIDAL
SILICICLASTICS — LOWER

PK

PK

10m

5

0
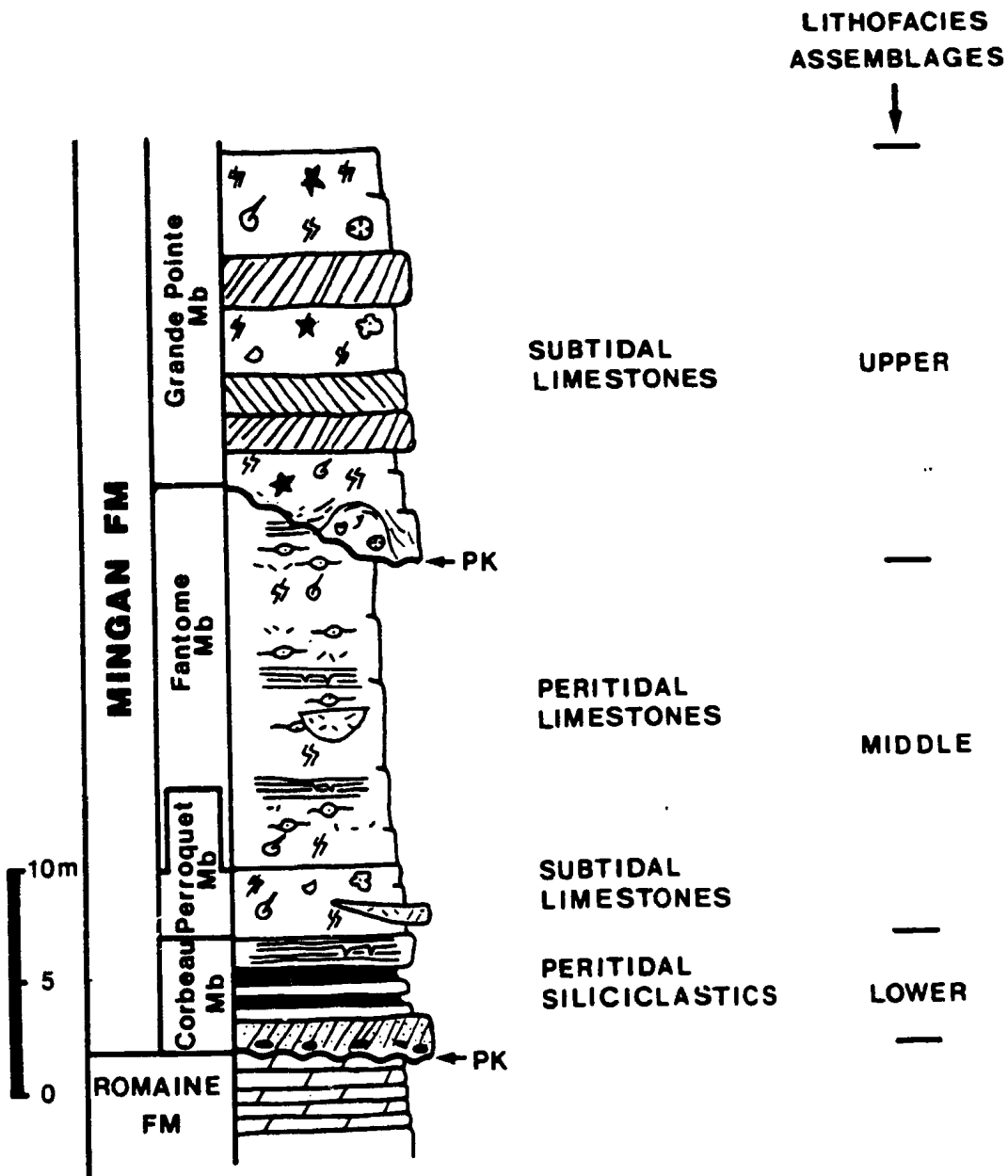
LITHOFACIES DESCRIPTION AND INTERPRETATION

The Mingan Formation is subdivided into sixteen discrete lithofacies on the basis of their lithological characteristics. These lithofacies consist of shallow-water deposits which represent peritidal siliciclastic, peritidal limestone, and subtidal limestone environments.

Peritidal siliciclastic lithofacies (see table 4-1)

Lithofacies 1: Silty dololaminites

Description: This lithofacies is composed of silty laminated dolostones and forms a distinctive tan-weathered unit, up to 1.5 m thick, capping the lower siliciclastic assemblage (plate 4-1; A and B). Silty dololaminites exhibit sedimentary features similar to those of the previously described dololaminites in the Romaine Formation (lithofacies B, p. 39). They differ only in their green colour in fresh exposure due to presence of argillaceous material. Furthermore, evidence for evaporite precipitation is ubiquitous and consists of aggregates of salt hoppers preserved on mud cracks (plate 4-1; C and D). In thin-section, the millimetre laminae are composed of a mosaic of dolomite crystals with subhedral to euhedral rhombs averaging 30 μm in size. Undolomitized laminae exhibit alternating layers of terrigenous grains (mainly clays and quartz silts) and/or peloid-rich wackestones/packstones.

Interpretation: Rocks of this lithofacies represent dolomitized cryptalgalaminites deposited in the high intertidal/supratidal zone. Algal mats have been described from modern siliciclastic tidal flats (Reineck, 1975; Miller, 1975) where they cover unvegetated areas of the supratidal marshes. Dolomitization probably occurred soon after

PLATE 4-1

LITHOFACIES 1: SILTY DOLOLAMINITE

A. Field photograph (cliff exposure) of a silty dololaminite unit (50 cm thick) capping the Corbeau Member (arrow). Note the underlying laminated shales (s) and the sharp but conformable contact with the overlying fenestral mudstones (m) of the Fantome Member. Ile du Havre SW.

B. Field photograph (cross-section view) of lithofacies 1 showing cryptalgalaminites. Grande Ile E. Lens cap is 50 mm in diameter.

C. Field photograph of well-developed mud cracks on the bedding plane. Ile Quarry NW. Lens cap is 50 cm in diameter.

D. Field photograph (bedding plane view) of aggregate salt hoppers preserved on mud cracks. Close-up of (C). Ile Quarry NW.

TABLE 4-1. CHARACTERISTICS AND DEPOSITIONAL ENVIRONMENTS OF THE PERITIDAL SILICICLASTIC LITHOFACIES

LITHOFACIES	LITHOLOGICAL CHARACTERISTICS	INFERRED ENVIRONMENTS
1. Silty dololaminites	Planar to wavy laminations; mud cracks; evaporite pseudomorphs; lenestone, tepees; syneresis cracks; local bioturbation; lower siliciclastic assemblage	Supratidal flats
2. Laminated shales	Pin-stripe tidal bedding; lenticular siltstones with internal ripple laminations; unlossoliferous; moderate bioturbation; lower siliciclastic assemblage	Intertidal mud flats
3. Laminated sandstones	arkosic compositions; flaser, wavy, and lenticular bedding; shale interbeds; wave and current ripple marks; matricalure brachiopods; moderate to extensive bioturbation; lower siliciclastic assemblage	Intertidal sand flats
4. Cross-bedded sandstones	arkosic compositions; trough cross bedding; articulate and inarticulate brachiopods; vertical trace fossils; lower siliciclastic assemblage	Nearshore sand bars
5. Channelized sandstones	arkosic compositions; irregular margins; scoured base; lag deposit with shale clasts; inarticulate brachiopods; vertical trace fossils; lower siliciclastic assemblage	Tidal channels

-104-

PLATE 4-2

LITHOFACIES 2: LAMINATED SHALES

A. Field photograph of a cliff exposure on Ile aux Perroquets N where
    laminated shale (s) makes up most of the Corbeau Member and
    grades upsection into skeletal limestones (l) of the Perroquet
    Member.

B. Field photograph (cross-section view) of lithofacies 2 interlayered
    with thin lenses of fine sandstone (lighter coulored bed). Detail of
    (A). Ile aux Perroquets N. Metre stick is 1.2 m long.

C. Field photograph (cross-section view) of shales showing pin-stripe
    tidal bedding. Ile Saint-Charles E. Lens cap is 50 mm in diamter.
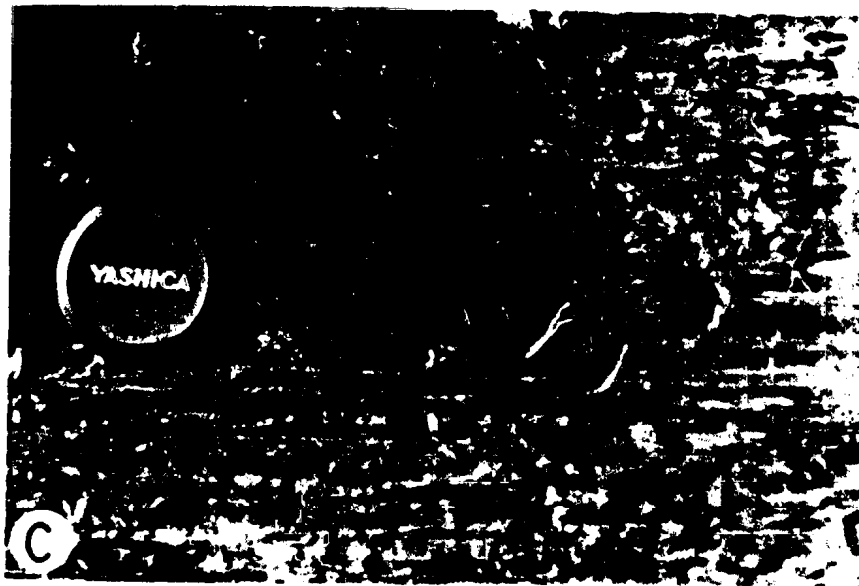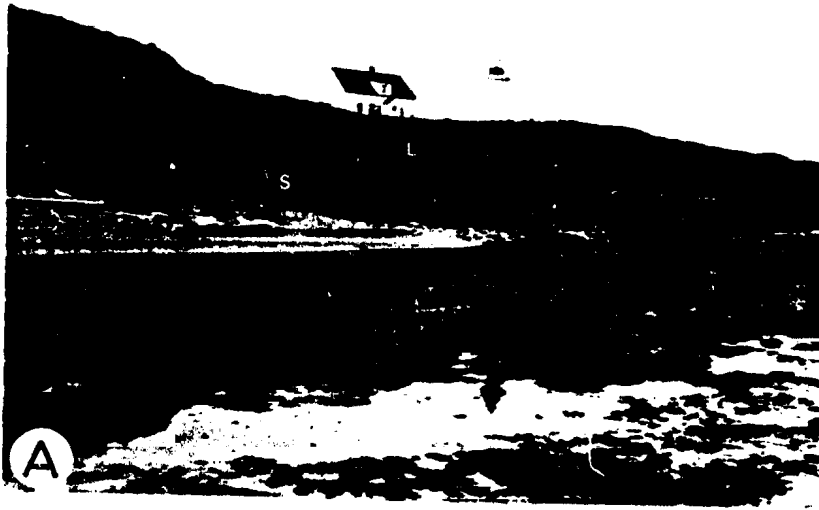
flats where they occur in the upper part of the intertidal zone

(Reineck, 1975; Weimer et al., 1982). The tidal transport processes

commonly generate both suspension and bedload transport deposition

(Klein, 1977).

Lithofacies 3: Laminated sandstones

Description: This lithofacies occurs in units that vary between 0.3

and 2.0 m in thickness and show gradational contacts with laminated

shales (lithofacies 2) in the lower siliciclastic assemblage. Rocks of

this lithofacies are composed of fine-grained arkosic sandstones

characterized by flaser (plate 4-3; A and B), wavy, and lenticular beds

(3-10 cm thick). The sandstones are separated by thin shale interbeds.

Both wave and current ripple forms are present on bedding plane surfaces

(plate 4-3; C). Primary sedimentary textures and structures are

sometimes obliterated by bioturbation. Skeletal biota is absent except

for lingulid brachiopod fragments. The sandstones are arkosic in

composition with up to 30% feldspar (mainly plagioclase). The quartz and

feldspar grains range from 0.1 to 0.3 mm in size, are subrounded to

subangular and are well-sorted within an individual layer. These grains

are cemented by euhedral dolomite crystals that predate a later stage of

blocky, iron-rich calcite cement (plate 4-3; D).

Interpretation: Based on modern environmental counterparts (i.e.

sand flats of Reineck, 1975), this lithofacies represents sediments

deposited in the lower part of intertidal flats, as evidenced by the

sediment type and texture as well as physical and biogenic structures.

Unlike upper tidal flat sediments (lithofacies 2), these sediments are

more sandy and characterized by ripple laminae and various bedding

PLATE 4-3

LITHOFACIES 3: RIPPLE-LAMINATED SANDSTONES

A. Field photograph (cross-section view) of flaser-bedded sandstones. Ile Saint-Charles NW. Scale in cm.

B. Field photograph (cross-section view) showing detail of the flaser bedding in (A). Ile Saint-Charles NW. Hammer for scale.

C. Field photograph of lithofacies 3 showing symmetrical wave ripple marks with interference patterns on the bedding surface. Ile Saint-Charles NW.

D. Thin-section photomicrograph (plane-polarized light) of laminated sandstones where well-sorted quartz and feldspar particles are subangular and cemented by an early dolomite (d) and late blocky calcite (b) cements. Note the dedolomitization (dark centers) in euhedral dolomite crystals. Scale bar is 1.0 mm.

types. Both wave and current action features suggest a depositional setting located near the low tide line. According to Ekdale et al. (1984, p. 179), sand flats are usually occupied by suspension feeders related to the local hydrodynamic conditions and, as a result, vertical dwelling burrows are common.

Lithofacies 4: Cross-bedded sandstones

Description: This lithofacies, if present, rests directly on the Romaine Formation and forms the basal unit (up to 3.0 m thick) of the lower siliciclastic assemblage (plate 4-4; A). It consists of coarse-grained arkosic sandstones with trough cross-bedding (plate 4-4; B). Cross-bedding sets range from 0.2 to 1.2 m in thickness and usually become thinner up section. The paleoflow currents based on cross-bed axes, show bipolar-bimodal (070°-250°, n=25) and rare, unimodal (230°, n=4) patterns (vector means). The restricted skeletal fauna includes inarticulate lingulid brachiopods and small articulate brachiopods (mainly rhynchonellids). The sandstones are sometimes punctuated by skeletal-rich layers (3-5 cm thick) composed of echinoderm, brachiopod, mollusk, and bryozoan fragments. Vertical dwelling trace fossils, Diplocraterion and Skolithos, are commonly found near the top of cross-bed sets (plate 4-4; B). These quartz sandstones are like the laminated sandstones in that they contain up to 30% feldspar. The sandstones are characterized by a bimodal grain size distribution with each mode composed of well-rounded grains (plate 4-4; D). Particles are mainly a mixture of coarse-grained sand (0.8-1.5 mm) with fine-grained sand (0.1-0.2 mm); however, intermediate grain sizes are also present. Intergranular porosity is filled by quartz and feldspar overgrowths with

- 111 -

PLATE 4-4

LITHOFACIES 4: CROSS-BEDDED SANDSTONES

A. Field exposure of the contact between dolostones of the Romaine
    Formation (foreground) and overlying cross-bedded sandstones (ss) of
    the Mingan Formation (Corbeau Member). Note the fossil rinnenkarren
    on top of the Romaine Formation. Grande Ile E.

B. Field photograph (cross-section view) of abundant vertical trace
    fossils, Diplocraterion, near the top of a cross-bed set (arrow).
    Ile du Havre E. Hammer is 30 cm.

C. Thin-section photomicrograph (cross-polarized light) illustrating
    the mature bimodal texture of quartz and feldspar particles in the
    sandstones. Scale bar is 1.0 mm.
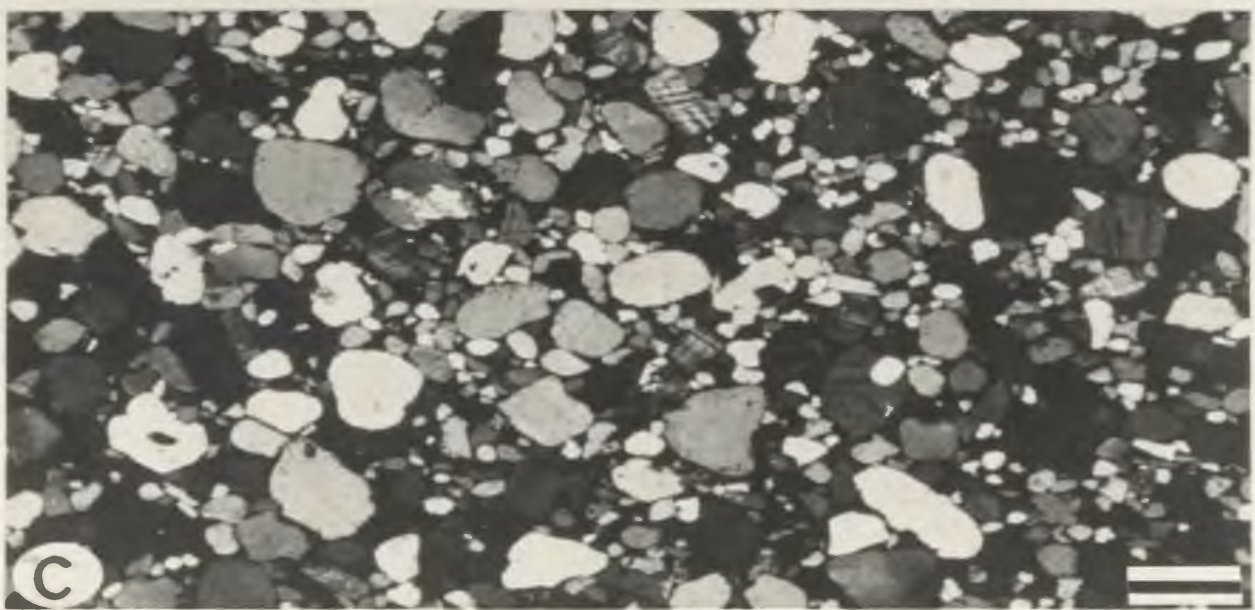
subordinate blocky, iron-rich calcite and/or dolomite cement. The present intergranular porosity locally reaches 10% of the total volume.

Interpretation: This lithofacies is interpreted as a series of inner shelf sand bars related to a marine transgression over the Romaine Formation. The sand bars are tidally controlled as indicated by the paleoflow currents but their progressive emergence could have caused sudden changes in the tidal flow directions (Klein, 1977). Trace fossils are characteristic of shallow nearshore zones that are dominated by physical sedimentary structures (Skolithos ichnofacies of Seilacher, 1967). These processes operated on a large scale during Early Paleozoic when unvegetated land areas were the norm. It is not clear whether this basal sandstone was due to a blanket of regolithic eolian sediments covering the Romaine Formation or to a distant Precambrian sand source that may have been reworked and subsequently transported across the shelf with renewed submergence. Studies of the paleokarst unconformity with smoothed solution sculptures (to be discussed later) beneath these sandstones, however, suggest that it was the former. Folk (1968) also pointed out that the bimodal size distribution in mature sandstones must result from deflationary eolian processes. On the other hand, evidence suggests deposition in a subtidal, marine environment. Sediments in the nearshore zone are normally retained within the littoral energy fence due to the landward wave-driven currents along the coastline (Brenner, 1980). This energy fence may be inhibited by shoreface bypass mechanisms (storm surge reflux, spring tidal current) resulting from the erosional retreat of the shoreface during a marine transgression, as shown by studies on Recent continental shelves (Swift, 1976). It is possible that the residual sand blanket overlying the Romaine Formation was similarly

reworked during marine trangression and deposited in the inner shelf by shoreface bypassing.

Lithofacies 5: Channellized sandstones

<u>Description</u>: This lithofacies occurs in the lower siliciclastic assemblage and is laterally associated with the laminated shales and the laminated sandstones (lithofacies 2 and 3). Rocks of this lithofacies consist of coarse-grained arkosic sandstones which form channellized units, up to 3.0 m thick (plate 4-5; A). The channels have irregular margins and scoured bases as well as abundant shale clasts forming a lag deposit at the base (plate 4-5; B). They are usually formed by slightly-inclined, alternating layers of sandstone (5-30 cm thick) and shale (3-10 cm thick).The restricted skeletal fauna includes inarticulate lingulid brachiopods (plate 4-5; C) with some small articulate brachiopods. The trace fossils are mostly vertical burrows (mainly <u>Skolithos</u>).

<u>Interpretation</u>: This lithofacies is interpreted as a series of point bar deposits in tidal channels. Like tidal channels on modern muddy tidal flats (Bridges and Leeder, 1976; Mowbray, 1983), this lithofacies is formed by lenticular sand-mud layered units with a lag concentrate overlying an erosional surface. Their internal structure is characterized by individual layers dipping (5 to 15) from the channel floor (Bridges and Leeder, 1976, fig. 18). These deposits differ from fining-upward sequences generated by fluvial point bars (for comparison, see Walker and Cant, 1984) because the scouring and lateral accretion occurs only during a limited period of the tidal cycle, most commonly the late ebb flow. The vertical dwelling burrows are compatible with

PLATE 4-5

LITHOFACIES 5: CHANNELLIZED SANDSTONES

A. Field photograph (cliff exposure) of a sandstone channel within laminated shales. Note the irregular channel margin (arrows). Ile du Havre E.

B. Field photograph showing the scoured base (sole bedding plane) from channel shown in (A) containing numerous shale clasts. Ile du Havre E. Lens cap is 50 mm in diameter.

C. Polished slab (cross-section view) illustrating the coarse-grained nature of sandstones in lithofacies 5. Note the presence of inarticulate brachiopod valves (black flaky particles). Ile du Havre E.
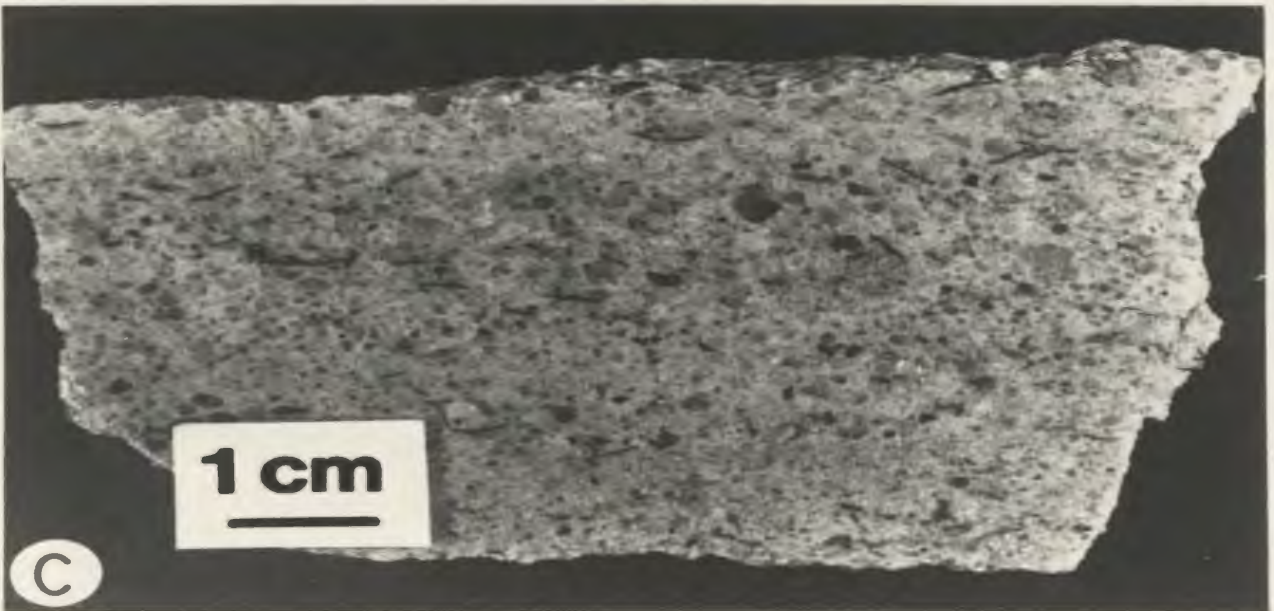
tidal point bar deposits that are subject to rapid erosion and deposition (Ekdale et al., 1984).

Peritidal limestone lithofacies (see table 4-2)

Lithofacies 6: Cryptalgalaminites

Description: Most of this lithofacies is composed of planar-laminated mudstones on a millimetre scale cut by abundant mud cracks (plate 4-6; A and B). The restricted fauna contains only disarticulated ostracod valves and some gastropod fragments. The millimetre laminae exhibit three discrete microfabrics (plate 4-6; C): 1) peloid laminae, characterized by well-sorted peloids ranging from 40 to 60 μm in size; 2) algal laminae formed of Girvanella filaments; and 3) structureless micritic laminae. The Girvanella algal laminae (plate 4-6; D) vary from vertical, self-supporting filaments to closely-packed fragmented filaments with interstitial micrite. Idiotopic dolomite rhombs are ubiquitous in the micritic laminae and range from 10 to 20 μm in size. The fenestrae structures are usually laminoid in shape but irregular forms are also present. The cryptalgalaminites form thin units (10-50 cm thick) in the middle limestone assemblage.

Interpretation: This lithofacies represents sediments deposited in the supratidal zone as evidenced by abundant diagnostic sedimentary features (mud cracks, restricted biota, fenestrae). Millimetre laminae in supratidal flat sediments are commonly regarded as resulting from periodic storm-induced flooding and sedimentation with subsequent algal mat growth (Hardie and Ginsburg, 1977; Shinn, 1983b). The laminae microfabrics are strikingly similar to the algal-laminated sediments in

TABLE 4-2. CHARACTERISTICS AND DEPOSITIONAL ENVIRONMENTS OF THE PERITIDAL LIMESTONE LITHOFACIES

LITHOFACIES	LITHOLOGICAL CHARACTERISTICS	INFERRED ENVIRONMENTS
6- Cryptalgalaminites	planar laminations; mud cracks; _Girvanella_ layers; fenestrae; restricted fauna; middle limestone assemblage	Supratidal mud flats
7- Fenestral mudstones	abundant fenestrate pores; rare mud cracks; restricted biota; intraformational intraclasts; middle limestone assemblage	Intertidal mud flats
8- Intraclast grainstones	fenestral mudstone intraclasts; ripple laminations; restricted biota; middle limestone assemblage	Tidal channels
9- Gastropod packstones	restricted biota dominated by gastropods; solution cavities; generations of internal sediment and fibrous calcite cement; middle limestone assemblage	Lagoons
10- Mudstones/ skeletal wackstones	Moderate to strong bioturbation; restricted marine biota; middle and upper limestone assemblages	Semi-restricted shelf

PLATE 4-6

LITHOFACIES 6: CRYPTALGALAMINITE

Photomicrographs - Plane polarized light

A. Field photograph (cross-section view) of lithofacies 6 showing
mudstones, planar laminated on a millimeter scale. Ile Nue de Mingan
NW. Lens cap is 50 mm in diameter.

B. Field photograph (bedding plane view) of mud cracks in lithofacies
6. Ile Quarry E. Hammer for scale.

C. Thin-section photomicrograph showing microfabrics in
cryptalgalaminite. Note the alternating algal (a) and peloid (p)
laminae. Detail in (D). Scale bar is 1.0 mm.

D. Thin-section photomicrograph of algal laminae showing abundant
self-supporting Girvanella filaments. Scale bar is 100 µm.
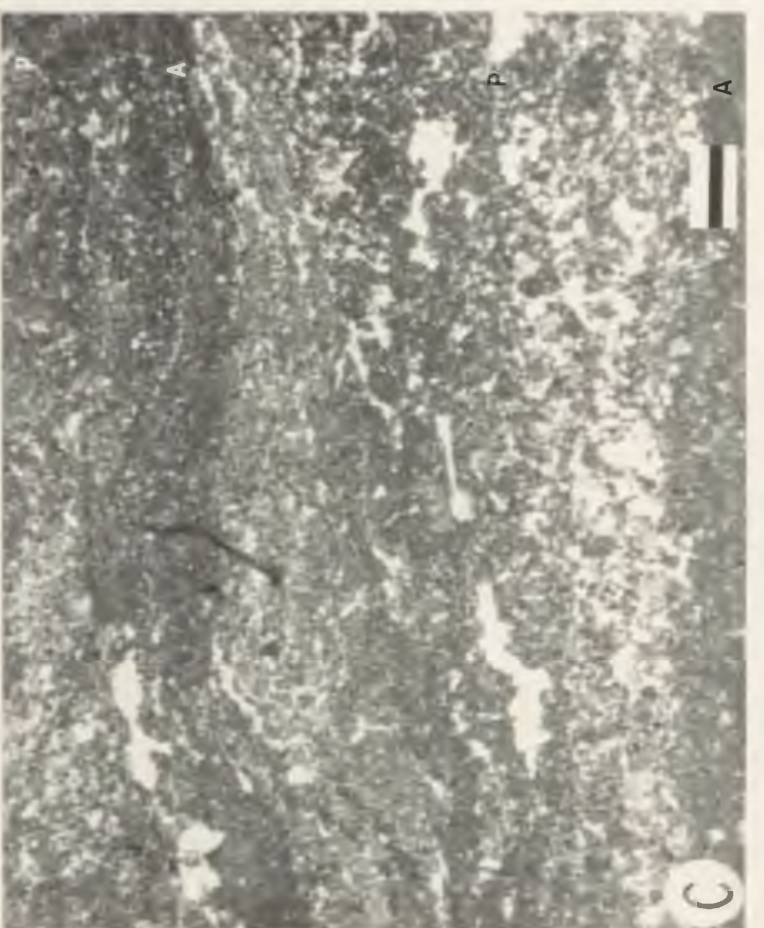
coastal supratidal marshes of western Andros Island, Bahamas (Monty and Hardie, 1976; Hardie, 1977). The algal layers or "tufas" in these sediments are composed of well-preserved and calcified Scytonema filaments and make fine modern analogues for the Girvanella algal laminae (see for comparison Monty and Hardie, 1976, figs. 9 and 10). According to Monty and Hardie (1976), the presence of algal-laminated sediments is indicative of relatively humid climate and the presence of a flat, low-lying, locally ponded, tidal platform.

Lithofacies 7: Fenestral mudstones

Description: The fenestral mudstones are the most common lithofacies in the middle limestone assemblage and occur in units ranging from 0.3 to 5.0 m in thickness. This lithofacies consists of structureless to peloidal micrite with abundant fenestrae (plate 4-7; A and B). The fenestrate pores are laminoid and irregular in shape and can make up to 40% of the total volume (plate 4-7; C). Laminoid fenestrae are planar in shape (0.2 to 0.5 mm high; 1.0 to 5.0 mm long) and are oriented parallel to the bedding. Irregular fenestrae are equidimensional to highly irregular in shape (0.5 to 4.0 mm in size). Both fenestrae types are randomly distributed and form an interconnected network. The restricted biota includes leperditiid ostracods, gastropods, and calcareous green algae (mainly Hedstroemia). Girvanella fragments are ubiquitous. Furthermore, intraclast-rich layers (2.0 to 8.0 cm thick) are common and consist of sand to pebble-sized intraformational clasts (i.e. fenestral mudstones). Other observed features are planar to scalloped erosion surfaces and rare mud cracks. In thin section, most of the fenestrate and intragranular pores are filled by blocky, equant calcite cement

- 122 -

PLATE 4-7

LITHOFACIES 7: FENESTRAL MUDSTONE

A. Field photograph (cross-section view) of lithofacies 7 showing abundant fenestrate pores. Ile a Firmin S. Scale in cm.

B. Polished slab (cross-section view) of fenestral mudstone. Note that the fenestrate pores are interconnected and laminoid to irregular in shape. Ile NIapiskau E.

C. Thin-section photomicrograph (plane polarized light) showing interconnected laminoid and irregular fenestrate pores in fenestral mudstone. Scale bar is 1.0 mm.
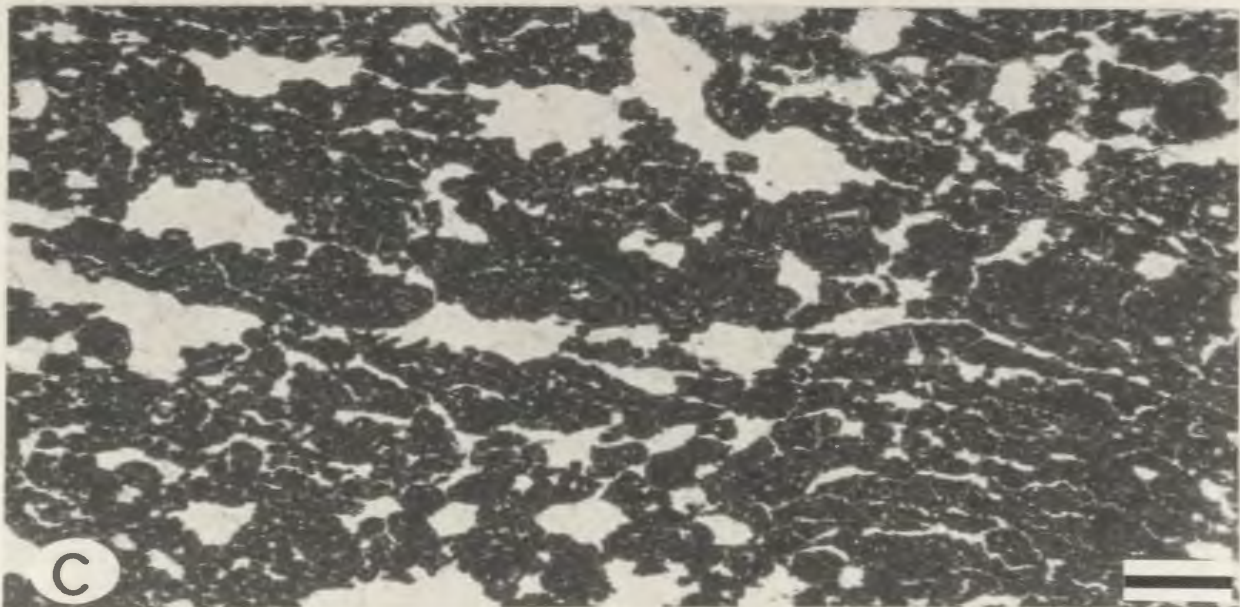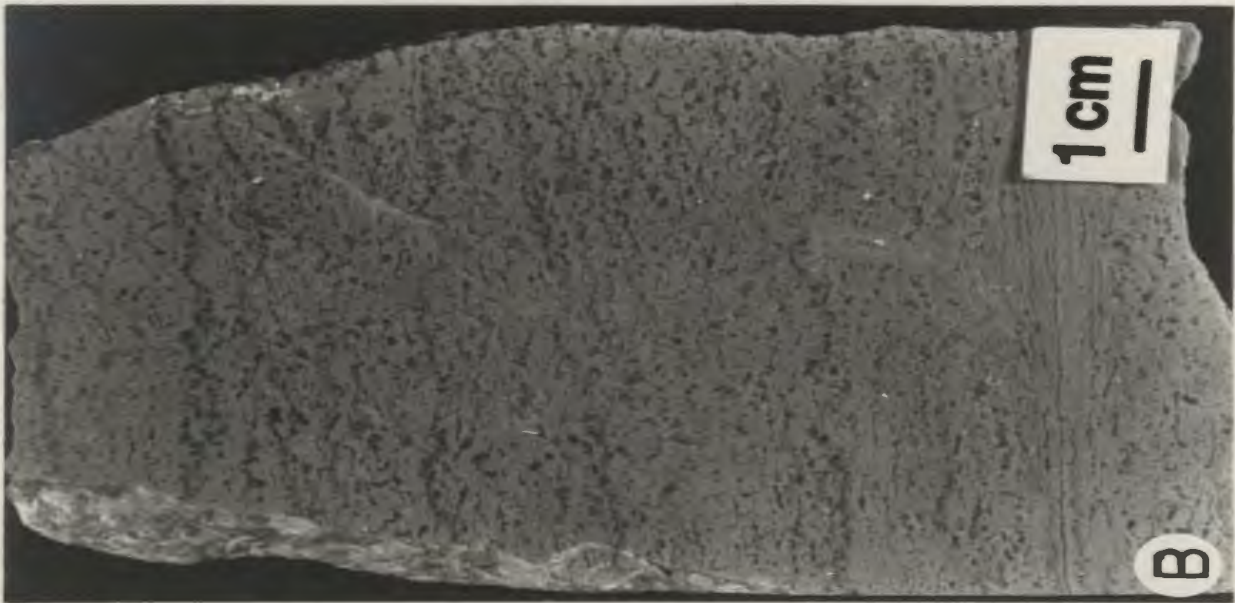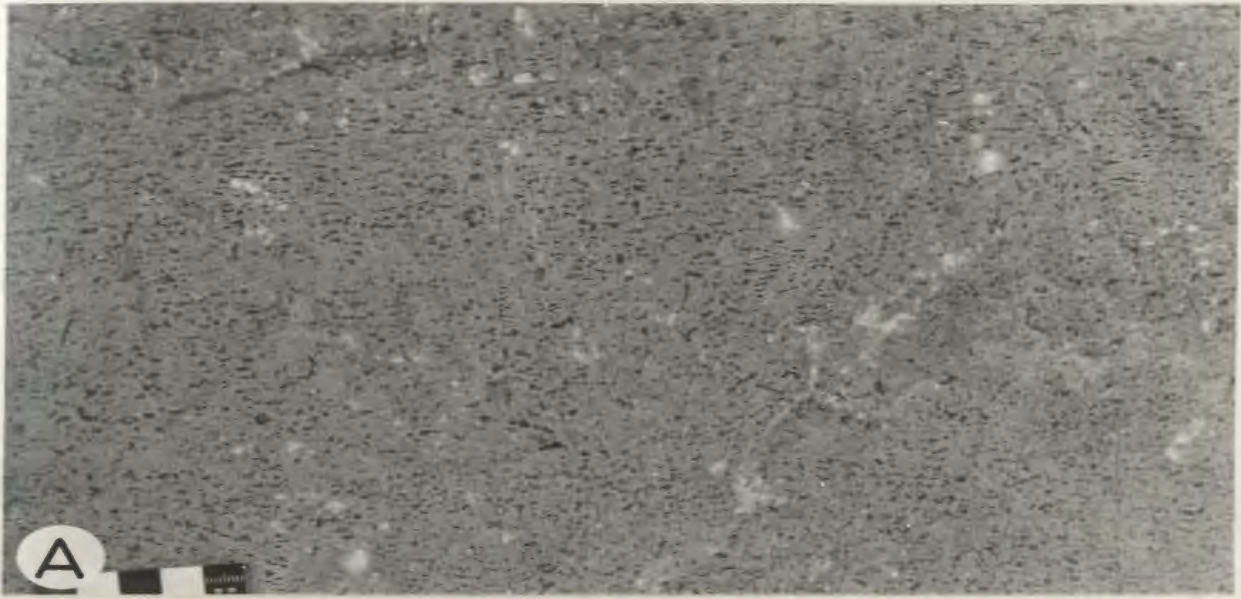
which is sometimes predated by fibrous calcite cement and micritic geopetal sediment.

Interpretation: This lithofacies represents sediments deposited in intertidal mud flat environments. The sedimentary layering commonly observed in supratidal sediments is usually lacking but indications of subaerial exposure (fenestrae structures, mud cracks) are still present. The restricted biota, dominated by euryhaline forms, is compatible with such high-stress environments. The fenestrae are considered to be reliable intertidal indicators in muddy sediments by Shinn (1983 a). The origin of fenestrae is explained by several mechanisms, such as decay of organic material (mainly algal); gas bubble formation; air escape during flooding; and shrinkage and expansion (Shinn,1968; Logan et al, 1974). Several of these mechanisms, which operate concurrently in modern tidal flats are probably responsible for formation of the complex fenestrae network. Some large irregular pores (up to 8 mm in size), however, are more likely secondary solution vugs as indicated by their smooth outlines and by truncated fossils. These sediments were lithified early as suggested by the numerous intraformational intraclasts and by the preservation of fenestrae (Shinn and Robbin, 1983). Early lithification probably inhibited extensive reworking of sediment by burrowing organisms.

Lithofacies 8: Intraclast grainstones

Description: Intraclast grainstones are found as channellized units (plate 4-8; A), up to 2.0 m thick, in the middle limestone assemblage and are laterally associated with the fenestral mudstones (lithofacies 7). This lithofacies is composed of micritic intraclasts with minor

PLATE 4-8

LITHOFACIES 8: INTRACLAST GRAINSTONE

A. Field photograph (cross-section view) of channellized unit of intraclast grainstone. Note the scoured channel base (arrows) truncating fenestral mudstones. Pointe Enragee N. Hammer is 30 cm.

B. Polished slab (cross-section view) of lithofacies 8 showing mechanical layering. Pointe Enragee N.

C. Thin-section photomicrograph (plane polarized light) illustrating intraclasts of fenestral mudstone. Note the presence of internal geopetal sediment (m). Scale bar is 1.0 mm.
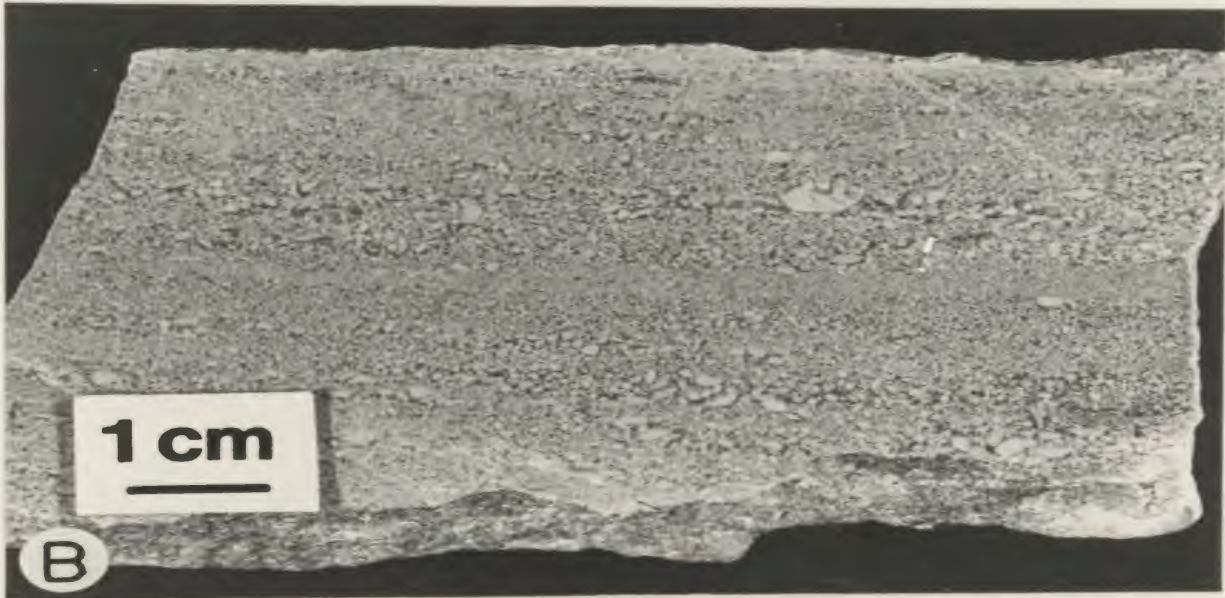
skeletal debris (plate 4-8; B). The sand to pebble-sized intraclasts

consist of homogeneous to fenestral micrites and are subrounded to

highly irregular in shape (plate 4-8; C). The skeletal biota consists of

gastropod, calcareous green algae, and ostracod fragments. Mechanical

layering is barely identifiable but ripple cross-laminae are sometimes

present. In thin-section, the primary intergranular pores are mainly

filled by blocky, equant calcite cement.

Interpretation: The intraclast grainstones represent sediments

deposited in channels within a tidal flat system. The inferred

environment is supported by abundant intraclasts derived from laterally

associated lithofacies, local slumped blocks at channel margins and

irregular scoured bases or margins truncating the fenestral mudstones.

Tidal channels like those on the Andros Island tidal flat are fine

modern analogues for this lithofacies (Shinn et al, 1969; Hardie, 1977).

Lithofacies 9: Gastropod packstones

Description: This lithofacies occurs as a laterally persistent unit

(0.5-0.8 m thick) in the lower part of the middle limestone assemblage.

Most of the lithofacies consists of muddy skeletal sediments which are

characterized by packstone to wackestone depositional textures. The

abundant but restricted fauna is dominated by gastropods (plate 4-9; A

and B), with leperditiid ostracods, calcareous green algae (Hedstroemia,

Garwoodia), and bathyurid trilobites. Stenohaline taxa are rare. The

depositional matrix is mainly composed of structureless micrite with

some silt-sized peloids. Associated diagenetic features include

selective dissolution of the gastropod skeletons which were subsequently

filled by several generations of internal geopetal sediments (locally

PLATE 4-9

LITHOFACIES 9: GASTROPOD PACKSTONES
LITHOFACIES 10: MUDSTONE/SKELETAL WACKSTONES

A. Field photograph of lithofacies 9 showing abundant high-spired gastropods on the bedding plane. Ile Niapiskau W. Lens cap is 50 mm in diameter.

B. Polished slab (cross-section view) of gastropod packstones. Note the selective dissolution of the gastropods skeletons which are later filled by internal geopetal sediment (s) and/or fibrous calcite cement (f). Ile du Havre SW.

C. Polished slab (cross-section view) of lithofacies 10 illustrating bioturbated lime mud with floating fragments of ostracods and bathyurid trilobites. Ile Niapiskau W.

D. Field photograph of the common trace fossil, <u>Chondrites</u>, exposed on the bedding plane in lithofacies 10. Ile Niapiskau W. Lens cap is 50 mm in diamter.
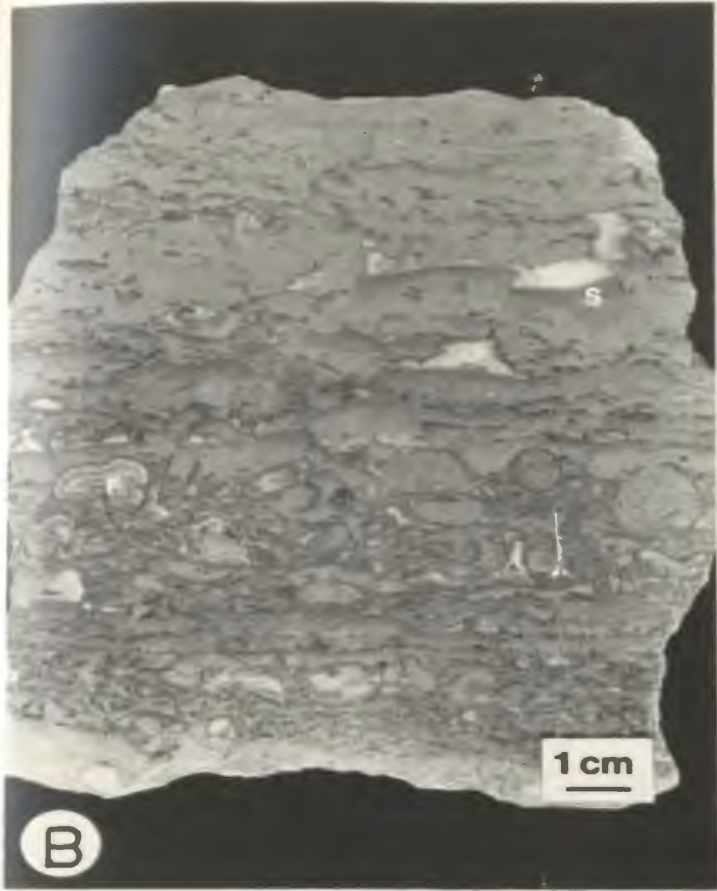
red in colour) and/or fibrous calcite cement.

Interpretation: This lithofacies is interpreted as sediments deposited in semi-restricted, low-energy environments. The abundant but restricted biota with a few well-adapted organisms is commonly indicative of semi-restricted settings such as lagoons that are not frequently invaded by normal marine waters (Enos, 1983). The depositional textures also reflect relatively quiet environments. Garret (1977) described a similar low-diversity biota and lithological characters in nearshore sediments of western Andros Island, Bahamas. These sediments contain a semi-restricted, shallow water community of organisms living on bioturbated sandy mud bottom.

Lithofacies 10: Mudstones/skeletal wackestones

Description: This lithofacies occurs in two distinct stratigraphic settings; 1) wavy-bedded units (0.4- 2.0 m thick) in the upper limestone assemblage and 2) thin lenticular units (0.1-0.4 m thick) or wavy-bedded units (up to 3.0 m thick) in the middle limestone assemblage. The wavy-bedded units are sometimes interlayered with ripple-laminated grainstones that are mainly composed of biomicritic intraclasts. The thin lenticular units are laterally associated with the fenestral mudstones (lithofacies 7). This lithofacies consists of bioturbated muddy sediments with less than 20% skeletal grains (plate 4-9; C). The depositional matrix is composed of structureless to peloidal micrite. Laminations are rarely visible due to sediment reworking by burrowing organisms. Chondrites and Palaeophycus are the most common trace fossils (plate 4-9; D). The biota includes gastropods, leperditiid ostracods, and calcareous green algae (mainly Hedstroemia). Stenohaline skeletal

taxa are rare.

Interpretation: This lithofacies represents sediments deposited in low-energy shelf environments with poor water circulation (lagoons, bays). The low-diversity biota, moderate to intense bioturbation, lack of sedimentary structures and absence of subaerial exposure are usually diagnostic of semi-restricted, subtidal environments (Enos, 1983). The depositional textures also suggest relatively quiet environments only disturbed by storm waves. Modern examples of semi-restricted, subtidal settings include the Florida Bay restricted by Pleistocene limestones forming the Florida Keys (Enos and Perkins, 1977) and the inner shelf adjacent to western Andros Island tidal flat (Hardie, 1977). Unlike the mudstones/skeletal mudstones, the lenticular units associated with the fenestral mudstones are more likely deposited in small ponds forming low depressions on tidal flats.

Subtidal limestone lithofacies (see table 4-3)

Lithofacies 11: Skeletal wackestones/packstones

Description: This lithofacies occurs in both middle and upper limestone assemblages and forms units ranging from 1.0 to 6.0 m in thickness (plate 4-10; A and B). Most of the lithofacies consists of burrowed muddy sediment with an abundant fossil assemblage and wackestone to packstone texture (plate 4-10; C). The skeletal grains are mainly whole to slightly fragmented, but unabraded, bioclasts. The biota is dominated by echinoderms, brachiopods, gastropods, ostracods, Girvanella oncolites, and trilobites. Lithistid sponges, cephalopods, ramose bryozoans, calcareous algae (Hedstroemia, Nuia, Solenopora), and

- 132 -

TABLE 4-3. CHARACTERISTICS AND DEPOSITIONAL ENVIRONMENTS OF THE SUBTIDAL LIMESTONE LITHOFACIES

LITHOFACIES	LITHOLOGICAL CHARACTERISTICS	INFERRED ENVIRONMENTS
11- Skeletal wackstones/ packstones	moderate to strong bioturbation; diverse marine biota; _Girvanella_ oncolites; dolomitized burrows, middle and upper limestone assemblages	Low-energy, open shelf
12- Skeletal/oord grainstones	mixed abraded bioclasts and ooids; herringbone cross-bedding; diverse marine biota; oomoldic pores; associated lithologies with intraclasts and peloids; middle and upper limestone assemblages	High-energy sand shoals
13- Reef limestones	Massive mound-shaped to stratiform structures; sponges, bryozoans, tabulate corals, calcareous algae,; associated diverse biota; wackestone to bafflestone, locally bindstone texture; middle and upper limestone assemblages	Patch reefs and reef mounds
14- Basal intraclast grainstones	intraclasts with skeletal grains; diverse biota dominated by crinoid and lithistid sponges; keystone vugs; marine fibrous cement with pendulous orientation, patchy distribution; base of the upper limestone assemblage	Beachrock
15- Nodular mudstones	Siliciclastic interbeds; restricted biota; moderate bioturbation; patchy distribution; base of the upper limestone assemblage	Semi-restricted shelf
16- Brachiopod coquinas	Restricted fauna dominated by rhynchonellid brachiopods; quartz sands; patchy distribution; base of the upper limestone assemblage	Semi-restricted shelf

PLATE 4-10

LITHOFACIES 11: SKELETAL WACKESTONE/PACKSTONE

A. Field photograph (cross-section view) of lithofacies 11 forming an unevenly-bedded unit. Ile du Havre SE. Hammer is 30 cm.

B. Close-up of (A). Note the presence of solution seams. Ile du Havre SE. Lens cap is 50 mm in diameter.

C. Polished slab (cross-section view) of lithofacies 11 illustrating numerous bioclasts (mainly echinoderm fragments) floating within a bioturbated lime mud matrix. Ile du Havre NE.

D. Thin-section photomicrograph (plane polarized light) of lithofacies 11 showing various skeletal particles (echinoderms, bryozoans, brachiopods, gastropods, trilobites, ostracods). Scale bar is 1.0 mm.

tabulate corals are also present. The lack of sedimentary structures is due to extensive burrowing. The burrows are dense and form distinctive mottled fabrics. In thin-section (plate 4-10; D), the burrows are usually delimited by concentric haloes of micron-sized dolomite rhombs and/ or microspar. Planolites, Palaeophycus, and Chondrites are the most common trace fossils.

The Girvanella oncolites may compose up to 40% of the total volume but are usually less than 5% (plate 4-11; A and B). These oncolites range in size from about 0.3 to 2.0 cm in diameter. The oncolite microstructures are best described using a three-end member classification: 1) distinctly laminated, concentric filaments, 2) distinctly laminated, asymmetric filaments (plate 4-11; C), and 3) indistinctly wavy to dome-like filaments intergrown (plate 4-11; D)with small Ortonella bushes. In larger oncolites, the microstructures are sometimes transitional from types 1 or 2 in the inner, core areas to type 3 in the outer areas. Skeletal grains are the most common nuclei.

Interpretation: This lithofacies represents low-energy, subtidal sediments deposited in normal marine environments. The abundant and diverse biota, including various stenohaline taxa, is commonly associated with open marine conditions (Wilson and Jordan, 1983). The absence of sedimentary structures, slightly fragmented fossils, and depositional textures suggest relatively quiet depositional environments but oncolites indicate periods of intermittent turbulence. The oncolite microstructures are related to the degree of agitation during the oncolite growth (Logan et al, 1964; Wright, 1983). According to Wright (1983), forms which grew in higher energy conditions are subspherical and well laminated (type 1) while the forms that grew in lower energy

PLATE 4-11

LITHOFACIES 11:
SKELETAL WACKESTONE/PACKSTONE (ONCOLITIC)

Photomicrographs - Plane polarized light

A. Field photograph (cross-section view) of oncolite-rich layers (arrows) within lithofacies 11. Ile de la Maison. Lens cap is 50 mm in diameter.

B. Field photograph (bedding plane view) of a oncolite-rich layer in which oncolites are standing out in relief. Ile de la Maison. Lens cap for scale.

C. Thin-section photomicrograph showing distinctly laminated, asymmetric oncolites. Scale bar is 1.0 mm.

D. Thin-section photomicrograph illustrating the microstructure of Girvanella oncolites with indistinctly intergrown filaments. Scale bar is 100 um.
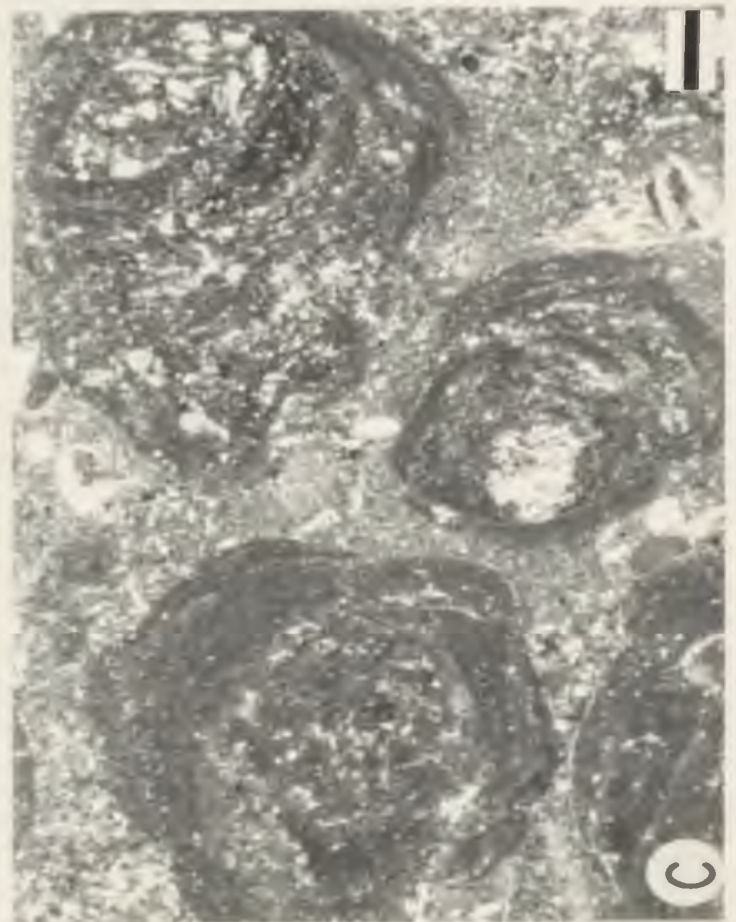
conditions are irregular and less well laminated (types 2 and 3).

Furthermore, Peryt (1981; 1983) regarded Girvanella oncolites as an

indicator of deposition under conditions of slow sedimentation. Similar

features are observed in modern open shelf deposits which are generally

muddy, with packstones and wackestones dominating the shelf environments

(Wilson and Jordan, 1983). A good Holocene example is the Hawk Channel

which forms a localized low depression on the Florida Shelf filled by

muddy skeletal carbonates (Enos, 1977).

Lithofacies 12: Skeletal-ooid grainstones

Description: The grainstones display sets, up to 1.0 m thick, of
trough cross-bedding characterized by bimodal-bipolar paleoflow
directions (plate 4-12; A). This lithofacies occurs as sets of
len-shaped units (2.0-8.0 m, thick) in both middle and upper limestone
assemblages and grades laterally into skeletal wackestones/packstones
(lithofacies 11). In general, the grainstone units are traced laterally
for several tens of metres but those in the upper assemblage are more
widespread (up to 10 km). Most of these grainstone units are capped by
paleokarst surfaces which exhibit several minor solutional forms (i.e.
karren, kamenitzas). In the upper assemblage, the intraclast content is
high (20-30%) where small wedge-shaped lenses with scoured bases occur
within the cross-bedded grainstones. In addition, small, well-sorted
peloids or small intraclasts are also present where the grainstone units
become more burrowed (mainly large Chondrites) and grade into laterally
associated lithofacies (plate 4-12; D).

This lithofacies is made up primarily of well-winnowed grainstones
with various percentages of skeletal debris and ooids (plate 4-12; B and

- 139 -

PLATE 4-12

LITHOFACIES 12: SKELETAL-OOID GRAINSTONE

Photomicrographs - Plane polarized light

A. Field photograph (vertical cliff exposure) of trough cross-bedding in lithofacies 12. Grande Pointe. Hammer is 30 cm.

B. Thin-section photomicrograph of lithofacies 12 with abundant skeletal debris of echinoderms, brachiopods, bryozoans and mollusks. Scale bar is 1.0 mm.

C. Thin-section photomicrograph of lithofacies 12 with abundant ooid particles. Note the spar-filled cortex and oomoldic pores (upper right corner). Scale bar is 1.0 mm.

D. Thin-section photomicrograph of lithofacies 12, found in units grading laterally into lithofacies 11, with abundant well-sorted peloids. Scale bar is 1.0 mm.
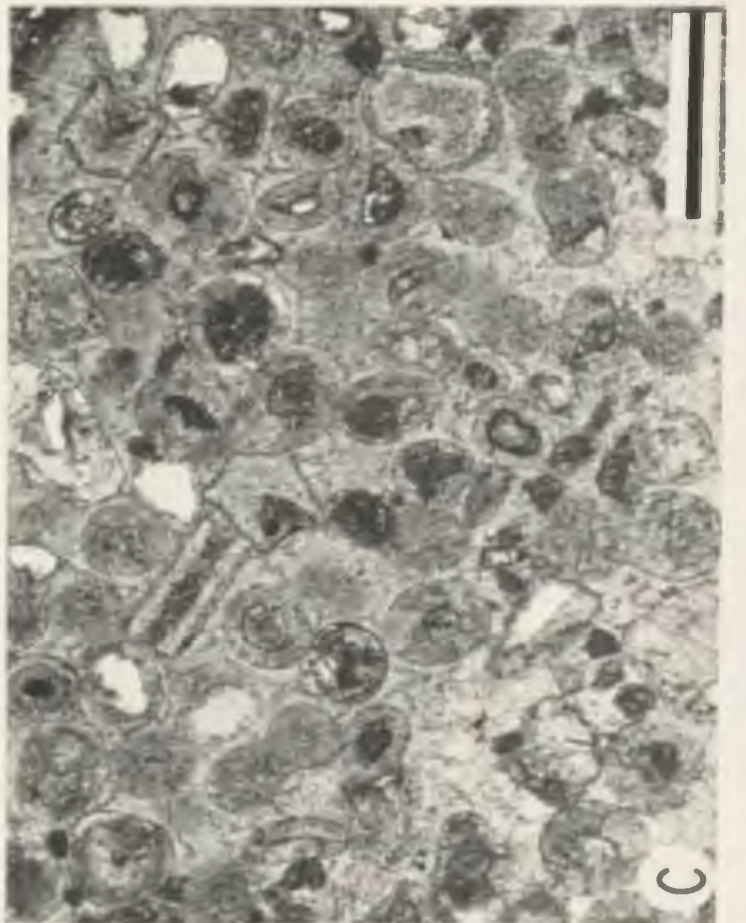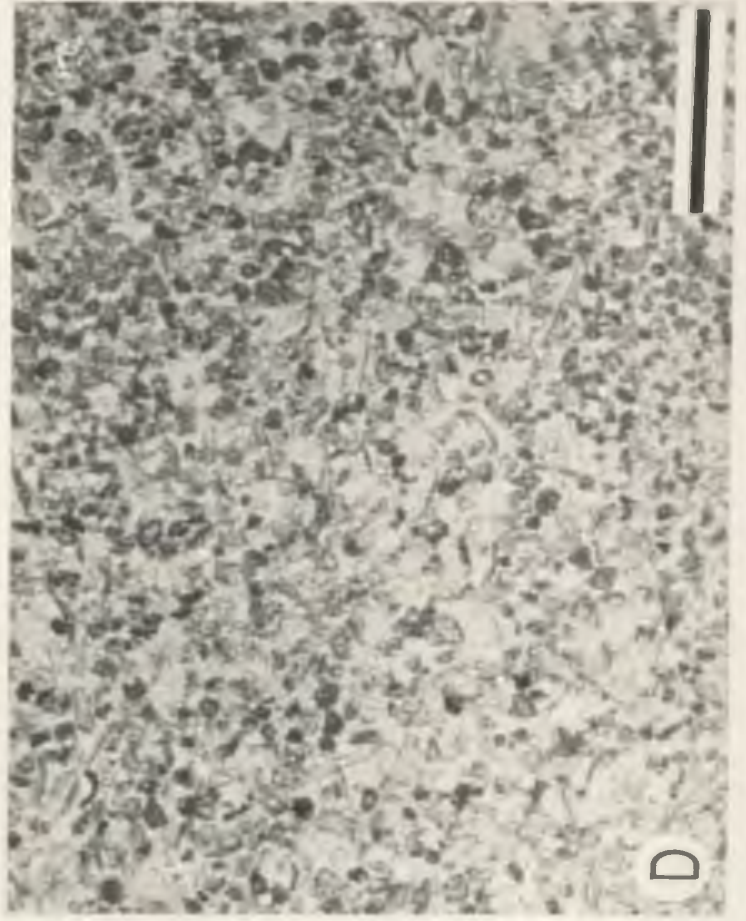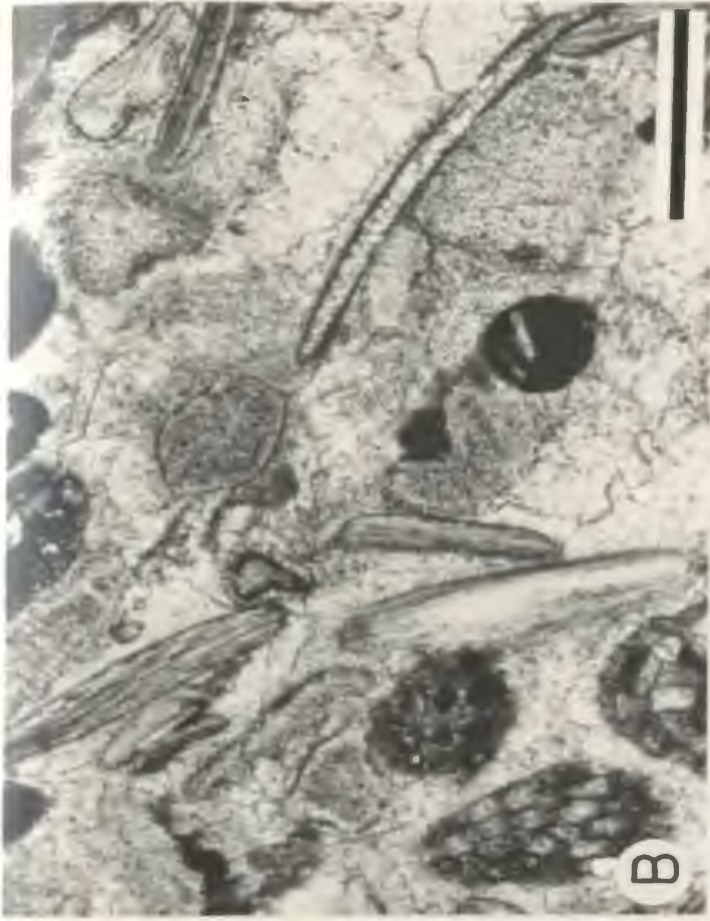
C). Micritic intraclasts are sometimes present. Skeletal debris is usually abraded grains derived from a diverse biota dominated by crinoids, gastropods, ramose bryozoans, brachiopods, trilobites, and ostracods. Cephalopods, lithistid sponges, tabulate corals, and calcareous algae (_Nuia_, _Girvanella_) are also present. The ooids may comprise up to 40% of the grains, but usually less than 10%. They are well-sorted, averaging 0.3 to 0.5 mm in diameter. The cortex is variable even within a single thin-section and displays a complete spectrum from well-preserved radial and/or concentric fabrics to spar-filled cortices. Small intraclasts or peloids are the most common nuclei. Secondary oomoldic (intragranular) pores created by selective dissolution of the ooids can locally make up 10% of the total rock volume. This lithofacies is discussed in further detail in chapter 7.

Interpretation: This lithofacies represents well-washed carbonate sands in shoal environments. The sedimentary structures, oolitic grains and obvious rounding of skeletal grains are indicative of high energy, shallow water conditions. In addition, the biota, including several stenohaline taxa, suggest an open marine setting with sea water of near normal salinity. Shoal environments were mainly influenced by tidal currents. Active sand shoals characterized by open marine fauna have been reported from several Holocene carbonate banks and platforms (Wilson and Jordan, 1983). Most of these shoals are only few metres below sea level. In some cases, shoal development may result in the formation of small islands that rise as much as 5 m above sea level (Harris, 1979). The extent of these on-shelf shoals are much less than their counterparts forming extensive sand bodies at the bank margin (Halley et al., 1983).

Lithofacies 13: Reef limestones

Description: The term "reef" is used here in a broad sense to encompass both bioherm and biostrome structures which characterize this lithofacies. The bioherms occur either alone or as an aggregate of small, massive mound-shaped structures. Individual bioherms are 0.5 to 2.0 m high, 2.0 to 10.0 m in diameter, and circular in plan. The biostromes are massive, poorly-bedded structures (0.8-2.0 m) that are laterally persistent, at least for several tens of metres. Larger skeletal metazoans are also commonly found in growth position in a lime mudstone matrix and include lithistid sponges, tabulate corals (Billingsaria sp. and Eofletcheria sp.), ramose and encrusting bryozoans, calcareous algae (Parachaetetes sp.). The bulk of the bioherms are dominated by branching, digitate, and domal metazoans with wackestone to floatstone (locally boundstone) depositional textures. They are sometimes capped by more tabular, lamellar, and encrusting metazoans with a bindstone texture. Crinoids, brachiopods, gastropods, trilobites, ostracods and cephalopods are also present. The skeletal content represents 40% to 60% of the total volume. Well-laminated stromatolite mats are ubiquitous. Of particular interest is the micritic matrix containing numerous elongate to tubular fenestrae (vermiform microstructure of Pratt, 1982b) and forming a crust (algal ?) that clearly encrusts the larger metazoans. The bioherms are surrounded by haloes of well-winnowed skeletal sands dominated by crinoid and ramose bryozoans but other bioherm-forming organisms are also present. These sands flank the bioherms with slopes up to 20 . The isolated bioherms and biostromes, however, are more commonly interbedded with skeletal wackestone/packstones (lithofacies 11) with only minor grainstone

lenses. This lithofacies occurs in both middle and upper limestone assemblages. In general, aggregated bioherms rest directly on the intra-Mingan paleokarst unconformity while the isolated bioherms and biostromes directly overlie the skeletal/ooid grainstone units (lithofacies 12).

Interpretation: The skeletal metazoan buildups are interpreted as patch reefs and reef mounds or blankets. The patch reef mounds represent wave-resistant structures which grew under relative high-energy conditions as evidenced by their flanking beds. The algal crust probably played an important role in binding and strengthening the larger building organisms. The reef mounds and blankets form "in situ" accumulations of large skeletal metazoans which grew under more quiet conditions. The poorly-developed zonation conforms to a growth model for reef mounds proposed by James (1984b) where only a colonization and sometimes a thin domination (i.e. mound cap) stages are present, but differences are also observed. The stabilization stage (basal bioclastic pile) is usually missing. The buildups rest directly, on paleokarst surfaces that formed during periods of subaerial exposures. These surfaces provided hard substrates on which building organisms could directly grow with subsequent marine invasion. Similar features (dimension, composition, structure) have been described from other Middle Ordovician on-shelf buildups (Pitcher, 1964; Kapp, 1975; Klappa and James, 1980). This lithofacies is discussed in further detail in chapter 5.

Lithofacies 14: Basal intraclast/skeletal grainstones

Description: This lithofacies forms the basal unit (0.5 to 3.0 m) in

the upper limestone assemblage where it directly overlies the intra-Mingan paleokarst unconformity, however, its distribution is patchy. The bedding attitude with slopes up to 30° is locally related to the irregular erosional topography generated by the paleokarst unconformity. Rocks of this lithofacies are mainly composed of grainstones or well-winnowed calcarenites to calcirudites (plate 4-13; A). Grainstones consist of a mixture of intraclasts and skeletal grains (plate 4-13; B) and display faint, inclined, trough cross-bedding. The intraclasts are sand to small pebble-sized, subrounded grains with a subspherical to irregular shape. Fenestral mudstones are the most common intraclasts. The abraded skeletal grains include several stenohaline taxa dominated by crinoids and lithistid sponges. Skeletal fragments of mollusks, brachiopods, bryozoans, trilobites, and ostracods are also present. Scattered ooids with a well-defined radial cortical layer are sometimes observed. Of particular interest are the numerous irregular shaped voids which are usually larger than the particles, and as a result both roofs and floors are bounded by more than one grain (plate 4-13; B). Associated diagenetic features include isopachous, locally gravitational, fringes of inclusion-rich, fibrous calcite cement (up to 0.5 mm, thick) around the particles.

Interpretation: This lithofacies represents well-winnowed sand bodies deposited near the strandline with development of beachrock deposits. They are interpreted to be beachrock (Donaldson and Ricketts, 1979; James and Choquette, 1983) because: 1) fibrous calcite cement of marine origin is the most common cement and 2) pendulous cement orientation which implies vadose precipitation in a two-phase air-water environment. Furthermore, the irregular shaped voids (plate 4-13; B),

PLATE 4-13

LITHOFACIES 14: BASAL INTRACLAST-SKELETAL GRAINSTONE
LITHOFACIES 15: NODULAR MUDSTONE
LITHOFACIES 16: BRACHIOPOD COQUINA

A. Polished slab (cross-section view) of lithofacies 14 composed mainly of a mixture of intraclast (light-coloured particles) and echinoderm fragments. Note the presence of keystone vugs (spar-filled pores); detail in (B). Ile Nue de Mingan E.

B. Thin-section photomicrograph (plane polarized light) showing irregular shaped voids, called keystone vugs (v), in intraclast-echinoderm grainstone. Scale bar 1.0 mm.

C. Field photograph (cross-section view) of nodular mudstones overlying laminated shales (beneath the hammer). The mudstone-shale contact represents the intra-Mingan unconformity in the upper part of the siliciclastic assemblage on Grosse Ile au Marteau. Detail in (D). Hammer is 30 cm.

D. Field photograph (cross-section view) showing interbedded nodular mudstones and shales in lithofacies 15. Lens cap is 50 mm.

E. Unpolished slab (bedding plane view) of lithofacies 16 showing abundant rhynchonellid brachiopods (<u>Rostricellula sp.</u>) standing out in relief. Ile du Havre E.
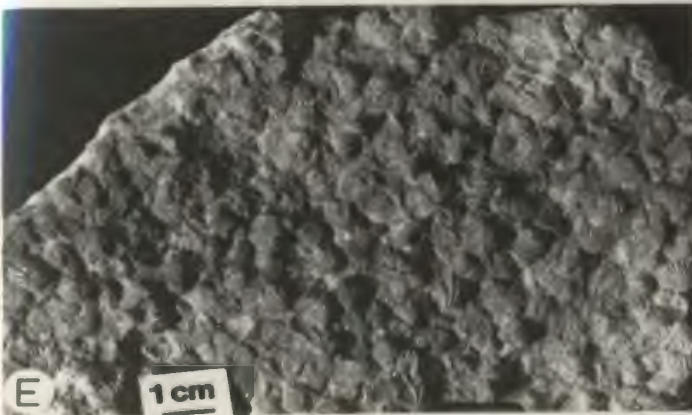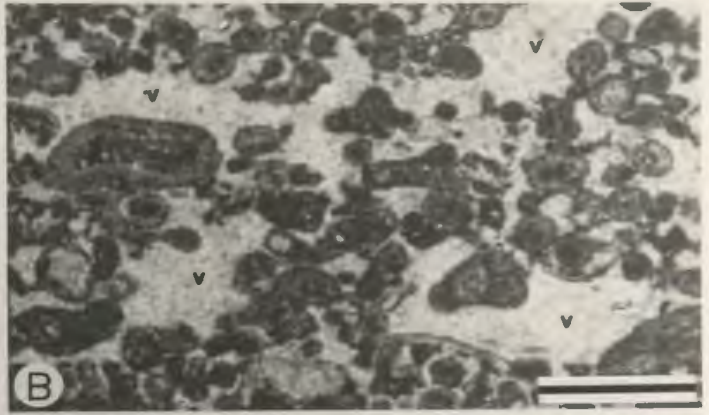
commonly termed "keystone vugs", are believed to result from air escaping in the intergranular pores as they are flooded with marine waters during the flood tidal cycle (Inden and Moore, 1983). The bedding attitude, sedimentary structures, and depositional textures are also compatible with the inferred depositional environment. Uncemented beach sediments were subsequently removed during marine transgression; this could explain the patchy lithofacies distribution at the base of the upper assemblage. Inden and Moore (1983) point out that the beach facies have low preservation potentials, especially those deposited above the effective wave base (beach foreshore and shoreface).

Lithofacies 15: Nodular mudstones

Description: This lithofacies locally occurs in units ranging from 0.3 to 2.0 m in thickness in the basal part of the upper limestone assemblage (plate 4-13; C). Its distribution is related to the intra-Mingan paleokarst unconformity. It is made up of thinly interbedded nodular mudstones and shales (plate 4-13; D). The mudstone interbeds (2.0-8.0 cm) are composed of homogeneous, slightly burrowed micrite. The restricted biota is dominated by ostracod and gastropods, however, the biota content is less than 5%. The shale interbeds (1.0-5.0 cm) consist of siliciclastic particles (shales and quartz silts).

Interpretation: This lithofacies represents muddy, sediments deposited in restricted, subtidal environments under relatively quiet conditions. The environmental restriction is inferred from the impoverished biota. These sediments were deposited in depressions surrounded by higher paleokarst landscapes following the onset of marine trangression but before complete shelf inundation. The siliciclastic

material in the shale interbeds is derived from a local source, more likely the lower siliciclastic assemblage which was locally exposed at this time.

Lithofacies 16: Brachiopod coquinas

Description: This lithofacies occurs as patchy lenticular units (10-40 cm) at the base of the upper limestone assemblage and overlies the intra-Mingan paleokarst unconformity. The lithofacies is commonly associated with the nodular mudstones (lithofacies 15). Most of the lithofacies consists of rhynchonellid brachiopods (Rostricellula sp.) making up to 50% of the total volume (plate 4-13; E). The brachiopod valves are whole to slightly fragmented. Although ostracods and gastropods are present, stenohaline skeletal taxa are rare or absent. Small intraclasts are ubiquitous. Siliciclastic content sometimes reaches 30% (mainly quartz sand).

Interpretation: Like the nodular mudstones, this lithofacies represents sediments deposited in relatively restricted, subtidal environments. Restricted settings may have a low diversity biota with only few well-adapted organisms. The lithofacies distribution suggests that the coquinas were preferentially concentrated in depressions related to the unconformity which first experienced marine inundation. Siliciclastic material was also derived from the lower assemblage. Basal lag coquinas are reported at the base of some Pleistocene shallowing-upward cycles overlying subaerial exposure surfaces and result from the onset of a transgression (Pierson, 1980).

LITHOFACIES DISTRIBUTION

The Mingan Formation can be subdivided into three distinct stratigraphic and paleoenvironmental assemblages (figs. 4-1 and 4-2). They are called the lower siliciclastic, middle limestone, and upper limestone assemblages. Of particular importance is the intra-Mingan paleokarst unconformity which influences distribution of both underlying lower and middle assemblages and sedimentation in the overlying upper assemblage.

The lower assemblage is composed of peritidal siliciclastic lithofacies and is characterized by an overall fining-upward texture (fig. 4-3). Dolomite and chert pebbles are sometimes present at the base of the assemblage which unconformably overlies the Romaine Formation. The assemblage consists, from the base to the top of: cross-bedded sandstones (lithofacies 4); laminated sandstones (lithofacies 3); and laminated shales (lithofacies 2). The sequence is commonly capped by silty dololaminites (lithofacies 1). Channellized sandstone units (lithofacies 5) are sometimes associated with the laminated shales and/or sandstones. Lateral lithofacies variations also occur within the lower assemblage. When the cross-bedded sandstones are absent, the assemblage is mainly composed of laminated shales with laminated sandstones (e.g. Ile du Perroquet and Ile Saint-Charles sections). Furthermore, the upper part, if not most, of the assemblage is locally eroded by the intra-Mingan unconformity (e.g. Grande Pointe and Ile du Fantome sections). Its thickness is relatively constant, averaging 5 m, but the Ile Innu section is only 1.5 m thick and is probably related to some erosional relief associated with the Romaine-Mingan unconformity which is used as a datum.

Figure 4.2- Stratigraphic cross-section showing the distribution of the lithofacies assemblages in the Mingan Formation. Note the position of the intra-Mingan unconformity (PK). Datum base is the Romaine-Mingan contact. C: Corbeau Member; P: Perroquet Member; F: Fantome Member; G: Grande Ile Member.

LITHOFACIES ASSEMBLAGES

G — UPPER

F }
P } MIDDLE

C — LOWER

W   E

G

?

G

F

P

F

F

F

C

PK

Romaine Formation

10 M

15 KM   0
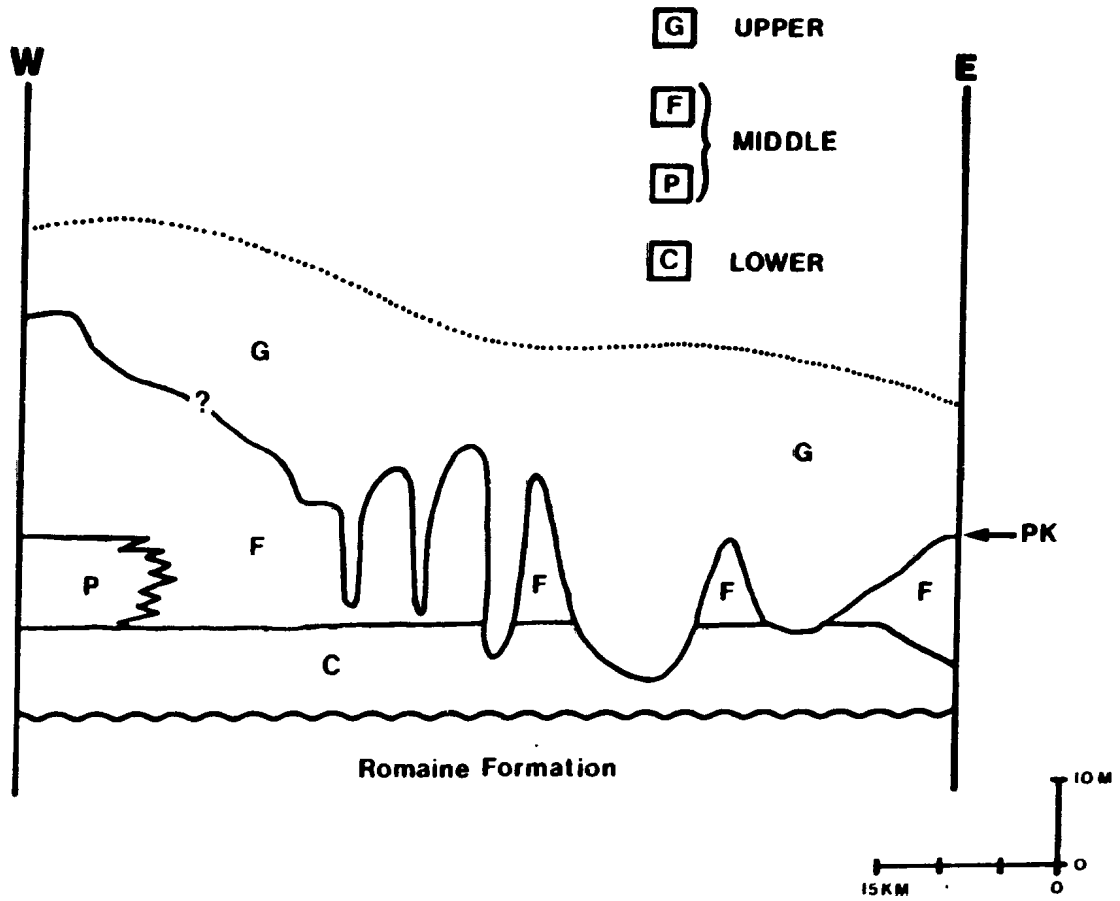
Figure 4.3– Schematic description of the peritidal lithofacies in the lower siliciclastic assemblage which is characterized by a fining-upward character. Major lithofacies are, in ascending order: trough cross-bedded sandstones (lithofacies 4); ripple-laminated sandstones (lithofacies 3); channeilized sandstones (lithofacies 5); ripple-laminated shales (lithofacies 2) and silty dololaminites (lithofacies 1).

LOWER SILICICLASTIC ASSEMBLAGE

SILTY
DOLOLAMINITES

SUPRATIDAL
ALGAL MARSH

RIPPLE-LAMINATED
SHALES

INTERTIDAL
MUD FLAT

CHANNELLIZED
SANDSTONES

TIDAL
CHANNEL

RIPPLE-LAMINATED
SANDSTONES

INTERTIDAL
SAND FLAT

CROSS-BEDDED
SANDSTONES

NEARSHORE
SAND BARS
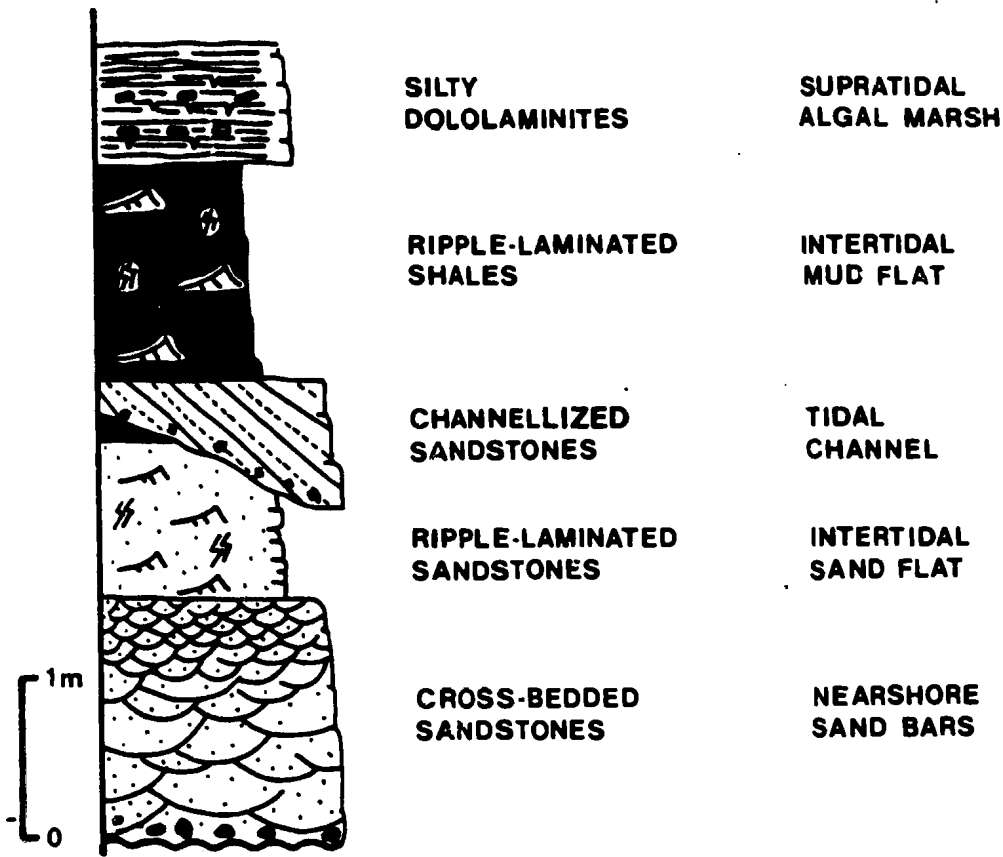
The <u>middle</u> <u>assemblage</u> consists of peritidal and subtidal limestone lithofacies (fig. 4-1). This assemblage has a gradational and conformable contact with the underlying lower siliciclastic assemblage while its upper boundary is delimited by the intra-Mingan unconformity (fig. 4-2). The middle assemblage is characterized by a repetition of lithofacies on a metre scale (fig. 4-4). This "non-cyclic" repetition consists sometimes, from the base to the top of: mudstones/skeletal wackestones (lithofacies 10): fenestral mudstones (lithofacies 6): cryptalgalaminites (lithofacies 7). Gastropod packstones (lithofacies 9) and channellized intraclast grainstone (lithofacies 8) units are sometimes present. Most lithofacies cannot be correlated between adjacent sections only a few kilometres apart. The fenestral mudstone is the most common lithofacies making up to 50% of the total volume. The intra-Mingan unconformity, with its substantial relief, controls the distribution and thickness of the assemblage. Sections, up to 20 m thick, can be measured locally. Finally, subtidal lithofacies (mainly lithofacies 11 and 12) intertongue with the lower part of the middle assemblage in the easternmost part of the study area (fig. 4-2).

The <u>upper</u> <u>limestone</u> <u>assemblage</u> contains only subtidal limestone lithofacies (fig. 4-1). The lower boundary of this assemblage corresponds to the intra-Mingan unconformity while its upper boundary is covered by extensive Pleistocene deposits and still remains unknown in the study area (fig. 4-2). This assemblage directly overlies either the middle limestone assemblage or the lower siliciclastic assemblage depending upon local erosional relief of the unconformity. A pre-depositional topography also controls the lithofacies pattern of the upper assemblage. The assemblage consists of superimposed, lenticular

Figure 4.4- Schematic diagram showing the recurrent (non-cyclic) lithofacies association in the middle limestone assemblage. Major lithofacies are, in order of abundance: fenestral mudstones (lithofacies 7); cryptalgalaminites (lithofacies 6); intraclast grainstones (lithofacies 8) and bioturbated skeletal wackestones (lithofacies 10).

MIDDLE LIMESTONE ASSEMBLAGE

CRYPTALGALAMINITE

SUPRATIDAL
ALGAL MARSH

BIOTURBATED
LIME MUDSTONE

FENESTRAL
MUDSTONE

CHANNELLIZED
INTERTIDAL
BELT

INTRACLAST
GRAINSTONE

BIOTURBATED
WACKESTONE

SUBTIDAL
LAGOON

1 m
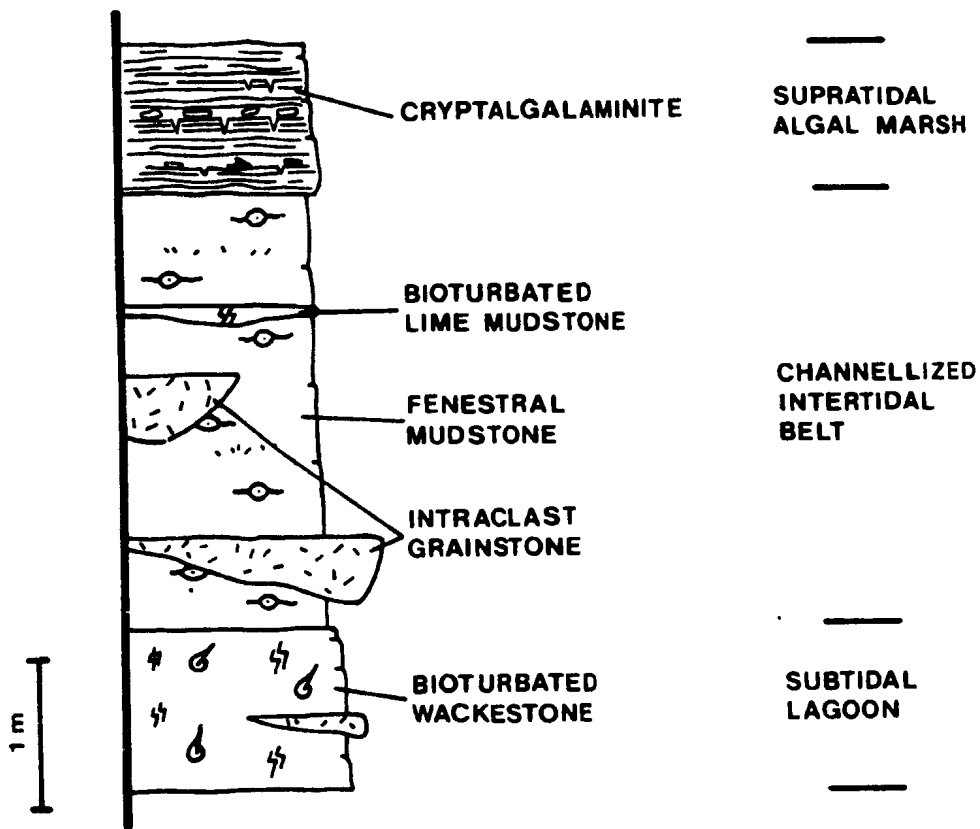
grainstone (lithofacies 12) units with their locus in topographic

depressions related to the unconformity. The lenticular grainstone

units grade laterally into equivalent skeletal limestones (lithofacies

10 and 11). Minor lithofacies such as nodular mudstones (lithofacies 15)

and brachiopod coquinas (lithofacies 16) are stratigraphically

restricted to the lower part of these depressions. Furthermore,

carbonate buildups (lithofacies 13) and intraclast grainstones

(lithofacies 14) are patchily distributed above the unconformity.

The lateral variation of lithofacies in the upper assemblage is

illustrated in greater detail in figure 4-5. Each lenticular grainstone

unit is usually capped by a paleokarst surface and consists mainly of

skeletal/ooid grainstones with some channellized, intraclast-rich

sub-units. The grainstone units become more burrowed and grade laterally

into adjacent skeletal limestones within 300 metres. These adjacent

limestones are dominated by mudstones and skeletal wackestones

(lithofacies 10) in the northern part of the study area whereas the

southern part is composed mainly of skeletal wackestones and packstones

(lithofacies 11).

DEPOSITIONAL MODELS

Some problems are raised by an integrated depositional model for the

Mingan Formation. Marked shifts from siliciclastic to carbonate

deposition is observed in peritidal lithofacies of the lower and middle

assemblages. Furthermore, the irregular pre-depositional topography

created by the intra-Mingan unconformity played a significant role in

the distribution of lithofacies within the upper assemblage. For these

reasons, each lithofacies assemblage is now treated as a distinct

- 158 -

Figure 4.5- Schematic cross-section showing the lateral variations of lithofacies in the upper limestone assemblage. Selected idealized sections display the spectrum of these variations within a lenticular grainstone unit bounded by paleokarst surfaces. SG: skeletal/ooid grainstones with well-defined trough cross-bedding. IG: intraclast grainstones in channellized unit, PG: bioturbated peloid grainstones with poorly-defined trough cross-bedding (lithofacies 12); MW: mudstone/skeletal wackestones (lithofacies 10); WP: skeletal wackestones and packstones (lithofacies 11). See figure 1.2 for symbols.
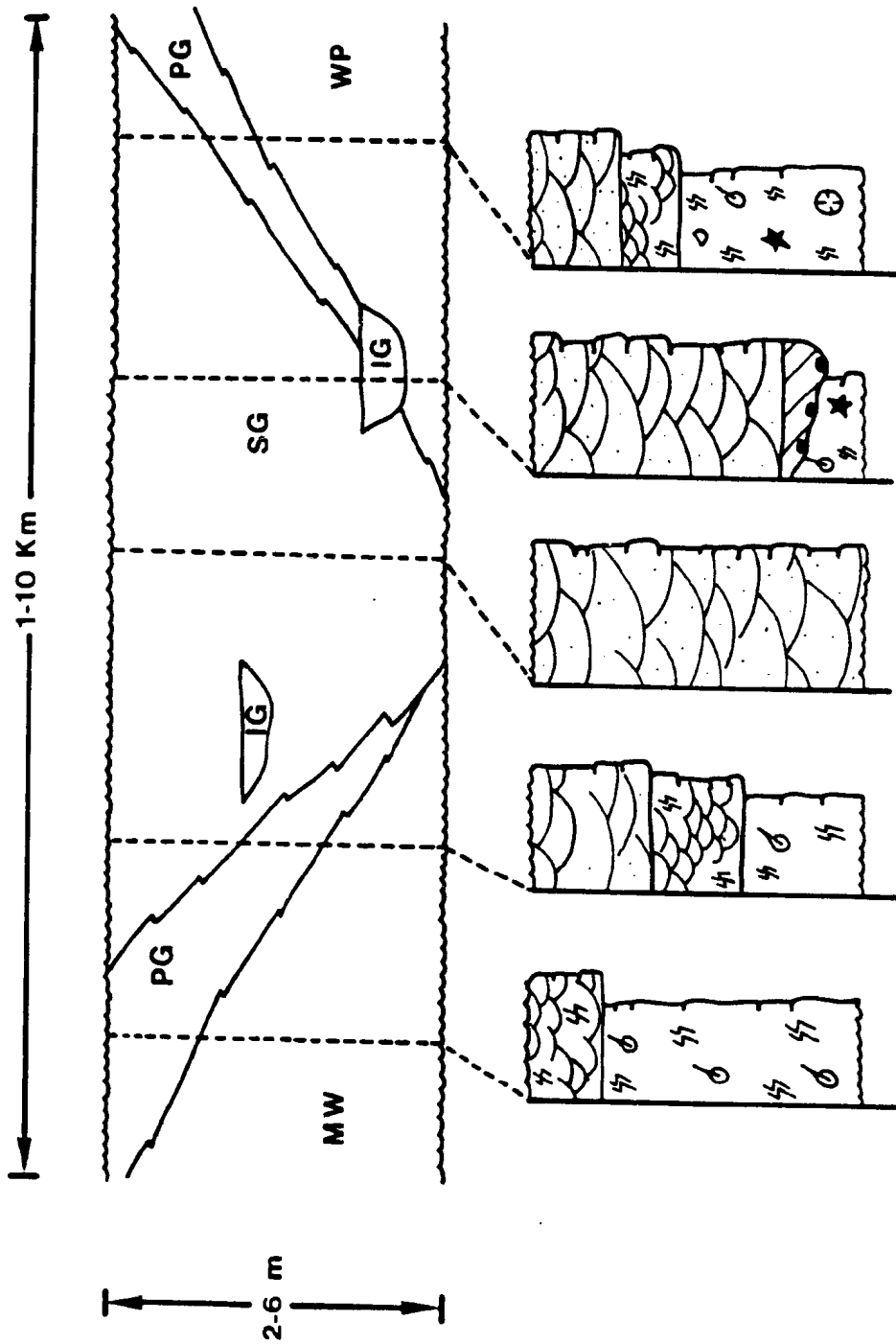
depositional phase.

Lower siliciclastic assemblage

The lower lithofacies assemblage is interpreted as a fining-upward
sequence deposited after a marine transgression occurred over the
subaerially exposed Romaine Formation. The basal sandstones with their
bimodal supermature texture (Folk, 1968) suggest that more or less
extensive deflationary eolian deposits covered the exposed platform and
were subsequently reworked by marine processes. The siliciclastic
material could have been transported by low-gradient rivers draining the
Canadian Shield during periods of more humid climate.

Of particular importance are the common Trypanites borings on the
Romaine unconformity and on pebbles immediately above it. Trypanites
borings are interpreted by most workers (Ekdale et al., 1984; Frey and
Pemberton, 1984) as being the product of marine organisms (probably
sipunculan worms). This suggests that the eolian deposits above the
unconformity were completely removed leaving only a pebble pavement as a
record of the transgressive event. The continuous shoreface erosion
(beach, barrier island) concomitant with shoreline advance is commonly
regarded as an important erosional process in most of the transgressive
situations (Reinson, 1984).

The fining-upward sequence is interpreted to result from the
migration of tidal flat sediments over nearshore marine sediments (fig.
4-3). This sequence displays similar lithofacies to those observed in
tidal flat systems along the coast of the Netherlands and Germany
(Reineck, 1975; Weimer et al., 1982). Diagnostic sedimentary structures
of these modern analogs are commonly observed in the sequence: mud

cracks, moderate to intense bioturbation, herringbone cross stratification, and wavy, lenticular, and flaser bedding. In accordance with Walter's rule of facies succession, sequential analysis suggests a depositional model (fig. 4-6) with two major environments; a tidal flat complex and a nearshore sand belt.

Tidal flat: The tidal flat represents a depositional system with three distinct morphological elements: supratidal algal marshes, intertidal flats, and tidal channels. The supratidal zone consisted of low-lying platforms on which algal mats flourished (lithofacies 1). This zone experienced long periods of subaerial exposure disturbed only by storm tides. The intertidal zone is further subdivided into a high intertidal mud flat and low intertidal sand flat. The mud flats occurred in the upper intertidal zone and usually contained slightly laminated muds with thin sand laminae (lithofacies 2). The sand flats were located in areas closest to the low tide line and consist of both sandy wave and current ripple laminae with some muddy lenses or layers (lithofacies 3). All of these sediments, however, were modified or reworked by bioturbation. Furthermore, the tidal flats are dissected by some tidal channels generating point bar deposits as they migrated laterally.

Nearshore sand: A sand belt was probably located seaward of the tidal flat system. The sand belt consisted of bars and large ripple bedforms demonstrating active bedload transport by tidal currents (lithofacies 4). Other depositional environments themselves are not now observable in the study area, however, the presence of skeletal grainstone lenses interlayered with these sands suggests that carbonate sedimentation was predominent in more offshore areas. The nearshore sand belt probably acted as a barrier that effectively inhibited the influx

Figure 4.6- Depositional model of the lower siliciclastic assemblage, showing the progradation of peritidal environments over adjacent subtidal environments. Two major depositional environments are recognized: 1)tidal flats with algal marshes, tidal channels, mud and sand flats and 2) a belt of nearshore sand bars.

LOWER SILICICLASTIC ASSEMBLAGE
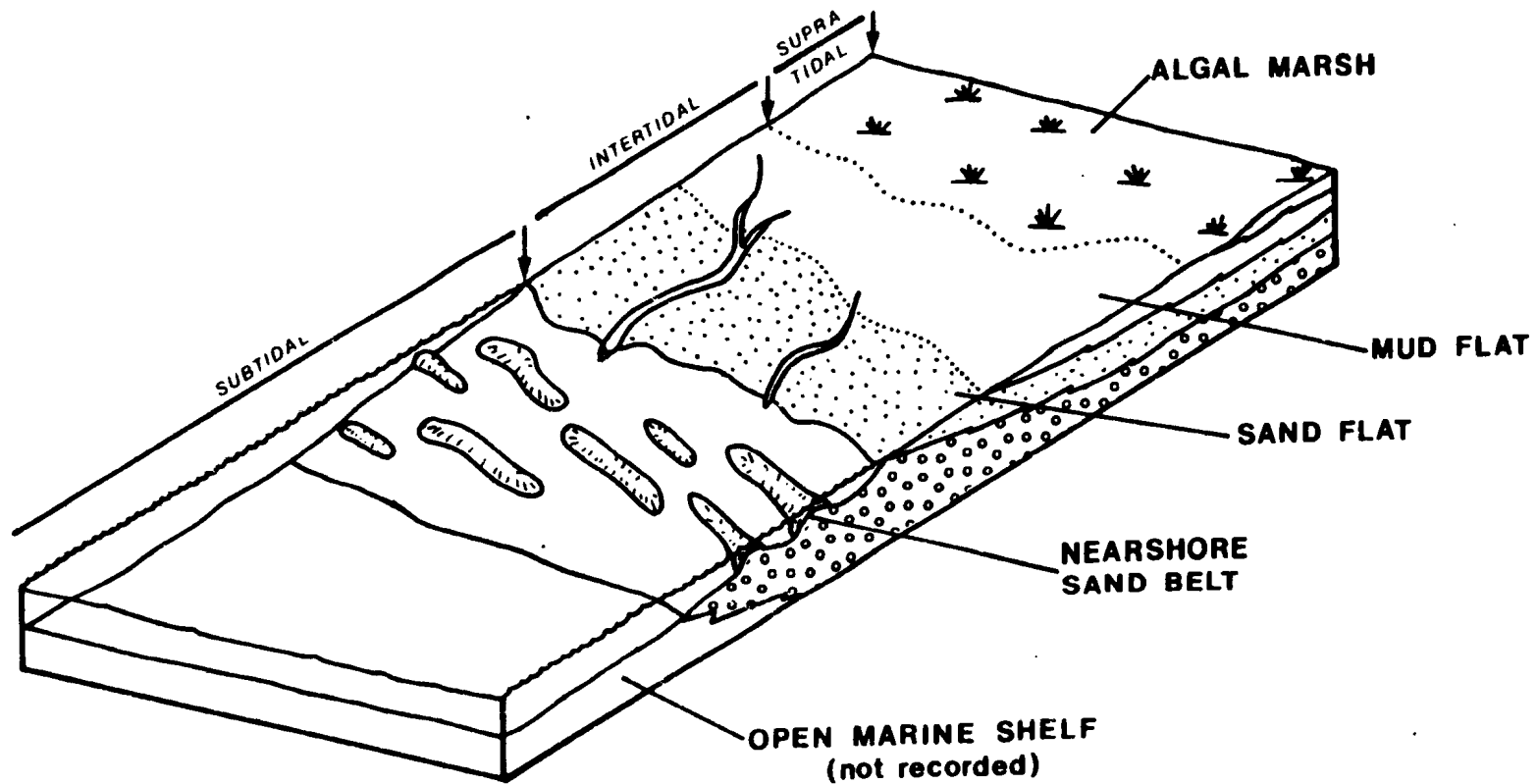
of terrigenous clastic material onto the shelf.

Middle limestone assemblage

The middle assemblage is composed mainly of recurrent peritidal lithofacies interdigitated with subtidal lithofacies in the eastern part of the study area. Cycles associated with the peritidal lithofacies can only be inferred because most of them cannot be traced between two closely-spaced sections, and as result the individual lithofacies are laterally gradational, even in a single bed. A complete "cycle" is illustrated in figure 4-4 and is based on both lateral and vertical lithofacies association with respect to the fenestral mudstones; the most common lithofacies in this assemblage. The overall sequence results from lateral migration of peritidal sediments over open shelf sediments. The suggested depositional model (fig. 4-7) is represented by the following morphological elements: tidal flat complex, lagoon, and open shelf.

Tidal flat: The tidal flats formed a complex environmental mosaic which is subdivided into supratidal algal marshes and an intertidal belt. The supratidal coastal marshes were low-lying plains which contained mud-cracked, algal-laminated sediments (lithofacies 6). The layering is thought to have resulted from alternating algal mat growth and flooding and deposition of marine sediments during storms (Monty and Hardie, 1976; Shinn, 1983b). The channellized belt consisted of intertidal mud flats with several channels and ponds. The intertidal flat deposits are muddy in composition and display evidence of subaerial exposure (fenestrae, mud cracks) (lithofacies 7). They were truncated by tidal channels which were filled by intraclastic material derived from

- 165 -

Figure 4.7- Depositional model of the middle limestone assemblage illustrating the major depositional environments.

MIDDLE LIMESTONE ASSEMBLAGE

ALGAL MARSH MUD FLAT

TIDAL CHANNEL

POND

LAGOON

SUPRA TIDAL

INTERTIDAL

SUBTIDAL

SAND SHOAL

OPEN SHELF
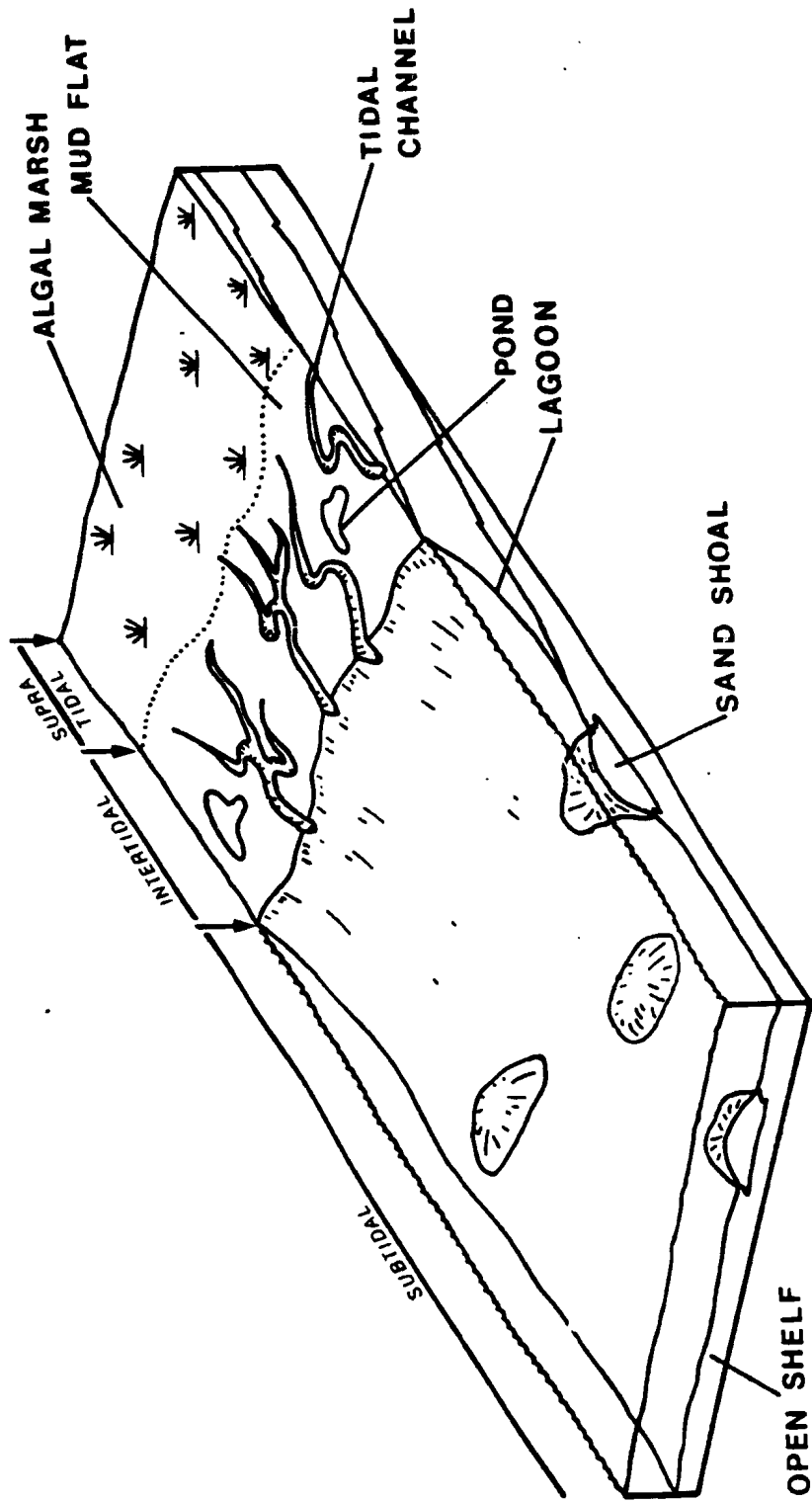
lithified tidal flat sediments (lithofacies 8). Scattered ponds were found in gentle topographic depressions over the intertidal mud flats. Sediments in these ponds, characterized by limited stratigraphic extent, are composed of highly bioturbated muds with little biotic content (lithofacies 10). In general, the tidal flats had a restricted fauna dominated by ostracods and gastropods. These sediments are similar to the Andros Island tidal flat deposits which presently develop under relatively low-energy and non-arid climatic conditions.

Lagoon: A subtidal zone formed a belt located seaward of the tidal flats and represents semi-restricted, lagoonal environments. In general, the lagoon deposits consist of burrowed muddy sediments with little biotic content (lithofacies 10). The low diversity biota was dominated by few well-adapted organisms (ostracods, gastropod, calcareous green algae) and invokes the existence of environmental restriction (geographic, salinity). Stenohaline organisms were rare or absent. Furthermore, the lagoon was vital for the tidal flat system because it was its source of sediment (Shinn, 1983b).

Open Shelf: The tidal flat system and lagoon were flanked by open shelf sediments characterized by a normal marine fauna including various stenohaline forms. The open shelf deposits are mainly composed of bioturbated muddy sediments (lithofacies 11) deposited below the normal wave base, however, sand shoals (lithofacies 12) also occur. These sand shoals probably inhibited water circulation onto the shelf and affected sedimentation in the inner shelf areas.

Upper limestone assemblage

The upper assemblage contains only subtidal limestone lithofacies

which occur as thin, shallowing-upward sequences. In general, these sequences grade upward from fine-grained, subtidal wackstones and packstones to well-winnowed, subtidal grainstones. They are usually capped by ancient subaerial exposure surfaces. Some sequences, however, are formed only by one or the other lithofacies. Such lateral variations (fig. 4-5) result from local hydrodynamic conditions related to the underlying intra-Mingan unconformity.

The intra-Mingan unconformity represents a prolonged period of subaerial exposure that preceded deposition of the upper assemblage. The erosional processes (mainly karstic) created an irregular topography (ridges, depressions, pits) with relief as much as 20 metres. With subsequent sea level rise, the landward migration of discrete sedimentary belts was inhibited by pre-depositional topography, and as a result more local hydrodynamic conditions controlled the facies pattern. The style of sedimentation on modern carbonate platforms is also thought to be influenced to varying degrees by antecedent topography of the Pleistocene basement (Purdy, 1974; Goreau and Land, 1974; Enos, 1977; Harris, 1979; Hine, 1983).

Minor fine-grained sediments (lithofacies 15 and 16) which show evidence of environmental restriction were first deposited in topographic depressions with the subsequent sea level rise. A period of sediment transport and winnowing occurred only with further marine inundation across the shelf. Strong tidal currents were focussed into the topographic depressions where carbonate sand bodies formed. Several environments are recognized in the proposed depositional model (fig. 4-8): island, restricted shelf, tidal delta, patch reef, and open shelf.

Island: The islands correspond to partially submerged ridges related

Figure 4.8- Depositional model of the upper limestone assemblage illustrating the major depositional environments. Tidal deltas are located between inter-island gaps.

UPPER LIMESTONE ASSEMBLAGE

ISLAND

TIDAL DELTA

RESTRICTED SHELF

BEACH

PATCH REEF

OPEN SHELF
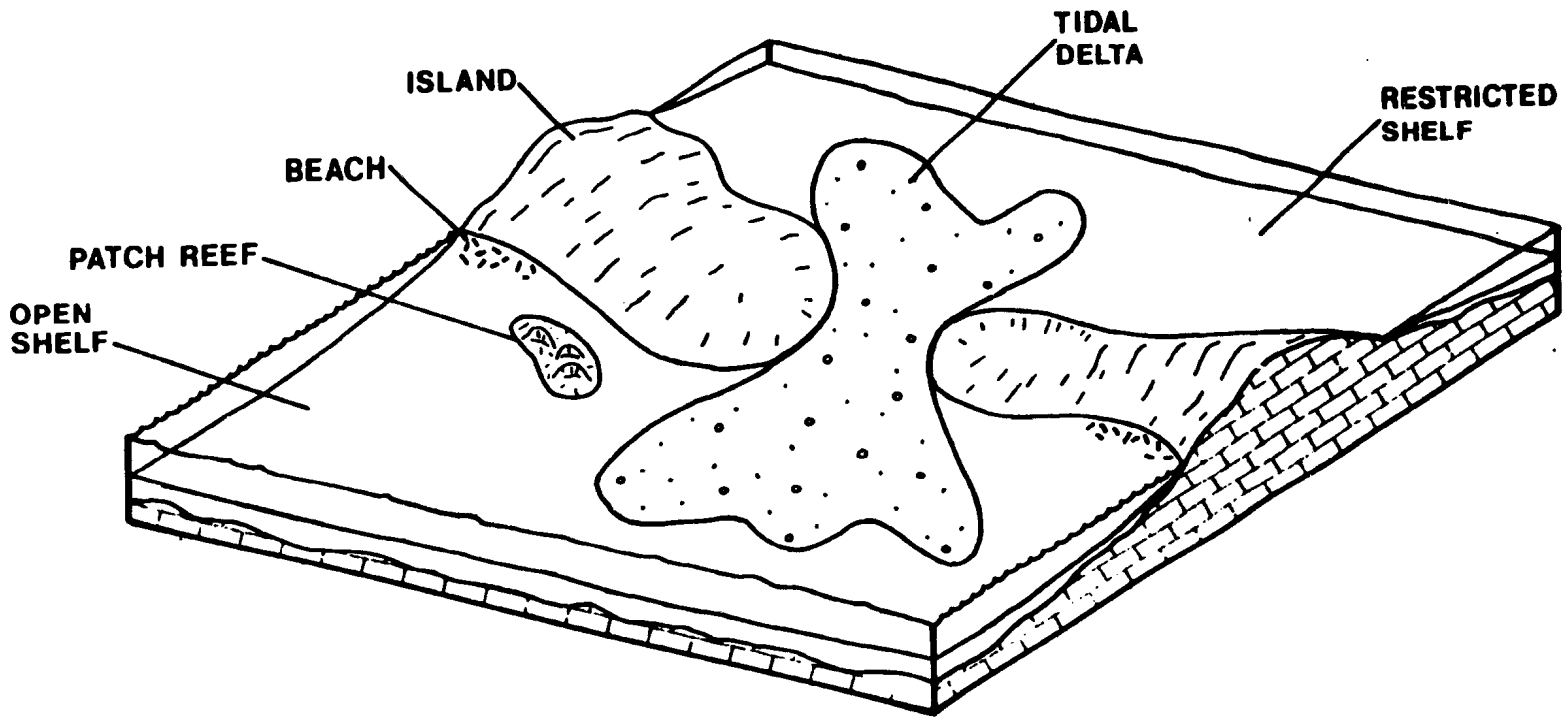
to the intra-Mingan unconformity. Their shorelines were characterized by rocky coasts and beach deposits. Rocky shorelines sometimes exhibited intertidal notches associated with small-scale littoral karst forms and encrusting marine organisms. The beaches were patchy and consisted of seaward dipping sand deposits that were lithified by marine fibrous cements (lithofacies 14).

Restricted shelf: A semi-restricted, low-energy shelf was located shoreward of the islands. These islands prevented adequate water circulation, and as a result restricted conditions prevailed over most of the area. The sediments were predominantly muddy with little or no biotic content (lithofacies 10). The biota included few stenohaline forms.

Tidal delta: Carbonate sand bodies were generated in response to strong tidal currents funnelled into depressions between the islands. They formed fan-shaped flood and ebb tidal deltas dissected by some channels. The ebb-dominated tidal currents probably built larger deltas that extended seaward. In general, these tidal deltas are composed of ooid and skeletal sands (lithofacies 12) but more intraclastic material is found in the channels. The tidal deltas actively migrated over the adjacent fine-grained shelf sediments. The transition consists of burrowed peloid muddy sands. Fine modern analogs are found in the southern Florida Keys (Multer, 1969; Enos, 1977) and in the Bahamas (Halley et al, 1983, figs. 17 and 18) where tidal deltas are located in the passes between islands.

Open shelf: An open marine, subtidal shelf was located seaward of the islands. The shelf contained mainly burrowed muddy sediments reflecting bottom conditions probably below fairweather wave base. The

biota was normal marine with various stenohaline taxa.

Patch reef: Small reefs and organic blankets were patchly distributed in the open shelf. Reefs were sometimes grouped in clusters and surrounded by well-winnowed sands composed of reef-derived bioclasts. Their distribution was controlled by underlying subaerial exposure surfaces which also provided a lithified substrate for the growth of building organisms such as sponges, tabulate corals, bryozoans, and calcareous algae.

SUMMARY

1) In comparison with the Romaine Formation, the Mingan Formation represents a more complex environmental mosaic where fifteen lithofacies, grouped into three distinct assemblages, can be recognized. Styles of sedimentation in the Mingan Formation changed through time from a siliciclastic peritidal regime following the initial transgression over the post-Romaine unconformity to a dominantly peritidal limestone regime to finally an open marine, subtidal limestone regime.

2) With the Chazyan trangession, a blanket of possibly eolian (residual) sediment overlying the post-Romaine paleokarst unconformity was reworked and redeposited at, or near, the strandline.

3) The fining-upward composition of the lower siliciclastic assemblage (Corbeau Member) resulted from the progradation of tidal flat sediments over strandline sands. Four distinct sub-environments in this tidal flat system can be examined: supratidal algal marshes, intertidal

mud and sand flats, and tidal channels.

4) Siliciclastic sedimentation changed abruptly to carbonate
sedimentation with the deposition of the middle assemblage composed of
peritidal limestones (Fantome Member) and to a lesser extent of subtidal
limestones (Perroquet Member). This assemblage, dominated by fenestral
mudstones, is non-cyclic and displays abrupt lateral facies changes. Its
depositional evolution indicates that an extensive Bahamas-style tidal
flat system prograded laterally over adjacent lagoonal and open shelf
sediments, limited to areas in the eastern Mingan Islands.

5) A period of subaerial exposure occurred prior to deposition of
the upper lithofacies assemblage (Grande Pointe Member), resulting in
the formation of a regional paleokarst with substantial relief. With
subsequent reinundation, sedimentation was locally controlled by this
irregular basement topography. Of particular importance, was the
development of sand shoals in the basement depressions, forming tidal
deltas (1-10 km wide). Three distinct depositional cycles of these sand
shoals and associated sediments, are present (see chapter 7 on
calcarenite cycles). Other recognized environments include: islands,
semi-restricted shelf, beaches, local patch reefs and open shelf.

CHAPTER 5

MINGAN REEF LIMESTONES

Reef limestones in the Mingan Formation, deposited during early
Middle Ordovician time, are commonly associated with shallow-water
carbonate sediments on an open shelf setting. Although most reefs are
small, mound-shaped bioherms, biostromes are also present. Of particular
importance is their common association with paleokarst surfaces which
served as foundations during reef growth.

The reefs were constructed primarily by lithistid sponges,
bryozoans, tabulate corals, and calcareous algae, together with algal
stromatolites. They display a remarkable degree of variation in organic
composition with several distinct end-member assemblages.

The Mingan reefs are similar in several respects (size, internal
composition, associated deposits) to other Early and Middle Paleozoic
reefs (James and Kobluk, 1978; Toomey and Nitecki, 1979; Klappa and
James, 1980; Pitcher, 1964; Scoffin, 1971; Riding, 1981). They grew
during one of the most important periods in the evolution of reefs
because several reef building taxa first appear in abundance in the
fossil record at this time. The stratigraphic relationships, lithology,
organisms, diagenesis, and deposition history of the Mingan reef
limestones are reported here.

TERMINOLOGY

As discussed in chapter 4, the term "reef" is used here in the broad

sense, to include all sorts of biostromes and bioherms regardless of their internal composition. The terms "biostrome" and "bioherm", when used, refer exclusively to the shape of the reef limestones; biostrome denotes a stratiform unit and bioherm denotes a massive mound-shaped structure. Depositional textures in the reef limestones are described using Embry and Klovan's (1971) classification, which is a modification of Dunham's (1964) classification applied to reefal carbonates.

Mingan reefs like other small Phanerozoic reefs may be subdivided into three distinct facies (James, 1984b): 1) "core facies", represented by massive limestones of _in situ_ remains of building organisms in a matrix of skeletal debris and lime mud; 2) "flank facies", represented by calcirudites and calcarenites of reef-derived material dipping and thinning away from the core and 3) "inter-reef facies", represented normal shallow-water, subtidal limestones, unrelated to reef formation.

REEFS AND ASSOCIATED DEPOSITS

Reefs are present in both Perroquet and Grande Pointe Members of the Mingan Formation where they are associated with various subtidal limestone lithofacies. These reefs occur at more than twelve localities in the study area (fig. 5-1) and may be grouped into three distinct types: 1)biostromes; 2) bioherms and 3) bioherm complexes.

Biostromes

Biostromes are massive, stratiform units up to 2.0 m thick (fig. 5-2) and can be traced for several tens of metres at the scale of outcrop (plate 5-1; A). Paleokarst surfaces capping underlying calcarenite cycles acted as a foundation for these reef limestones (see

Figure 5.1- Location map showing the distribution of reef types within
the Mingan Formation. 1) lithistid sponge/bryozoan/tabulate
biostrome; 2) tabulate coral bioherm; 3) bryozoan bioherm; 4)
solenoporacean algae/tabulate coral bioherm complex; 5) lithistid
sponge/bryozoan/tabulate coral bioherm complex. See figure 1-1 for
locality names.

MINGAN REEF LIMESTONES

① SPONGE-BRYOZOAN-CORAL BIOSTROME
② CORAL BIOHERM
③ BRYOZOAN BIOHERM
④ CORAL-ALGAE BIOHERM COMPLEX
⑤ SPONGE-BRYOZOAN-CORAL BIOHERM COMPLEX

N

0   5   10   15 KM
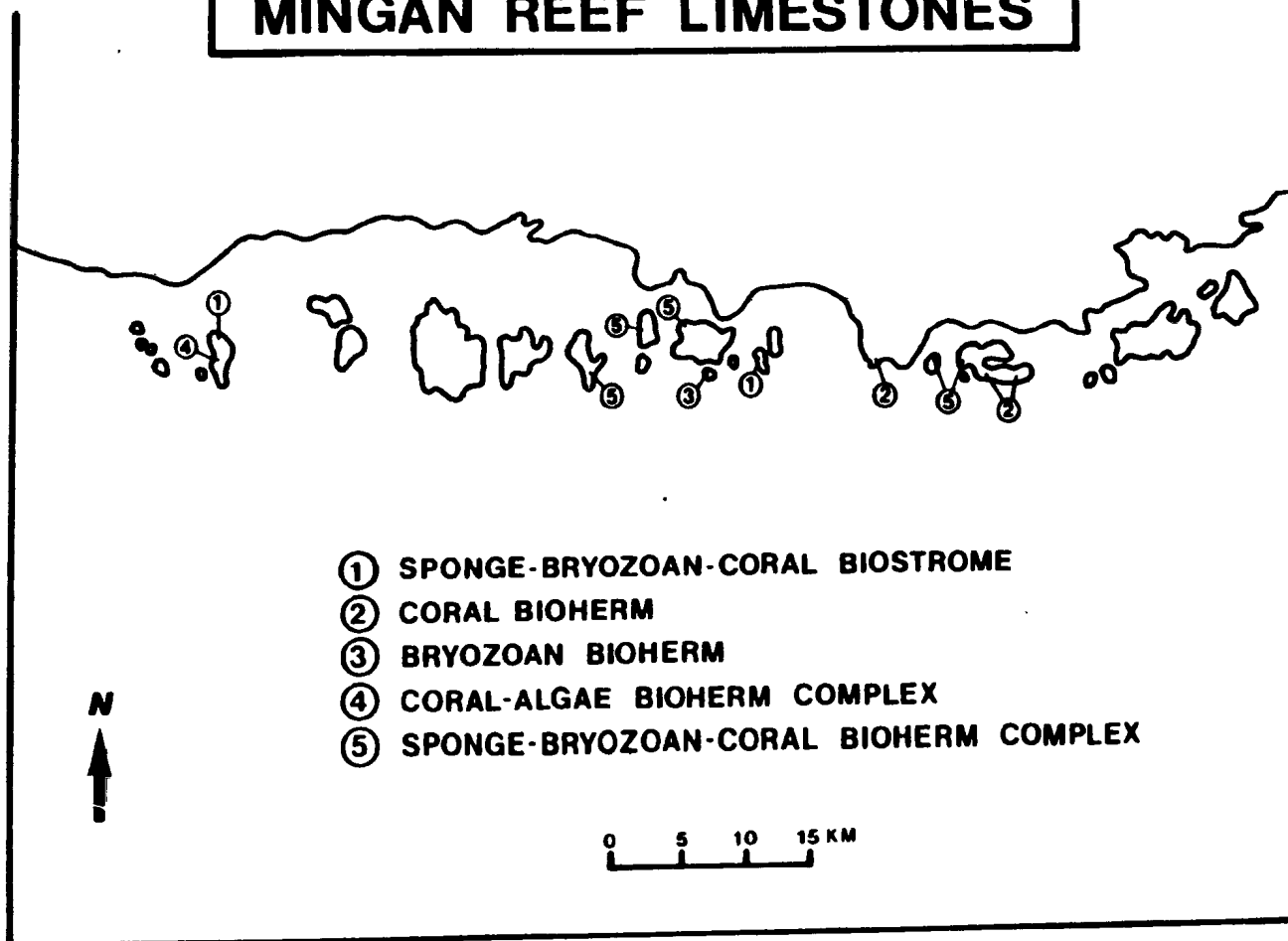
Figure 5.2- Schematic diagrams showing the stratigraphic relationships
between the core, flank, and inter-reef facies in the Mingan reef
limestones. Three types of reef limestones are recognized: 1)
biostromes, 2) bioherms and 3) bioherm complexes with either
composite or scattered reef cores. See text for description.

BIOSTROME
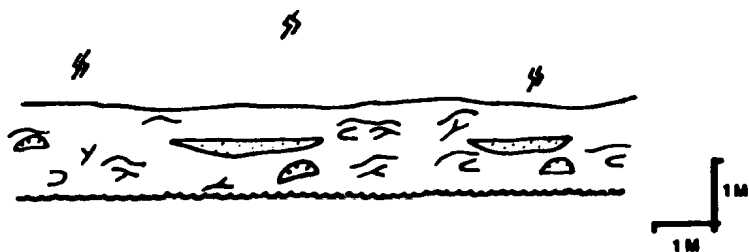
BIOHERM
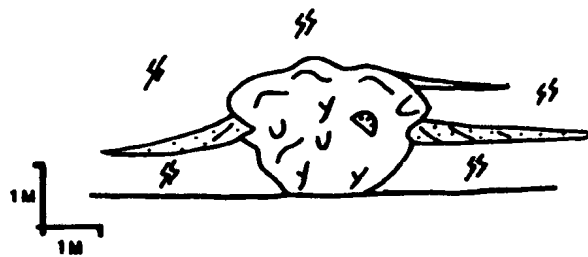
BIOHERM COMPLEX

COMPOSITE REEF CORE
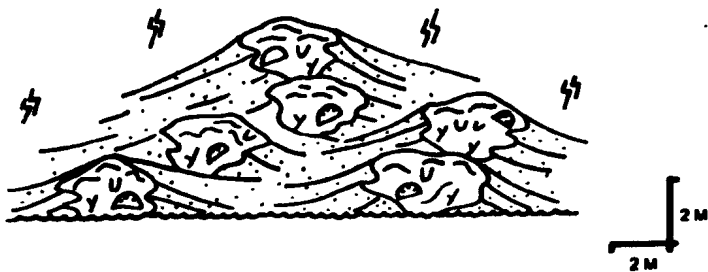
SCATTERED REEF CORE
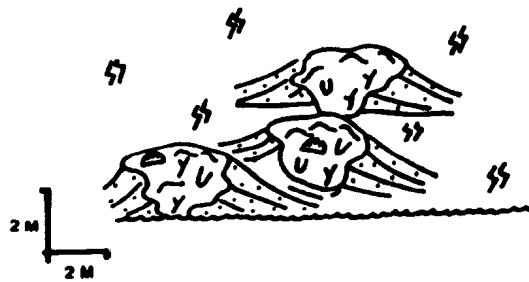
REEF CORE
FACIES

REEF FLANK
FACIES

INTER-REEF
FACIES

PLATE 5-1

REEF LIMESTONES - SPONGE-CORAL-BRYOZOAN BIOSTROMES

A. Field photograph (cross-section view) of a sponge-coral-bryozoan biostrome forming a massive stratiform unit (b) and overlying cross-bedded grainstones (g). The sharp contact with grainstones corresponds to a paleokarst surface capping calcarenite cycles (see plate 7-1). Ile Nue de Mingan N. Hammer is 30 cm.

B. Field photograph (cross-section view) showing reef organisms in a sponge-coral-bryozoan biostrome. Organisms include encrusting, sheet-like corals (c), Billingsaria, tubular lithistid sponges(s), and delicate ramose bryozoans (d) . Detail in (C). Ile Nue de Mingan N. Lens cap is 50 mm in diameter.

C. Close-up of (B) showing tubular lithistid sponges (s) and ramose bryozoans (b) encrusted by Billingsaria (c). Note that the sponges and bryozoans are not found in life position but display no evidence of transport. Lens cap for scale.

D. Polished slab (cross-section view) showing tubular (s) and globular (g) sponges, oriented parallel to bedding plane, in a sponge-coral-bryozoan biostrome. Ile Nue de Mingan N.
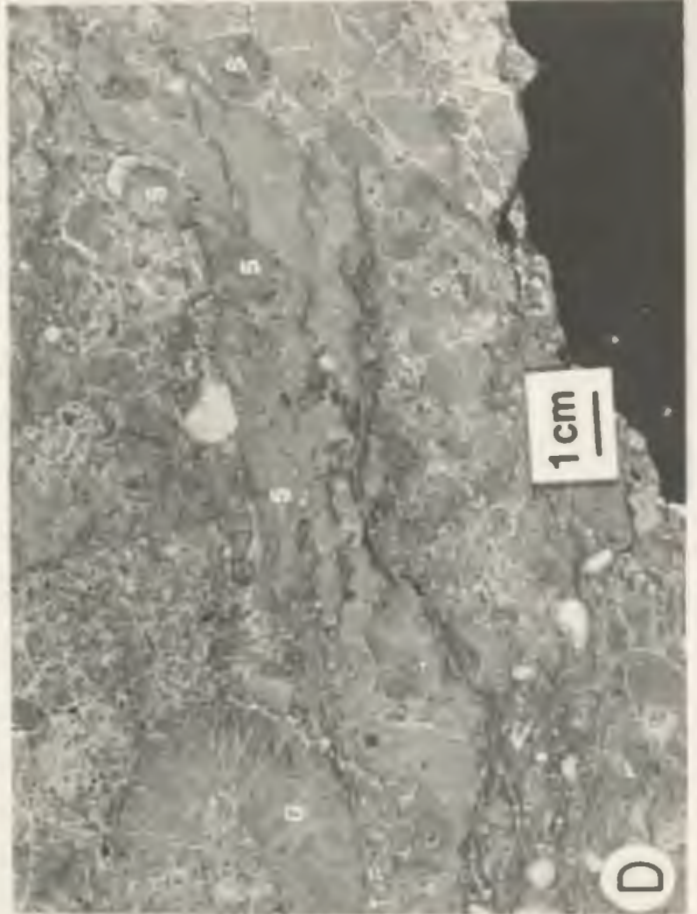
chap. 7).

Biostromes are usually composed of massive-weathering rudstones with a skeletal wackestone matrix. The units are made up a consortium of lithistid sponges, bryozoans, and tabulate corals (plate 5-1; B). Most reef-building taxa are not found in life position but display no evidence of transport (plate 5-1; C and D).

The matrix consists of homogeneous to peloid lime mud, is slightly to moderately burrowed, and may compose up to 50% of the total rock volume. Other fragmented, but unabraded skeletons include: echinoderms, brachiopods, gastropods, ostracods, trilobites, an' cephalopods. Small grainstone lenses composed of echinoderm and bryozoan fragments are also present.

Bioherm

These reef limestones consist of biohermal units forming small mound-shaped structures (plate 5-2; A) that range from 0.5 to 5.0 m across and 0.2 to 1.5 m high (fig. 5-2). These structures are isolated, subcircular in plan and irregular to oblong in cross-section. They display convex tops, slightly concave bottoms and irregular margins interfingering with adjacent lithologies. Bioherms rest directly on grainstones which form the upper part of calcarenite cycles. Paleokarst surfaces do not form bases. In general, reef mounds are surrounded by inter-reef facies with only minor flank facies.

The Mingan bioherms are composed primarily of in situ reef building organisms with a matrix of skeletal wackestone to lime mudstone and exhibit depositional textures ranging from bafflestone to bindstone. The reef builders are commonly dominated by a single taxon, generally

- 183 -

PLATE 5-2

REEF LIMESTONES - CORAL BIOHERM

A. Field photograph (cross-section view) of coral bioherm forming a small, isolated mound-shaped structure. Scale bar is 2 cm. Grande Pointe SO.

B. Field photograph (cross-section view) of reef organisms in a coral bioherm. Organisms consist of intergrown sheet-like _Billingsaria_ (b) and hemispherical _Eofletcheria_ (e). Ile Saint-Charles SW. Lens cap is 50 mm in diameter.

tabulate corals (plate 5-2; B) with only subordinate builders
(bryozoans, lithistid sponges, cyanobacterial mats).

The bioherm matrix consists of lime mud and may comprise from 40% to
60% of the total rock volume. The mud matrix, in which float a variety
of skeletal remains, is structureless and disturbed only by
bioturbation. Syndepositional cavities which are common features in
reefs (Krebs, 1971; Scoffin, 1972; James and Kobluk, 1978) are absent;
the interskeletal space being always filled with lime mud.

Bioherms are commonly flanked by skeletal wackestones and packstones
which consist of burrowed muddy sediments with a diverse biota. These
sediments were deposited in subtidal, open marine environments under
relatively quiet conditions (see description lithofacies 11). In some
cases, thin lenses of echinoderm-rich grainstone/packstone extend short
distances (1-2 m) away from the mounds but are rare and show no
preferential orientation.

Bioherm complexes

Bioherms may also form complexes when they occur in clusters of massive
mound-shaped structures surrounded by lime sands (fig. 5-2). These reef
complexes may reach 3 to 6 m in height and several tens of metres in
length (plate 5-3; A). Individual mound-shaped structures (plates 5-3; B
and 5-4; A) are randomly distributed within a reef complex and similar
in shape and in size to bioherms described earlier. Reef complexes occur
only in the Grande Pointe Member where they rest directly on the
intra-Mingan paleokarst unconformity.

The most common reef builders are lithistid sponges, bryozoans,
tabulate corals, and solenoporacean algae. These organisms are commonly

PLATE 5-3

REEF LIMESTONES -
SPONGE-BRYOZOAN-CORAL BIOHERM COMPLEX

A. Field photograph (cliff exposure) of sponge-bryozoan-coral bioherm complex illustrating several mound-shaped structures (b) surrounded by bedded grainstones. This bioherm complex (top 3.0 m) is separated from the underlying, well-bedded fenestral mudstones (m) by the intra-Mingan paleokarst unconformity (black line). Detail in plate 7-7; B). Exposed section is approximately 8.0 m thick. Ile de la Fausse Passe E.

B. Field photograph (cross-section view) showing the irregular margin between bioherm (b) and flanking grainstones (g). Note the presence (beneath the hammer) of a debris apron (d) composed of reef builders transported away from the reef core (detail in D). Ile du Fantome W.

C. Field photograph (bedding plane view) of the bioherm shown in (B). Note the abundance of in situ globular sponges in the reef core with their central cavity facing upward. Ile du Fantome W. Scale bar is 2 cm.

D. Field photograph (bedding plane view) of the debris apron shown in (B). Note the abundance of transported globular sponges with a random orientation. Ile du Fantome W. Hammer is 30 cm.

E. Polished slab (cross-section view) of bryozoan-rich grainstone surrounding bioherms in a bioherm complex. The strap-shaped bifoliate bryozoan, Stictopora, is particularly abundant. Ile du Fantome W.
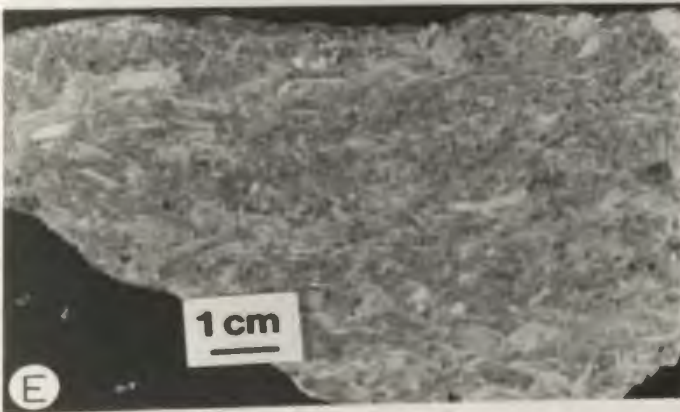
PLATE 5-4

REEF LIMESTONES -
CORAL-ALGAE BIOHERM COMPLEX

A. Field photograph (wave-cut platform) of the coral-algae bioherm
complex showing a massive reef core more resistant to weathering
than the flanking grainstone beds. Detail in (B). Ile Nue de Mingan
W. Hammer is 30 cm.

B. Field photograph (low tangential view along the bedding plane) of
reef organisms in coral-algae bioherm complex. Organisms include
massive, tabular Billingsaria (c) intergrown with layers of
sheet-like solenoporacean algae (s). Detail in (C and D). Ile Nue de
Mingan W. Lens cap is 50 mm in diameter.

C. Polished slab (cross-section view) of massive tabular Billingsaria
shown in B.

D. Polished slab (cross-section view) of sheet-like to lamellar
solenoporacean algae shown in (B).

E. Polished slab (cross-section view) illustrating growth cavities
between closely-intergrown solenoporacean algae. Cavities are
partially filled by geopetal sediment (s) pre-dating fibrous calcite
(thin fringe) and blocky calcite (last void-filling). Ile Nue de
Mingan W.

F. Polished slab (cross-section view) of flanking grainstone
immediately adjacent to a reef core in coral-algae bioherm complex.
Skeletal particles include large transported fragments of coral,
solenoporacean algae, bryozoans and sponges. Ile Nue de Mingan W.
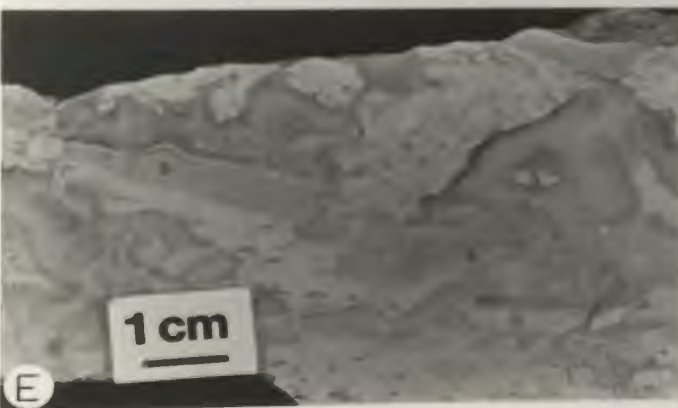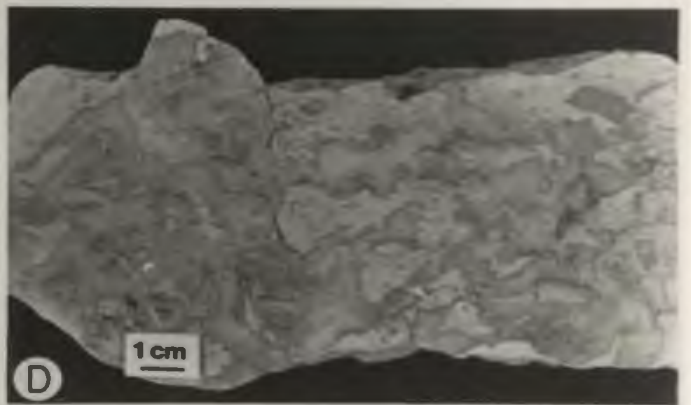
found in growth position and performed baffling and trapping roles during reef growth (plate 5-3; C and 5-4; B-D).

The floatstone matrix consists of lime mudstone (40-50%) with a sparse but diverse skeletal content. Of particular importance is a micritic crust with tubular fenestrae that surrounds large skeletal metazoans. Otherwise the lime mud matrix is structureless and disturbed only by burrows characterized by circular cross-sections with distinct burrow margins and filled by late diagenetic void-filling blocky calcite.

Syndepositional or growth cavities are sometimes observed when larger reef building taxa are closely intergrown. These cavities, ranging from 1 to 5 cm long, are partially filled by geopetal sediment which is overlain by void-filling blocky calcite (plate 5-4; E). In some cases, fibrous calcite cement lines cavity walls.

The mound complexes are surrounded by bedded grainstones forming piles with slopes up to 20° (plate 5-3; B,D,E and 5-4; F). On a smaller scale, individual reef mounds have sharp but irregular margins which interfinger with flanking grainstone facies, indicating that they grew as sediments accumulated around them. Flanking grainstones grade laterally into skeletal wackestone and packstones within 10-15 m. Grainstones may be rare or absent if individual mounds are closely spaced within a given reef complex.

REEF ORGANISMS

The most important organisms in·the reef limestones are: lithistid sponges, bryozoans, tabulate corals, and calcareous algae. Other organisms, which did not contribute directly to the reef construction,

are: echinoderms, molluscs, arthropods, and brachiopods.
Stromatoporoids, which are common in the classic reefs from the Chazy
Group in New York and Vermont (Pitcher, 1964; Kapp, 1975), are rare in
the Mingan reefs. The relationships between the growth forms and
functions of the major building organisms are summarized in the table
5-1.

Sponges

The systematics of the Mingan sponge fauna are presently under
study; however preliminary results indicate that they are lithistid
sponges belonging exclusively to the family Anthaspidellidae (K. Rigby,
pers. comm. 1983). The most common genera are _Hudsonospongia_, _Eospongia_,
Anthaspidella, _Zittelella_, _Lissocoelia_, _Psarodictyon_, _Rhopolocoelia_,
Calycocoelia, and _Archaeoscyphia_. All of them were previously
undescribed from the study area but _Eospongia_ which was originally
recorded by Billings (1865) has been reported by Twenhofel (1938).
Twenhofel, however, did not describe the internal morphology of these
sponges which is of primary importance for taxonomic classification. It
should be pointed out that this classification has been revised only
recently (Levi, 1973; Rigby, 1983). For the purpose of the present
study, most lithistid sponges are referred to by their growth form.

Lithistid sponges are abundant in reef limestones, especially in
reef cores, and occupy from 10 to 30% of the rock volume. In some cases,
reef cores may contain up to 50% of _in situ_ lithistid sponges with
densities up to 30 sponges/m on some bedding plane surfaces. In
contrast, lithistid sponges are rare in the inter-reef facies but
sponge-rich debris piles commonly flank the reef cores.

Table 5-1. Functions of the major fossil organisms in the Mingan reef limestones.

REEF ORGANISM	GROWTH FORM	FUNCTION
Lithistid sponges	globular to hemispherical	frame builders
	encrusting, lamellar	binders
	tubular to conical	bafflers
Tabulate corals	encrusting, lamellar	binders
	massive, tabular	frame builders
	hemispherical	frame builders
Bryozoans	hemispherical	frame builders
	encrusting, sheet-like	binders
	ramose, branching	bafflers
	bifoliate, strap-shaped	bafflers
	encrusting, lattice-like	binders
Algae	encrusting, lamellar to tabular	frame builders
	encrusting, sheet-like	binders

Various growth forms are recognized which are in order of importance: 1) globular forms, 3-15 cm in size (plate 5-5; A); 2) thin-walled lamellar forms which are bowl-shaped, 1-3 cm thick and 10-80 cm long (plate 5-5; B); 3) conical forms which are cup- to horn-shaped, 5-10 cm long (plate 5-5; C) and 4) tubular forms which are rod-shaped, 1-5 cm in diameter and 5-15 cm long Plate 5-5; D and E). Most of these sponges are single but some tubular and conical forms are branched (plate 5-5; F). The growth forms of these lithistid sponges within reef cores exhibit no obvious distribution pattern.

Bryozoans

Twenhofel (1938, p.42-44) identified several bryozoan species in the Mingan Formation that belong to geologically younger species. This is due to the fact that the bryozoan fauna from the Chazy type area in New York and Vermont were described much later by Ross (1963 a,b,c,d). Ross (1964) in a summary paper recognized 11 bryozoan genera from the New York-Vermont area of which most, if not all, are new taxa and restricted to the Chazy stage. These bryozoans were widespread in shallow-shelf environments especially in reef mound and flank facies as well as in sand shoal and more quiet open shelf facies (Ross, 1972; 1981).

Preliminary taxonomic study of the Mingan bryozoan fauna indicates that it is much more diverse and complex than previously recognized by Twenhofel (R.J. Cuffey, pers. comm. 1984). Nine bryozoan genera are present in the reef limestones and all of them are also described from the Chazy type area. They include: 1) cryptostome bryozoans represented by Ceramoporella sp. and Constellaria islensis; 2) trepostome bryozoans represented by Batostoma chazyensis/campensis, Nicholsonella sp.,

PLATE 5-5

REEF ORGANISMS - LITHISTID SPONGES

A. Field photograph (bedding plane view) of globular sponges. Ile du Fantome W. Scale in cm.

B. Field photograph (bedding plane view) of a bowl-shaped sponge with thin, lamellar wall. Petite Ile au Marteau W. Scale in cm.

C. Field photograph (bedding plane view) of a large cup-shaped sponge (tangential section). Ile Nue de Mingan W. Scale in cm.

D. Field photograph (bedding plane view) of tubular sponges showing rod-shaped forms in longitudinal section and circular forms in transversal section. Ile Nue de Mingan W. Scale in cm.

E. Field photograph (cross-section view) of tubular, locally branching, sponges in sponge-bryozoan-coral biostrome. Ile Nue de Mingan N. Scale in cm.

F. Polished slab (cross-section view) of branching, tubular sponges in coral-algal biohem complex. Ile Nue de Mingan W.
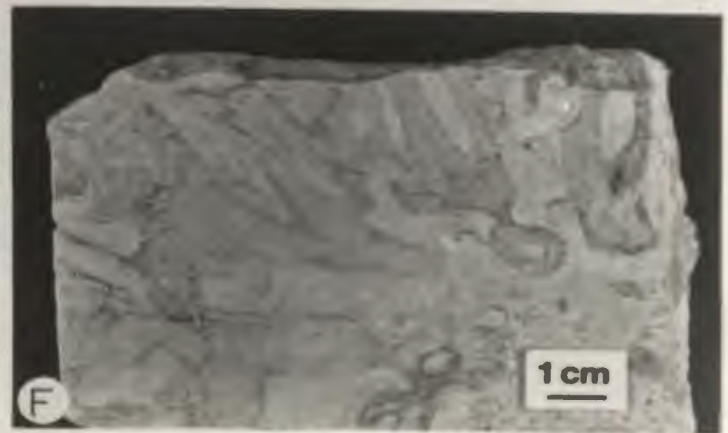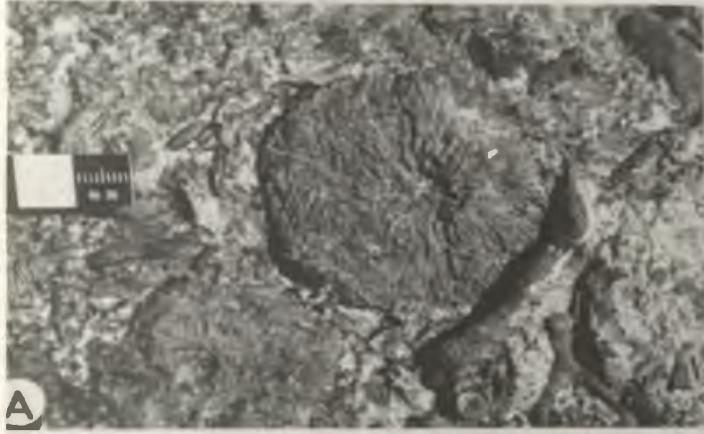
Nicholsonella ? sp. indet., Lamottopora duncanae, and Jordanopora heroensis; 3) bifoliate bryozoans represented by Stictopora fenestrata, Eopachydictya gregaria, Chazydictya chazyensis and 4) fenestrate bryozoans represented by Phylloporina sp..

Bryozoans in the reef limestones display various growth forms which include: encrusting sheet-like, ramose branching, strap-shaped, and encrusting lattice-like. Some bryozoans have at least two different growth forms, usually ramose and sheet-like (plate 5-6; A-C). Encrusting forms are locally intergrown to form small nodular masses or knobs ranging from 3 to 15 cm in size. These nodular masses are restricted to reef core facies and dominated by Batostoma. The ramose, branching forms are present in both reef core and flank facies (mainly Batostoma and Nicholsonella), but are more important in the reef core. In contrast, the strap-shaped bifoliates (plate 5-6; D) are more common in reef flank facies (mainly Stictopora). Lattice-like fenestrates (Phylloporina) are present in both facies. The bryozoan distribution and growth habit in the reef limestones are summarized in table 5-2. The relative proportion of bryozoan species in reef limestones is also included in table 5-2; "X" indicating less than 1% of the total bryozoan fauna, "rare" indicating 1 to 5%, "common" indicating 5 to 20% and "abundant" indicating more than 20%.

Tabulate corals

Tabulate corals are common in reef limestones, making up to 20% of the total volume in some reef cores. Large broken fragments or upturned coral colonies are present in reef flank facies (plate 5-4; F) but absent in inter-reef facies. The coral fauna is fairly simple and

Table 5-2. Distribution of the bryozoan species and growth forms in the Mingan reef limestones.

SPECIES	GROWTH FORM	CORE FACIES	FLANK FACIES
Ceramoporella sp.	encrusting, sheet-like	rare	X
Constellaria islaendis	massive, nodular	rare	X
Batostoma chazyensis/campensis	massive, nodular	common	X
" " "	encrusting, sheet-like	abundant	X
" " "	ramose, branching	abundant	abundant
Nicholsonella sp.	encrusting sheet-like	rare	X
" "	ramose, branching	common	X
Nicholsonella sp. indet.	ramose, branching	common	common
Lamottopora duncanae	ramose, branching	common	X
Jordanopora heroenis	ramose, branching	common	X
Stictopora fenestrata	bifoliate, strap-shaped	common	abundant
Lopachydictya gregaria	bifoliate, strap-shaped	X	rare
Chazydicta chazyensis	bifoliate, sheet-like	X	rare
Phylloporina sp.	fenestrate, lattice-like	common	rare

PLATE 5-6

REEF ORGANISMS - BRYOZOANS

Photomicrographs - Plane polarized light

A. Field photograph (cross-section view) of _in situ_ ramose bryozoans
    (Batostoma) within a lime mudstone matrix. Sponge-bryozoan-coral
    bioherm complex. Ile du Fantome W. Scale in cm.

B. Field photograph (bedding plane view) showing transported fragments
    of ramose bryozoans (Batostoma) in sponge-bryozoan-coral biostrome.
    Petite Ile au Marteau W. Scale in cm.

C. Thin-section photomicrograph of encrusting, sheet-like bryozoans
    (Batostoma) from the reef core (upper part) of sponge-bryozoan-coral
    bioherm complex. Scale bar is 1.0 mm.

D. Thin-section photomicrograph of strap-shaped bifoliate bryozoans
    (Stictopora) from the reef flank of sponge-bryozoan-coral bioherm
    complex. Echinoderm grains are also present. Scale is 1.0 mm.
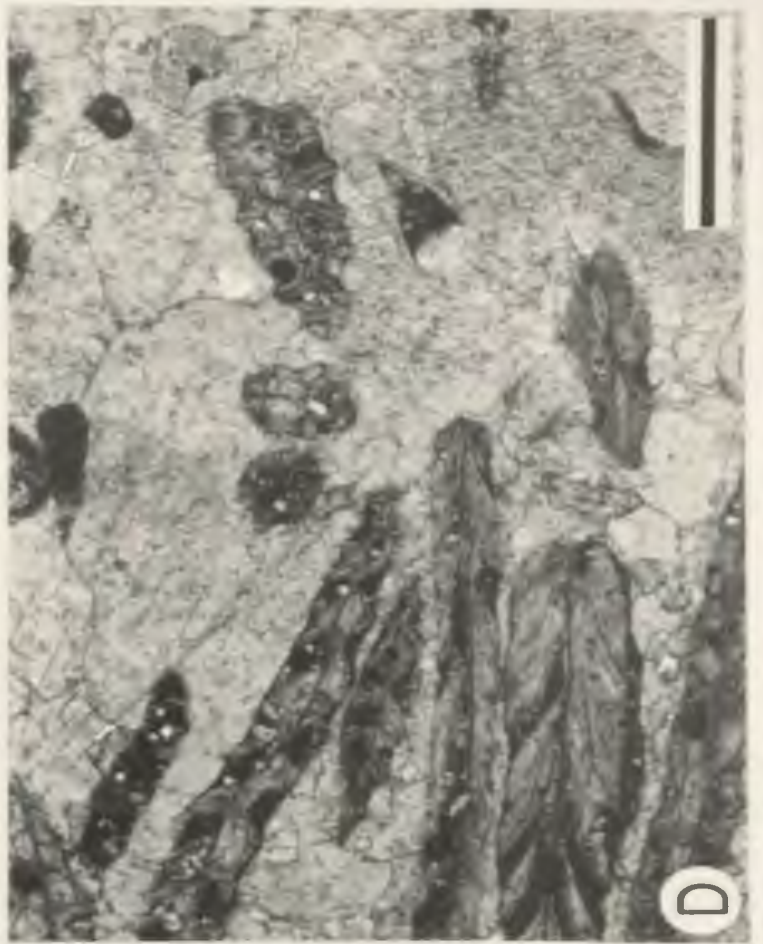
consists of <u>Billingsaria parva</u> and <u>Eofletcheria incerta</u> (T. Bolton,
pers. comm. 1982). <u>Billingsaria</u> occurs commonly as encrusting,sheet-like
growth forms, ranging from 0.2 to 3.0 cm thick and 5 to 15 cm long
(plate 5-7; A and B). It may form nodular masses (5 to 20 cm in size)
when several layers of <u>Billingsaria</u> are superimposed on top of one
another. It may also occur as more robust, tabular sheets, up to 10 cm
thick and 60 cm long (plate 5-4; B and C), which have been observed only
in one locality (i.e. Ile Nue de Mingan west). <u>Eofletcheria</u> is usually
hemispherical to slightly elongate upward and ranges from 5 to 20 cm in
size (plate 5-2; B and 5-7; C).

In thin-section, rare, encrusting, sheet-like tabulate corals that
are intergrown with bryozoans exhibit offsets near the margins of
corallites, and more likely belong to the genus <u>Lichenaria</u> (plate 5-7;
D).

Algae

Algal material in the reef limestones includes: rhodophytes,
cyanophytes, and minor <u>incertae sedis</u>. Rhodophytes are abundant but
restricted to the reef mound complex in Ile Nue de Mingan (west) where
they occur either as in place lamellar to sheet-like skeletons in the
reef core facies or as large broken fragments in the reef flank facies.
Their original microstructure is commonly obliterated by coarse
neomorphic calcite (plate 5-8; A). Relic features (plate 5-8, B),
however, are present and outline the reticulate structure of the
perithallus which appears to be distinctive of genus <u>Parachaeletes</u>
(Guilbeault, 1979; Bourque et al., 1981). These solenoporacean algae, if
superimposed, may form irregular laminar masses a few tens of

PLATE 5-7

REEF ORGANISMS - TABULATE CORALS

A. Polished slab (cross-section view) of thin, tabular corals, Billingsaria, in a coral-algae bioherm complex. Ile Nue de Mingan W.

B. Polished slab (cross-section view) of encrusting, sheet-like corals, Billingsaria, in coral bioherm. Note the presence of micritic algal crusts (c) in light gray (detail in plate 5-8; D-F) and bioturbated lime mudstone matrix (m) in darker gray. Ile Saint-Charles SW.

C. Polished slab (cross-section view) showing intergrown colonies of hemispherical corals, Eofletcheria, in coral bioherm. Ile Saint-Charles SW.

D. Thin-section photomicrograph (plane polarized light) of the coral, Lichenaria. Note the presence of common offsets (arrows) near the margins of corallites. Scale bar is 1.0 mm.

- 202 -
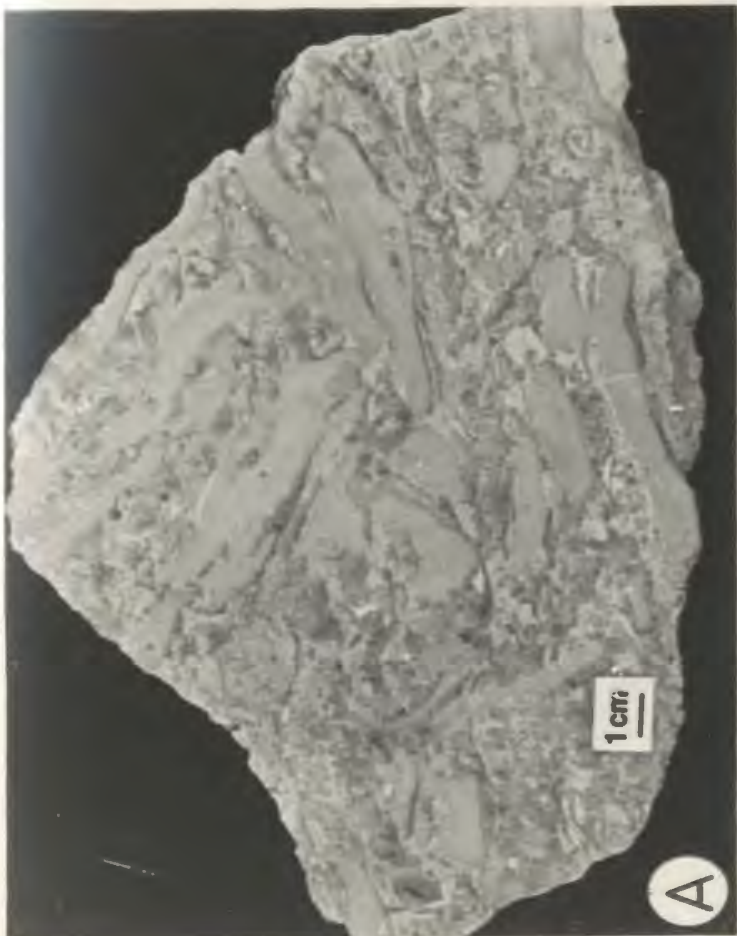
PLATE 5-8

REEF ORGANISMS - ALGAE

Photomicrographs - Plane polarized light

A. Thin-section photomicrograph of poorly-preserved solenoporacean algae (Parachaetetes). Note the relic cross-partitions (left). Scale bar is 1.0 mm.

B. Thin-section photomicrograph of relic fabrics in solenoporacean algae showing the reticulate structure of the perithallus, characteristic of the genus Parachaetetes. Scale bar is 1.0 mm.

C. Thin-section photomicrograph of stromatolite mats (s) encrusting sheet-like bryozoans (b) in sponge-bryozoan-coral bioherm complex. Scale bar is 1.0 mm.

D. Thin-section photomicrograph of micritic algal crust alternating with sheet-like bryozoans. Note the abundance of elongate to tubular fenestrae (vermiform microstructure). Detail in (F). Scale bar is 1.0 mm.

E. Thin-section photomicrograph of micritic algal crust surrounding erect ramose bryozoans in sponge-bryozoan-coral bioherm complex. Note the bioturbated lime mudstone matrix. Scale bar is 1.0 mm.

F. Thin-section photomicrograph illustrating the vermiform microstructure of micritic algal crust. Scale bar is 1.0 mm.
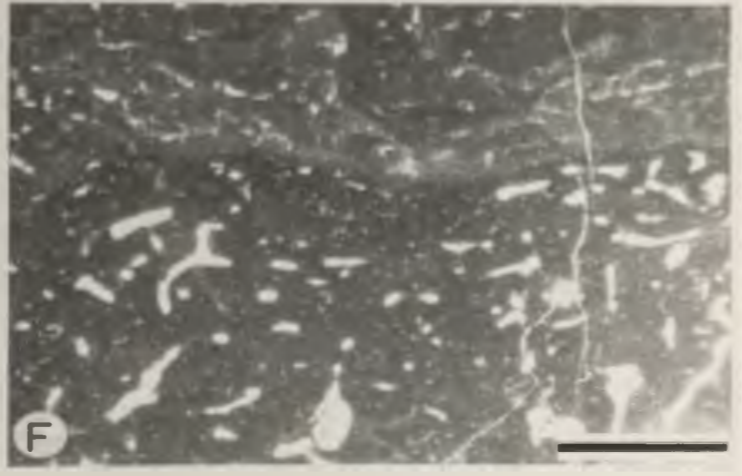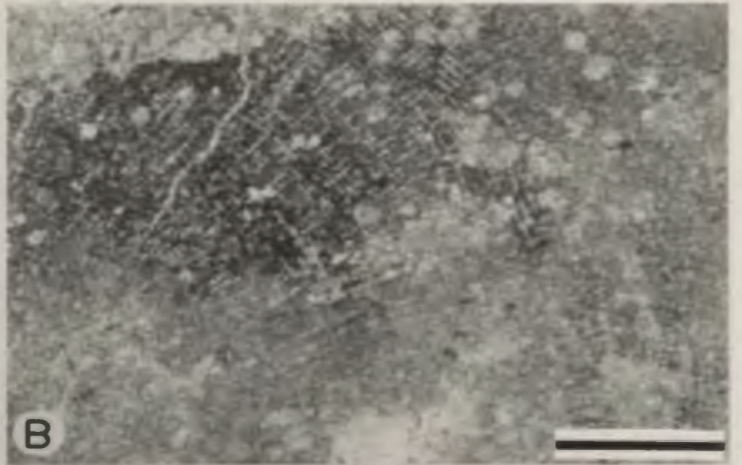
centimetres thick which interfinger at their edges with the surrounding sediment. They may also intergrow with the tabulate coral <u>Billingsaria</u>.

Cyanophytes are ubiquitous but subordinate building organisms (usually less than 10%) in most of the reef core facies and consist of stromatolitic mats or algal crusts . Stromatolitic mats are lamellar sheets with faint millimeter-thick laminae that encrust or bridge between other metazoan skeletons (plate 5-8; C). In addition to these mats, irregular micritic crusts (5-15 mm thick), characterized by a faint peloid microstructure, encrust skeletal material or grow as sheets over the sediment (plate 5-8; D and E). The micritic crusts contain numerous elongate to tubular fenestrae (0.1-0.5 mm in diameter) which are filled by geopetal sediment and/or void-filling spar (plate 5-8; F). Similar worm-like or vermiform microstructure has been recognized in the lime mud matrix of other early Paleozoic reefs (Ross et al., 1975; Kapp, 1975; Klappa and James, 1980). Pratt (1982b) argued that such a microstructure is common in cryptalgal structures and could probably represent original spaces occupied by algal filament bundles that were not calcified. Although direct evidence for an algal origin is missing, microstructures that come closest to these micritic crusts are the pelletoidal network of sponge-constructed mud mounds in the Silurian of Gaspe (Bourque and Gignac, 1983). The microstructure of these Gaspe mud mounds, however, is characterized by a well-defined pelletoidal network, more irregular fenestrae, and ubiquitous sponge spicules which are conspicuously absent in the Mingan micritic crusts.

<u>Girvanella</u> tubules and the problematic algae <u>Wetheredella</u>, <u>Nuia</u>, and <u>Halysis</u> are sometimes present in the lime mud matrix.

Pelmatozoans

Pelmatozoan fragments (unidentified crinoids and blastoids) make up
a substantial proportion of the reef limestones, especially in sediment
flanking the reef cores, where they may reach 50% of the rock volume.
These fragments, however, are less abundant in the lime mud matrix of
reef cores where they occur in small pockets or clusters. Articulated
echinoderm plates are rare. Pelmatozoan holdfasts, characterized by a
rhizoid morphology, are present in the lower parts of some reef cores.

Stromatoporoids

Stromatoporoids are a minor component in the reef limestones and
occur only in reef flank facies on Ile Nue de Mingan (west). They are
bulbous to domal in shape and 10 to 50 cm in size. Stromatoporoid
coenostea display in place growth positions but are not aggregated
together or with other organisms to form reefs. Their internal
morphology is poorly preserved and appears stromatolitic, without
stromatoporoid texture. In thin-section, some areas, however, show
cyst-plates forming convex-upward domes which are characteristic of the
genus Labechia (C.W. Stearn, pers. comm. 1985).

Other skeletal remains

Molluscs, brachiopods, and arthropods are also present in the reef
limestones but are accessory and average only 1% or 2%. In general,
these skeletal remains are slightly to moderately fragmented but
unabraded, although more complete specimens occur in the reef cores.

Nautiloids and gastropods are the only molluscs in the reef
limestones. Complete orthocone nautiloids (mainly Spyroceras spp. ?)
are

not important skeletal components but in one locality (i.e. Ile Nue de Mingan west) they occur as piles or pockets of 5 to 30 specimens surrounding the reef cores. The low-spired gastropod Maclurites is also present. Other low-spired and high-spired gastropods are found but are less abundant.

The brachiopod fauna is fairly simple, rhynchonellids and orthids being the most common. This contrasts with more diverse fauna in the inter-reef facies.

Bumastus and Illeanus are the dominant trilobite genera in the reef limestones but are rarely found complete (Shaw, 1980). Leperditiid ostracodes are even less common and characterized by smooth-shaped valves which are sometimes articulated.

SEDIMENTOLOGICAL ROLES

Reef organisms performed several functional or sedimentological roles during reef construction as indicated by the wide variety of skeleton morphology. These organisms can be separated into two groups, those that contributed directly to reef building and include in situ framebuilders, bafflers, and binders and those that produced sediment in reef interstices because of post-mortem disintegration. In general, reef cores are dominated by baffling organisms in the lower part whereas binding organisms are generally more common in the upper parts. Small framebuilding organisms are ubiquitous. Similar functional roles are played by corals or algae in modern reefs, however a major difference is the absence of large framebuilders able to resist high wave energy.

Framebuilders

Tabulate corals are the only true framebuilders which may form
mutually encrusted or closely packed skeletons. They consist of
hemispherical Eofletcheria or lamellar to tabular Billingsaria or
combination of both. Solenoporacean algae are locally intergrown with
robust, tabular Billingsaria and form a solid framework as reflected by
the presence of syndepositional or growth cavities. Small nodular masses
composed of superimposed sheet-like organisms (i.e. tabulate corals,
bryozoans) may also have functioned as framebuilders. These nodular
masses, however, are generally isolated and are only few tens of
centimetres in size. Globular lithistid sponges were also potential
framebuilders.

Bafflers

In situ ramose bryozoans and conical to tabular lithistid sponges
were probably more effective as bafflers and were too small and delicate
to act as framebuilders. These organisms allowed some of the suspended
sediment to settle out around their base. Echinoderms were also bafflers
prior to their post-mortem disintegration as judged by the large amount
of echinoderm particles released in the sediments surrounding the reef
cores.

Binders

Encrusting, lamellar to sheet-like organisms played an important
role in reef construction by binding other reef-building organisms and
the intervening sediment, thus stabilizing the reef structure. These
organisms include lithistid sponges, bryozoans, tabulate corals, and

cyanophytes. Echinoderms with their holdfasts were also effective
sediment binders.

Sediment producers

All the reef building organisms, especially bafflers, were
potentially sediment producers. Echinoderms and bryozoans (mainly ramose
and strap-shaped, bifoliate forms) constitute a substantial proportion
of the gravel and sand-sized sediments within and around the reef cores.
Other whole and broken skeletal remains added loose matrix. These
remains originated from segmented benthic organisms (echinoderms,
brachiopods, ostracods) or from free-living organisms (gastropods,
trilobites, cephalopods) which may have fragmented after death.

Most of the reef-building taxa performed several sedimentological
roles during the construction of reef limestones; for instance bryozoans
were small framebuilders, encrusters, trappers, binders, and sediment
producers. Such variety in constructional roles by bryozoans is common
in several Phanerozoic reefs (Cuffey, 1977).

BIOTIC ASSEMBLAGES IN REEF LIMESTONES

The larger biotic constituents in reef limestones are characterized
by different assemblages which may be either dominated by a single taxon
or composed of several principal taxa. Five distinct biotic assemblages
are recognized in the different types of reef limestone.

Lithistid sponge/bryozoan/tabulate coral biostromes

This assemblage forms massive biostromal units (fig. 5-1) in the
northern part of Ile Nue de Mingan and in Petite Ile au Marteau (plate

5-1). These units are developed on paleokarst surfaces capping the calcarenite cycles.

The large biotic constituents are bryozoans (30-50%) and lithistidsponges (30-40%) together with the tabulate coral Billingsaria (10-20%). Most of these organisms, especially hemispherical, globular and ramose forms, are rarely found in growth position but are only slightly fragmented or overturned. Encrusting, sheet-like metazoans, however, are more commonly found in situ, encrusting the latter forms.

Tabulate coral bioherms

Small metre-sized bioherms (fig. 5-1) with a substantial proportion of tabulate corals occur in Grande Pointe and in the southern part of Ile Saint-Charles (plate 5-2). These bioherms in the Grande Pointe Member directly overlie grainstone units associated with calcarenite cycles but not paleokarst surfaces.

The reef builders are generally found in situ and include tabulate corals (70-80%) with subordinate bryozoans (10-20%) and lithistid sponges (5-10%). Tabulate corals consist of stacked, hemispherical Eofletcheria either alone or in concert with encrusting, sheet-like Billingsaria.

Bryozoan bioherms

Small hemispherical masses built by bryozoans occur on Ile a Calculot (fig. 5-1) where they also conformably overlie grainstone units at the top of calcarenite cycles in the Grande Pointe Member. These masses average only 30 cm in height and 100 cm in diameter. Masses similar in size and in composition are sometimes associated with

lithistid sponge/bryozoan/ tabulate coral blankets.

The bioherms are composed primarily of encrusting, sheet-like and branching, ramose bryozoans. The most common bryozoan genera are Batostoma and Ceramoporella; other large skeletons are rare or absent.

Solenoporacean algae/tabulate coral bioherm complexes

This biotic assemblage is present only in the western part of Ile Nue de Mingan (fig. 5-1) and forms closely-spaced bioherms surrounded by skeletal lime sands (plate 5-4). Individual bioherms are hemispherical, 1-2 m high, and 3-15 m in diameter. These bioherms rest directly on the intra-Mingan paleokarst unconformity with a slight angular relationship between both.

Reef builders within these bioherms consist of an intergrowth of the solenoporacean algae Parachaetetes (40-50%) and the tabulate coral Billingsaria (30-40%). Other in situ builders are less common and include lithistid sponges (10-20%) and bryozoans (5-10%).

Lithistid sponge/bryozoan/tabulate coral bioherm complexes

Bioherm complexes (fig. 5-1), composed of several principal taxa, are well exposed in Ile du Fantome, Ile de la Fausse Passe, and the western part of Ile Saint-Charles (plate 5-3). Other occurrences are known in Ile Niapiskau and Ile du Havre but were not studied in detail due to limited exposure. These complexes have grown directly on the intra-Mingan paleokarst unconformity.

The biotic assemblage in the bioherm complexes consists of lithistid sponges, bryozoans (mainly Batostoma) and tabulate corals (mainly

Billingsaria). The relative importance of these constituents is
extremely variable between different bioherm complexes or even between
different bioherms of the same complex. Consequently this biotic
association may be regarded as a three end-member assemblage.

ZONATION IN THE REEF LIMESTONES

Reef facies in bioherm and bioherm complexes display commonly, but
not always, both lateral or vertical zonations in the distribution of
their biotic and sedimentologic components (fig. 5-3). These zonations
are best developed in the mound complexes: biostromes exhibit no obvious
patterns.

Lateral zonation

The reef flank facies, if present, is characterized by a distinct
lateral zonation of biotic and sedimentologic components which vary with
distance away from the reef core. This is indicated by: 1) decrease in
percentage of the skeletal remains; 2) decrease in size of the particles
and 3) textural change from grain-supported to matrix-supported fabrics.
Such lateral gradations may occur within 5 to 15 m depending on spacing
of the reef cores. Furthermore, debris aprons composed of slightly
transported and overturned reef builders are observed only a few metres
away from the reef cores. In contrast with the reef flanks, reef cores
do not display a lateral zonation.

Vertical zonation

The reef cores, which may be dominated by a single taxon or composed
of several principal taxa, exhibit a vertical biotic zonation with

Figure 5.3– Biotic and sedimentologic variations in the core and flank facies of Mingan reef limestones. Lateral variations are observed only in reef flanks whereas the reef cores exhibit a crude vertical zonation.

REEF FLANK

GRAINSTONE

DEPOSITIONAL
TEXTURE

PACKSTONE-WACKESTONE

GRAVEL-SIZED

SKELETAL
DEBRIS

SAND-SIZED

BRYOZOAN REMAINS

DOMINANT
BIOTA

ECHINODERM REMAINS

0.5-2.0 m

5.15 m

REEF CORE

FRAMEBUILDERS

BAFFLERS

BINDERS
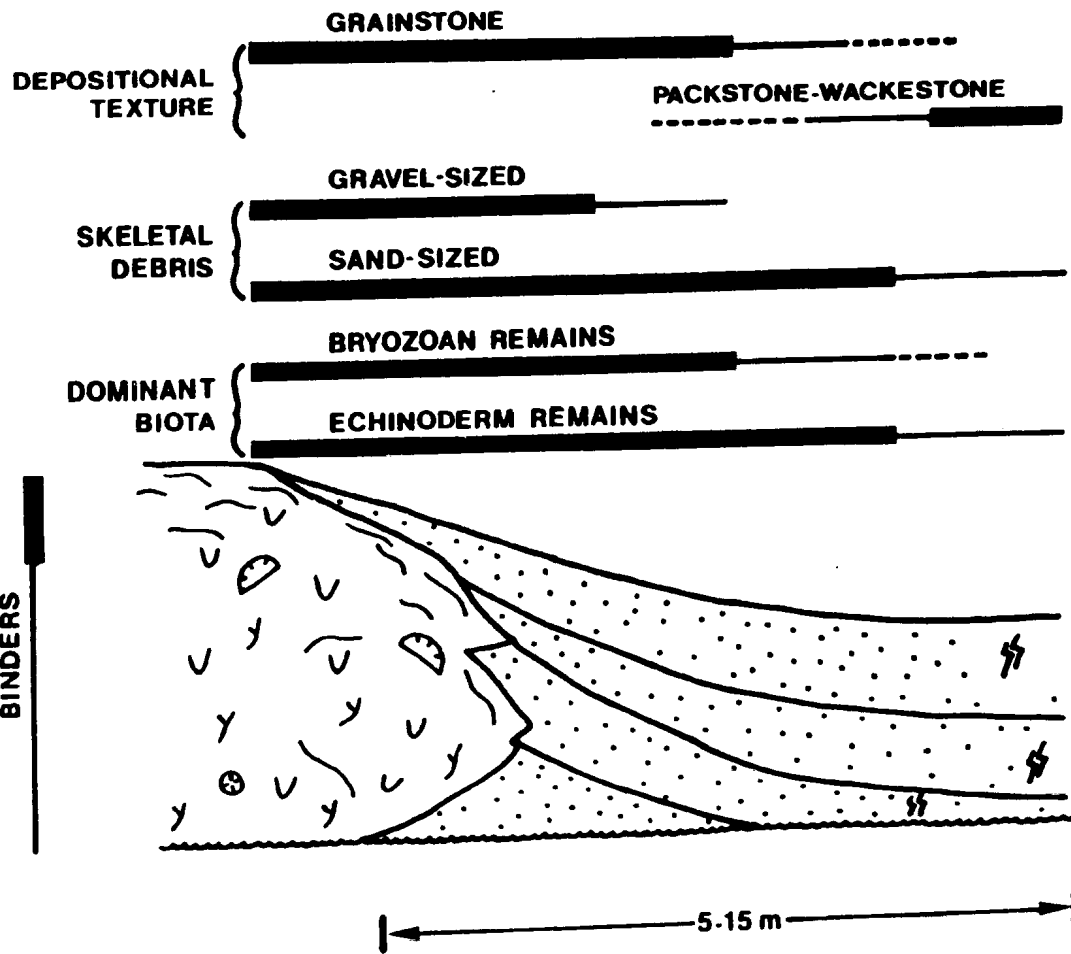
respect to the growth forms of the reef building organisms. In general, baffling organisms with ramose, tubular, and globular forms are common throughout the reef core facies but the upper part is usually dominated by binding organisms with encrusting lamellar to tabular forms. The most common binders are either the trepostome bryozoan *Batostoma* or the tabulate coral *Billingsaria* or a combination of both. Some reef cores in bioherm complexes are capped almost entirely by a layer of encrusting, lamellar bryozoans, up to 50 cm thick. Small framebuilding organisms with hemispherical forms are ubiquitous but display no preferential distribution within the reef cores. Vertical zonation in the sediments flanking the reef cores is absent.

DIAGENESIS

Early diagenesis

The reef limestones appear, at least locally, to have experienced early marine lithification. Inclusion-rich fibrous calcite cement which is commonly regarded as an early marine precipitate (Ginsburg and Schroeder, 1973; James et al, 1976) is found in the reef cores of some mound complexes. Its distribution is patchy and limited to small interskeletal pores or cavities, if present, and intraskeletal pores. The early nature of this cement is indicated by the following: 1) it is the first generation of cement; 2) isopachous layers line the pore walls; 3) it is interlayered with internal marine sediments (mainly peloids) and 4) it is restricted to reef core facies.

Early lithification of the lime mud matrix is more equivocal. Nevertheless, burrows are common throughout the matrix, indicating a

depositional origin for the mud. The burrows, however, display distinct circular cross-sections and are filled by late diagenetic, blocky calcite cement. Similar burrow features in the rubbly calcilutites of the Silurian Douro Formation in the Arctic Islands have been interpreted as reflecting minor compaction of the lime mud matrix due to a firm substrate or early lithification of the sediments (Narbonne, 1984). It is possible that these muddy sediments were lithified early by micritic cement but this can be only inferred since diagnostic features are missing (i.e. macroborings truncating the matrix or broken fragments similar in composition in the flanking sediments). In fact, the lime mud in reef limestones is regarded by some workers (Klappa and James, 1980; Narbonne and Jones, 1984) as polygenetic in origin and may be from: 1) deposition of lime mud in the reef interstices due to baffling organisms; 2) skeletal disintegration of reef organisms, especially algal material; 3) micritization of skeletal material and 4) inorganic precipitation of micrite.

Another synsedimentary diagenetic feature is the dissolution of the spicules in lithistid sponges. These spicules, by analogy with modern lithistid sponges (Rigby, 1983), were originally composed of siliceous material (probably opaline silica). Such material is not recognized in the Mingan lithistid sponges, instead the spicules have been dissolved and voids later filled with late diagenetic, sparry calcite. Furthermore, sponge spicules in the sediments flanking the Mingan reefs are rare despite the abundance of sponge skeletons in the reefs. Dissolution of the silica must have occurred after the spicules were encased in lithified micritic material but before the precipitation of calcite cement. This micritic material is quite different from

darker-coloured micrite with microbioclastic debris that filled the sponge canals and chambers or surrounded the sponge skeletons. The study of other fossil sponge reefs has shown that the rapid encasement in lime mud and subsequent dissolution of the lithistid spicules occurred at the same time as reef growth (Palmer and Fursich, 1981; Narbonne and Dixon, 1984). Palmer and Fursich (1981) interpreted the encasement of the spicules in lime mud to be due either to passive settling with early lithification or to precipitation of micrite. The synsedimentary lithification of lithistid sponges in the Mingan reef limestones is also supported by the presence of broken sponge fragments in the sediments flanking the reef cores. Siliceous spicules in modern reefal environments are unstable opaline silica and dissolve rapidly (Land, 1976; Hartman, 1977). Dissolution is thought to be even more pronounced under conditions of rapid sedimentation and synsedimentary cementation (Wiedenmayer, 1980a).

Meteoric and burial diagenesis

Postsedimentary diagenesis is characterized by the occlusion of the intraparticle, interparticle, and biomoldic pores by blocky calcite cement which is, in some localities, preceded by prismatic calcite precipitation. Unlike synsedimentary cements, all the sediments in reef limestones contain blocky calcite cement which displays an increase in both crystal size and iron content toward the pore centers. Similar cement is observed in fractures that are truncated only by sheet cracks. These cracks that formed in response to local horizontal stress, are sub-horizontal fractures, 0.2-1.0 cm high, 3-15 cm long, and filled later with coarse blocky calcite (mainly ferroan). Ferroan dolomite is

sometimes present as the last void-filling cement in larger pores. Stylolites and stylolitic seams are common and affect all the preexisting fabrics. This diagenetic suite is thought to reflect progressive burial of the reef limestones by younger Ordovician sediments that have since been eroded in the study area.

Neomorphism of larger reef organisms (calcareous algae, bryozoans, tabulate corals, and stromatoporoids) which was concomitant with the precipitation of blocky calcite is important to the extent that it is sometimes difficult to recognize their skeletal fabrics. These organisms display various styles of fabric retention which probably reflect their original mineralogy (aragonitic vs calcitic). Further details concerning the diagenesis of reef limestones are found in chapter 8.

INTERPRETATION

Depositional environment

Bioherm complexes- These structures, compared to isolated bioherms and biostromes, represent reefs that grew in turbulent environments. This is indicated by the volumetrically important flanking facies which consists of well-winnowed grainstones. These "clean" echinoderm-bryozoan sands cannot be explained simply as in situ accumulations of avalanche-type debris. Indeed, marine erosion by steady waves and/or currents was probably responsible for the formation of reef-derived bioclastic halos surrounding each individual core within a bioherm complex. Furthermore, the presence of these halos flanking and dipping away from the cores suggests that the reef structures exhibited topographic relief above the seafloor. This relief, however, was no

more than 1 m judging from the interlayering relationship between flank and core facies.

Patch reefs growing in Bermuda lagoons are good modern analogs for the Mingan bioherm complexes. The Bermuda reefs are generally unzoned knobs which occur either singly or in clusters and result from the intergrowth of corals, algae and associated organisms (Garret et al., 1971). The Mingan reefs differ only in the absence of large, massive reef building organisms.

Unlike the Bermuda patch reefs, the Mingan structures did not grow in lagoonal environments but under open marine conditions as indicated by the diverse and abundant normal marine fauna in the associated inter-reef facies (i.e. lithofacies 11). The Mingan limestones in the study area occur in a shallow water position but pass basinward into deeper water muddy carbonates and basinal shales which are present in subsurface of Anticosti Island located only 30 km to the south. This suggests that the reefs grew along the outer part of an open shelf or ramp which was not separated by a marked break from the basin. Furthermore, scattered occurrences rather than a continuous trend in the Mingan reef limestones is typical of carbonate ramp deposits (Ahr, 1973). Modern examples with shallow water ramp reefs include the Yucatan shelf in Mexico (Logan et al., 1969) and the Persian Gulf (Purser, 1973).

Bioherms- In contrast to the bioherm complexes, isolated bioherms, dominated by a single taxon (tabulate corals or bryozoans), grew under more tranquil conditions. These bioherms are generally flanked by skeletal wackstones and packstones that are similar to the widespread inter-reef deposits. Bioclastic halos are rare but if present,

extend only a few metres away from the reef core and show no
preferential orientation. These halos represent in situ accumulations of
skeletal muddy sand. This is suggested by the absence of evidence of
transport (abraded grains) and the presence of significant amounts of
lime mud (packstone/grainstone). A possible depositional setting may
have been protected sites behind sand shoal deposits because the
bioherms are always found overlying the ooid-skeletal grainstones that
are associated with calcarenite cycles.

Modern reefs, built by corals and calcareous algae, offer only few
examples for a comparison with these Mingan bioherms. Such examples are
possibly the small scattered reefs growing across the Joulter Cays ooid
sand shoal just north of Andros Island (Cuffey et al, 1977; Wyedenmayer,
1980). These living reefs, accumulating on sand bottoms, are rounded to
flat-topped, vertical-sided masses (few metres in size) dominated by a
single taxon (bryozoans or sponges) as framebuilders. Other accessory
framebuilders (corals, coralline algae, serpulids), however, also
contribute to reef growth. The Mingan bioherms are probably closest to a
reef type, referred as " reef mounds" which occur in the rock record,
especially at periods of time when the full spectrum of reef-building
organisms was absent (James, 1984b). Reef mounds grew in quiet water
environments and are more commonly found in the interior part of the
platform and in a downslope position near the platform margin.

Biostromes- Biostromes represent in situ accumulations of potential
reef building organisms that are dominated by fragile, sometimes
branching forms. Most of these organisms, however, are not found in life
position, especially those with elongate growth forms that are
conspicuously oriented parallel to bedding planes. The depositional

setting of these biostromes was one of relatively low-energy conditions. This interpretation is supported by several lines of evidence: 1) the association with mud matrix-supported deposits; 2) the slightly fragmented nature of unabraded organisms and 3) the absence of sedimentary structures. Furthermore, large skeletal metazoans with encrusting, sheet-like growth forms that are generally found in place in the biostromes, probably stabilized sediment from wave or current reworking.

The Mingan biostromes are strikingly similar to some modern inshore banks built by branching corals and algae in the interior part of the Florida reef tract (Turmel and Swanson, 1976). James (1983) points out that these inshore banks left little or no evidence of a coral and algal frame because most of the bank building organisms are branched and segmented and more prone to post-mortem breakdown. In fact, cores through these banks are characterized by branching coral floatstone to rudstone with a platy and branching algae grainstone to packstone matrix very similar to the depositional textures present in the Mingan biostromal units.

Growth stages

The Mingan reef limestones exhibit two distinct growth stages which are best developed in bioherm complexes (fig. 5-4). Suitable substrates appear to be one of the main controls on reef location and development. In most cases, paleokarst surfaces with renewed marine sedimentation provided lithified substrates on which various reef building organisms could grow. Following initial development, reef cores as well as reef-derived flanking sediments were used as substrates for subsequent reef growth. In some cases, stabilized portions of sand shoal deposits

Figure 5.4- Comparison between the stages of development in some Lower and Middle Ordovician bioherms. Source of data: El Paso Group in west Texas and New Mexico (Toomey, 1970; Toomey and Nitecki, 1979); Table Head Group in western Newfoundland (Klappa and James, 1980); Mingan Formation (this study); Crown Point Formation in New York and Vermont and the Carters Formation in Tenessee (Alberstadt et al, 1974; Walker and Alberstadt, 1975). Legend:

:Bryozoans;

:Lithistid sponges

:Stromatoporoids

:Tabulate corals

:Pelmatozoans

:Calathium

:Pulchrilamina

DOMINATION

DIVERSIFICATION

COLONIZATION

PIONEER

EL PASO GROUP   TABLE HEAD GROUP   MINGAN FM   CROWN PT FM   CARTERS FM

← H   ← PK

-224-
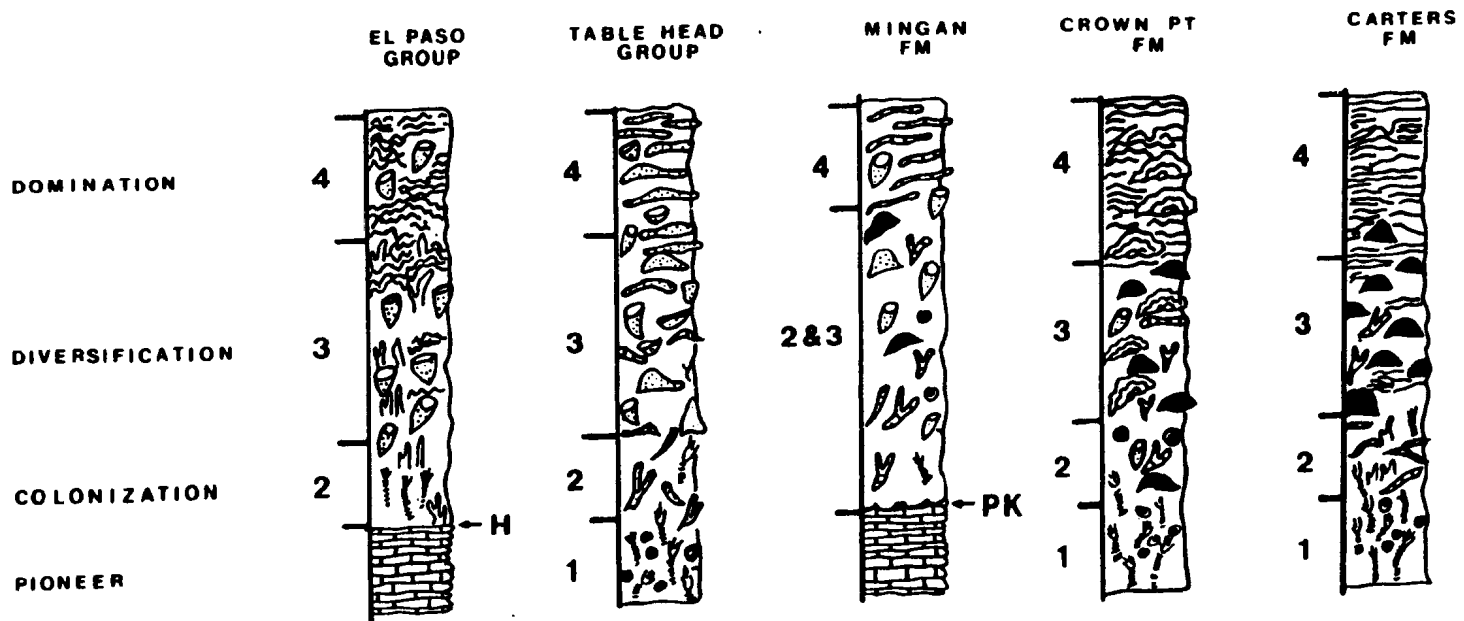
GROWTH STAGES

were also used as a foundation during the growth of some isolated bioherms.

The initial stage is a bafflestone unit which also forms the bulk of the reef core. This unit is composed of in situ organisms with delicate, branching forms within a skeletal wackestone matrix. During this stage, no obvious distribution pattern with respect to the growth forms or diversity of the reef building organisms is noticeable within a given reef core. Most of these builders acted as bafflers with some subordinate binders. Small framebuilders were ubiquitous.

The final stage is a bindstone unit capping the reef core. This unit consists of a thin layer of organisms with encrusting, sheet-like forms but other forms do occur. The biotic diversity is usually low compared to the first growth stage.

Phanerozoic reefs can exhibit four separate stages of growth which are thought to represent ecological successions (Walker and Alberstadt, 1975; Frost, 1977; James, 1984b). These stages are commonly called, following the terminology of Walker and Alberstadt (1975): 1) stabilization stage; 2) colonization stage; 3) diversification stage and 4) domination stage. The stabilization or pioneer stage is usually a local accumulation of skeletal debris, colonized by rooted organisms (mainly pelmatozoans in the Paleozoic) that bind and stabilize the substrate. Once stabilized, this substrate is colonized by numerous delicate organisms (mainly branching) during the colonization stage. The diversification stage consists of a diverse assemblage of baffling, binding, and frame-building organisms that form the bulk of the reef mass. The domination stage occurs at the top of the reef and is characterized by a low diversity assemblage of lamellar and encrusting

binders.

In the Mingan reefs, the usual stabilization stage in which piles of skeletal debris are stabilized by rooted organisms is absent, and lithified substrates (i.e. paleokarst) provided suitable surfaces for delicate, branching reef builders to grow on. The colonization and diversification stages in the Mingan reefs are apparently unrecognizable due to the homogeneous nature of the reef cores, thus stage 1 is thought to represent both. This is not surprising because the diversification stage is relatively thin when compared to the other growth stages (Walker and Alberstadt, 1975). Nevertheless, more delicate branching metazoans are more common at the base of the Mingan reefs. The domination stage, characterized by a low-diversity assemblage of encrusting and lamellar binders, is represented by stage 2.

Stages of reef growth have been also recognized in some Ordovician bioherms but most of other Ordovician bioherms appear to be homogeneous structures. A zonation with the four, or at least most of the four, growth stages has been described from bioherms of the Canadian El Paso Group in west Texas and Mexico, the Whiterockian Table Head Formation in western Newfoundland, the Chazyan Crown Point Formation in New York and Vermont, and the Rocklandian Carters Formation in Tennessee (fig 5-4).

The bioherms in the Crown Point and Carters Formations exhibit all four stages: 1) a stabilization stage, composed of a basal pelmatozoan grainstone; 2) a colonization stage, composed of the first organisms to participate in reef growth; 3) a diversification stage, composed of the core of the bioherm with a diverse assemblage of corals, bryozoans, algae, sponges and stromatoporoids and 4) a domination stage, composed almost entirely of encrusting stromatoporoids. These bioherms, similar

in their overall sequential development, however, show some differences in their faunal composition; the most important being the rarity of sponges and the presence of a distinctive 1-2 m zone of encrusting echinoderms, Calathium, and encrusting bryozoans above the basal grainstones in the Carters bioherms (Alberstadt et al, 1974). In spite of their small size, the four growth stages are also present in bioherms of the Table Head Group (Klappa and James, 1980). These bioherms are dominated by a single taxon, lithistid sponges, and within that taxon the organisms were sufficiently diverse to produce a structure with separate stages of growth.

The older bioherms in the El Paso Group, on the other hand, display three stages (Toomey, 1970; Toomey and Nitecki, 1979) which correspond to the upper three stages of the ideal zonation seen in previous Ordovician bioherms. These stages include: 1) a colonization or "pioneer colony" stage, composed of rooted echinoderms with some sponges, Calathium, and clusters of in situ brachiopods; 2) a diversification or "mature" stage with a diverse assemblage of digitate stromatolites, lithistid sponges (mainly Archaeoscyphia sp.) and Pulchrilamina and 3) a domination or "climax" stage, dominated by the problematic Pulchrilamina. A stabilization stage, formed by a pile of pelmatozoan sand is conspicuously absent beneath the El Paso bioherms. Indeed the substrate on which these reefs grew is a burrowed skeletal lime mud, now dolomitized. It is possible, however, that this substrate was a hardground developed during a period of non-deposition and was subsequently used by the first reef-building organisms which commonly prefer lithified substrate for their growth (Walker and Alberstadt, 1975). For instance, the presence of hardgrounds played an important

role in the formation of Silurian stromatoporoid-coral bioherms in Gaspe (Desrochers, 1981). Nodular to parted mudstones and skeletal wackestones beneath these bioherms were lithified early, just below the sediment-water interface (Noble and Howells, 1974), and acted as a foundation for the initial growth of delicate branching colonies of rugose corals. Thus, a hardground origin may help to explain the aberrant relation between a muddy substrate and reef development observed in the El Paso Group.

In summary, the sequence of growth stages found in other Ordovician reefs and in the El Paso Group in particular, is similar to that present in the Mingan bioherms. The absence of the basal stabilization stage in some bioherms may be explained by the presence of lithified surfaces (paleokarst, hardground) beneath these surfaces.

Trophic structure in reef limestones

The Mingan reefs represent a complex and highly-ordered community where most of the feeding or trophic groups of benthic organisms are present (table 5-3). The reef biota, when compared to the adjacent inter-reef biota, is characterized by a marked increase in abundance and diversity. The terminology used in the present trophic analysis, is that of Walker and Bamback (1974).

The main reef building organisms include lithistid sponges, bryozoans, and tabulate corals, which are all epifaunal organisms that were fixed to, or sat on, either a hard substrate or other organisms. Both lithistid sponges (Rigby, 1983) and bryozoans (Brood, 1978), based on our knowledge of the feeding habits of modern taxa, belong to suspension feeding trophic groups. Tabulate corals may represent either

- 228 -

Table 5-3. Trophic group distribution of fossil in Mingan reef limestones

FOSSIL ORGANISM	ECOLOGY	TROPHIC ANALYSIS
Lithistid sponge	epifaunal, attached	suspension feeder
Tabulate coral	epifaunal, attached	suspension feeder/ passive predator
Bryozoan	epifaunal, attached	suspension feeder
Algae	epifaunal, attached	primary producer
Stromatoporoid	epifaunal, attached	suspension feeder
Echinoderm	epifaunal, attached	suspension feeder
Brachiopod	epifaunal, attached	suspension feeder
Gastropod	epifaunal, vagile	browser
Cephalopod	nektobenthonic	scavenger
Ostracod	epifaunal, vagile	deposit feeder/ scavenger
Trilobite	nektobenthonic	scavenger
Burrower	infaunal	suspension feeder/ deposit feeder

suspension feeding or passive carnivorous trophic groups by analogy with modern living coelenterates (Cooper, 1974). Echinoderms were suspension feeders (Broadhead and Waters, 1980) but represent accessory reef builders. Solenoporacean algae, locally common as small framebuilders were primary producers, occupying the photosynthetic niche (Wray, 1977). In addition to calcareous algae, cyanophytes which are accessory builders, provided a food source for browsers. Unlike the absence of cyanophyte mats in modern subtidal environments (Garret, 1970), the presence of mats within Mingan reef interstices suggests that grazing pressure by gastropods was insufficient to inhibit their development. Pratt (1982a) pointed out that the Phanerozoic period is replete with examples of reefs containing stromatolites which coexisted with grazing and burrowing organisms under normal marine conditions. Stromatoporoids are thought to be suspension filter-feeding organisms. This interpretation is based on their affinity with sponges (Stearn, 1983). Stromatoporoids did not directly participate in reef construction.

In addition to these reef builders, various organisms were dwellers within reef interstices. Trilobites and ostracods were epifaunal, vagile organisms feeding as deposit feeders or scavengers at the sediment-water interface (Puri, 1964). Brachiopods based upon their modern living counterparts were epifaunal suspension feeders and may be either attached or free-lying organisms depending on the presence or absence of a pedicle opening (Grant, 1972). Cephalopods were nektobenthic, bottom feeding carnivores (Flower, 1957). Gastropods were vagile, epifaunal organisms that browsed algal mats that encrusted various reef builders (Copper, 1974).

Infaunal burrowers were common in the muddy matrix between the reef builders. These burrowers belonged to both suspension feeders and deposit feeders as suggested by the presence of burrows back-filled with peloidal material and burrows filled with blocky calcite (Ekdale et al, 1984). Their taxonomic affinities, however, remain unknown at this stage. Other soft-bodied organisms, if present, left no obvious record. Macroborings made by endolithic organisms are not observed even though they are present at the post-Romaine paleokarst unconformity and have been reported from other Early Paleozoic reefs (Kobluk et al., 1978). This may suggest that the Mingan reefs, and their lime mud matrix in particular, were not cemented as they grew on the sea floor.

The trophic structure of benthic communities is ruled by some basic principles (summarized by Walker, 1972) in order to minimize competition for food; these rules are: 1) each community is dominated by one trophic group; 2) of the several dominant species in the community, each belongs to a different trophic group and 3) one species dominated each trophic group in the community. The Mingan reefs reflect this as they are sometimes dominated by a single taxon (mainly a suspension feeder) while the others are subordinate or absent. Reef building taxa from other trophic groups (e.g. solenoporacean algae) are always present but their relative abundance is variable. In contrast, some reefs are build by several principal taxa which are all suspension feeders (i.e. lithistid sponges, bryozoans, tabulate corals). This may be explained by the fact that these taxa represent different feeding levels due to various growth forms and sizes. Such level stratification of the suspension feeders could minimize competition for food within the same trophic group.

DISCUSSION

Comparison with other Middle Ordovician reefs.

The composition, organism diversity and depositional environments
outlined for the Mingan bioherms are not unique but are similar to other
lower Paleozoic reefs and to Lower and Middle Ordovician bioherms
ofNorth America in particular (see table 5-4). A comparison with other
bioherms is needed here to understand the importance of the Mingan
bioherms at this critical time of reef development (Copper, 1974; James,
1983).

Klappa and James (1980) discussed the evolution of Early Paleozoic
reefs and suggested a basic pattern of development. Early Paleozoic
bioherms are generally mound-shaped structures composed of abundant
skeletons and rich in lime mud. These structures occur either as single
mounds or as large bioherms composed of an aggregate of numerous small
mounds, and represent stratigraphic reefs (sensu Dunham, 1970). They
commonly exhibit a vertical zonation. The most common reef-building
organisms are: bryozoans, corals, stromatoporoids, lithistid sponges,
calathids, and the problematic Pulchrilamina. Pelmatozoan debris is
common both within and surrounding the bioherms. The matrix of these
bioherms is generally a burrowed, skeletal wackestone, ranging from 40
to 60 per cent of the rock volume. In the matrix, pelmatozoan debris,
spicules, trilobites, ostracods, and brachiopods are present. This basic
pattern in Lower Paleozoic bioherms was established as early as the
Lower Cambrian (James and Kobluk, 1978).

Lower and Middle Ordovician bioherms can be grouped into three
distinct classes according to Klappa and James (1980), and include by

Table 5.4- Reef-building organisms in Lower and Middle Ordovician bioherms.

| AGE | REEF BUILDING ORGANISMS | |
LOCATION REFERENCE	MAJOR TAXA	ACCESSORY TAXA
EARLY CANADIAN		
St. George Group Western Newfoundland (Pratt and James, 1982)	thrombolites/corals/ <u>Renalcis</u>	lithistid sponges/ <u>Pulchrilamina</u>
LATE CANADIAN		
Southern Oklahoma (Toomey & Nitecki, 1979) Western Utah (Rigby, 1968; 1971)	lithistid sponges	stromatolitic algae/ <u>Renalcis/Epiphyton</u>
El Paso Group West Texas, New Mexico (Toomey & Nitecki, 1979)	<u>Calathium/Pulchrilamina/</u> lithistid sponges	calcareous algae
WHITEROCKIAN		
Table Head Group Western Nfld. (Klappa & James, 1980)	lithistid sponges	<u>Pulchrilamina</u>/bryozoans
CHAZYAN		
Chazy Group New York, Vermont (Pitcher, 1964; 1971)	lithistid sponges	bryozoans/corals/ <u>Rothpletzella</u>
	bryozoans	
	corals	stromatoporoids/bryozoans/ lithistid sponges/<u>Solenopora</u>
	stromatoporoids/corals/ lithistid sponges/<u>Solenopora</u>	bryozoans
Mingan Formation (This study)	bryozoans	
	corals	lithistid sponges/bryozoans
	Lithistid sponges/bryozoans/ corals/cyanophyte mats	
	Solenoporacean/corals	lithistid sponges bryozoans stromatolitic mats
BLACKRIVERAN		
Lourdes Limestones Western Newfoundland (James & Stevens, 1982)	corals	lithistid sponges/bryozoans stromatoporoids
Rockdell Formation Tennessee (Ruppel & Walker, 1982)	bryozoans	calcareous algae, sponges
TRENTONIAN		
Carters Formation Tennessee (Alberstadt & al , 1974)	corals/stromatoporoids	bryozoans/calcareous algae

order of increasing faunal complexity: 1) mud mounds; 2) bioherms dominated by a single taxon and 3) bioherms with several taxa. The simplest of these bioherms are mud mounds which possess no obvious large skeletons and are composed for the most part of lime mud and stromatactis (James, 1984b). Mud mounds in Middle Ordovician strata are the first ones in the rock record and occur in the Antelope Valley Limestone of southern Neveda (Ross et al, 1975); in the Effna Formation in Virginia (Read, 1982) and locally in the Houlston Formation in Tennessee (Walker and Ferrigno, 1973; Ruppel and Walker, 1982). These mud mounds, however, are quite different from the Mingan bioherms and grew almost exclusively in deeper water on carbonate slopes (Pratt, 1982b).

The two other classes of bioherm are more similar to the shallow-water Mingan structures. They differ only with respect to their primary biotic constituents which can be subdivided into several types. These types of bioherms are described briefly for different stages in Lower and Middle Ordovician time.

Canadian (Ibexian) bioherms. Bioherms in the earliest Ordovician, recently documented by Pratt and James (1982), are a complex intergrowth of thrombolites (i.e. non-laminated cryptalgal structures), the coral Lichenaria, and Renalcis with rare lithistid sponges and Pulchrilamina. In some cases, bioherms are dominated by thrombolites either alone or with sponges and are similar to other "algal-sponge" bioherms from the early Canadian House Limestone of western Utah (Rigby, 1966).

Bioherms younger in age are found in the late Canadian strata of west Texas, New Mexico, and Oklahoma (Toomey, 1970; Toomey and Nitecki,

1979). They are generally small, mound-shaped structures, a few metres
in size, but larger mounds may reach 20 m high and 87 m across. Their
principal biotic builders are a consortium of lithistid sponges (mainly
Archaeoscyphia), calathids, and the problematic organism Pulchrilamina.
As mentioned earlier, these organisms are conspicuously zoned within
each bioherm. The relative abundance in these bioherms is variable; in
some cases they are dominated by the sponge Archaeoscyphia and regarded
as a separate type. These structures, found in southern Oklahoma (Toomey·
and Nitecki, 1979) and western Utah (Rigby, 1966, 1971), are associated
with stromatolitic mats and the calcified algae Renalcis and Epiphyton.

Whiterockian bioherms. Bioherms in slightly older strata than the
Mingan bioherms have been found only in the Table Head Group of western
Newfoundland (Klappa and James, 1980). They occur as small metre-sized
structures dominated by lithistid sponges with a wide variety of forms,
and also contain rare bryozoans and Pulchrilamina.

Chazyan bioherms. Bioherms, contemporaneous with the Mingan
bioherms, to date have been found only in the Chazy Group of New York
and Vermont where they are abundant and well kr wn (Pitcher, 1964, 1971;
Toomey and Finks, 1969; Kapp, 1975). The major building organisms in
these bioherms include stromatoporoids, bryozoans, lithistid sponges,
and the calcareous algae Solenopora (also referred to as Parachaetetes
by some workers). The relative abundance of these biotic elements varies
widely; many bioherms are dominated by a single taxon either sponges,
bryozoans, or corals.

In the lower part of the Chazy Group (Day Point Formation), small

bioherms, dominated by bryozoans, are homogeneous, highly irregular to linear in shape, and composed of numerous superimposed layers of the encrusting trepostome Batostoma and cyclostomate Ceramoporella (formerly Cheiloporella). They have been interpreted as relatively deeper water reefs that grew at wave base or below, compared to other Chazy bioherms (Kapp, 1975). Similar bioherms are also present in the Chazy Group in Quebec (Hofmann, 1963; Kobluk, 1981a).

Bioherms, dominated by tabulate corals, are ubiquitous throughout the Chazy Group but vary in character. In the Day Point Formation, coral bioherms are composed almost entirely of Lichenaria with subordinate encrusting bryozoans. Their origin, however, is equivocal, being interpreted either as a transported coral rubble by Pitcher (1964) or in situ accumulations by Finks and Toomey (1969). In the overlying Crown Point Formation, some bioherms, several meters in size, contain abundant corals (Billingsaria) with less common stromatoporoids, lithistid sponges, trepostome bryozoans, and the algae Solenopora. Bioherms in the upper part of the Chazy Group (Valcour Formation) consist mainly of superimposed layers of the massive coral Billingsaria, while others are dominated by the hemispherical coral Eofletcheria, and in some cases both corals occur together.

Bioherms, dominated by lithistid sponges (mainly Zittella), are present in the Crown Point Formation, together with encrusting trepostome bryozoans, the coral Billingsaria, and the algae Rothpletzella (also referred to as Spaerocodium by some workers). Sponges in these bioherms are characterized by a wide variety of forms and may represent over 50 per cent of the rock volume.

The first bioherms in which stromatoporoids are an important

constituent are in the Crown Point Formation. In addition to stromatoporoids, other primary biotic constituents are common in these bioherms and include: <u>Billingsaria</u>, <u>Solenopora</u>, lithistid sponges, and less abundant bryozoans. These bioherms exhibit all vertical growth stages in which the domination stage is generally dominated by a rigid framework of stromatoporoids as they grew under more turbulent conditions (Alberstadt et al, 1974).

<u>Blackriveran bioherms</u>. Bioherms in the succeeding Blackriveran time have been found in the Lourdes Limestone in western Newfoundland (James and Stevens, 1982) and in the Rockdell Formation in Virginia and Tennessee (Read, 1980; Ruppel and Walker, 1982). Individual bioherms in the Lourdes Limestone may reach 7 m high and 12 m across but are, on average, smaller. Each structure is for the most part composed of many stacked coral heads, mainly <u>Labyrinthites</u> with subordinate sponges, bryozoans, and stromatoporoids. The matrix between coral heads is filled with coarse skeletal debris.

The Rockdell bioherms, on the other hand, are dominated by encrusting bryozoans (fourteen genera in total), together with calcareous algae and rare sponges. These bioherms formed in significantly shallower waters than did the Houlston bioherms which were deposited contemporaneously basinward in Tennessee (Ruppel and Walker, 1982).

<u>Rocklandian bioherms</u>. Bioherms in the Carters Formation of Tennessee, estimated to be 160 m long and 15 m high, are made up of a consortium of stromatoporoids and large tabulate corals , up to 1 m in

- 237 -

diameter (Alberstadt et al, 1974). Calcareous algae and bryozoans are also present but less common. Like the bioherms in the Lourdes Limestone, substantial amounts of grainstone are found in these structures. They are characterized by a fourfold vertical growth succession.

It has been recognized by several workers that a major change in the style of bioherms occurred in the Early Paleozoic when bioherms in the Cambrian, dominated by algal structures (except archeocyathids in Early Cambrian) were replaced by other taxa in the Ordovician. This change has long been associated with the beginning of the Middle Ordovician, characterized by the first appearance of bryozoans, corals, and stromatoporoids in abundance and also coincident with a major trangression over the subaerially exposed North American craton. From the previous discussion, it is apparant that this change did not take place rapidly but occurred gradually throughout Early and Middle Ordovician time. As noticed by Klappa and James (1980), several biotic constituents (lithistid sponges in particular) appeared early and persisted for most of that time whereas other taxa disappeared were replaced by new taxa. By Chazyan time, bioherms were populated with numerous potential biotic builders which occur either alone or in complex assemblages, and as result a wide variety of reef types developed. It is only later in Middle Ordovician time that corals and stromatoporoids became prominent as successful reef builders with their large skeletons able to build larger and more complex bioherms.

From the previous discussion, the bioherms in the Mingan Formation represent an important stage in the evolution of reef development, and

particular, in the Lower Paleozoic. First, it should be pointed out that these bioherms are similar to most, if not all, other bioherms described in this section, and so conform to a general "basic pattern" observed in Lower Paleozoic bioherms (Klappa and James, 1980). Second, the Mingan bioherms differ only by their primary biotic builders when compared to other Lower and Middle Ordovician bioherms. These builders, however, are in part inherited from older bioherms (lithistid sponges and to a lesser extent calcareous algae and the primitive coral Lichenaria) and in part new taxa (tabulate corals, bryozoans). Some of these new and older builders in the Mingan bioherms in turn persisted through the Chazyan time and are present in young r bioherms. This is also consistent with a gradual transition in the style of bioherms during Lower and Middle Ordovician time. Third, it has long been recognized that bryozoans, corals, and stromatoporoids in reef communities first appear in abundance during the Chazyan. This needs to be revised now because stromatoporoids are conspicuously absent in the Mingan bioherms which are contemporaneous with those in the Crown Point and Valcour Formations of the Chazy Group (see chapter 2). This indicates that stromatoporoids were probably endemic (with the exception of Labechia) to the Chazy type area (Webby, 1980). Finally, it is also evident that environmental factors played an important role in the development of different reef types in the Mingan Formation. It is most likely that some of the numerous potential builders in the Chazyan time could have been more successful than others to colonize and dominate reef environments under specific environmental conditions. The most obvious factor controlling the relative number of these builders was water turbulence (see interpretation in this chapter). Variable water turbulence conditions

- 239 -

affect also indirectly factors such as food supply, light penetration, bottom substrate, and turbidity. By analogy, variations in water turbulence may explain the variety of reef types also present in the Chazy Group of New York and Vermont.

CHAPTER 6

PALEOKARST UNCONFORMITIES

INTRODUCTION

The lower paleokarst unconformity developed on the Romaine Formation
during Whiterockian time and corresponds to the Knox or Beekmantown
unconformity elsewhere in eastern North America. It represents an
extensive karst plain veneered by eolian sediments and exhibits a
variety of surface solution features ranging from karren to small
collapse dolines. Subsurface features are local and consist of small
caves filled by collapse breccias.

The upper paleokarst unconformity occurs within the Mingan Formation
and displays substantial karst relief which was modified by intertidal
erosion preceding renewed submergence. The surface is sculpted into a
variety of karren forms.

Both paleokarst unconformities are interpreted to be due to tectonic
movement in the basin caused by Taconic Orogenesis, some 500 km to the
east.

KARST PROCESSES AND CONTROLS

The formation of karst landforms, both surface and subsurface, is
related to the occurrence of soluble rocks such as evaporites,
carbonates, and quartzites (Bogli, 1980), although only those formed in
carbonate rocks are relevant to the following discussion. According to

Estaban and Klappa (1983), karst is best defined as:

> "a diagenetic facies, an overprint in subaerially
> exposed carbonate bodies, produced and controlled by
> dissolution and migration of calcium carbonate in
> meteoric waters, occurring on a wide variety of
> climatic and tectonic settings, and generating a
> recognizable landscape".

Solution is critical to the formation of karst, which can be inhibited if solution processes are inoperative, regardless of adequate climatic conditions. These processes are controlled in most natural conditions by the addition and removal of carbon dioxide (CO_2) to the water (Bathurst, 1975, chap. 6). Of particular importance is the partial pressure of the carbon dioxide (pCO_2) in the air (i.e. atmosphere, soil pores, subsurface caves) standing at the air-water interface and the temperature of the water, both of which control the amount of CO_2 soluble in water. In general, the amount of CO_2 dissolved in the water increases as the pCO_2 of the air increases and as the temperature of the water decreases. Several dissolution or corrosion processes can operate in the meteoric environment and the most important are: simple corrosion, biogenic corrosion, and mixing corrosion (Thrailkill, 1968; Ritter, 1978, p.473-475; Bogli, 1980).

Corrosion in its simplest form occurs on bare surfaces that are directly exposed to precipitation (i.e. air-rock interface). Rainwater is in equilibrium with atmospheric CO_2 (0.03% in content) and as a result, it forms a weak acid ("carbonic acid") able to dissolve carbonate substrates.

Biogenic corrosion occurs when water permeates through a soil supporting vegetation or a humus cover. Air in the soil is characterized by a high content of biogenic CO_2 which commonly averages 1-2% (up to

20-25% in some tropical soils) and always exceeds the CO_2 content in the atmosphere. Water in the soil is an aggressive solution agent when it reaches the soil-rock interface.

Another important solution process is mixing corrosion which occurs when two bodies of water with different temperature or CO_2 content are mixed. For instance, meteoric water saturated with respect to calcite may become undersaturated by being cooled or being mixed with water which is in equilibrium with a lower pCO_2 (Thrailkill, 1968). Mixing of water with different pH or salinity content may also have caused corrosion. Mixing corrosion in the meteoric environment commonly takes place at the water table and in the transition zone beneath the phreatic lens (James and Choquette, 1984).

The formation of karst is primarily controlled by climatic conditions that determine the amount of water circulating in the system. Karst features are more abundant and diverse in humid, subtropical to tropical areas where a combination of temperature, precipitation, and vegetation strongly favor corrosion processes. This is not to say that karst does not form in other areas with low precipitation and/or cold temperature, but development is significantly slower.

KARST PRODUCTS

Modern karst can be grouped into two types: surface and subsurface landforms. These landforms are briefly discussed here, however more detailed information about their geomorphology and classification can be found in several excellent references (Jennings, 1971; Sweeting, 1973; Bogli, 1980; Esteban and Klappa, 1983).

The surface landforms are subdivided into uncovered, subsoil,

and mantled karsts according to the presence or absence of cover and type of cover. Uncovered karst is a bare surface on which natural water flows unhindered. Subsoil karst is covered by soil, usually residual, supporting land plant vegetation. These soils are sites of intense microbial activity which add extra CO_2 in the system. Finally, mantled karst is overlain by a thin cover of sediment, usually transported. In summary, uncovered karst is formed by solution at the atmosphere- rock interface whereas solution in both subsoil and mantled karsts occurs at the cover-rock interface.

The most common landforms associated with karst surfaces are dolines, which form enclosed depressions ranging from a few metres to several hundreds metres wide and deep. They are formed by a combination of solution and collapse or subsidence, but solution is always the driving mechanism causing enlargement of joints or fractures and eventual settling of the soluble surfaces (Bogli, 1980, fig. 3.9). Large landforms with positive topography include several types of hills (towers, mongotes, pinnacles) which are developed only in tropical and subtropical areas characterized by high rainfall and extensive vegetal cover.

Small solution features, commonly termed "karren", are common on surface karst and range from tens of millimetres to a few metres in size. Karren forms display a wide spectrum of shapes, including: pits, flutes, grooves, pipes, basins (Sweeting, 1973; Allen, 1982, p. 225-252). Furthermore, karren are sometimes hierarchically organized with small forms developed on the larger ones. Their morphology is mainly controlled by slope and dip of the substrate, presence or absence of a cover, and solution processes. In general, karren produced beneath

sediment or soil cover are characterized by smooth and rounded solutional forms, whereas those developed on bare substrates display more sculpted forms. The cover on karst surface acts as a meteoric water storage, so the contact between CO_2 in the air, the water, and the rock surface lasts much longer than on bare surfaces where rainwater commonly disappears before it reaches $CaCO_3/CO_2$ equilibrium.

Major subsurface landforms consist of caves and solution breccias. Caves are underground, open spaces of solution origin, generally with a connection to the surface, and partially filled with speleothems and cave sediments. They are well developed in areas where mixing corrosion is intense (i.e. water table, transition zone beneath the phreatic lens). Furthermore, solution breccias can form by collapse of the cave roofs in response to the removal of the underlying soluble rocks.

Karst features (caves, karren) are sometimes formed contemporaneously with alteration and lithification of newly exposed marine carbonate sediments (syngenetic karst of Jennings, 1971). These sediments are dominated by metastable aragonite and Mg-calcite minerals which alter rapidly in presence of fresh water. The full development of karst landforms is therefore not commonly observed in these poorly-lithified carbonates.

It is assumed by most workers that karst features are equally developed in limestone and dolomite terranes (Sweeting, 1973; Bogli, 1980). Although it is not certain at this stage whether the same spectrum of karst features can form in dolomites or if these features can develop at the same rate (Pluhar and Ford, 1970).

COASTAL KARST

Coastal "karst" sometimes exhibits morphological features (pools, karren) similar to those observed on bare carbonates in subaerial environments (Kaye, 1959; Scheinder, 1976). This karst occurs along tropical to temperate limestone coasts in the intertidal zone (zone of wave and tide) and the supratidal zone (zone of wave splash and spray).

The formation of coastal karst has been attributed to a variety of physical, biological, or chemical processes (see Scheinder, 1976 for a good review). Several studies, however, have highlighted the importance of biological erosion in the destruction of marine carbonate coasts (Ginsburg, 1953; Scheinder, 1976, 1977). The morphological features along these coasts are not simply the result of inorganic solution, but are also due to simultaneous biologic corrosion caused by endolithic organisms (mainly cyanophytes) and biologic abrasion carried out by grazing organisms (molluscs, chitons, echinoids). Another destructive process is the chemical dissolution in tidal pools related to diurnal changes in temperature and respiration by plants and organisms, thus causing an increase in the CO content of water (Emery, 1946; Revelle and Emery, 1957). Physical processes are commonly limited to wave action removing material weakened by organisms. Wave erosion is rapid enough along exposed, high-energy coasts to inhibit colonization by organisms.

A typical profile of coastal karst (fig. 6-1) is characterized by 1) a tidal platform with colour zones and small-scale relief forms and 2) a notch lying below the mean high water line. The colour zonation of the tidal platform reflects the distribution of endolithic and epilithic cyanophytes with respect to the moisture gradient in the peritidal zone. Irregular to jagged relief forms (mainly pools and basins) are common in

- 246 -

Figure 6.1- Schematic cross-section of a coastal exposure surface showing the main features across a present-day tropical rocky shore (modified from Estaban and Klappa, 1983). These features include: 1) a notch lying below the mean high water line and 2) a tidal platform, characterized by small-scale ragged relief forms (mainly kamenitzas). Note the transition with the adjacent subaerial exposure surface which may occur within a few metres.

COASTAL EXPOSURE SURFACE

COASTAL — SUBAERIAL

KARST

SOIL

KAMENITZAS

NOTCH

SUPRATIDAL

INTERTIDAL

SUBTIDAL

SL
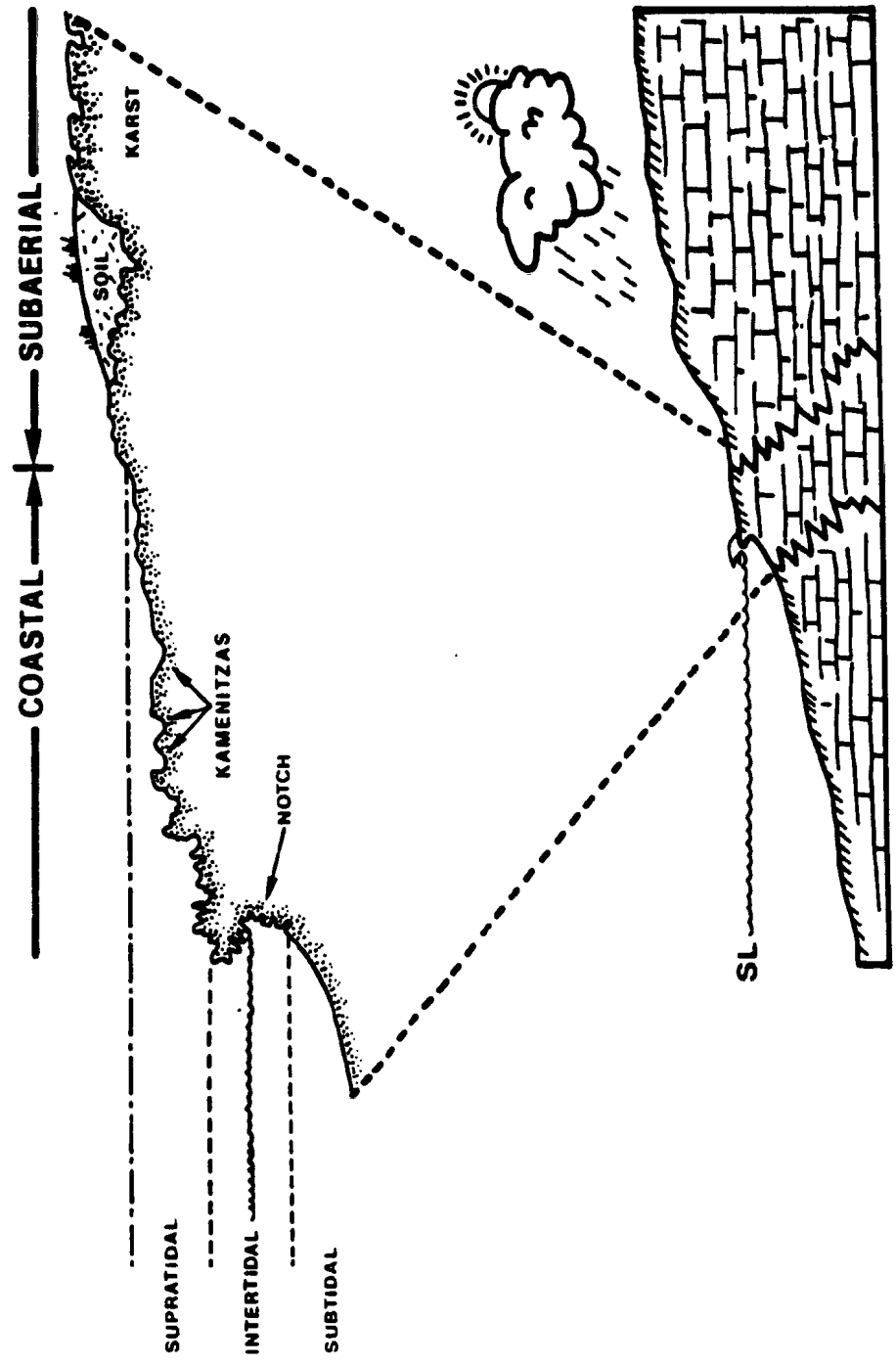
all colour zones. The intertidal notch displays a horizontal to overhanging roof and is best developed on relatively protected coasts. Coastal exposure surfaces may grade laterally landward within a few metres into subaerial exposure surfaces.

PALEOKARST

Paleokarst is used here in the broad sense to encompass any karst features (i.e. surface and subsurface) associated with a landscape of the past and buried by a sequence of post-karst strata. Detailed studies on paleokarsts are rare and listed in table 6-1.

Paleokarst landforms with substantial erosional relief are unusual in the geological record. Maslyn (1977), however, described tower karst forming steep-sided hills (up to 20 m) near the Mississippian- Pennsylvanian contact in central Colorado. In general, paleokarst surfaces are sub-horizontal with little erosional relief, usually less than 1-2 metres. Mammillated to potholed paleokarst surfaces in the Carboniferous of Britain were formed beneath a vegetation cover, with each depression developed around a single root system (Walken, 1974; Wright, 1982). They commonly cap small, shallowing-upward cycles (Sommerville, 1979; Bridges, 1982). In some areas, polyphase karst erosion caused superimposed generations of solution pipes filled by fluvial sediments (Walkden and Davies, 1983).

Other paleokarst surfaces exhibit irregular, scalloped to hummocky topography in vertical section (Read and Grover, 1977; Kobluk et al., 1977; Cherns, 1982; Kobluk, 1984). Their relief ranges from 10 to 50 cm, as small basins with steep walls and sharp ridges, and was produced mainly by tidal erosion along peritidal rock platforms. Both borings and

TABLE 6.1- EXAMPLES OF SUPERFICIAL KARSTS IN ANCIENT CARBONATE SEQUENCES.

OCCURENCE	DESCRIPTION	INTERPRETATION
Middle Ordovician Virginia, U.S.A. (Read and Grover, .977)	scalloped to planar erosion surfaces, relief up to 30 cm, basins (10-100 cm wide) with steep walls, borings, marine encrusting organisms, capping fenestral units and overlying subtidal units.	bare subaerial/littoral karren initiated on exposed karst and subsequently eroded in peritidal zone.
Upper Silurian Gotland, Sweden (Cherns, 1982)	irregular to scalloped erosional surfaces, relief of 40-50 cm, oriented ridges and basins on bedding planes, laterally associated planar surfaces, encrusting marine organisms, shallowing-upward sequence.	bare subaerial/littoral karren surfaces.
Silurian-Devonian Southern Ontario, Canada (Kobluk et al., 1977; Kobluk, 1984)	irregular to wavy erosional surfaces, relief up to 100 cm, solution-enlarged fractures, karren forms, pitting, leached and vuggy porosity, borings, microphyte mats, iron oxide crusts.	littoral karren formed by tidal erosion
Carboniferous(Visean) Britain (Walken, 1974; Wright, 1982)	mammillated to potholed erosional surfaces, relief of 50 to 100 cm, overlying k-bentonite clays, associated calcrete crusts.	paleokarst surface beneath a soil cover, pits associated with root systems, similar to "decken-karren".
Carboniferous(Visean) Britain (Wright, 1982)	rubbly horizon with clay-filled pipes and horizontal fissures, associated vadose diagenetic features.	paleokarst surface beneath a soil cover, similar to tropical kavor-nossen karren.
Carboniferous(Visean) Britain (Walken & Davies, 1983)	sandstone-filled pipes capping minor sedimentary cycles, up to 1.5 m wide and 3.0 m deep, associated with fluvial channels, superimposed generations of pipes	paleokarst surface associated with polyphase erosion, solution by overbank fluvial flooding
Late Mississipian Colorado, U.S.A. (Maslyn, 1977)	steep-sided hills, relief up to 20 m, hill sides mantled by conglomerates and breccias, associated sinkholes.	tower karst produced by jointing in massive limestones, sub-tropical to tropical landforms.
Late Mississipian Wyoming, U.S.A. (Sando, 1974)	large cavities associated with regional disconformity, up to 15 m wide and 30 m high, filled with angular blocks and red clastic sediments, delimited by vertical walls, associated with enlarged joints and irregular-shaped caves.	paleokarst surface and subsurface, dolines or sinkholes with associated caves.
Late Cretaceous Israel (Buchbinder et al., 1983)	circular to irregular depressions filled with collapse breccias and post-karst marine sediments, 10-80 m in diameter, overlying bedrock dipping toward centre of the depression.	Paleokarst surface landforms, collapse dolines.

encrusting marine organisms are usually present on these surfaces. Their morphology, however, needs to be interpreted with caution because bedding plane exposures are usually limited, if not totally missing.

Paleodolines associated with karst surfaces have been described from Tertiary strata in Israel (Buchbinder et al. 1983) and late Mississippian beds in Wyoming (Sando, 1974). They form circular to irregular depressions (10-80 m wide and deep) delimited by vertical walls and filled by post-karst sediments and angular blocks derived from the host rock. Subsurface collapse breccias without obvious connection to the karst surface are also present.

Paleokarst landforms with subsurface caves and collapse breccias are common in the geological record, probably reflecting good preservation potential from subsequent erosional phases. They are best known from mineral deposits which have been extensively drilled. Karstification played an important role in the development of lead-zinc deposits of several North American Paleozoic carbonate-hosted orebodies (Kyle, 1983). Subsurface caves and collapse breccias formed zones of secondary porosity acting as conduits for fluid migration and sites for ore precipitation.

RECOGNITION OF PALEOKARST

It is not clear whether infrequent karst occurrence in ancient carbonate sequences is due to inadequate outcrop or subsurface data or to any subsequent erosional phase. On the other hand, karst is also unfamiliar to most geologists.

Estaban and Klappa (1983) identified several diagnostic criteria of subaerial karst which are : 1) surface landforms, including dolines,

rounded karren forms, or any landforms covered by relict soils; 2) subsurface landforms, mainly caves; 3) speleothems or cave precipitates such as stalactites, stalagmites, flowstone, and cave pearls and 4) collapse structures due to the removal of the underlying carbonates. Other features are common in the karst environment but not restricted to them, including vadose cement textures, lichen structures, crystal silt, and leached and vuggy porosity.

Some problems are raised by the timing of karst formation in ancient carbonate sequences. For instance, intrastratal karst can easily be misinterpreted as surface paleokarst because it occurs in the subsurface along lithological boundaries and forms after deposition and lithification of the overlying rock. Paleokarst, however, refers only to features which formed at one time and were subsequently buried by younger formations, except for exhumed paleokarst which is today exposed due to subsequent erosion. Although exhumed paleokarst should be distinguished from relict karst which is part of the present landscape but was formed at an earlier time and never covered by younger strata. Furthermore, smaller scale features such as stylolites or hardgrounds are common in carbonate sequences and can sometimes be mistaken for paleokarst surfaces. The reader is refered to both Wright (1982) and Read and Grover (1977) who discuss these problems in greater detail and suggest criteria for their distinction.

POST-ROMAINE PALEOKARST UNCONFORMITY

A marked paleokarst unconformity occurs on top of the Romaine Formation and is usually overlain by the basal sandstone unit of the Mingan Formation. This sandstone is interpreted to be a deflationary

eolian deposit which veneered the paleokarst unconformity at one time but was reworked with renewed submergence. Conodonts suggest that most of Whiterock time is missing and represented by the paleokarst surface in the study area (Nowlan, 1981). The duration of the Whiterockian stage (sensu Barnes et al, 1981) is estimated to be about 10 m.y. (Ross et al, 1982). The paleokarst unconformity is characterized by 1) a regionally-wide mappable surface; 2) various solution surface features ranging from small collapse dolines to karren and 3) associated features such as collapse breccias, borings, and pebble lags.

Regional unconformity

The paleokarst unconformity is today exposed both in vertical section and as bedding planes at more than twenty localities. The unconformity can be traced laterally for several hundreds of metres at some of these localities (e.g. Ile Quarry and Grande Pointe). On a regional scale, this unconformity represents a smooth surface with little or no relief. This is also reflected by the uniform thickness (4-5 m) of the basal Corbeau Member of the Mingan Formation which is generally capped by a marker bed of silty dololaminite (lithofacies 1). In some localities (e.g. Ile Innu, Ile du Havre E, and Grande Ile) however, variations in thickness may result from local relief of few metres superimposed on the regional unconformity. The unconformity truncates older beds toward the east where the Mingan Formation directly overlies the Sainte-Genevieve Member of the Romaine Formation (fig. 3-2). As much as 25-30 m of this formation is probably missing in easternmost localities and resulted from tectonic tilting and erosion of the platform interior in response to Taconic orogenic events located

several hundreds of kilometres to the east (to be discussed later). On
the basis of dolomite texture, three distinct sectors are recognized at
the top of the Romaine Formation (fig. 3-2): 1) an eastern part with
sucrosic dolomites (i.e. Sainte-Genevieve Member); 2) a central part
with dolomicrites (i.e. lower part of the Grande Ile Member) and 3) a
western part with both dolomicrites and sucrosic dolomites (i.e. upper
part of the Grande Ile Member).

Solution surface features

Various solution features are present and include: collapse dolines,
two end-member karren forms (rundkarren, kamenitza) and planar pitted
surfaces.

Dolines: Small solution depressions (plate 6-1; A), associated with
the unconformity, are ubiquitous in the study area, especially in the
eastern Mingan Islands where they are particularly prominent. These
bowl-shaped basins range from 1-3 m in depth and 5-20 m in diameter
(plate 6-1; B and C). Intraformational breccias (see below for
description) are sometimes associated with the depressions but their
exact relationship is difficult to evaluate because pervasive
dolomitization obscures lithological fabrics. In some cases, breccia
masses characterized by flat floors, steep, irregular walls, and roofs
with a distinct v-shape, are present beneath the dolines.

Dolines at or near the top of the Romaine Formation are thought to
result from the subsurface development of discrete bodies of carbonate
breccia which formed by removal of the underlying carbonates and
subsequent foundering of cave roofs.

Rundkarren: Rundkarren or rounded solution runnels form sinuous to

PLATE 6-1

POST-ROMAINE PALEOKARST - DOLINES

A. Field photograph (vertical cliff exposure) showing a typical depression (arrows) or paleodoline present at the top of the Romaine Formation. Grande Ile W.

B. Field photograph (bedding plane view) of a doline forming a bowl-shaped basin on top of the Romaine Formation. Basin dimensions are 1.0 m in depth and 5.0 m in diameter. Baie des Puffins.

C. Field photograph (bedding plane view) of the northern flank of a doline forming a depression (arrows) estimated to 3 m in depth and 30 m in diameter. Baie des Puffins.

parallel grooves and ridges on the paleokarst unconformity (plate 6-2).
These features are common in the western part of the area on lithofacies
composed of sucrosic dolomites. Grooves are round to flat in
cross-section and separated by rounded-crest ridges. They are closely
spaced and range from 10 to 40 cm in width and 5 to 30 cm in depth.
Their length varies from a few metres to over 15 m in some parallel
forms.

Modern rundkarren are interpreted by most workers as solution
sculpture forming beneath a soil cover where only smooth and rounded
forms are created (Sweeting, 1973; Bogli, 1980). The presence of
biogenic CO_2, however, is not essential to their development (D. Ford,
pers. comm. 1985). More important is the sediment cover which is able to
retain or slow water movement at the cover/rock interface, etching away
all edges and crests. Furthermore, the orientation of these karren has
been clearly related to local drainage conditions which depend primarily
on the slope and dip of the cover/rock interface. Although it is also
possible that they first formed as bare rinnenkarren with sharp crested
forms and then modified to rundkarren when subsequently covered by
sediment.

Against this background, it is suggested that the "fossil
rundkarren" present at the top of the Romaine Formation were created
under a sediment cover. Furthermore, rundkarren with short and sinuous
forms were probably produced on slightly inclined to sub-horizontal
surfaces whereas longer and parallel rundkarren were formed on more
inclined surfaces.

Another possible explanation for the roundness of karren morphology
is that the solution processes on dolomite are different than those on

PLATE 6-2

POST-ROMAINE PALEOKARST - RUNDKARREN

A. Field photograph showing the bedding plane of the top of the Romaine Formation on Ile Quarry NW. Note the presence of well-oriented fossil rundkarren (arrows). Detail in (B) and (C).

B. Close-up of (A) showing fossil rundkarren on top of the Romaine Formation. Rundkarren consist of rounded grooves that are separated by rounded-crest ridges. Field notebook is 20 cm.

C. Close-up of (A) showing fossil rundkarren on top of the Romaine Formation. Rundkarren length is 5 m. Lens cap is 50 mm in diameter.

D. Close-up of plate 3-4 showing sandstone patches (s) of the overlying Mingan Formation preserved in the rundkarren grooves. Note the presence of abundant Trypanites borings, 2-3 mm in diameter, on the surface of rundkarren (see detail in plate 5-5). Lens cap for scale. Grande Ile W.

limestone, and so have little to do with the presence or absence of a sediment cover. In other words, rounded forms are perhaps characteristic of the solution processes on exposed dolomite substrates which inhibit the formation of sharp-crested features. This, however, appears to be an unlikely explanation as sharp-crested karren are forming today on subaerially exposed dolomite substrates (Pluhar and Ford, 1970; Cowell, 1976).

Kamenitza: Kamenitzas are solution basins with circular to oval outlines, flat bottoms, and rounded edges(plate 6-3; A). Well-developed basins occur commonly on the sucrosic dolomites in the western part of the study area. These small basins range from 10 to 50 cm (up to 100 cm) in diameter and from 5 to 30 cm in depth. They are commonly interconnected by sinuous rundkarren and rarely found alone (plate 6-3; B and C).

Modern kamenitzas are usually developed on horizontal to slightly inclined subaerial surfaces where solution by stagnant water forms pools and basins (Sweeting, 1973). On the other hand, kamenitzas also form today in the intertidal/supratidal zone through the destruction of limestone coasts by bioerosion and mixing corrosion, but they are characterized by sharp-crested forms (Scheinder, 1976; James and Choquette, 1984).

The Ordovician kamenitzas, developed at the top of the Romaine Formation, are interpreted to be subaerial solution sculptures developed beneath a sediment cover as evidenced by their smooth and rounded edges and their association with rundkarren.

Planar pitted surface: The unconformity is planar on dolomicrites;

PLATE 6-3

POST-ROMAINE PALEOKARST – KAMENITZA

A. Field photograph (bedding plane view) of a kamenitza on top of the Romaine Formation. Kamenitza consist of solution basins with circular outlines, flat bottoms, and rounded edges. Note the presence of abundant _Trypanites_ borings on the kamenitza surface (detail in plate 5-5). Ile Niapiskau W. Scale in cm.

B. Field photograph (bedding plane view) of kamenitzas (k) on top of the Romaine Formation. Ile Niapiskau W. Lens cap is 50 mm in diameter.

C. Field photograph (bedding plane view) of enlarged kamenitzas and sinuous rundkarren on top of the Romaine Formation. Ile Quarry NE. Hammer for scale.

ornamented only by ubiquitous cm-sized pits. Rundkarren and kamenitzas are rare and poorly developed if present.

Of particular interest is the work of Pluhar and Ford (1970) who studied dissolution of fresh dolomite blocks with dilute hydrochloric acid in the laboratory. On bare, sloping surfaces (5 to 30), small sharp-crested karren were produced whereas dolomite karsting was limited to micro-pitting on sloping surfaces covered with an artificial silica sand.

The formation of karren on the planar surfaces at the top of the Romaine Formation was similarly inhibited by the presence of a thin cover of residual eolian sand (mainly quartz) which caused spreading and diffusion of the meteoric water over the surface. Furthermore, the fined-grained nature of dolomite may have formed a non-porous substrate influencing the rate of karren formation. Pluhar and Ford (1970) describe similar relationships on modern karren developed in Silurian dolomites of southern Ontario.

Associated features

Collapse breccias: Small, local intraformational breccias are present in the central and western parts of the study area where they occur 10 to 30 m beneath the paleokarst unconformity. These breccias form irregular masses that reach a few metres in size and 20 m in length (plate 6-4; A). Breccia margins, at least in one locality, are parallel oriented and delimited by sharp, vertical fractures. Joints and fractures, however, have not been observed elsewhere. The breccias are usually clast-supported with a matrix of coarse, white dolomitic cement

- 263 -

PLATE 6-4

POST-ROMAINE PALEOKARST - COLLAPSE BRECCIA

A. Field photograph (vertical cliff exposure) of intraformational breccia (b). Note that the adjacent strata (s) display no evidence of disruption. Baie Puffin.

B. Field photograph (bedding plane view) showing chaotic, clast-supported breccia. Clasts are standing out in relief. Baie des Puffins. Scale bar is 2 cm.

C. Field photograph (cross-section view) of intraformational breccia with vertically-oriented clasts. Hammer is 30 cm.

D. Field photograph (cliff exposure) showing the collapse of strata overlying intraformational breccia. Baie Puffin.

or fine detrital dolomite grains. The clasts are angular to sub-rounded, and range from 1 to 10 cm in size (plate 6-4; B and C). Larger fragments exhibit a fitted fabric. They are poorly sorted, oligomictic in composition and clearly derived from the same stratigraphic horizon.

A tectonic origin is unlikely because the breccias are stratigraphically controlled and adjacent strata display no evidence of disruption. These intraformational breccias probably represent collapse features due to partial removal of soluble material. Fractures may have controlled the development and distribution of these features and facilitate circulation of superficial meteoric water in subsurface. On the other hand, the formation of these breccias may be also due to dissolution in a mixing zone concomitant with pervasive dolomitization. There is growing evidence that dissolution is important in the mixing zone (James and Choquette, 1984). For instance, the northeastern Yucutan coast exhibits scalloped morphology and related collapse features which apparently developed in the coastal mixing zone (Back et al., 1979, 1984). The second hypothesis, if correct, would mean that the breccias are relic, intrastratal features rather than breccias generated contemporaneously with the subaerial exposure during Whiterockian time.

Boring: Abundant borings (up to 40 tubes/cm^2) are developed on the paleokarst unconformity (plate 6-5; A and B) but are patchy in distribution and occur on both dolomicrites and sucrosic dolomites. These borings cut through sucrosic dolomite crystals. They are simple, unbranched tubes with a circular aperture to the surface and belong to the ichnogenus Trypanites (Pemberton et al., 1980). They are straight in longitudinal section and usually oriented normal to the surface

- 266 -

PLATE 6-5

POST-ROMAINE PALEOKARST - TRYPANITES BORINGS

A. Field photograph (bedding plane view) showing abundant Trypanites
    borings on a planar surface at the top of the Romaine Formation.
    Boring aperture is 1-2 mm in diameter. Grande Pointe.

B. Field photograph (cross-section view) of Trypanites borings at the
    top of the Romaine Formation. Borings are 3-5 mm long. Ile Niapiskau
    W.

C. Polished slab (cross-section view) of Trypanites borings. Note that
    the borings are straight, unbranched, and normal to the bedding
    surface. Grande Pointe.
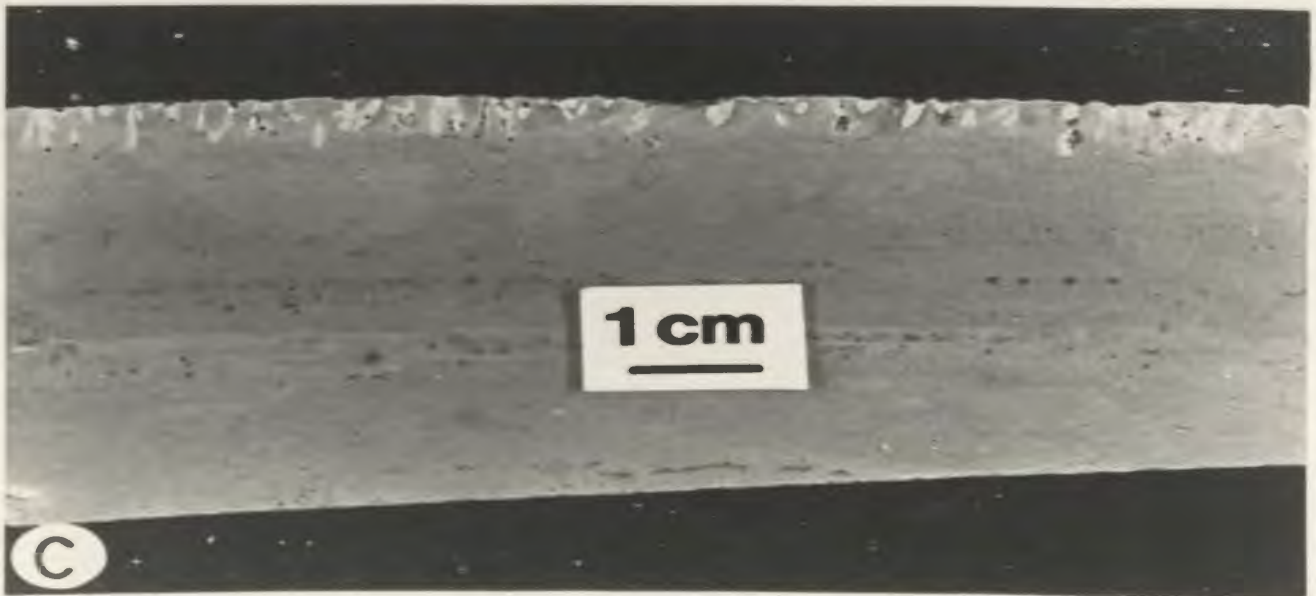
(plate 6-5; C). Their size averages 1-2 mm in width and 3-5 mm in length but larger forms are present. They are filled with terrigenous or dolomitic material.

Trypanites borings were formed after the karst surface developed on well lithified substrates and subsequently filled with sediments. It is not clear what organisms produced these borings but marine sipunculid worms are most likely, based on their overall morphology (Pemberton et al., 1980).

Pebble lag: Pebble lags, 10 to 30 cm thick, are found locally on top of the Romaine Formation (plate 6-6; A). These lags are lenticular and can be traced only for 50-100 m. They consist of chert and dolomite lithoclasts (plate 6-6; B and C) with a bimodal mature sandstone matrix (locally argillaceous). Lithoclasts are 1 to 20 cm in size, range from clast-supported to matrix supported, and are poorly sorted. Chert lithoclasts are subspherical in shape and have pitted surfaces (borings ?). Many of these chert pebbles are identical to chert nodules found in the Romaine lithofacies, especially dololaminites, and so suggest that they were eroded out and concentrated at the unconformity surface and redeposited with the sandstones. Dolomite lithoclasts are angular to rounded with flat, discoid shapes and are sometimes bored by Trypanites. These borings, however, are usually absent on the unconformity beneath pebble lags.

Pebble lags are probably a regolith (i.e. residual material) on top of the Romaine Formation that was slightly reworked but not completely removed by waves and currents with the renewed marine transgression. This is suggested by their stratigraphic position above the unconformity and locally derived material.

PLATE 6-6

POST-ROMAINE PALEOKARST - PEBBLE LAG

A. Field photograph (bedding plane view) of chert and dolomite lithoclasts in an argillaceous matrix overlying the Romaine Formation. Grosse Ile au Marteau. Lens cap is 50 mm in diameter.

B. Polished slab (cross-section view) of chert pebbles (dark particles) in arkosic sandstone overlying the Romaine Formation. Ile du Havre NW.

C. Polished slab (cross-section view) of dolomite lithoclasts in an argillaceous sandstone matrix immediately above dololaminite of the Romaine Formation (bottom). Note the sharp nature of the Romaine-Mingan contact. Grande Pointe.
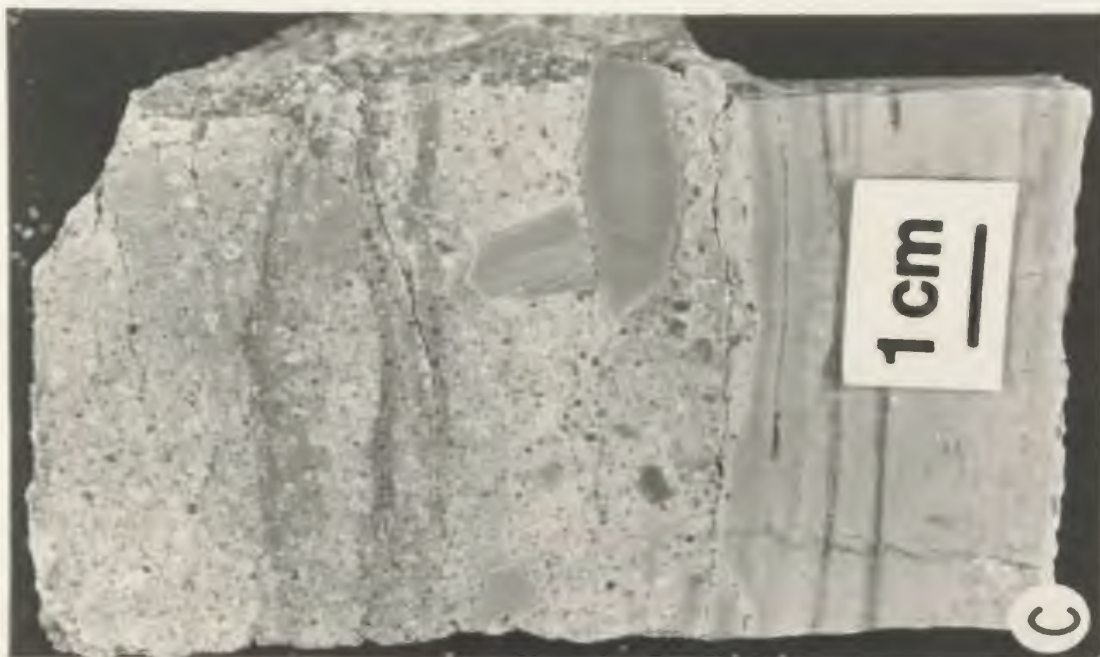
Interpretation

The sequence of events that occurred during the development of the paleokarst unconformity at the top of Romaine Formation is summarized in figure 6-2. The sequence began with a marine regression that exposed much of the "St-Lawrence" platform during early Whiterockian time. At that time, the Romaine lithofacies consisted of a lower unit of sucrosic dolomites and an upper unit of dolomicrites except in its upper part where a thin unit of sucrosic dolomites is present (fig. 6-2, stage 1). As discussed earlier, Romaine lithofacies were pervasively dolomitized prior to or at this time. Dolomicrites resulted from contemporaneous dolomitization of cyclic peritidal limestones and sucrosic dolomites formed early by replacement of subtidal limestones in a brackish mixing zone.

A peripheral bulge (see discussion later) associated with the Taconic Orogenic events in nearby western Newfoundland developed at about the same time and caused slight tilting of the exposed platform in the study area (fig. 6-2, stage 2). Paleotopographic features probably formed by differential chemical and physical weathering over the Romaine dolomites during the development of the unconformity. Scarce dolomite clasts in the post-unconformity sands, however, suggest that chemical weathering (i.e. dissolution) was the main process.

As time passed during stage 3 of the unconformity development, positive topographic elements were progressively eroded and eventually peneplaned to produce an extensive karst plain with little relief (fig. 6-2). Stratigraphic relief along the unconformity, however, increases from west to east where approximatively 30 m of upper Romaine strata are missing.

Figure 6.2- Schematic cross-sections illustrating the sequential development of the paleokarst unconformity capping the Romaine Formation. Stage 1: Romaine Formation prior to exposure consisted of a lower unit of sucrosic dolostones (Rsg or Sainte-Genevieve Member) and an upper unit of dolomicrites (Rgi or Grande Ile Member). Stage 2: epeirogenic movements caused tilting of the platform and differential weathering of the Romaine dolomites. Stage 3: progressive weathering resulted in an extensive karst plain with little relief on which a variety of solution features developed. Stage 4: Chazyan transgression reworked an eolian sand blanket overlying the post-Romaine paleokarst which was eventually exposed, at least locally, on the sea floor, bored by numerous endolithic organisms and finally covered by sandy material. Note the presence of the intraformational breccias beneath the paleokarst surface. See text for further detail.

POST-ROMAINE PALEOKARST

1

R_{gi}

R_{sg}

2

3

4
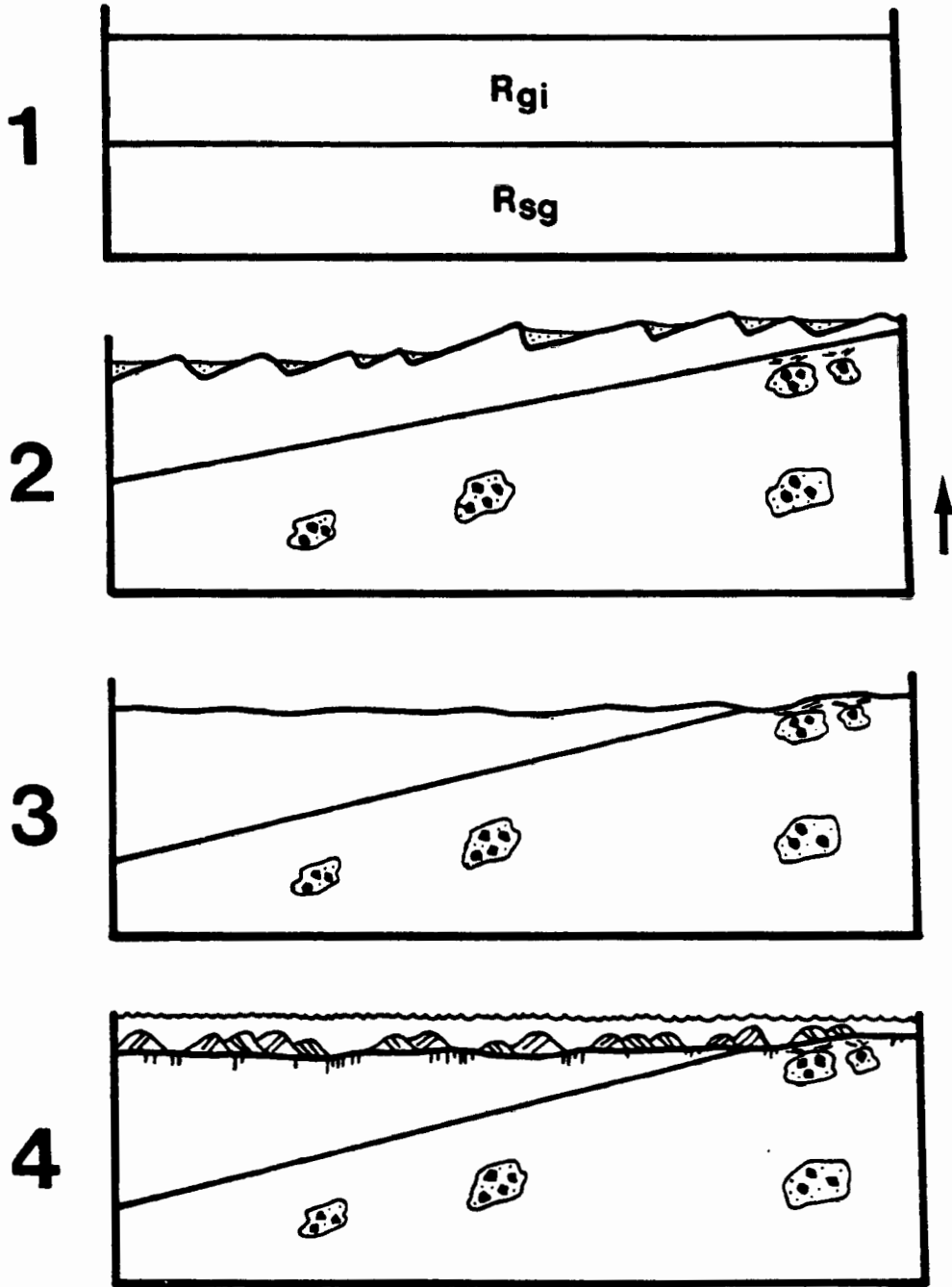
At that time, the unconformity was covered by a blanket of residual eolian sands characterized by a bimodal texture and arkosic composition. These sands are believed to be fluvial in origin and deposited during more humid periods by rivers draining the cratonic interior. Arkosic composition of these sands may reflect proximity of the source area and rapid transport which may have been more easily achieved under the absence of vascular plants during the early Paleozoic. Wind erosion which would have been more important was also a prominent transporting agent. There is growing evidence that many non-marine early Paleozoic sands have an eolian history (Dott and Byers, 1980). It is conceivable that alluvium and residual eolian deposits were present near the craton and that eolian sand dunes were transported away from these areas over the exposed platform. There is no way to test this hypothesis at this stage. Nevertheless, eventual examination of the basal Mingan sandstones beneath Anticosti Island could permit recognization of eolian, or at least marine-modified, dune sands characterized by an excellent sorting, mature composition due to prolonged eolian transport and abrasion, and thick cross-bed sets. In fact, the coeval St. Peter sandstone, which forms an extensive cratonic sand sheet in the upper Mississippi Valley region, is interpreted to be a mixture of coastal eolian and fluvial sands reworked by marine processes with renewed marine transgression (Mazzullo and Ehrlich, 1983).

A variety of small-scale karst features was formed on top of the unconformity and was controlled by: 1) the presence of a sediment cover; 2) the substrate nature (i.e. dolomicrite or sucrosic dolomite) and 3) the local drainage conditions. A sediment cover above the paleokarst surface is responsible for the development of smooth karren forms rather

than sculpted forms. Well-developed solution features were formed only over areas with substrates of sucrosic dolomite. This type of dolomite is porous and permeable due to high intercrystalline porosity, and so was probably more susceptible to dissolution than the impermeable dolomicrites. The style of these surface features, ranging from sub-parallel karren to kamenitza, indicate that local drainage conditions were present and controlled by the dip/slope of the substrate. It should be noted that substrates with a slope of only $1° -2°$ may develop sub-parallel solution forms (D. Ford, pers. comm. 1985). Local drainage conditions are probably relic from the earlier tectonic tilting of the platform (stage 2) because most runckarren form are oriented with a persistant east-west direction.

Subsurface solution features consist of intraformational breccias that are stratigraphically restricted to the lower unit of sucrosic dolomite. It is not clear whether their origin was due to concomitant dissolution and dolomitization of preexisting subtidal limestones or to dissolution by meteoric water percolating downward from the paleokarst unconformity. The first hypothesis is most likely because permeability was probably insufficient to permit downward water movement due to little or no primary porosity because to the dolomicrites capping the formation and poor secondary porosity, usually formed by joints and fractures. Furthermore, minor topographic relief following stage 2 of the unconformity development may have provided insignificant hydraulic gradient to assure groundwater circulation in the system. Permeability and groundwater circulation are two fundamental requirements for the development of an active karst system regardless of adequate precipitation (Stringfield et al., 1979). Thus, surface solution

processes were more likely favored over those operating in the subsurface. Nevertheless, large, bowl-shaped structures observed today on the top of the Romaine Formation are thought to result from the collapse of the rocks overlying the intraformational breccias. Whether these structures are true dolines or relic subsurface features exhumed by erosion at the unconformity surface, remains unclear.

The final stage of the unconformity development occurred with renewed marine transgression during Chazyan time. Beaches or barrier-island coasts were probably formed at, or near, the shoreline during the initial trangression. Evidence of these deposits in the basal Mingan sandstones is, however, lacking. Instead, these basal sandstone sheets were reworked as subtidal sand bars as demonstrated by their marine fauna and sedimentary structures. Furthermore, the cover of residual eolian sand overlying the paleokarst unconformity was completely reworked during the trangression but local accumulations of chert-rubble conglomerates remained in more protected sites. It is possible that the sediment cover and inferred shoreline deposits were destroyed by the transgression and reworked by marine currents in a process similar to the Holocene transgressive barrier of the U.S. middle Atlantic coast (Schwartz, 1967; Swift, 1975). The proposed mechanism consists of shoreface erosion and offshore deposition under conditions of relatively slow and steady sea level rise, and as result a transgressive disconformity or "ravinement" underlies sediments deposited in shelf environments (Swift, 1968). Deep shoreface erosion during the Chazyan trangression across the study area, however, was limited by well-lithified Romaine dolomites which have been eventually exposed on the sea floor, bored by marine endolithic organisms, and

finally covered by sandy material.

PALEOKARST WITHIN THE MINGAN FORMATION

Another paleokarst unconformity is present within the Mingan
Formation separating the uppermost member of this formation from the
underlying members (fig. 4-2). This unconformity exhibits substantial
relief which in turn controls present distribution of the underlying
members due to erosion and appears to have controlled sedimentation in
the uppermost member with renewed submergence. In general, peritidal
carbonate deposits are present beneath the paleokarst unconformity. In
contrast, the overlying beds consist of subtidal carbonates deposited in
a variety of shallow water shelf environments (tidal deltas,
semi-restricted lagoons, patch reefs, open shelf). Of particular
importance is the presence of discontinuous beachrock deposits (i.e.
lithofacies 14) directly overlying the paleokarst unconformity. These
deposits were probably more widespread at one time but unconsolidated
beach sediments were removed during marine transgression.
Biostratigraphic data (conodonts and shelly fossils) indicate that the
intra-Mingan paleokarst unconformity represents a relatively short
depositional break in the Mingan sequence which occurred during Chazyan
time (Nowlan, 1981; Shaw, 1980). The Chazy biostratigraphy in eastern
North America, however, is equivocal because it is represented by only
two overlapping conodont faunal intervals (Mid-continent zones 5-6 of
Sweet et al., 1971) and is bounded above and below by unconformities in
its type area. This precludes the development of fine stratigraphic time
intervals within the Chazyan stage which is approximately 5 m.y. long
(Ross et al., 1982). The intra-Mingan paleokarst unconformity is also

characterized by 1) a regionally-wide mappable surface; 2) abundant sharp-crested karren and 3) associated features.

Regional unconformity

The paleokarst unconformity exhibits irregular, but smooth topographic features or landforms (ridges, depressions, pinnacles) on a regional scale. Landforms demonstrate up to 20 metres of relief as measured either by correlation of key beds between closely-spaced sections or by mapping along extensive seacliff exposures (fig. 6-3). The unconformity in the eastern half of the study area is characterized by two regional depressions (6-10 km wide), respectively centered on Grande Pointe and Ile Saint-Charles (fig. 4-2). In contrast, the unconformity in the western half is more irregular with closely spaced depressions and ridges or pinnacles, usually less than 2-3 km apart (plate 6-7; A-D). The topographic gradient associated with the unconformity generally ranges from $1°$ to $5°$ but may reach $20°$ in some areas (e.g. Ile du Fantome, Ile du Havre SW).

Minor solution features

Small superficial karren (plate 6-8; A-D) are superimposed on the paleokarst unconformity and consist of sculpted runnels (rinnenkarren) and basins (kamenitza). Their surface is in sharp contact with underlying beds. In thin-section, both grains (intraclasts, bioclasts) and cements are truncated along this surface.

Rinnenkarren: Rinnenkarren or crested solution runnels are similar in size and in shape to rundkarren except that their steep to vertical sides are characterized by sharp edges. They have rounded to scalloped

Figure 6.3- Outcrop sketches showing the paleokarst unconformity in cross-section; a) profile A-A' located at Grande Anse on Ile du Havre (SW) and b) profile B-B' located at Anse a Michel on Ile du Fantome (West). Note the vertical exaggeration (1:10). Mc: Corbeau Member; Mp: Perroquet Member; Mf: Fantome Member; Mg: Grande Pointe Member; Rgi: Grande Ile Member of the Romaine Formation.

INTRA-MINGAN PALEOKARST UNCONFORMITY

ILE DU HAVRE

ILE DU FANTOME
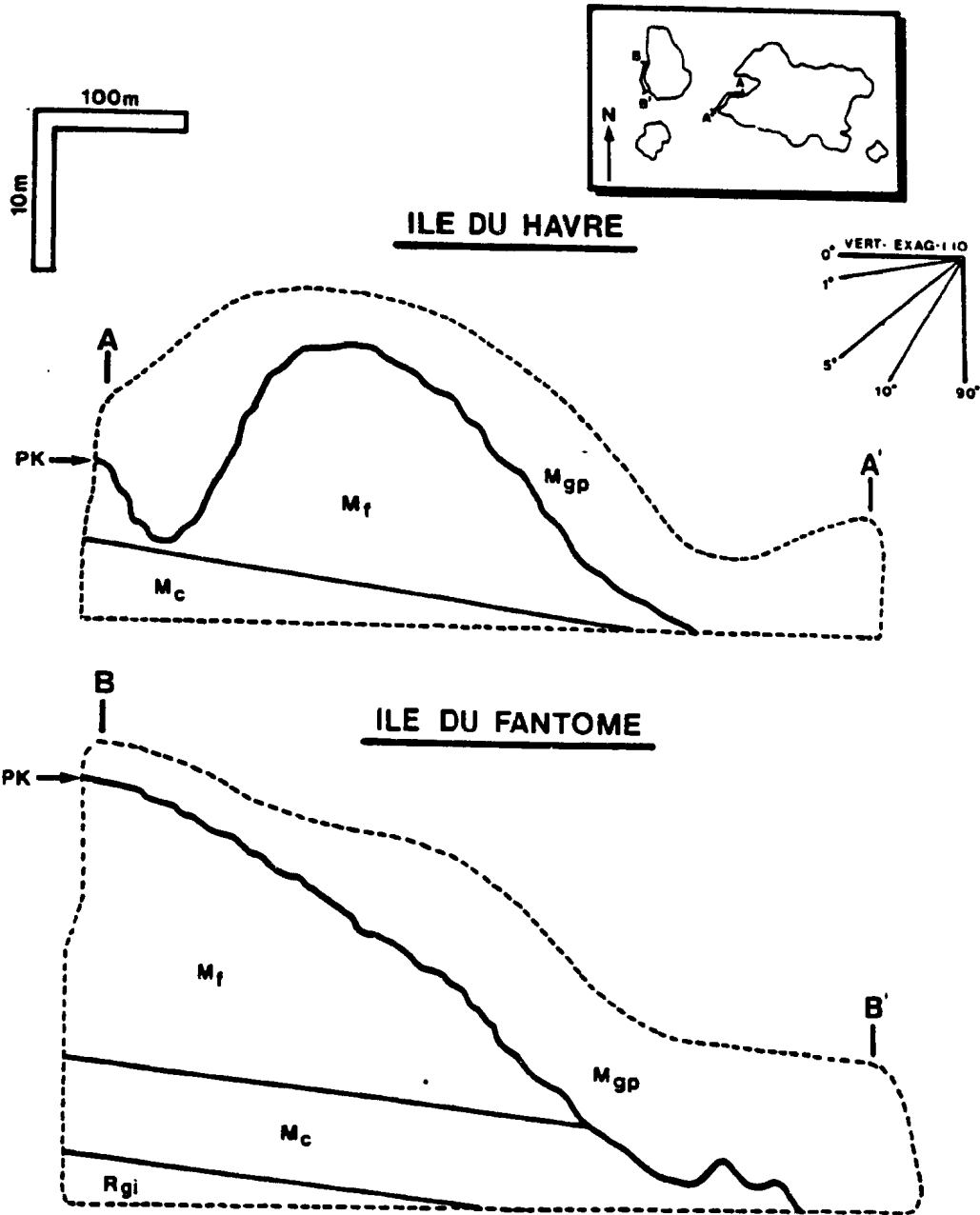
PLATE 6-7

INTRA-MINGAN PALEOKARST –
REGIONAL UNCONFORMITY

A. Field photograph (vertical cliff exposure) of the intra-Mingan
    paleokarst unconformity (black line). The unconformity is irregular
    and directly overlain by a cluster of small sponge-bryozoan
    bioherms. Ile du Fantome W. Hammer for scale.

B. Field photograph (cliff exposure) of the intra-Mingan paleokarst
    unconformity (black line). The unconformity is characterized by a
    regular topographic gradient from the right to the left where 3.5 m
    of relief is present. Note the presence of numerous coral bioherms
    forming small massive units above the unconformity. Field assistant
    is 2.0 m high (arrow) for scale. Ile de la Fausse Passe E.

C. Field photograph (cliff exposure) of the intra-Mingan paleokarst
    unconformity (arrows). The unconformity is characterized by a
    regular topographic gradient from the left to the right where 4.0 m
    of relief is present. Note the slight angular relationship between
    strata on both sides of the unconformity. Ile du Fantome S.

D. Close-up of (C) illustrating the unconformable contact between
    well-bedded fenestral mudstones of the Fantome Member (m) and
    overlying skeletal wackestones/packstones (p) of the Grande Pointe
    Member. Hammer is 30 cm.

PLATE 6-8

INTRA-MINGAN PALEOKARST - MINOR SOLUTION FEATURES

A. Field photograph (cross-section view) of small superficial karren or kamenitzas overlain by skeletal limestones of the Grande Pointe Member. Note the steep to vertical sides of sculpted karren characterized by sharp edges. Ile de la Fausse Passe E. Hammer is 30 cm.

B. Field photograph showing small superficial karren in cross-section along the intra-Mingan paleokarst unconformity. Ile de la Fausse Passe E. Field notebook is 20 cm.

C. Field photograph showing kaminetza and karren in cross-section along the intra-Mingan paleokarst unconformity. Ile du Fantome. Lens cap for scale .

D. Field photograph of sinuous karren exposed on the bedding plane of the intra-Mingan paleokarst unconformity. Ile du Fantome W. Hammer for scale.

bottoms. They are usually short (20-50 cm) and randomly oriented. In some areas, they are longer (up to 5 m) and oriented parallel with respect to local paleoslopes, usually greater than 5°.

Modern rinnenkarren form only on bare surfaces where meteoric water flows unhindered (Sweeting, 1973; Bogli, 1980). Length and parallelism usually increase with increasing slope. A similar origin is envisaged for rinnenkarren present at the top of the intra-Mingan paleokarst unconformity.

Kamenitza: Kamenitzas are similar to those described from the paleokarst unconformity capping the Romaine Formation but have steep sides with irregular and sharp edges that may sometimes overhang. Kamenitzas are commonly associated with short and sinuous rinnenkarren and grade laterally into sub-parallel rinnenkarren within tens of metres.

These "fossil kamenitzas" formed either in a subaerial or coastal settings. Kamenitzas with similar sculpted edges are observed today on slightly inclined to horizontal surfaces lacking cover where running water is more stagnant and forms pools and basins. They are also present in the tidal zone of modern tropical to temperate limestone coasts (Scheinder, 1976, 1977).

Associated features

Diagenesis: A detailed account of diagenesis is presented in Chapter 8. A brief summary, however, is given here because distinct diagenetic processes affect subaerially exposed carbonates (Longman. 1980; James and Choquette, 1984). The diagenesis of the lithofacies beneath the paleokarst unconformity has taken place in several stages and is

complex. These lithofacies, especially fenestral mudstones, were cemented early and well lithified prior to subaerial exposure. The most important diagenetic features, in approximate order of development, are: 1) neomorphism and dissolution (biomoldic and vuggy porosity) during initial exposure; 2) fissuring; 3) internal marine sediment and fibrous calcite cement (radiaxial) in both primary and secondary pore systems; 4) precipitation of iron-poor, clear calcite cements associated with shallow ground water and surface meteoric waters; 5) final karst erosion; 6) renewed marine submergence and deposition of the upper part of the Mingan sequence; 7) precipitation of iron-rich, blocky calcite and baroque dolomite during burial; 8) late-stage fracturing and 9) stylolitization.

Sediment-filled fissures: Fissures with sedimentary fillings are locally present beneath the paleokarst unconformity (plate 6-9; A and B). These fissures form a complex network and link together more porous horizons with abundant biomoldic and vuggy pores. Vertical fissures are planar to slightly curved and commonly oriented east-west. Most of them are less than 100 m long and 8 cm wide. They are occasionally cut by minor secondary fissures which show no preferred orientation. They are filled by internal sediments and/or marine fibrous cements similar to those found in adjacent moldic pores (plate 6-9; C and D). The most common internal sediment is red and fossiliferous (mainly ostracods) but an earlier generation is light olive-gray. These sediments commonly display laminations and consist mostly of carbonate mud. Angular, cm-sized clasts of host material (fenestral mudstones) are sometimes present in the fissures. In some cases, several generations of internal sediment are laterally superimposed in these fissures, suggesting that

PLATE 6-9

INTRA-MINGAN PALEOKARST - SEDIMENT-FILLED FISSURES

A. Field photograph (cross-section view) of a vertical sediment-filled
fissure (arrow) in fenestral mudstones (m) truncated by the
intra-Mingan paleokarst (black line). Ile du fantome S. Hammer is 30
cm.

B. Field photograph (cross-section view) of vertical sediment-filled
fissures (arrow) occurring in fenestral mudstones of the Fantome
Member beneath the intra-Mingan paleokarst. Ile du Fantome S. Lens
cap for scale.

C. Polished slab (cross-section view) of a sediment-filled fissure.
Note the geopetal nature of the sediment filling (f), carbonate mud
with abundant ostracods (oval particles in the upper half of the
fissure).

D. Field photograph (cross-section view) of a vertical fissure (f)
filled with fibrous (radiaxial) calcite cement. Ile du fantome S.
Lens cap for scale.
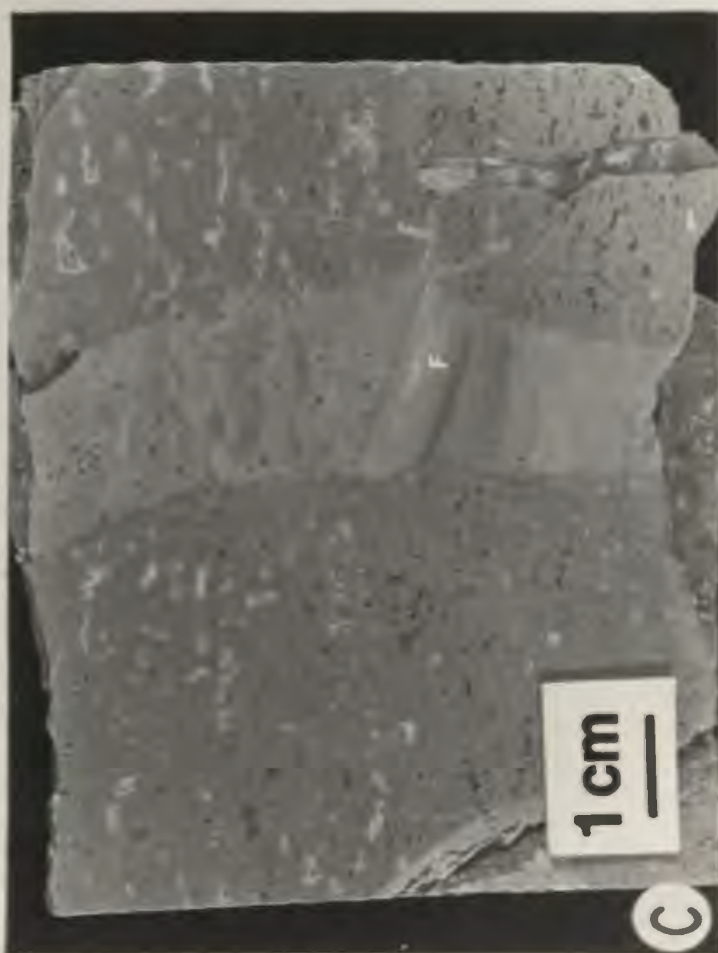
additional material was injected as the fissures were opening.

· Fissuring of the rock was most likely a product of fracturing and solution widening associated with subaerial exposure of the Mingan sequence. Fissures probably acted as conduits bringing internal sediment into porous subsurface units. Subsequent filling of these features indicates that the sequence was, at least periodically, in contact with circulating marine waters during incipient exposure as indicated by ostracod-rich internal sediment and marine fibrous cement. Unlike modern ostracods that are ubiquitous in all aquatic environments, ostracods during the Early Paleozoic are found only in marine environments (Horowitz and Potter, 1971). In fact, the oldest, non-marine ostracods in North America are from late Mississippian (Namurian A) strata of Virginia (Sohn, 1985). On the other hand, red sediment, often referred to as terra rossa, is a common fill in cracks of emergent rocks in such places as the Bahamas (Roehl, 1967). Terra rossa is considered as the by-product of pedogenic processes and subaerial solution of limestones and consists of red noncalcareous mudstone (Pye, 1983). On that basis, the red sediment filling the fissures beneath the paleokarst surface cannot represent a true residual soil. Although it is possible that minor insoluble residues (oxidized clays) were washed into the fissures and mixed with internal marine sediment, staining them a characteristic red colour. Furthermore, karren with sharp-crested forms argues against a significant development of soil above the paleokarst surface.

Paleonotch: The paleokarst surface is locally characterized by steep, vertical, sometimes sloping upward, walls (50-150 cm, high) (plate 6-10; A-C) which are morphologically similar to intertidal-subtidal notches observed along tropical carbonate coasts (Neumann,

PLATE 6-10

INTRA-MINGAN PALEOKARST - ASSOCIATED FEATURES

A. Field photograph (cross-section section) of a paleonotch along the intra-Mingan paleokarst. Note the steep vertical wall of the paleonotch (1.0 m high). Ile du fantome E. Hammer is 30 cm.

B. Field photograph (cross-section view) of a paleonotch along the intra-Mingan paleokarst showing two different levels with steep vertical walls. Grande Ile SE.

C. Field photograph (cross-section view) of a paleonotch along the intra-Mingan paleokarst (black line). The paleokarst separates the well-bedded fenestral mudstones of the Fantome Member (m) from the overlying skeletal limestones of the Grande Pointe Member (l). Ile Quarry SW. Hammer for scale.

D. Field photograph (bedding plane view) of crinoid holdfasts (arrows) encrusting the surface of the intra-Mingan paleokarst. Penny for scale. Ile Quarry N.
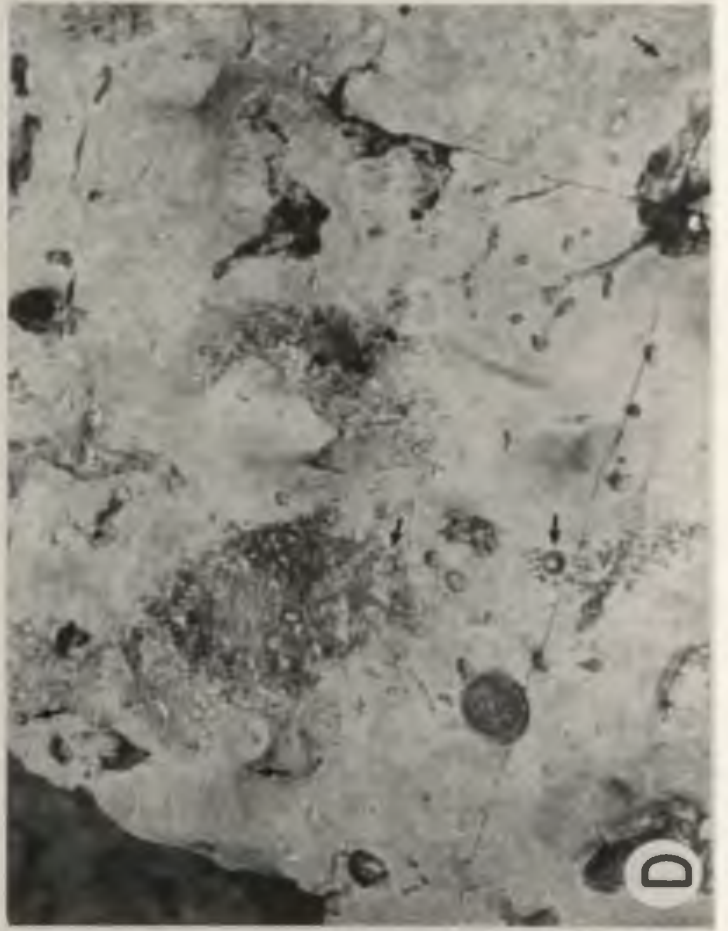
1966; Torunski, 1979). The "paleonotches" generally exhibit smooth pitted surfaces but some with irregular contacts are also present. Borings such as _Trypanites_ are absent.

The ecological zonation of modern carbonate shorelines is expressed in both epilithic and endolithic animals and plants which play an important role in their destruction (Scheinder, 1976). The origin of these Ordovician features is unclear as we know little about bioerosion of carbonate shorelines during the Early Paleozoic. Absence of unquestionable borings suggests that either physical destruction due to wave action or dissolution at the shoreline (i.e. mixing) was responsible. Against the first hypothesis, erosional blocks at, or near, the unconformity contact are never observed. Nevertheless, there is growing evidence for the presence of endolithic sponges in the geological record as early as Middle Ordovician (Kobluk, 1981b; Pickerill and Harland, 1984). Endolithic sponges are important in the bioerosion of modern limestone coasts (Neumann, 1966).

Encrusting organisms: Rare encrusting organisms are found _in situ_ on the paleokarst unconformity. The most common fossils are laminar trepostome bryozoans. Crinoid holdfasts with simple discoid forms are present but are noticeably less common (plate 6-10; D). In addition to these organisms, lithistid sponges with various growth forms (globular, cylindrical, saucer) are commonly present above the paleokarst surface but display some evidence of slight reworking and transport.

These marine organisms colonized or lived attached to the paleokarst surface which provided a hard substrate for their growth during marine transgression.

Interpretation

Sequential development of the paleokarst unconformity within the
Mingan Formation is illustrated in figure 6-4. Prior to subaerial
exposure, the Mingan sequence was composed of a lower siliciclastic unit
(shales, sandstones) and an upper limestone unit (fig. 6-4.1).
Depositional environments indicate that peritidal conditions were
prominent across the study area, and so any minor sea level fall would
simultaneously affect the entire area.

A second episode of epeirogenic movement during the Chazyan time
influenced sedimentation over the "St. Lawrence" platform. This episode
reflects the diachronous evolution of the Taconic Orogeny in nearby
Quebec (to be discussed later). The Mingan sequence was gradually
exposed due to tectonic uplift associated with the migration of a second
peripheral bulge across the area (fig. 6-4.2). This caused extensive
fissuring of the lithified early Mingan limestones. Subaerial exposure
was also accompanied by dissolution in the upper limestone unit as
evidenced by common biomoldic and vuggy porosity. Dissolution, however,
did not apparently affect the underlying Romaine sequence possibly
because shales in the upper part of the siliciclastic unit acted as an
aquiclude, inhibiting downward movement of meteoric fluids. During
initial exposure however, the sequence was periodically affected by
marine waters as the strandline was still fluctuating. Marine waters
circulating in the fissure network were saturated with lime mud that
eventually filled them and connected porous horizons. The co-existing,
fibrous cement indicates that marine waters were rapidly circulating
through the fissures. Diagenetic environments fluctuated from shallow
marine phreatic to shallow meteoric phreatic, the transition being

Figure 6.4- Schematic cross-sections illustrating the sequential
development of the intra-Mingan paleokarst unconformity. Stage 1:
the Mingan Formation, prior to subaerial exposure, consisted of a
lower unit of peritidal siliciclastics and upper unit of peritidal
limestones. Stage 2: epeirogenic movements caused extensive
fissuring of the early lithified Mingan limestones. Stage 3: karst
landform formed with further sea level fall and its surface was
sculpted into a variety of small karren forms. Stage 4: restricted,
subtidal carbonate sediments with renewed submergence were deposited
first in the lowest depressions but eventually into a wide spectrum
of normal marine sub-environments as marine circulation increased.
See text for further detail.

INTRA-MINGAN PALEOKARST

1 ← SL

2 ← SL

3 ←?=SL

4 ← SL
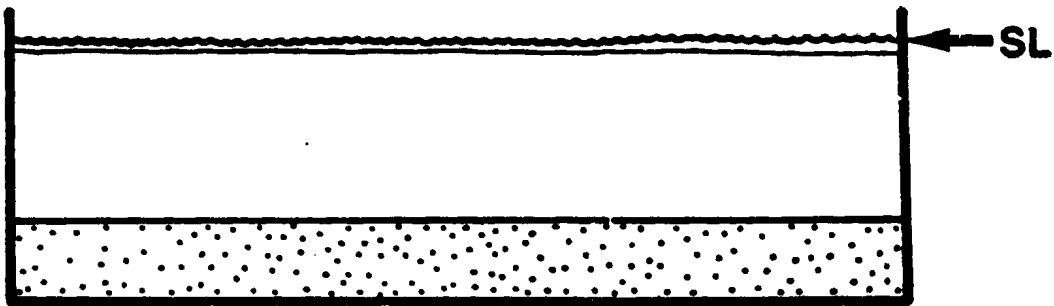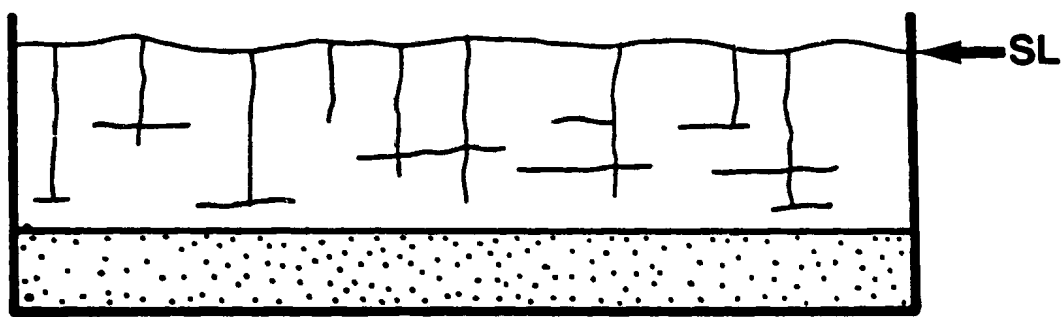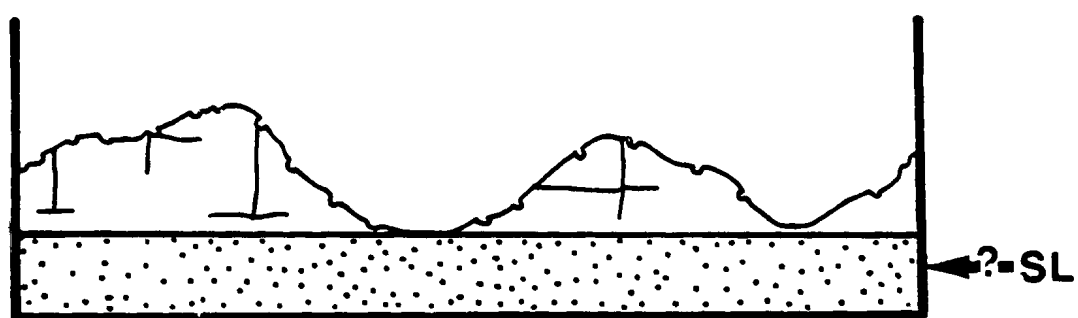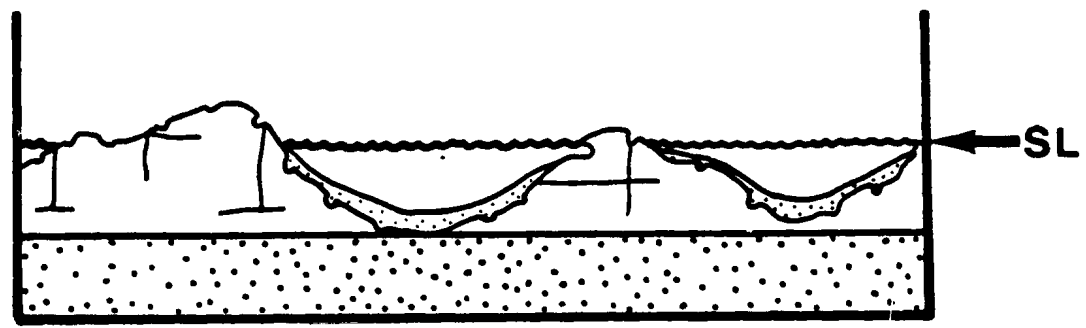
locally marked by petrographic changes within fibrous calcite crystals (inclusion-poor banding, brightly luminescent zones). Subsequent sea level fall definitively established a meteoric diagenetic regime over the Mingan sequence. The circulation of shallow groundwater and surface meteoric waters was active beneath the exposed surface and resulted in the precipitation of phreatic cement which occluded most of the primary and remaining secondary pore systems.

A minimum sea level drop of 20 m is indicated by erosional relief of the Mingan sequence observed on Ile du Fantome. A period of 200,000–400,000 years would have been necessary to produce karst landforms with similar relief today. This is based on known rates (50-100 mm/1,000 yrs) of limestone corrosion in different areas (Sweeting, 1973, p.42). During this stage (fig. 6-4.3), it is possible that non-filled or reopened fissures and fractures were progressively enlarged by dissolution and eventually developed karst landforms with topographic ridges and pinnacles. Absence of erosional blocks indicates that chemical weathering was also important here, however, physical weathering, if present, left no record. The downward development of karst landforms was generally limited by the presence of the underlying siliciclastic unit. In a few areas (Grande Pointe, Ile du Fantome) where the unconformity occurs within the siliciclastic unit erosion was more likely caused by physical processes.

Small, sharp-crested solution sculptures, superimposed on the larger scale karst landforms, developed on bare substrates. The morphological style of these sculptures appears to be controlled by the local topography of karst landforms. Today, in areas where weathering predominates, soils are commonly formed (Klappa, 1983); this contrasts

with their absence above the intra-Mingan paleokarst surface. It is

possible that chemical weathering (mainly dissolution) was not conducive

to the breakdown of rock into unconsolidated sediments and that erosion

by run-off waters was sufficient to remove all weathered detritus or

insoluble material above the paleokarst surface. Esteban and Klappa

(1983), however, pointed out that weathering and soil-forming processes

were probably different without the influence of land vegetation during

Early Paleozoic time.

The final stage in the development of the intra-Mingan unconformity

occurred with renewed transgression over the study area (fig. 6-4.4).

With initial submergence, sediments in the lowest topographic

depressions were deposited in more restricted marine environments.

Continued submergence enhanced marine circulation and sediment

deposition occurred in a variety of open, normal marine environments.

The submerged karst surface provided a rigid substrate for the growth of

various encrusting organisms and also acted as foundation for the

development of reef structures. Paleoshorelines were characterized by

beaches and rocky coasts. Rocky shorelines modified slightly the

pre-existing karst surface and exhibited distinctive intertidal notches

and kamenitzas but their origin (dissolution vs biological erosion)

remains uncertain.

THE CAUSE OF PALEOKARST UNCONFORMITIES

The formation of regional paleokarst unconformities requires either

tectonic uplift or eustatic drop in sea level, or a combination of both.

The paleokarst unconformities in the study area were formed during

Middle Ordovician time (Whiterockian-Chazyan) when both global marine

transgressions (Fortey, 1984; Barnes, 1984) and significant change in the Appalachian tectonic regimes (Rodgers, 1971; Williams, 1979;) are well documented.

Recent plate tectonic models have been proposed to explain regional unconformities above passive margin sequences during the transition to an active margin characterized by a reverse polarity (Jacobi, 1981; Cohen, 1982). The formation of these unconformities is thought to result from a migrating continental flexure or "peripheral bulge" as the passive margin becomes convergent. Modern oceanic trenches upon which are based the tectonic models are characterized by a bathymetric and gravimetric high, termed "outer rise", landward of subduction zones (Watts and Talwani, 1974; Dubois et al., 1974, 1975). The outer rise forms by a lithospheric flexure in response to vertical loading. Regional unconformities resulting from migrating continental flexure are common throughout the geological record. For instance, unconformities above ancient shelf sequences are present in the Antler orogenic belt of the western United States (Johnson and Murphy, 1984), in the Persian Gulf province adjacent to the Zagros thrust front (Murris, 1980; Searle et al., 1983), and in the Early to Mid-Cretaceous Caribbean mountain system in northern Venezuela (Maresch, 1974).

The Ordovician Taconic orogeny resulted from collision of the ancient eastern continental margin of North America with a volcanic arc, along a southeastward- dipping subduction zone (Malpas and Stevens, 1977). A pre-Middle Ordovician unconformity, recorded along the entire Appalachian system, above the "Great American Bank" (term proposed by R.N. Ginsburg), however, is commonly regarded as one of the first manifestations of the Taconic Orogeny (Rodgers, 1971; Williams and

Stevens, 1974). Sloss (1963) suggested that this regional break in sedimentation, observed in North American cratonic sequences, was due to a global sea level lowering during the early Middle Ordovician. Biostratigraphic data, however, indicates that the unconformity is significantly variable in both age and time length across the Appalachians (Savoy et al, 1981; Shanmugam and Lash, 1982; 1983). The unconformity cannot be explained by sea level changes alone, but also requires tectonic causes, as suggested by Lowry and Tillman (1974). Attempts to explain this unconformity in terms of modern tectonic environments have been recently presented for the Canadian Appalachians (Jacobi, 1981), New England Appalachians (Rowley and Kidd, 1981), Central Appalachians (Shanmugam and Lash, 1982), and Southern Appalachians (Shanmugam and Walker, 1980; Shanmugam and Lash, 1982; Mussman, 1982). All these studies suggest that uplift and erosion of the carbonate bank resulted from a peripheral bulge related to rapid subsidence of the bank margin. It is unclear whether subsidence was due to loading of the lithosphere by emplacement of thrust sheets (Hiscott et al. 1983; Quinlan and Beaumont, 1984) or to downwarping of the shelf margin as it approached the subduction zone (Shanmugam and Lash, 1982). Nevertheless, a peripheral bulge, based on rheological models, must form adjacent to any flexural downward of the lithosphere regardless of its cause (Walcott, 1970).

This unconformity also marks a transition from passive margin to convergent margin sedimentation which left an extensive record in rocks from Newfoundland to Tennessee (Klappa at al., 1980; Read, 1980, Belt and Buissiere, 1981; Ruppel and Walker, 1984). Post-unconformity carbonates and siliciclastics were respectively deposited in platform

and foreland basin settings located landward of the previous passive shelf margin. Carbonate platforms rapidly subsided to bathyal depth with deposition of black, graptolite-rich shale which in its turn was covered by a flysch succession that spread progressively cratonward away from the rising orogenic belt. In general, subsidence developed in a diachronous manner from east to west and an adjacent peripheral bulge also migrated simultaneously toward the craton to form an east-west diachronous unconformity.

Recent studies have pointed out the striking similarities in both structural and sedimentological record of the Taconic foreland basins (Shanmugam and Lash, 1983; Hiscott, 1985). This suggests that these basins evolved by analogous tectonic mechanisms, however, obvious temporal differences across the length of the orogen indicate a diachronous evolution. Taconic orogenesis began earlier in Newfoundland and Southern Appalachians then in the central part of the orogen. This is clearly shown by the age of autochthonous flysch which occurred from late Llanvirn to middle Caradoc in Western Newfoundland and Tennessee but generally from middle Caradoc to Ashgill elsewhere (Hiscott, 1985). There are some possible explanations for the diachronous evolution across the Appalachian system but it is not now possible to select the correct explanation from present plate-tectonic reconstructions of the Taconic Orogeny (Hiscott, 1985). It is possible that continent-arc collision occurred in a scissor-like manner and involved a mosaic of small plates, back-arc basins, and islands. Age variations may be also related to the geometry of the platform margin in which collision took place at different times in different places.

A modern analog is present in the Sahul-Timor area, north of Australia where similar depositional settings are found along an active continental margin (Veevers et al., 1978; Von der Borch, 1979). A late Miocene-early Pliocene unconformity separates ancient stable shelf carbonates from an overlying transgressive sequence (late Miocene-Recent). This latter sequence includes shallow water carbonate sediments of the Sahul shelf which pass into foreland basin with flysch deposits derived from the Timor tectonic highlands to the northwest.

From the above discussion, it is suggested that paleokarst unconformities in the Mingan sequence were formed by similar causal mechanisms (i.e. migrating peripheral bulge), although their stratigraphic superimposition must reflect diachronous evolution of the Canadian Appalachians, from western Newfoundland to Quebec. Emplacement of the Canadian Taconic allochthons across the continental margin took place between Llanvirnian and mid-Caradocian times in Newfoundland and Llandeilan to mid-Ashgill times in Quebec (Keppie, 1985). This means that a pre-Llanvirnian peripheral bulge migrated away from a rapidly subsiding shelf margin in western Newfoundland whereas a similar, but diachronous event in Quebec created a pre-Llandeilan peripheral bulge. The paleokarst unconformities in the study area may be explained by two interfering but temporally different peripheral bulges associated with the emplacement of the Taconic allochthons in western Newfoundland (350 km to the east), followed shortly thereafter by those in Quebec (about 150 km to the southwest). The remaining discussion compares the timing of possible eustatic and tectonic events with post- unconformity carbonates and siliciclastics deposited in the study area and adjacent Canadian Appalachians. The age of the stratigraphic units under

- 302 -

discussion are summarized in figure 6-5.

Prior to the arc-continent collision, the "St. Lawrence" platform recorded typical sedimentation on a passive-type continental margin and is well illustrated in figure 6-6 at its fullest state of development, reached only in late Canadian-earliest Whiterockian time. It reflects long-term structural stability and subsidence of its margin originally formed by rifting and opening of the Iapaetus Ocean during late Precambrian (Williams, 1979). The sequence consists of Cambro-Ordovician miogeoclinal carbonates resting conformably above Cambrian miogeoclinal siliciclastics and rift-related volcanics and immature siliciclastics. Thicknesses across the basin are greater near the more rapidly subsiding margin, although peritidal conditions were also maintained there (Pratt, 1979; Pratt and James, in press). The sequence thins toward the west where younger beds directly overlie the Precambrian basement. For instance, the sequence in the Mingan Islands comprises only late Canadian beds and is 65 m thick.

The paleokarst unconformity capping the Romaine Formation formed on exposed miogeoclinal carbonates as the passive margin became convergent in western Newfoundland, probably during a time of global sea level lowstand. Fortey (1980, 1984) suggested that a worldwide drop in sea level occurred during the Whiterockian time (late Arenig) as he recognized major regressive phases in both shelf and off-shelf localities from widely separated cratonic areas. Barnes (1984) also noticed similar regressive patterns around the ancient Laurentian craton in Canada. As discussed earlier, eustatic sea level lowering alone cannot explain age variations of the sequences overlying the exposed Cambro-Ordovician passive margin along the Appalachian system, including

Figure 6.5- Correlation diagram of the principal stratigraphic units under discussion, adapted from Barnes et al. (1981) and Hiscott (1985). 1: Gaspe Peninsula and Anticosti Island (subsurface), 2: Mingan Islands, and 3: western Newfoundland (Port-au-Port Peninsula). The Cloridorme Formation in the Gaspe Peninsula is structurally overlain by thrust sheets. In western Newfoundland, final thrust emplacement is dated by the neoautochthonous Long Point Group as early Caradoc in age.

LOWER ORD.	MIDDLE ORDOVICIAN					
Canadian	Whiterock		Chazy	Blackriver	Trenton	
Arenig	Llanvirn	Llandeilo	Caradoc			Ashgill

GASPE & ANTICOSTI

MINGAN   MᶜKASTY   CLORIDORME

MINGAN ISLANDS

MINGAN

ROMAINE FM

WESTERN NFLD

TABLE HEAD   MAINLAND   LONG POINT

ST-GEORGE GR
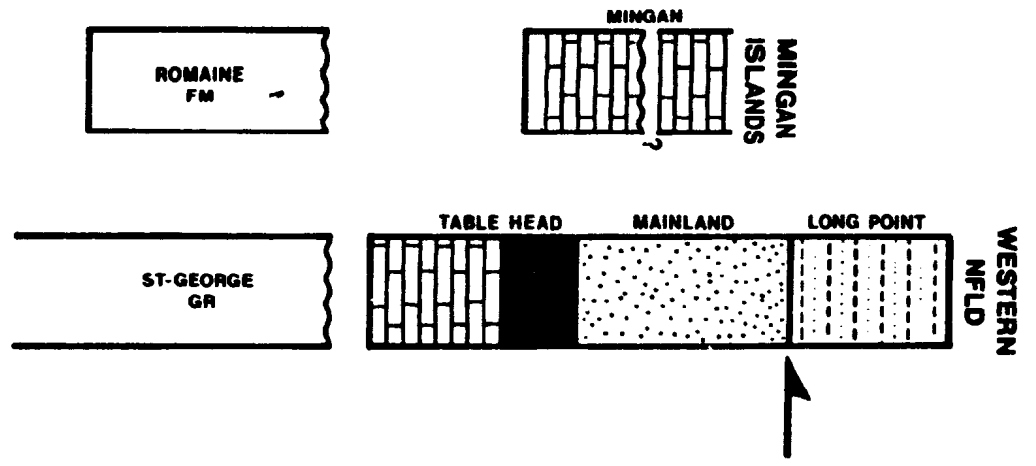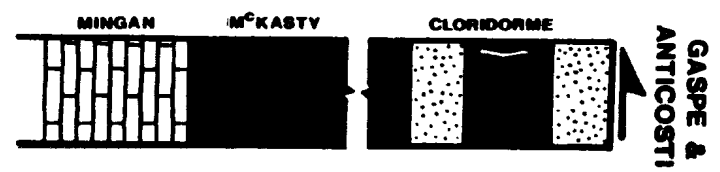
LEGEND

Platform carbonate

Black shale & shaly flysch

Autochthonous flysch

Neoautochthon

- 305 -

Figure 6.6- Section across the "Saint-Lawrence" platform from the Mingan
    Islands to Port-au-Port Peninsula in western Newfoundland. The
    platform is illustrated here at its fullest state of development,
    reached only during late Canadian-early Whiterockian time. This
    profile is characteristic of carbonate platforms of extensional
    margins which are commonly developed over a basal sequence of rift
    volcanics and immature siliciclastics (not illustrated) and more
    mature shelf siliciclastics. Deep water facies are observed in the
    allochthonous Humber Arm Supergroup in western Newfoundland. On the
    other hand, the rim or margin facies is never observed and probably
    hidden beneath the allochthon. Erosional fragments of this margin
    facies, however, are present in contemporaneous slope deposits of
    the allochthonous Cow Head Group in western Newfoundland.
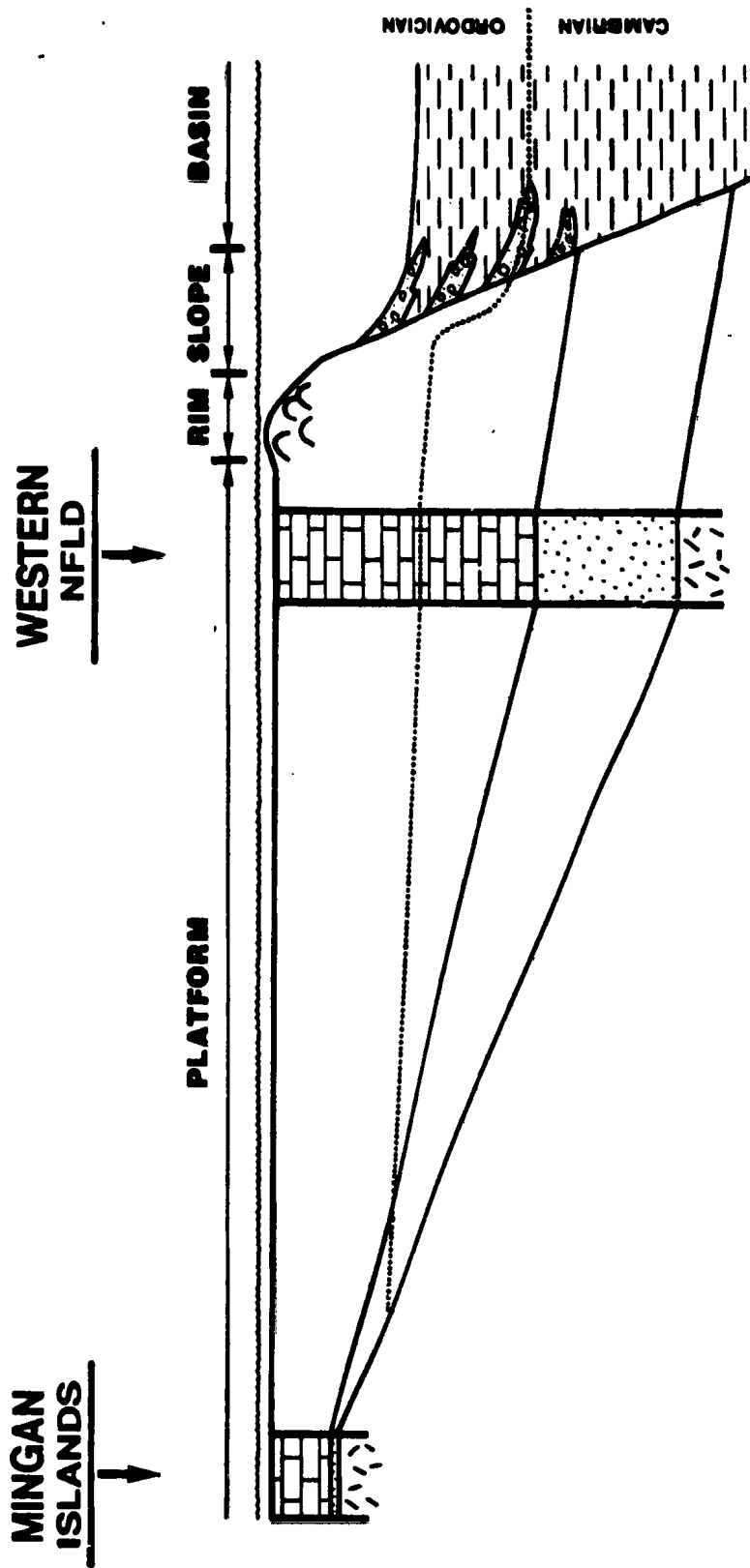
its Canadian segment.

A model with two sequential phases is envisaged for the development of the paleokarst unconformity and overlying deposits in the Mingan Islands (fig. 6-7). During the first phase, rapid subsidence of the shelf margin and onset of black shale deposition occurred in western Newfoundland as recorded by the Table Head Group (Klappa et a.., 1980). Foreland basins with similar deepening sequences in the Southern Appalachians may have subsided to as much as 700 to 1000 m in as little as 1 to 2 m.y. (Shanmugam and Walker, 1978, 1980). At the same time, a peripheral bulge formed in response to the downward flexure of the shelf margin and caused uplift and erosion of the shelf in areas located to the north such as the Mingan Islands. Prior to rapid subsidence of the shelf margin in western Newfoundland, the peripheral bulge was responsible for uplift, at least 100 m (Jacobi, 1981), accompanied by the local development of karst over the early Ordovician St-George Group (James and Stevens, 1982). The unconformity is only early Whiterockian in age there, while in the Mingan Islands it encompasses most of Whiterockian time. During the second phase, synorogenic flysch in western Newfoundland progressively spread cratonward away from the rising Taconic belt. Final nappe emplacement above this autochthonous flysch is dated early Caradoc, possibly late Llandeilan (i.e. Chazyan) as indicated by the neoautochthonous Lourdes limestones overlying the Humber Arm Allochthon (Williams and Stevens, 1974). The peripheral bulge migrated further toward the cratonic interior, and as a result deeper water facies were deposited in a diachronous manner toward the west. A marine transgression occurred above the exposed Romaine Formation during the Chazyan and peritidal sedimentation began in the Mingan Islands.

Figure 6.7- Schematic cross-sections illustrating the development of
the paleokarst unconformities and overlying transgressive sequences.
The formation of the paleokarst unconformity capping the Romaine
Formation is shown here in two stages. Stage 1: an upward flexure or
peripheral bulge formed in response to the shelf collapse to basinal
depths characterized by the deposition of black graptolitic shales
of the Table Head Group in western Newfoundland. Stage 2:
progressive development of a pericratonic foreland basin in western
Newfoundland forced the peripheral bulge to migrate toward the
cratonic interior and the deposition of the onlap facies of the
Mingan limestones and siliciclastics. A similar model but operating
in a diachronous fashion is also used to explain the intra-Mingan
paleokarst unconformity. See text for further detail.

PERIPHERAL BULGE MODEL
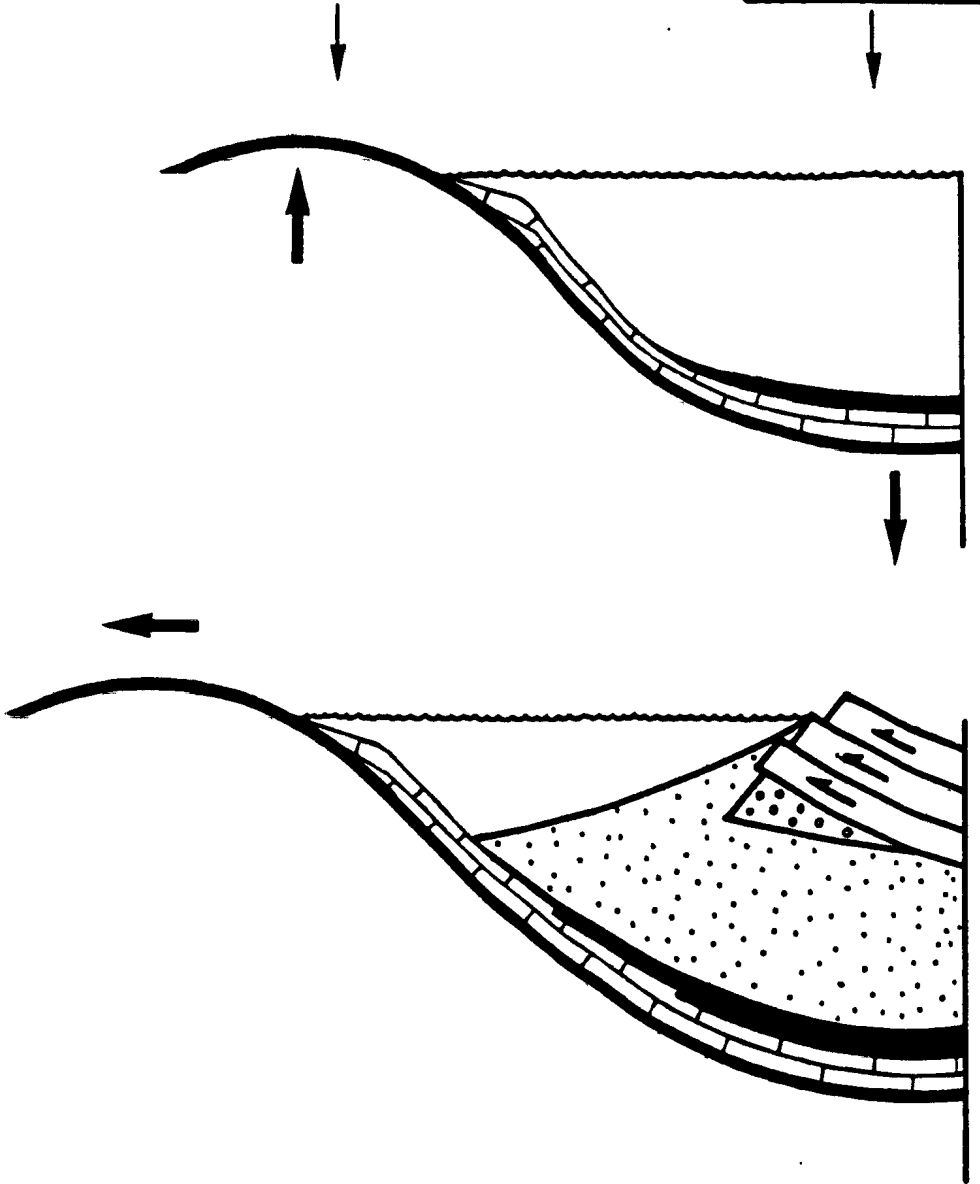
The flexure or peripheral bulge model, if correct, explains some
aspects of the depositional history of the Mingan sequence. Assuming a
W-NW emplacement for the Taconic allochthons (Keppie, 1985), it was
possible for a peripheral bulge migrating in a similar direction to
affect more strongly the western part of the Mingan Islands. This may
explain the apparent, eastward increase of stratigraphic relief
associated with the unconformity above the Romaine Formation.

On the other hand, the intra-Mingan paleokarst unconformity formed
above peritidal carbonates of the Mingan Formation as the passive margin
became convergent in Quebec, probably during a global sea level rise.
In spite of local regressive-transgressive sequences reported by Fortey
(1984) from the Llanvirnian-Llandeilan (i.e. Chazyan) of Britain, there
is not yet evidence of a sea level fall during Chazyan time. In fact,
evidence for such a depositional trend with karst development is unknown
in the Chazy Group of New York and Vermont where small on-shelf reefs
grew in shallow water above the fairweather wave base for most of the
Chazyan time (Pitcher, 1964; Kapp, 1975). This strongly argues in favor
of local tectonic movements as being responsible for the formation of
this paleokarst unconformity. It should be noted that the Taconic
Orogeny took place later in the New England Appalachians and that a
post-Chazyan unconformity in this area is thought to record the
migrating peripheral bulge (Rowley and Kidd, 1981).

A flexural model similar to that previously described is suggested
for the formation of the intra-Mingan paleokarst unconformity (fig.
6-7). A peripheral bulge formed as the shelf margin collapsed in Quebec
during the Llandeilan time. It was followed later by progressive
deposition of east-derived flysch and eventual emplacement of the

Quebec Taconic allochthons. This forced the peripheral bulge to migrate

further landward and renewed marine transgression over the exposed lower

Mingan sequence.

In summary, both paleokarst unconformities in the Mingan Islands are

believed to result from epeirogenic movements associated with the

diachronous evolution of the Canadian Taconic Orogenesis several 100 km

to the east. Eustatic sea level changes also occurred but were probably

of less importance.

CHAPTER 7

SHALLOWING-UPWARD CALCARENITE CYCLES

INTRODUCTION

In addition to major paleokarst unconformities, numerous local paleokarst horizons are also associated with metre-scale, shallowing-upward calcarenite cycles in the Mingan Formation. The lower part of each cycle is generally subtidal burrowed, skeletal wackestone or packstone. The upper part is a sand shoal of cross- bedded grainstone. Cycles are usually capped by a paleokarst surface.

The paleokarst surface reflects subaerial emergence, lithification of newly exposed carbonate sediments and karst erosion forming sharp karren. If exposure was prolonged, karren progressively widened and eventually developed into an extensive planar surface.

CALCARENITE CYCLE

Stratigraphic setting

Calcarenite cycles occur only in the Perroquet and Grand Pointe Members of the Mingan Formation which are composed of a variety of subtidal carbonates (fig. 4-1). The Perroquet Member, restricted to the western part of the study area, grades upward and laterally into peritidal carbonates of the Fantome Member. The uppermost Grande Pointe Member is separated from underlying members by the intra-Mingan paleokarst unconformity.

Each cycle consists of five different but related lithofacies which display important lateral transitions. In most cases, upper grainstone units are lens-shaped and interdigitate laterally with the underlying wackestone/packstone units. Paleokarst surfaces occur only on top of grainstone units. Vertical and lateral lithofacies associations within an "ideal" calcarenite cycle are summarized in figures 7-1 and 7-2. Individual cycles range from 2 to 6 m in thickness and can be laterally traced over from 1 to 10 km.

Depositional lithofacies

Carbonate lithofacies include, in ascending order: 1) reef limestone; 2) mudstone and skeletal wackestone; 3) skeletal wackestone/ packstone; 4) peloid grainstone and 5) skeletal-ooid grainstone. Although all are present only the last three lithofacies are significant in the calcarenite cycles. Details concerning the description and depositional environment of these lithofacies may be found in chapters 4 and 5.

Reef limestones

Reef limestones, as described in chapter 5, rest directly on paleokarst surfaces capping the grainstone units (figs. 7-1 and 7-2). These limestones are overlain and flanked by skeletal wackestones and packstones. They form small, biohermal and biostromal units which are composed of abundant lithistid sponges, tabulate corals, bryozoans, and calcareous algae within a skeletal wackestone matrix. These large metazoans are found in growth position except in biostromes which display slight evidence of transport. Bioherms and biostromes are

Figure 7.1– Description of an "ideal" calcarenite cycle developed in
    sand shoal deposits and capped by a paleokarst surface (PK).
    Sediments, deposited in the inter-shoal areas however, are composed
    of burrowed, muddy lithofacies deposited under more restricted
    conditions when the sand shoal areas became exposed.   Not
    illustrated is the possibility of thin tidal flat deposits
    (fenestral mudstone) in the upper part of a few calcarenite cycles
    which formed immediately behind exposed sand shoals. See figure 1.2
    for symbols.

CALCARENITE CYCLE

SHOAL

INTER-SHOAL

PK

2·6 m

SKELETAL-OOID GRST

PELOID GRST

MDST–SKELETAL WKST

SKELETAL WKST-PKST

REEF LMST

PK
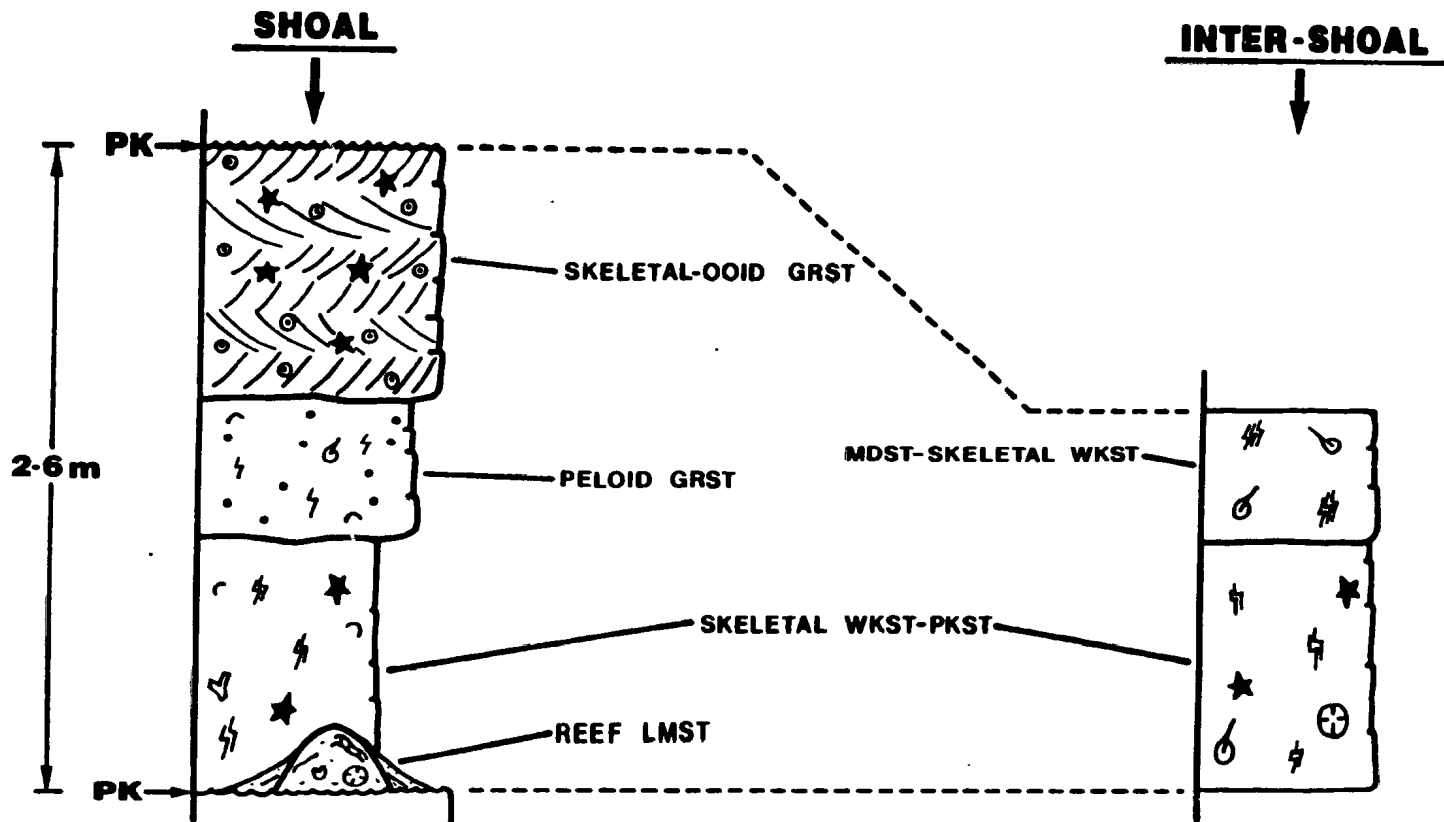
Figure 7.2– Schematic diagram illustrating the lateral lithofacies
association in calcarenite cycles.

CALCARENITE CYCLE

1-10 Km

2-6 m

PG

SG

PG

MW

WP

RL
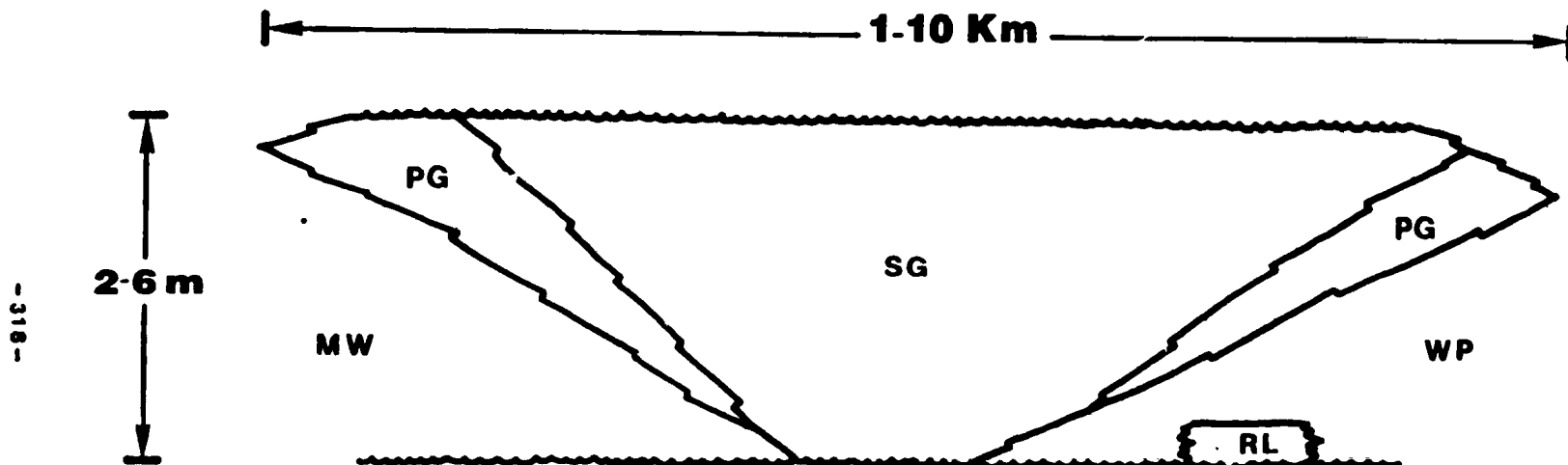
| SG | SKELETAL-OOID GRST | PG | PELOID GRST | WP | SKELETAL WKST-PKST |
| MW | MDST- SKELETAL WKST | RL | REEF LMST | ~~~~ | PALEOKARST SURFACE |

interpreted as reef mounds and blankets forming in situ accumulations of
skeletal metazoans under relatively low-energy conditions. These
organisms which require hard substrates for their growth colonized
locally the paleokarst surface with renewed submergence.

Mudstones/skeletal wackestones

This lithofacies consists of burrowed muddy sediments with less than
20% skeletal grains, mainly the remains of euryhaline organisms
(gastropods, ostracods). Sediments were deposited in low-energy,
subtidal environments, probably in semi-restricted lagoons behind the
higher energy sand shoals as they became exposed (chap. 4, lithofacies
10). This interpretation is also supported by the lithofacies
distribution where it occurs in the lower part of calcarenite cycles
(fig. 7-2). This lithofacies is generally found in the northernmost
sections and grades laterally into the grainstone units toward the south
(fig. 7-3).

Skeletal wackestones/packstones

These rocks are burrowed, muddy sediments with an abundant and
diverse fossil assemblage (chap. 4 lithofacies 11). They represent
low-energy, subtidal sediments deposited in open shelf environments. The
lateral gradation into the grainstone units is generally marked by
gently dipping beds with common Girvanella oncolites indicating some
degree of agitation. This lithofacies is more common in the southernmost
sections (fig. 7-3).

Figure 7.3- Schematic panel diagram showing the lithofacies distribution and location of the paleokarst surface in a portion of the study area. Sections are constructed using the Romaine-Mingan contact as a datum (not shown in diagram). Note that the grainstone lithofacies form a lenticular unit which dies out laterally in all directions. Sections include: 1: Pointe de Chasse (Ile du Havre); 2: Anse a Guemon (Ile du Havre); 3: Pointe Enragee (Ile du Havre); 4: Petite Ile au Marteau, 5: Grosse Ile au Marteau; 6: Cap Ferre (Grande Pointe); 7: Pointe Enragee; 8: Ile de la Fausse Passe; 9: Grande Pointe north); 10: Grande Pointe (south).

CALCARENITE CYCLE

PALEOKARST SURFACE

E — SKELETAL-OOID GRST

D — PELOID GRST

C — SKELETAL WKST-PKST

B — MDST-SKELETAL WKST

A — REEF LMST

INTRA-MINGAN PALEOKARST

3 Km
0
8 m
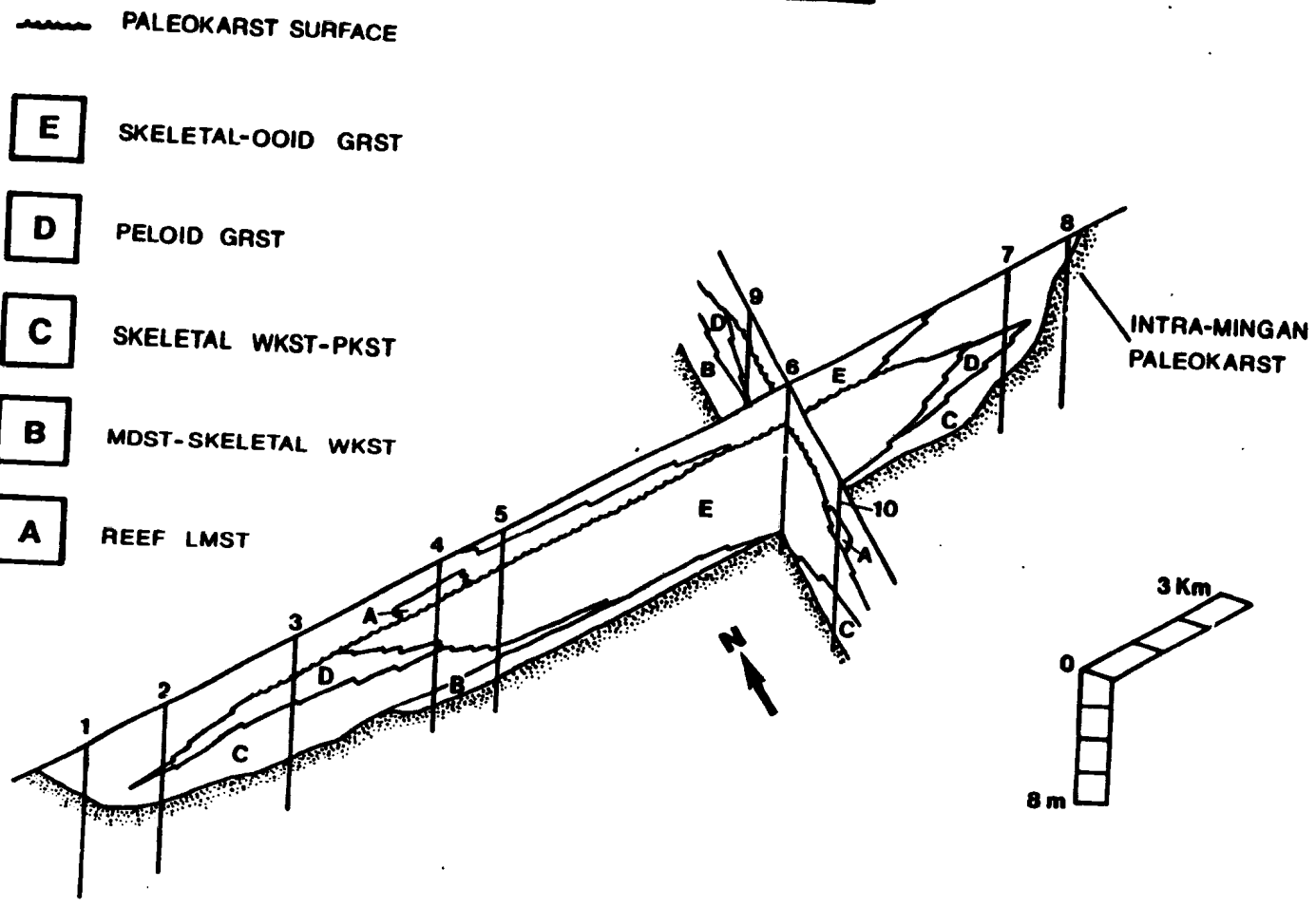
Peloid grainstones

Peloid grainstones (described with lithofacies 12 in chapter 4) are composed of well-sorted peloids or small intraclasts with only minor skeletal particles and ooids. Cross-bedding is common but may be locally destroyed by extensive bioturbation (mainly Chondrites). Peloid grainstones represent a gradational unit found between laterally adjacent skeletal-ooid grainstones and muddy lithofacies (figs. 7-2 and 7-3). This lithofacies is best explained as sediments deposited on relatively quiet sand flats away from the most active ooid shoal areas.

Skeletal-ooid grainstones

This lithofacies consists of mud-free, grainy sediments composed of skeletal fragments (mainly crinoids) and ooids in varying amounts. Ooid grains are less common in cycles of the Perroquet Member. These sediments were deposited as sand shoals controlled mainly by tidal currents, as indicated by trough cross- bedding with bipolar-bimodal paleoflow directions. This lithofacies is volumetrically important in core and crest of calcarenite cycles and dies out laterally in all directions (fig. 7.3). The ooid-skeletal sands interfinger laterally with peloid grainstones (fig. 7-2). Fossiliferous intraclast sands are sometimes common and occur, at least in one locality (Grande Pointe), as wedge-shaped lenses with scoured bases in the ooid-skeletal sands. They are interpreted as tidal channels truncating the sand shoals.

Fenestral mudstones

This lithofacies occurs only at one locality (i.e. Ile Saint-Charles SE) where it forms the upper half meter of a calcarenite cycle but is

laterally discontinuous. It consists of structureless to peloid micrite characterized by common fenestrae and restricted biota. These sediments are intertidal to supratidal deposits which could probably accumulate in small protected pockets behind a sand shoal.

Depositional sequence

The vertical lithofacies association within an individual calcarenite cycle is characterized, from the base to top by: increasing grain size, better sorting, more sedimentary particles (i.e. bioclasts, ooids), more grain-supported fabric, and better stratification (fig. 7-1). These features indicate that each cycle records the development of progressive shallowing conditions, eventually culminating in subaerial emergence. Such cycles are present throughout the geological record (Purser, 1972; Wilson, 1975) and reflect the fact that carbonate sediments can easily catch up to most rises of sea level due to tectonic subsidence and/or eustatic changes (Schlager, 1981). Harris (1979, 1984) documented a similar vertical sequence, developed during the Holocene transgression, by coring of modern ooid sand shoals on the Great Bahama Bank. Unlike these extensive modern shelf-margin sand bodies, the Ordovician calcarenite cycles represent smaller sand shoals as indicated by their limited lateral extent. They were, however, deposited into two distinct settings: 1) sand shoals in the Perroquet Member were located seaward of tidal flat and lagoonal facies, and 2) sand shoals in the Grande Pointe Member formed in tidal deltas in response to funnelled tidal currents between topographic depressions associated with the intra-Mingan paleokarst unconformity. As mentioned earlier in chapter 5, the exact nature of the shelf to margin transition is equivocal, being

hidden beneath the Gulf of St. Lawrence. Nevertheless, a discontinuous reef trend in the study area and the absence of shallow water-derived clasts in deeper carbonates beneath Anticosti Island strongly argue in favour of an open shelf or ramp setting. Carbonate ramps are characterized by shallow, agitated facies of the nearshore zone that pass downslope into deeper water, low-energy deposits without a marked break in slope (Ahr, 1973). The Mingan sand shoals along a ramp profile probably developed in the inner, shallow part of the ramp and formed a baffle zone to offshore wave and current activity. A break in the slope, if present, occurred many kilometres offshore away from these high-energy sand shoals and left no obvious record in contemporaneous slope and basinal deposits.

In contrast to these sand shoals, the inter-shoal facies consists only of muddy carbonate sediments (fig. 7-1). These sediments, however, were never subaerially exposed as indicated by the conspicuous absence of paleokarst surface or other diagnostic features associated with meteoric diagenesis. Indeed the subaerial exposure of the sand shoals resulted in the progressive environmental restriction of adjacent subtidal areas, especially in the northern part of the study area. This suggests also that the sand shoals had a synoptic relief of several metres over the inter-shoals areas.

PALEOKARST SURFACES

Three superimposed cycles, each capped by a paleokarst surface, are present in both Perroquet Member (Ile Nue de Mingan) and Grande Pointe Member (Ile du Havre E). Paleokarst surfaces, if present, always occur on top of the calcarenite cycles (plate 7-1; A-D). These surfaces may

PLATE 7-1

CALCARENITE CYCLE - PALEOKARST SURFACE

A. Field photograph (vertical cliff exposure) of cross-bedded
    grainstones (g) capped by a karst surface (arrow) at the top of a
    calcarenite cycle. Grainstones are sharply overlain by reef
    limestones (r) occurring in a massive biostromal unit. Detail in
    (B). Ile Nue de Mingan N. Hammer is 30 cm.

B.   Close-up of (A) showing the sharp contact at the top of the
    calcarenite cycle. Note the presence of sculpted karren, here shown
    in cross-section, at the contact (arrow). Lens cap is 50 mm in
    diameter.

C. Field photograph (vertical cliff exposure) of a planar erosive
    surface (arrow) capping a calcarenite cycle and separating
    grainstones (g) from overlying skeletal muddy limestones (l). Ile du
    Havre SE.
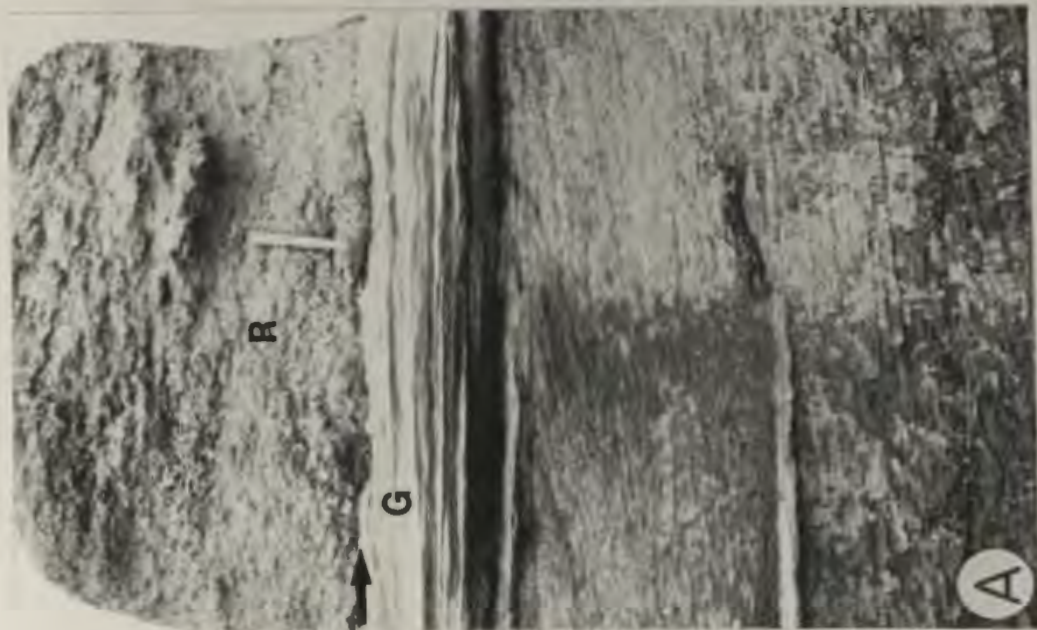
be traced over several kilometres from one outcrop to another (fig.
7-3). They are laterally discontinuous and stop where grainstones grade
into the gently dipping beds of skeletal wackestone/packstone on the
shoal flanks. The surfaces are irregular, scalloped to planar in
vertical section with less than 30 cm of relief (plate 7-2; A). They are
exposed on extensive bedding planes which permits recognition of four
distinct forms when compared with modern karst (Sweeting, 1973; Bogli,
1980; Allen, 1982, p.222-251). These forms include: 1) rinnenkarren; 2)
kamenitza; 3) trittkarren and 4) planar surface.

Rinnenkarren and Kamenitzas

These features are similar in size and in shape to those observed on
the intra-Mingan paleokarst unconformity and characterized by steep
walls with irregular and sharp edges. Rinnenkarren are randomly oriented
but small forms are sometimes superimposed on larger depressions which
may form channels up to 1 m wide and several tens of metres long (plate
7-3; C and D).

Comparison with modern karst indicates that they developed on bare
limestone substrates exposed to rainwater. The randomly-oriented
rinnenkarren and their common association with kaminetzas probably
reflect slightly inclined substrates disturbed only by minor topographic
gradients which locally controlled the water flow.

Trittkarren

Trittkarren (plate 7-3; A and B), which are best described as
resembling the imprint of a heel, are asymmetrical in vertical section
with a flat tread (20-40 cm long) and a vertical riser (5-15 cm high).

PLATE 7-2

CALCARENITE CYCLE - PALEOKARST SURFACE

A. Field photograph (bedding plane view) of a paleokarst surface illustrating well-developed and oriented karren on top of a calcarenite cycle. Ile Nue de Mingan N. Hammer is 30 cm.

B. Field photograph (bedding plane view) of a paleokarst surface showing karren with widened forms but still recognizable oriented ridges. Ile Nue de Mingan N. Scale bar is 2 cm.

C. Field photograph (bedding plane view) of a paleokarst surface showing more flattened karrens with discontinuous ridges. Scale in cm. Ile Nue de Mingan N. Scale bar is 2 cm.

D. Field photograph (bedding plane view) of a paleokarst surface characterized by a planar surface with only relic features such as small pinnacles. Note the paleokarst surface disappearing beneath overlying limestones (top left). Scale in cm. Ile du Havre SE. Scale bar is 2 cm.

Note: Photographs in plate 7-2 represent a transition in the style of paleokarst surfaces capping the calcarenite cycles.
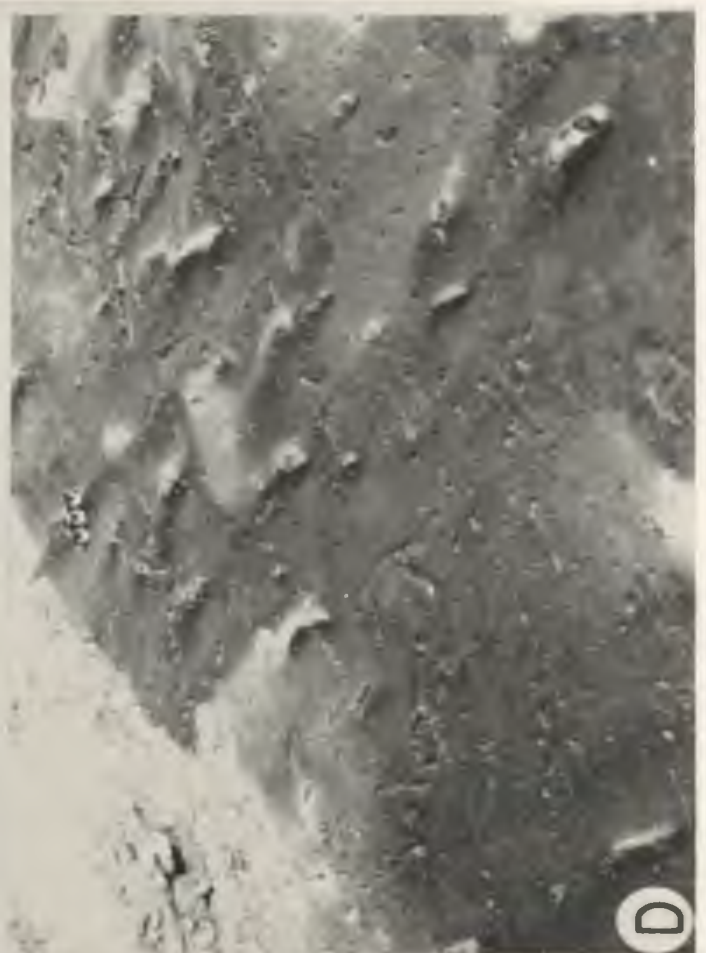
PLATE 7-3

PALEOKARST SURFACE - SOLUTION SCULPTURES

A. Field photograph (bedding plane view) of trittkarren on top of a calcarenite cycle. Trittkarren are asymmetrical in vertical section with a flat tread and a vertical riser. Field notebook is 20 cm. Grande Pointe.

B. Same as (A). Note that trittkarren are semi-circular and laterally coalescent on the bedding plane. Hammer is 30 cm.

C. Field photograph (bedding plane view) of sculpted karren on top of a calcarenite cycle. Karren are separated by well-oriented depressions or channels filled by overlying skeletal limestones. Detail in (D). Grande Pointe. Hammer for scale.

D. Close-up of (C) showing a depression partially filled with skeletal limestones (see bottom). Hammer for scale

They are semi-circular and laterally coalescent on the bedding plane.

Furthermore, they are commonly organized in steps and oriented

perpendicular with respect to other karren forms, such as rinnenkarren.

Modern trittkarren are present only on slightly inclined substrates

directly exposed to rainwater. They are thought to result from a two

water layer process; the upper layer is more "aggressive" on the

vertical back-wall, the lower layer is highly alkaline on the flat tread

(Sweeting, 1973). Solution by water flowing perpendicular to their

orientation causes preferential solution of the back-wall.

Planar surface

The paleokarst surfaces are also characterized by extensive planar

surfaces which can be traced for several hundred metres, if not

kilometres, with little or no relief. Relief on these planes consists

only of oriented ridges (5-10 cm high, 20-150 cm long) and isolated

pinnacles (5-15 cm high) (plate 7-2: B-D). In some areas, they pass

laterally, over a few tens of metres, into surfaces with well-developed

karren (plate 7-2; A). Centimetre-sized pits are ubiquitous features

that are superimposed on the planar surfaces (plate 7-4; A). These pits

are circular to irregular in plane view and have a smooth relief that is

filled by the overlying limestones. Furthermore, large Chondrites

burrows (Hofmann, 1979; Filion and Pickerill, 1984) with branches up to

80 cm long are truncated just at the base of their mastershaft where

they generally branch to form an horizontal dendritic network (plate

7-4; C). The planar surfaces are clearly erosional because both grains

and cements are truncated along the surface (plate 7-4; B).

PLATE 7-4

PALEOKARST SURFACE - PLANAR EROSIVE SURFACE

A. Field photograph (bedding plane view) of a planar surface on top of a calcarenite cycle. Note the presence of pitting and relic features, small pinnacles (p). Ile du Havre SE. Scale in cm.

B. Field photograph (bedding plane view) of gastropod shell truncated by a planar surface capping a calcarenite cycle. Ile du Havre SE. Lens cap is 50 mm in diameter.

C. Field photograph (bedding plane view) of the trace fossil, Chondrites, truncated by a planar surface capping a calcarenite cycle. Ile du Havre SE. Lens cap for scale.
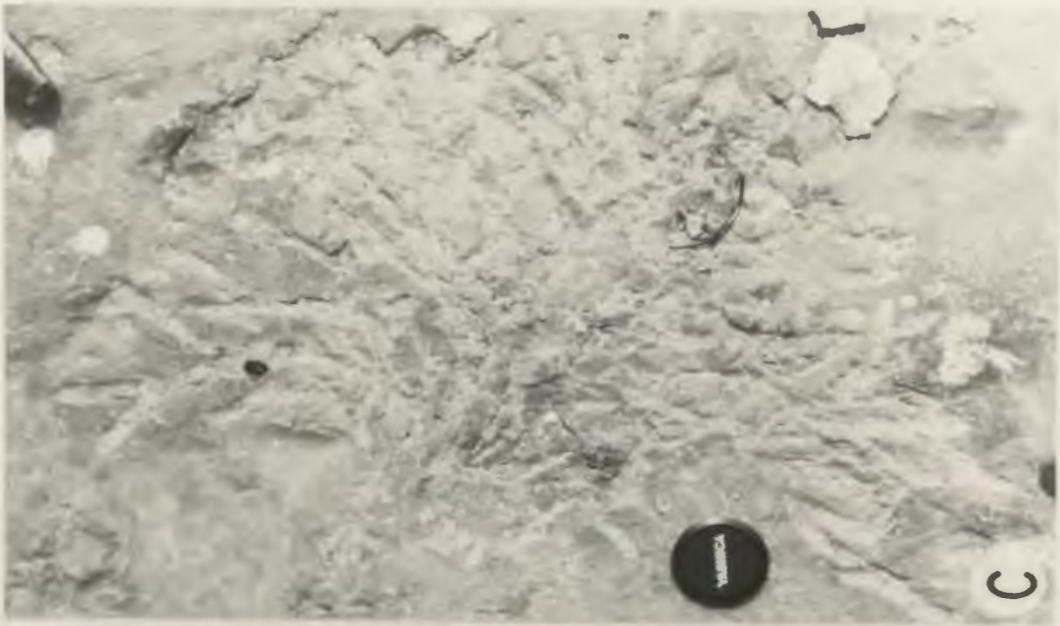
Karren forms in modern karst terrains converge toward flat surfaces at the lower end of the topographic gradient where flowing water becomes more stagnant and sideways enlargment is promoted. It is believed that the Ordovician planar surfaces were similarly formed by the progressive enlargment of karren and eventual development of extensive flat surfaces which are textured only by relic features (i.e. small ridges and pinnacles). The truncated mastershafts of Chondrites burrows suggest that at least several tens of centimeters were removed at the top of calcarenite cycles by karst erosion.

The origin of the small pits is more equivocal. Sharp circular pitting on modern exposed surfaces, sometimes considered as small kamenitzas, are thought to be a direct result of precipitation where as pits with smoother and irregular form are most likely the result of biological activity (Corbel, 1963). The problem with the second hypothesis is the absence of higher plants during the early Paleozoic time. Lichens and algae, present at this time however, are known to produce strong organic acids (Moore and Bellamy, 1974). Cowell (1976) interpreted pitting forming today as a product of biological solution by lichens and algae growing directly on the carbonate bedrock. This offers a possible explanation for small pits observed on the planar surfaces in this study.

In summary, the paleokarst surfaces represent exposure surfaces which formed contemporaneously with sedimentation and developed only on sand shoal deposits in response to minor fluctuations in sea level. The style of solution sculpture (karren) was controlled by the absence of soil or sediment cover and by the local drainage conditions at the

developed into peneplaned surfaces. With subsequent sea level rise, such a surface would have been rapidly submerged and most likely preserved without significant modification for the rock record.

Diagenesis

All grainstones below paleokarst surfaces represent newly exposed marine carbonate sediments which were severely affected by various meteoric diagenetic processes. The diagenetic history of these sand shoal deposits can be grouped into three distinct phases: 1) synsedimentary marine diagenesis; 2) meteoric diagenesis and 3) deeper burial diagenesis. Diagenesis is briefly outlined here, however details concerning this topic may be found in chapter 8.

The precipitation of calcite cement began in the marine environment, but evidence is equivocal. Synsedimentary marine cements occur as isopachous fibrous calcite (10-50 μm thick) around grains and clearly predate internal marine sediment. Furthermore, rounded intraclasts similar in composition, are lithified by the same cement and represent probable erosional remnants of these early lithified sediments. Cementation is patchy and suggests that small portions of the sand shoal deposit experienced seafloor lithification prior to subaerial exposure. Hardgrounds (i.e. marine cemented sediments) in modern sand shoals occur in stable-bottom areas commonly covered by algae where a combination of water turbulence and stabilized sediments is favorable to their development (Dravis, 1979).

Following this synsedimentary phase, sediments underwent significant alteration in a meteoric diagenetic environment. The most important

- 336 -

diagenetic features include: cementation, neomorphism and fabric-selective dissolution (biomoldic, oomoldic). Calcite cements are generally iron-poor, clear, and isopachous. They are strongly zoned under cathodoluminescence and probably formed under continually fluctuating chemical conditions which is most typical of meteoric waters. These cements, truncated by the paleokarst surfaces, fill virtually all of the pore spaces and occur in three basic forms: prismatic, syntaxial overgrowth and blocky. All three forms appear to have formed at the same time in different pore spaces and reflect the highly variable character (saturation state, water flow) in space and in time of the percolating meteoric waters. The sediment became well lithified near the surface as demonstrated by the conspicuous absence of grain-to-grain pressure solution. Gravitational cement, which is considered as an excellent criterion for vadose precipitation (James and Choquette, 1984) is rare and found only in fenestral mudstones, underlying the paleokarst surface on Ile Saint-Charles SE. Study of the cement stratigraphy (see chap. 8) clearly indicates that moldic pores formed in a near-surface diagenetic setting. Furthermore, these pores are sometimes floored with internal sediment and silt- to sand-sized crystal debris. Of particular importance is the repeated occurrence of these diagenetic features in the calcarenite cycles. This suggests that each cycle repeats similar diagenetic episodes, caused by a separate period of subaerial emergence.

There are two potential sources of calcium carbonate supplying the near-surface cements: 1) dissolution of metastable sediments, and 2) surface dissolution. Newly exposed marine sediments were initially cemented soon after meteoric waters began to percolate through the

sediments. Cementation occurred simultaneously or prior to the selective

dissolution of metastable particles (aragonitic ?) such as ooids and

skeletal components (mainly molluscs with some bryozoans). This caused

induration of these sediments and eventual development of surface karst

features. Most of the calcite cement of phreatic origin, however, is

thought to come from the dissolution of surface sediment associated with

the karst erosion.

All of the remaining pore spaces were filled with blocky calcite

cement which exhibits an iron-poor to iron-rich zonation toward the pore

centers. This cement grew over other previous cements and is also

present in fractures cutting all preexisting fabrics. Stylolitization,

however, is generally the latest diagenetic feature and is rarely cut by

fractures. Iron-rich cement and stylolites formed during progressive

burial of the Mingan sequence during Middle Ordovician time.

DISCUSSION

Origin of calcarenite cycles

The association of paleokarst surfaces with shallowing-upward cycles

is important as it may provide some insight into the cause of cyclicity.

Wilkinson (1982) summarized mechanisms that could explain the repetition

of such small-scale cycles. He recognized two end-members models: an

allocyclic model, influenced by extrinsic mechanisms and an autocyclic

model, influenced by intrinsic mechanisms. As Wilson (1975) pointed out,

these models are not necessarily independant of one another.

Extrinsic mechanisms are external to the depositional systems and

affect depositional processes by controlling the absolute position of

sea level and by changing in a non-uniform or periodic manner. Tectonic

and sea level fluctutations are two possible, extrinsic mechanisms that could affect cycles, reported in this study.

One possibility is that small epeirogenic movements persisted even after the passage of a peripheral bulge over the study area. This is not totally unreasonable considering the proximity of the Mingan Islands to the ancestral Appalachians, which were actively rising at that time in the Gaspe Peninsula, about 150 km to the south. In this hypothesis, each trangression was induced by a sudden tectonic pulse and basin subsidence. Eustatic sea level changes are also a possible mechanism for these cycles. Glacial eustatic sea-level changes and fluctuations in the rates of sea-floor spreading are often cited as factors controlling sea level changes (Donovan and Jones, 1979). There is widespread evidence of continental glacial deposits on the former Gondwanaland continent during the Ashgill time (Beuf et al., 1971). Fortey (1984) assumed that major ice sheets were established long before this time because there were large continental masses in the south polar region in the earlier Ordovician. Since the same period has been identified as one where subduction (and presumably concomitant sea-floor spreading) was active along the eastern margin of the North American craton, it is possible that global tectonic and glacial causes were operating together at this time.

In contrast, intrinsic mechanisms are totally independant of external influences and have to be self-regulating to develop cyclic deposits. These mechanisms are controlled by variation in the rates of sediment production and deposition without changes in the absolute position of sea level.

Ginsburg (1971) proposed an autocyclic model for prograding tidal

flat environments where the sedimentation rates are controlled by the source area. As tidal flats prograde, the adjacent, subtidal source area decreases or becomes too deep and sedimentation rates cannot keep pace with subsidence, thus a transgression occurs. This model can be modified to explain shallowing-upward sequences resulting from the shoaling of lime sand bodies such as those described in this study. In this modified model, sand shoals, characterized by some depositional relief, are prograding or expanding into deeper waters either at the bank margin or on the shelf. As the shoals move into deeper waters, more sediment is needed for vertical buildup rather than lateral progradation which may be progressively slowed and eventually stopped. The end result is also a shallowing-upward sequence.

Although there is no criterion at present that allows the distinction between these two models which generate virtually similar sequences. The fact that each of the Mingan calcarenite cycles is capped by a paleokarst surface may provide a clue in the evaluation of extrinsic versus intrinsic mechanisms. Surface karst, in general, is considered as a destructive process because its formation involves chemical dissolution of the parent limestone and represents a net loss of calcium carbonate. The paleokarst surfaces in this study represent weathered surfaces which removed the upper part of the calcarenite cycle which are inferred to be sand shoal deposits as indicated by several lines of evidence: 1) paleokarst surfaces are directly superimposed upon subtidal lithofacies; 2) cross-bedding in subtidal lithofacies is truncated by paleokarst surfaces and 3) absence of vadose diagenesis, in spite of subaerial exposure. Furthermore, the formation of these paleokarsts would have necessitated a relative sea-level fall such that

carbonate sediments were subaerially exposed for a reasonable period of time to produce a peneplaned surface. These observations provide unequivocal support for some extrinsic mechanisms that could maintain carbonates at a relatively significant elevation above sea level. The amount of sea level drop, however, is in metres because the inter-shoal areas, located in deeper water, are apparently not affected by subaerial exposure. Indeed these areas became the sites of more restricted deposition (i.e. mudstone-skeletal wackstone) caused by poor water circulation behind the exposed sand shoals. Either or both, small eustatic sea level changes or tectonic events could have produced the Mingan calcarenite cycles.

Comparison with other calcarenite cycles

Numerous examples of shallowing-upward cycles (see later) have been described by other workers and sometimes referred to in the literature as oolite-grainstone cycles (Wilson, 1975, p.283-297) or grainy sequences (James, 1984a). Examples include Middle Mississippian cycles from the Illinois Basin (Cluff, 1984) and Williston Basin (Smith, 1972; in Wilson, 1975), Middle Jurassic cycles of the Paris Basin (Purser, 1969, 1972; in Wilson, 1975), late Cretaceous cycles of east Texas (Wiggins and Harris, 1984), and late Cenozoic cycles of the southeastern Bahamas (Pierson, 1980; 1982).

These examples, including the Mingan calcarenite cycles, have several characteristics in common:

1) They are usually associated with larger scale shallowing-upward sequences with as many as 15 cycles which become usually thinner higher in the section.

2) Individual cycles range from a few metres to a few tens of metres in thickness.

3) The lower part of each cycle consists of open, marine subtidal deposits (skeletal wackestones and packstones).

4) The upper part of each cycle is composed of high-energy, sand shoal deposits which are generally influenced by tidal currents. Grainstones are commonly oolitic, especially near the top of cycle, but pelmatozoan grainstones may be also important.

5) no major reef development is associated with these cycles.

Most of these examples, however, are commonly found in carbonate platforms marginal to basins (Wilson, 1975). They may occur at the margins of either wide platforms and be traced for several tens of kilometres (e.g. Illinois, Williston, and Paris Basin) or smaller banks and be traced for only a few kilometres (e.g. southeastern Bahamas). In contrast, the Mingan calcarenite cycles represent sand shoals and tidal deltas probably deposited in the inner part of a gently sloping carbonate ramp. This suggests that typical calcarenite cycles are not unique to the platform margin but may also form in a carbonate ramp setting, the location of the zone of effective wave and current activity along the platform profile being a more important factor.

The nature of the surface capping these examples is variable. Some are capped by a submarine hardground and overlain by deeper basinal sediments (e.g. Paris Basin). Others exhibit evidence for subaerial exposure and include: 1) paleosols such as calcrete and terra rossa (Pierson, 1980); 2) paleokarst (this study) and 3) thin intertidal/supratidal deposits (Cluff, 1984). These variations most

likely reflect local environmental factors (climate, land vegetation).
In some, there are no obvious subaerial/vadose features and the contact
is sharp and apparently conformable. The lack of these features,
however, does not necessarily mean that the limestone was never
subaerial exposed because the surface may not have been exposed long
enough to form them.

As Wilson (1975) pointed out, such cycles do not form behind a
well-developed barrier reef because the flow of tidal current is
singularly restricted. Calcarenite cycles should be particularly common
in the record at times when only small delicate, branching and
encrusting reef builders were present. At these times, the shelf margin
must have been a complex of oolitic or skeletal (generally crinoidal)
sand shoals (James, 1984). On the other hand, environmental factors are
not always conducive to the development of marginal reefs, and so cycles
may also occur at any time during the Phanerozoic.

CHAPTER 8

LIMESTONE DIAGENESIS

INTRODUCTION

A detailed petrographic analysis (fossil skeletons, ooids and cement) of the Mingan Formation indicates that its components were lithified and altered in three distinct diagenetic environments (submarine, near-surface, and deeper burial). It is apparent that meteoric water penetrated via numerous subaerial exposure surfaces and left the most distinctive and varied diagenetic imprint, including: neomorphism, early dissolution (both fabric and non-fabric selective), and pervasive cementation before much compaction took place. Weathering and destructive diagenesis rather than calcite precipitation commonly marked the final episode of subaerial exposure. In spite of widespread evidence of emergence during the deposition of the Mingan Formation, vadose diagenetic features are virtually absent.

The objectives of this chapter are: 1) to document the petrographic character of sedimentary grains (fossils, ooids) and cement in the Mingan limestones; 2) to determine the diagenetic evolution of the Mingan sequence and 3) to discuss major findings or applications of this study to limestone diagenesis, in particular meteoric diagenesis.

PETROGRAPHY OF FOSSIL SKELETONS

Trilobites

The trilobite shells are ubiquitous particles (usually less than 1-2%) in subtidal lithofacies where nineteen genera, in total, have been identified by Shaw (1980). The trilobite **Bathyurus**, however, may compose substantial proportions (up to 10%) of some peritidal lithofacies. In thin-section, the shell microstructure of trilobites consists of fine calcite prisms oriented perpendicular to the skeletal surface. These prisms which are barely distinguishable with the light microscope are composed of iron-poor calcite. The carapaces are non-luminescent under cathodoluminescence and display no evidence of dissolution or neomorphism. Similar petrographic observations of trilobite cuticles have been consistly observed throughout the Paleozoic (Bathurst, 1975; Horowitz and Potter, 1971).

The well-preserved microstructure of trilobite cuticles is thought to reflect an original calcitic mineralogy, but of uncertain magnesium content. James and Klappa (1983) suggested that trilobites of different families secreted differing amounts of magnesium. Their suggestion is based on observations of Cambrian to Permian trilobites which may be replaced by ferroan calcite with preservation of the original skeletal texture. As Richter and Fuchtbauer (1978) pointed out, this indicates that the skeleton of some trilobites may have been Mg calcite.

Ostracods

The ostracod shells are ubiquitous in all limestone lithofacies, being only a significant component (1-5% in content) in peritidal limestones. Most of the ostracods have rather smooth valves and belong

to the family Leperditiidae. The petrographic attributes of ostracod cuticles are similar to those observed in trilobites. Cuticles are also non-luminescent under cathodoluminescence.

The retention of the cuticle microfabric in most ostracods strongly suggests that their original mineralogy was calcite. Modern ostracods have calcite skeletons with magnesium content ranging from 1 to 5 mole % but sometimes reaching up to 10 mole % (Cadot et al., 1972).

Brachiopods

Both inarticulate and articulate brachiopods are present in the Mingan Formation where they are common but subordinate particles, averaging 1-2% in content. The inarticulate brachiopods belong to the genus Lingulella and occur only in peritidal siliciclastics. All of the inarticulates have chitinophosphatic shells that are characterized by a crude laminated microfabric oriented slightly oblique to the shell structure.

The articulate brachiopods are present in all subtidal limestone lithofacies, and at least 12 different genera (mainly orthids and rhynchonellids) have been recognized (Cooper, 1956). In some areas, coquina beds are sometimes found at the base of the Intra-Mingan paleokarst unconformity and consist almost only of Rostricellula orientalis, an early rhynchonellid not recorded outside the study area (plate 4-13; E). In thin-section (plate 4-12; B), all the articulates exhibit the typical fibrous brachiopod fabric with a well-developed secondary layer of fibres oriented oblique to the shell surface. The primary layer made of fine fibres of calcite elongated perpendicularly to the shell surface, however, is poorly preserved or absent. The

calcite fibres are always iron- poor and non-luminescent under cathodoluminescence. Neither dissolution nor neomorphism of the brachiopod shells have been observed.

The shell microfabric in articulate brachiopods is consistently well preserved in the geological record, suggesting that their original mineralogy was calcite. There is general agreement that recent and fossil articulate brachiopods secrete calcite shells which usually contain less than 4 mole % $MgCO_3$ (Chave, 1954; Bathurst, 1975). This is also supported by geochemical studies using stable isotopes and trace elements that indicate the brachiopod shells suffered only minor diagenetic alteration with meteoric waters due to their low-magnesium calcite composition in comparison to other skeletal components (Brand and Veizer, 1980, 1981; Al-Aasm and Veizer, 1982).

Echinoderms

Echinoderms are common in all subtidal lithofacies, especially in grainstones associated with the calcarenite cycles or reef limestones. The echinoderm skeletons, however, are rarely preserved and consist mostly of disarticulated plates forming sand-sized particles. In thin-section (plate 4-12; B), these plates act optically as a single crystal of calcite and are surrounded by extensive epitaxial overgrowths. They are inclusion-rich and iron-poor although some are iron-rich. Under cathodoluminescence (plate 8-7; F), echinoderm particles appear non-luminescent to blotchy.

Mineralogical data and ultrastructure observations suggest that Recent crinoids secrete highly porous endoskeletons composed of high-Mg calcite, usually ranging from 8 to 16 mole % (Chave, 1954; Milliman,

1974). Echinoderm particles in Pleistocene limestones are characterized by both internal and external cements that are always in optical continuity with the particles. Ancient crinoids, composed of diagenetic low-Mg calcite are believed to have been originally high-Mg calcite as suggested by: 1) well preserved crinoidal material of Pennsylvanian age containing from 5 to 12 mole % $MgCO_3$ (Lowenstam, 1963; Brand, 1981); 2) presence of microdolomite inclusions in echinoderm particles (Macqueen and Ghent, 1970; Lohmann and Meyers, 1977) and 3) similar petrographic attributes consistently observed throughout the geological record. On the basis of the microdolomite content, Leutloff and Meyers (1984) estimated the average composition of Mississippian crinoids to 10.4 mole % $MgCO_3$ in comparison to 14.5 mole % for modern low-latitude crinoids, with the difference being ascribed to Mg loss during diagenesis.

Mollusks

Cephalopods and gastropods are present in all limestone lithofacies although both low- and high-spired gastropods are more common in peritidal lithofacies. Mollusk skeletons always appear as spar-filled molds (plates 4-10; D and 4-12; B). The calcite precipitated in these molds, is generally iron-poor, blocky and exhibits zoned luminescent properties under cathodoluminescence. Gastropod molds in peritidal lithofacies are frequently filled by an earlier stage of either fibrous (iron-poor, blotchy luminescent) or prismatic (iron-poor, non-luminescent) calcite sometimes preceded by internal geopetal sediment.

There is a general consensus that most Recent and fossil gastropods

and cephalopods secrete an aragonite skeleton (Bathurst, 1975). In general, skeletons in fossil specimens are almost always cement-filled molds. In some exceptionally, well-preserved cases, the original mineralogy and shell microstructure of these mollusks has been recognized in strata as old as Pennsylvanian (Yochelson et al., 1967; Brand, 1981).

Tabulate corals

Tabulate corals in the Mingan Formation are generally found in reef limestones and consist of four genera: Eofletcheria, Billingsaria, Lichenaria, and Tetradium?. The first two genera are common whereas the last two are much more rare having been identified only in thin-section. There is no general consensus as to whether the original mineralogy of the tabulate corals was aragonite or calcite (James, 1974; Sandberg, 1975a). Well-preserved microstructures in some of them have been used to suggest a primary (Mg-?) calcitic mineralogy. Squires (1973) reported that the skeletons of tabulate corals contain 5 to 8 mole % $MgCO_3$ in the Middle Pennsylvanian Buckhorn asphalt of Oklahoma, which also has an abundant, still preserved, aragonite fauna. On the other hand, some tabulate corals exhibit replacement or neomorphic microfabrics similar to those observed in "calcitized" scleractinian corals from Pleistocene limestones. Furthermore, the systematic status of the extinct Paleozoic Tabulata, although commonly regarded as coral, remains unclear because some workers have attempted to interpret them, or at least some, as sclerosponges (Hartman and Goreau, 1975; Flugel, 1976).

The skeleton of Eofletcheria spp. is characterized by loosely-packed corallites which are connected by short, horizontal syringoporoid tubules (plate 8-1; E). Tabulae are poorly developed and septa are

absent. The skeletal microstructure exhibits a fibrous fabric oriented
normal to the surface that form walls ranging from 200-400 μm in
thickness. Tabulae have similar but thinner fibrous fabric. This fibrous
fabric appears always as iron-poor calcite and non-luminescent under
cathodoluminescence.

The tabulate coral Billingsaria spp. is characterized by massive
corallites with septal trabeculae dilated edge-wise to form a thick wall
(plate 8-1; A and C). The tabulae are well-developed and septa are
short. In contrast to Eofletcheria, its skeleton microstructure is
completely obliterated by calcite crystals truncating the internal
skeleton macrostructures which are delimited by abundant inclusions
(plate 8-1; A-D). The calcite crystals in longitudinal section are
100-300 μm wide, 500-2,000 μm long and have length/width ratios
averaging 5-6. The same crystals in transverse section are
equidimensional and blocky in appearance. They are characterized by
zig-zag boundaries that interlock with adjacent crystals. The calcite
blades are oriented normal to the tabulae, mimic the direction of growth
changes and have undulose extinction under polarized light. These
crystals are iron-poor and form non-luminescent to dull subzones under
cathodoluminescence.

Lichenaria spp. exhibit prismatic, massive corallites (1 to 5 mm in
width) with offsets arising near their margins (plate 5-7; D). The
skeleton microstructure is composed of micritic crystals (less than 10
μm) that are iron-poor.

Another tabulate coral cannot be identified positively because it
always occurs as molds filled with a mosaic of iron-poor prismatic
calcite crystals (plate 8-1; F). Some corallites, however, are filled

PLATE 8-1

FOSSIL SKELETONS - TABULATE CORALS

Photomicrographs - Scale bar=1.0 mm

A. Thin-section photomicrograph (plane polarized light) illustrating
    massive corallites with septal trabeculae of the tabulate coral,
    Billingsaria. Detail in (C).

B. Same as (A) under cross-polarized light. Note the calcite crystals
    forming elongate blades oriented normal to the tabulae and the
    zig-zag boundaries between crystals.

C. Close-up of (A) showing calcite crystals truncating the internal
    skeleton macrostructure delimited by inclusion-rich zones. Plane
    polarized light.

D. Same as (C) under cross-polarized light.

E. Thin-section photomicrograph (plane polarized light) showing
    corallites, connected by short syringoporoid tubules, of the
    tabulate coral, Eofletcheria. Skeletal microstructure is fibrous and
    oriented normal to the corallite surface.

F. Thin-section photomicrograph (plane polarized light) of the tabulate
    coral, Tetradium ?. Note the spar-filled skeleton and the
    shamrock-like sections of corallites filled with lime mud.
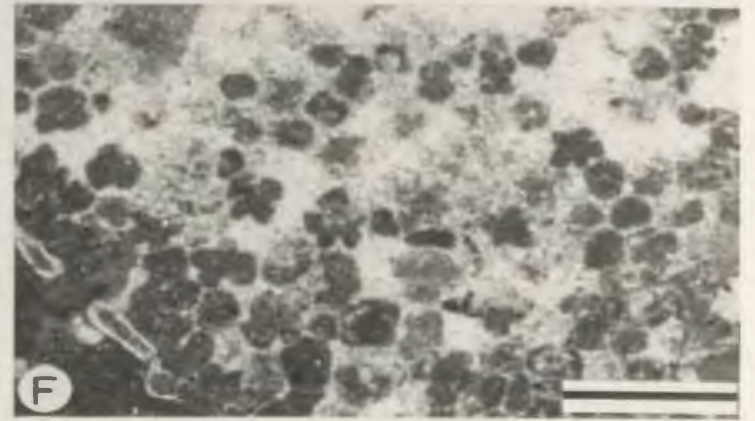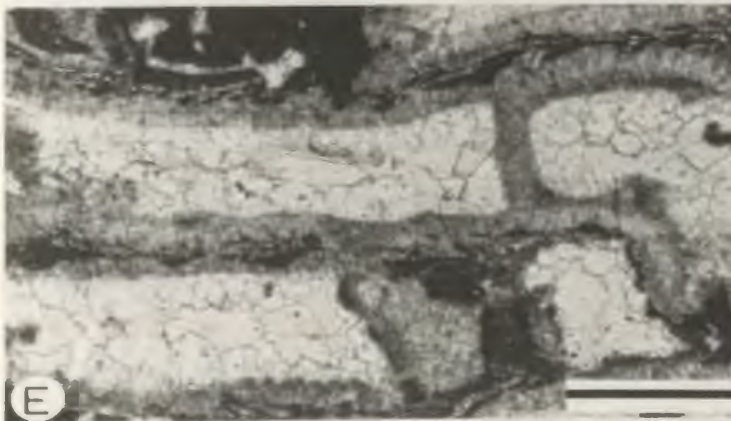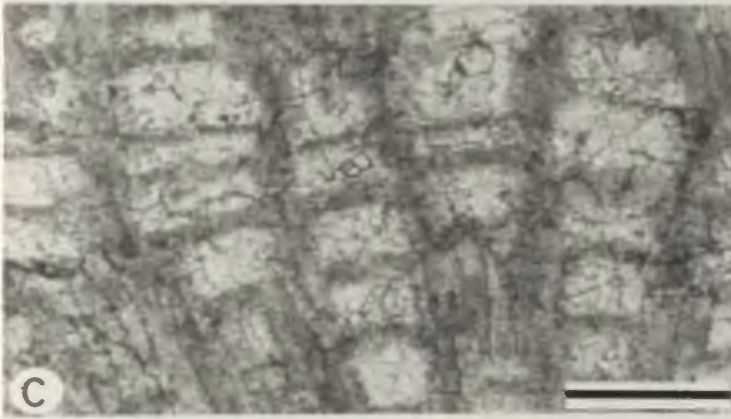
with micritic material at or near the skeleton margins and exhibit in transverse view shamrock-like sections delimited by the presence of four short septa which are characteristic of Tetradium spp.

Solenoporacean algae

Solenoporacean algae are restricted to reef limestones in the Mingan Formation. These algae show a high degree of development of horizontal layers or cross-partitions within vertical threads of cells (plate 5-8; A and B). This reticulate networks of cells averaging 50 µm in size appear to be characteristic of the genus Parachaetetes (Bourque et al., 1981). The preservation of the skeleton microstructure, however, is highly variable even within the same specimen ranging from poorly-preserved fabrics, outlined by abundant inclusions in sparry calcite crystals to fabrics obliterated by blocky calcite. The blocky calcite is iron-poor, inclusion-rich, 0.1 to 0.5 mm in size, and equidimensional to slightly elongate in shape. Under cathodoluminescence, skeletons appear always as non-luminescent disturbed only by some blotchy luminescent areas.

The solenoporacean algae Parachaetetes is part of an extinct family of calcareous red algae ranging from late Cambrian to the Paleocene (Wray, 1977). The skeletal structure of solenoporacean algae is poorly known although some workers have reported other Ordovician occurrences of Parachaetetes (including some formerly Solenopora spp.) with similar "recrystallized" fabrics (Kapp, 1975)

Bryozoans

Bryozoans are ubiquitous particles in all subtidal limestone

lithofacies but are significant sediment contributors only in reef limestones. These bryozoans are characterized by skeletons with a tubular architecture that is frequently observed in Paleozoic bryozoans (Boardman and Cheetham, 1969). In total, nine bryozoan genera have been identified with taxa belonging to the orders Cystoporata, Trepostomata, and Cystoporata. The skeletal microstuctures of these bryozoans exhibit three styles of preservation: 1) well-preserved skeletons with various combinations of lamellar, granular, and fibrous microstructures (plate 5-6; C and D); 2) poorly-preserved skeletons truncated by blocky calcite crystals (plate 8-2; A and B) and 3) obliterated skeletons outlined by spar-filled molds (plate 8-2; C and D). All these preservation styles may be present within the same thin-section. The transitions from one style to another, however, are <u>never</u> observed within the same bryozoan skeleton. The bryozoans with style 2 appear to be more common in trepostomates with ramose, branching growth habits whereas those with style 3 are common in trepostomates with encrusting, lamellar forms. The lamellar to fibrous calcites of style 1 are iron-poor, sometimes iron-rich, and non-luminescent under cathodoluminescence. The calcite crystals observed with style 2 have similar replacement fabric to that replacing the tabulate coral <u>Billingsaria</u> but differ only by their smaller size (less than 200 μm long). The calcite, precipitated in the bryozoans molds, generally consists of two stages: 1) first stage of iron-poor, prismatic calcite crystals oriented normal to the void margin, and 2) second stage of iron-rich, blocky calcite crystals filling the void. In some cases, only blocky calcite is present although an early iron-poor stage can be recognized in the blocky calcite. Under cathodoluminescence (plate 8-7; G and II), the first stage shows

PLATE 8-2

FOSSIL SKELETONS — BRYOZOANS

Photomicrographs - scale bar=1.0 mm

A. Thin-section photomicrograph (plane polarized light) of an
    unindentified trepostomate bryozoan with poorly-preserved skeleton
    truncated by calcite crystals.

B. Same as (A) under cross-polarized light. Note the undulose
    extinction of bladed calcite crystals.

C. Thin-section photomicrograph (plane polarized light) of spar-filled
    bryozoans (s) with encrusting, sheet-like forms. Zooecia are
    sometimes filled with lime mud.

D. Thin-section photomicrograph (plane polarized light) of spar-filled
    bryozoans (s) with internal sediment, crystal debris (d) flooring
    the bryozoan mold.
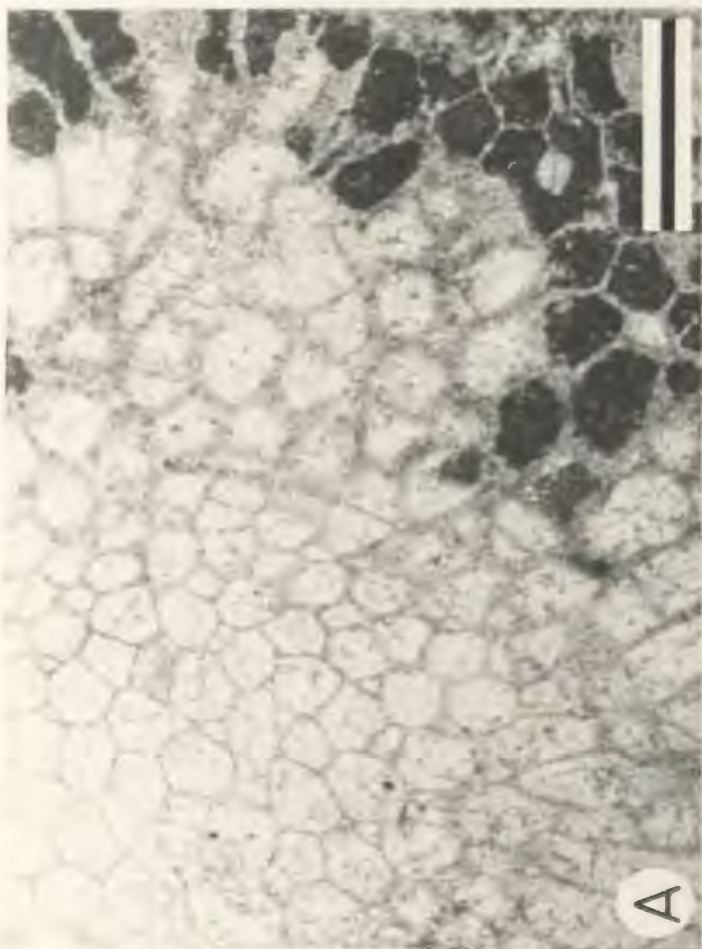
substages of non-luminescent to bright properties while the second stage displays only dull luminescence.

The mineralogy of the Recent bryozoans is highly variable, being related to phylogenic, ontogenic, and environmental factors (Milliman, 1974). Detailed studies have shed some light on the mineralogy and fabric of some cheilostomes which dominated the post-Paleozoic bryozoan fauna (Rucker and Carver, 1969; Sandberg, 1975a). They found that the encrusting species of the suborder Anasca tend to be calcitic, while free forms are aragonitic or contain a mixture of aragonite and calcite. In the suborder Ascophora, some species are all calcite, others all aragonite, but many have a mixed mineralogy with aragonite occurring as a late thickening of the frontal wall. The amount of $MgCO_3$ within the calcite generally ranges from 4 to 8 mole %, with a maximum of 13 mole %. The mineralogy of the Paleozoic bryozoans, however, is poorly known because occurrences of bryozoan skeletons with their original calcite or aragonite mineralogy have not been discovered. Ritcher and Fuchtbauer (1978) suggested an original high-Mg calcite mineralogy on the basis that well-preserved bryozoan skeletons are commonly stained by potassium ferricyanide. James and Klappa (1983) pointed out that the bryozoan skeletons that they studied are inconsistently stained by potassium ferricyanide even within the same thin-section, and so this reflects, more likely, their variable Mg content.

Summary

On the basis of their petrographic characteristics, fossil skeletons in the Mingan limestones can be separated into three distinct groups: 1) skeletons with well-preserved microfabrics; 2) skeletons with

spar-filled molds and 3) skeletons with relic microstructures. In general, fabric-preserved skeletons (group 1) are characterized by iron-poor calcite, non-luminescence under cathodoluminescence and absence of dissolution or neomorphism. Ostracods, trilobites, articulate brachiopods, echinoderms and the tabulate coral, Eofletcheria always appear with fabric-preserved skeletons.

Spar-filled skeletons (group 2) are now molds filled with iron-poor calcite cement sometimes followed in larger pores by a final stage of iron-rich, blocky calcite cement. Such skeletons include mollusks and possibly the tabulate coral Tetradium.

Finally, the tabulate coral Billingsaria and solenoporacean algae are replaced by coarse, iron-poor calcite crystals having no relationship with the original skeleton microstructure, present only as relics. Furthermore, all three styles of fabric retention are present in bryozoan skeletons. The transition, however, from one style to the other is never observed within the same bryozoan skeleton.

OOID CHARACTERISTICS

Two distinct types of ooids occur in the Mingan limestones. The first is made up of relatively small grains (0.2-0.4 mm in size) that are sometimes found in grainstones associated with peritidal lithofacies. These ooids are thought to represent local patches of oolitic sands that were subsequently transported and deposited in peritidal environments, only short distances from their place of generation. In thin-section (plate 8-3; A), their cortical layer is micritic to acicular with a marked radial fabric oriented normal to the ooid surface. The nucleus consists of a cryptocrystalline grain, either

PLATE 8-3

OOIDS
SYNSEDIMENTARY CEMENT - FIBROUS CALCITE

Photomicrographs - Plane polarized light
- Scale bar=1.0 mm

A. Thin-section photomicrograph of ooids (o) with radial cortex mixed with echinoderm grains and intraclasts (lithofacies 14: basal intraclast-skeletal grainstone).

B. Thin-section photomicrograph of spar-filled ooids in skeletal-ooid grainstone (lithofacies 12). Note the oomoldic pores and ooid distortion (arrow) caused by the collapse of surrounding prismatic cement.

C. Thin-section photomicrograph of fibrous calcite cement (f) lining solenoporacean algae (a) in coral-algae bioherm complex. Coarse, blocky calcite (b) is the last void-filling cement.

D. Thin-section photomicrograph of fibrous calcite cement (f) filling intraparticle pores around intraclasts and echinoderm grains (lithofacies 14: basal intraclast-skeletal grainstone). Fibrous calcite with meniscus fabric in the bottom left corner.
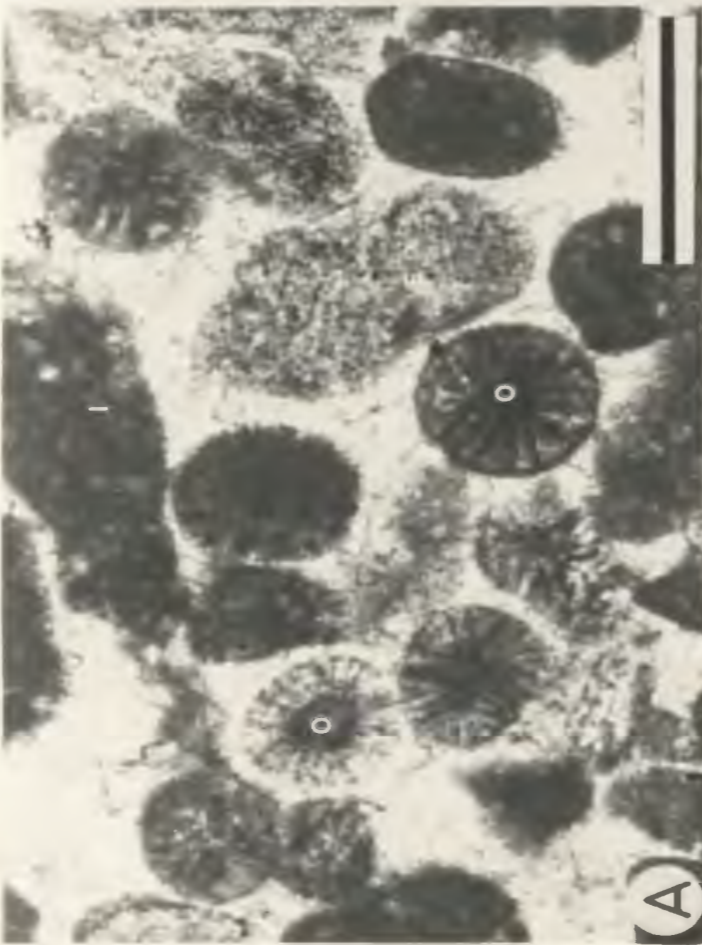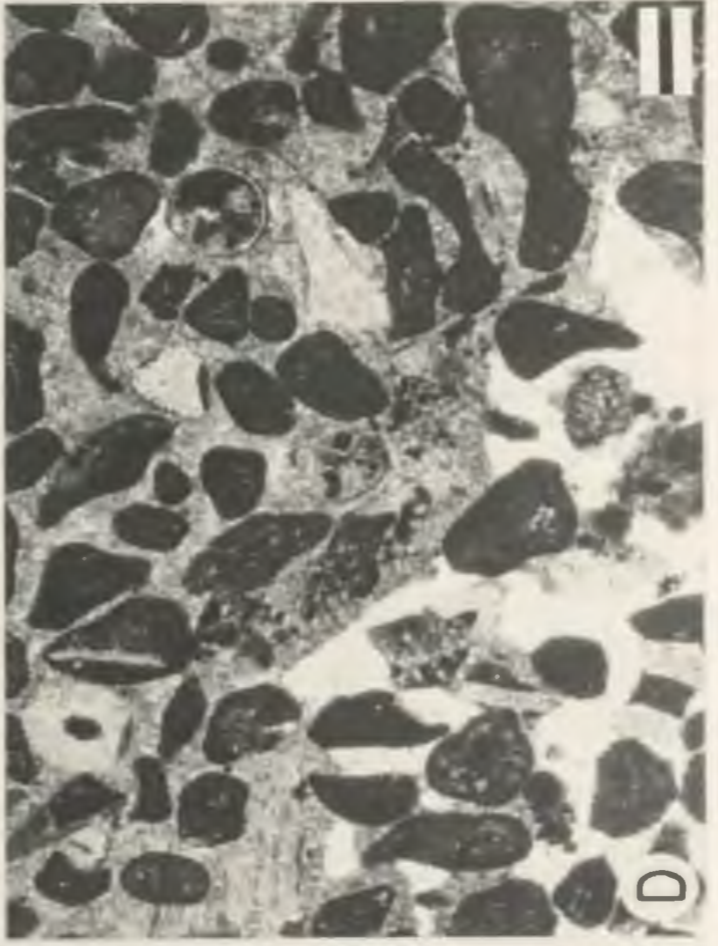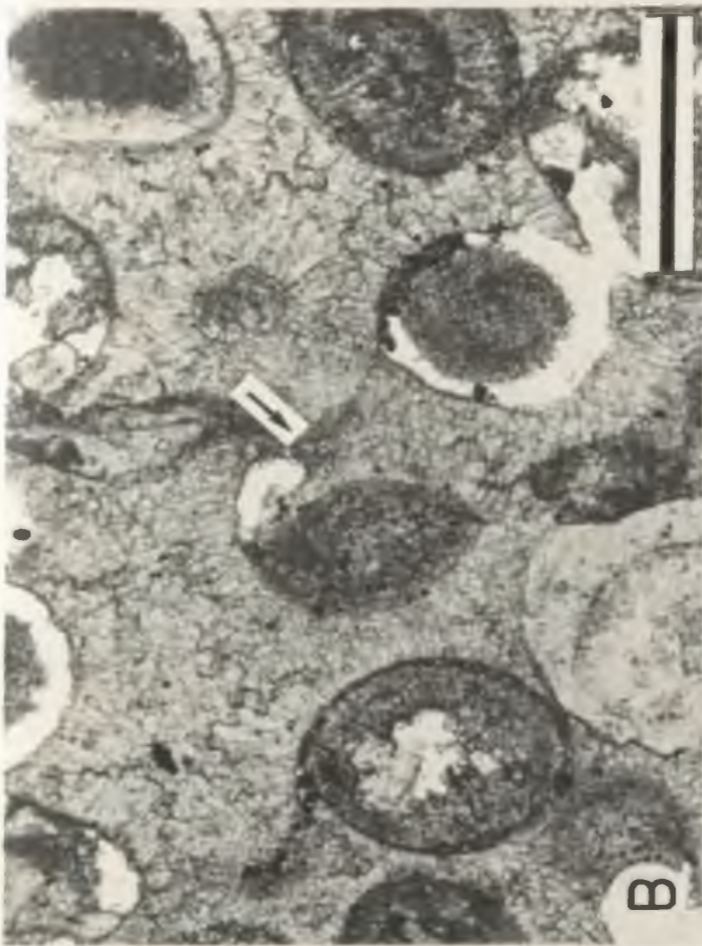
a peloid or a small rounded intraclast which averages 0.1 mm in size. In some cases, the cortical layer is partially obliterated due to post-accretionary micritization or replacement by dolomite crystals. The radial cortex is iron-poor calcite crystals that are non-luminescent under cathodoluminescence.

The second type of ooids occurs in the upper part of grainstone units capping the calcarenite cycles. These grainstones represent the most active portion of sand shoals that formed in tidal deltas. In contrast to the first type, these ooids are slightly larger (0.3 to 0.6 mm in size) and volumetrically more important making up to 40% of the rock volume. Their cortical layers appear always as spar-filled molds and consist of a single, large or several calcite crystals that are iron-poor (plates 4-12; C and 8-3; D). The void-filling nature of these calcite crystals is well illustrated under cathodoluminescence where they display substages of bright to dull luminescence similar those observed in adjacent gastropod molds. The calcite crystals, however, are sometimes inclusion-rich and characterized by a vague concentric banding. The most common nucleus is peloids or small, rounded intraclasts but the nucleus is sometimes absent. Oomoldic pores (plate 4-12; C) are common and sometimes partially filled with late ferroan dolomite cement. The first type of ooids are rare in these grainstones, although some ooids with an inner, radial and outer, spar-filled cortical layers are present. The primary interparticle pores are generally occluded by clear, iron-poor prismatic calcite which is non-luminescent under cathodoluminescence. Because compactional fractures caused ooid distortion and cement collapse, it is inferred that both calcite cementation and ooid dissolution have predated any

significant sediment accumulation.

On the basis of similar fabric retentions, the first type of ooids may be included in group 1 with fabric-preserved fossil skeletons whereas the second type is characteristic of spar-filled skeletons (group 2).

The microstructure and mineralogy of modern marine ooids have been recently summarized by Simone (1981) and Ritcher (1983). The cortical layer in aragonite ooids is characterized by either tangentially oriented crystals, or radially oriented crystals or a combination of both. In contrast, only radially-oriented crystals have been observed in the cortical layer of marine Mg-calcite ooids. Furthermore, ooids may frequently contain layers of cryptocrystalline, randomly-oriented crystals, either aragonite or Mg-calcite. The cortical layer in fossil ooids, however, consists of cryptocrystalline calcite with either tangentially- or radially-oriented crystals. The preservation of their original structure is generally thought to indicate a previous calcitic or Mg-calcitic composition, while previous aragonite is indicated by sparry calcite (Sandberg, 1975b; Tucker, 1984; Wilkinson et al., 1984). In the latter case, the primary structure is destroyed during diagenesis, because aragonite is dissolved to form oomoldic porosity which may be filled with cement, or the aragonite is calcitized in situ as shown by relics of the original laminae. Oomoldic porosity in oolitic limestones strongly suggests an original aragonitic composition for the ooids in spite of the equivalence of Mg calcite and aragonite solubilities and rare occurrences of molds developed during high-Mg calcite dissolution as pointed out by Wilkinson et al. (1985).

CALCITE CEMENTATION

Synsedimentary cement

Fibrous calcite.

Fibrous calcite cement is relatively rare and occurs only in beachrocks, fenestral mudstones, and reef limestones, especially in larger mound complexes. In reef limestones (plates 5-4; E and 8-3; C), it lines growth cavities and fills some intraparticle pores in various fossil skeletons. In beachrock (plate 8-3; D), it lines or completely fills interparticulate pores around intraclasts and skeletal debris, including echinoderm grains. When the pores are partially filled, fibrous cement commonly displays microstalactitic and/or meniscus fabrics. In fenestral mudstones, fibrous calcite sometimes fills fenestrate and other primary pores but may be truncated at the margin of vuggy pores resulting from non-fabric selective dissolution.

In thin-section, the fibrous calcite consists of bladed to prismatic crystals which are oriented normal to the pore wall or substrate. Individual crystals are 0.05 to 0.5 mm wide, up to 0.5 mm long, iron-poor, and inclusion-rich but some crystals may have clear terminations. These crystals exhibit a faint sweeping extinction under crossed polars. Subcrystals are hardly identifiable. Under cathodoluminescence, the fibrous calcite is blotchy to non-luminescent. This type of cement is commonly referred to as "radial-fibrous" calcite (Mazzullo, 1980; Kendall, 1985). Furthermore, this cement is strikingly similar to submarine cements described from several modern reefs (Ginsburg and Schroeder, 1973; James et al., 1976) and beachrocks

(Moore, 1973, 1977).

The synsedimentary nature of the fibrous calcite cement is supported by several lines of evidence: 1) it is always the first generation of cement, if present; 2) it fills only primary void systems; 3) it predates and/or alternates with internal marine sediments (mainly peloid/skeletal wackstones); 4) it predates compaction and 5) the presence of various petrographic characteristics (fibrous fabric, inclusion-rich, nonluminescent) which are common to fossil sea floor precipitation (Longman, 1980; James and Choquette, 1983).

Postsedimentary cements

Radiaxial fibrous calcite

This cement occurs only in fissures and associated vuggy and biomoldic pores beneath the intra-Mingan paleokarst unconformity (plate 8-4; A). It forms either as pervasive, isopachous crusts filling all the pore spaces (plate 8-4; C) or as thin, isopachous fringes (0.3 to 2.0 mm thick) post-dated by iron-poor, blocky calcite (plate 8-4; B). Isopachous crusts consist of either a single layer of cone-shaped crystals or several poorly-layered nested cones (plate 8-4; D) separated by internal marine sediment. Fibrous calcite is sometimes characterized by a preferential downward growth that is most likely due to internal sediment present at the bottom of the pores, thus inhibiting upward growth of this cement. In some cases, the isopachous crusts are layered with alternating, inclusion-rich and inclusion-poor bands (100 to 300 um thick) which may form up to three couplets within some crystals. These inclusion-poor bands are generally iron-poor and brightly luminescent

PLATE 8-4

POST-SEDIMENTARY CEMENT - RADIAXIAL FIBROUS CALCITE

Photomicrographs - Scale bar is 1.0 mm

A. Polished slab (vertical view) showing internal geopetal sediment and radiaxial fibrous calcite filling secondary biomoldic pores (arrows) in gastropod packstone (lithofacies 9). Ile du Havre SW.

B. Thin-section photomicrograph (plane polarized light) of gastropod mold filled with internal geopetal sediment (s) and radiaxial fibrous calcite (f) forming isopachous lining. Note the gastropod mold outlined by the original biomicrite matrix (m) and the last void-filling, blocky calcite (b).

C. Thin-section photomicrograph (plane polarized light) of inclusion-rich radiaxial fibrous calcite forming a pervasive crust in a gastropod mold. Note the presence of internal geopetal sediment with peloids (s).

D. Same as (C) under cross-polarized light. Note the presence of several poorly-layered nested cones of radiaxial fibrous calcite.

(plate 8-7; C). Individual crystals are petrographically similar to those in synsedimentary fibrous cement but contain microdolomite inclusions and have zig-zag interboundaries. In contrast, the crystals are mostly radiaxial fibrous calcite (Bathurst, 1959; Kendall and Tucker, 1973) but lateral transitions with radial-fibrous calcites commonly occur. Under crossed polars, they are characterized by a marked undulose extention and an opposing pattern of distally-convergent optic axes.

Radiaxial fibrous calcite is interpreted here as marine cement but is clearly post-depositional and filled only secondary pore spaces. Such cements are more commonly found in the depositional and early diagenetic cavities of reefs and mudmounds (Bathurst, 1959, 1982; Ross et al., 1975; Davies, 1977; Walls et al., 1979). They represent neomorphosed fibrous marine cement composed of laterally interfering bundles of radiating crystals (Kendall and Tucker, 1973). Its neomorphic origin, although has been recently questioned by Kendall (1985) and reinterpreted as a primary fabric resulting from the asymmetric growth within calcite crystals undergoing split growth. Its original mineralogy is inferred to be Mg-calcite on the basis of microdolomite and other evidence (Lohmann and Meyers, 1977).

Prismatic calcite

Prismatic calcite cement is widespread in the Mingan Formation and generally occurs as isopachous rinds: 1) in both interparticle and intraskeletal pores of most calcarenitic lithofacies (plate 8-5; A and B); 2) in growth cavities of some reef limestones; 3) in fenestrate pores of fenestral mudstones and 4) in vuggy and biomoldic pores, if

PLATE 8-5

POST-SEDIMENTARY CEMENT -
PRISMATIC AND STALACTITIC CEMENT

Photomicrographs - Scale bar=1.0 mm

A. Thin-section photomicrograph (plane polarized light) illustrating an isopachous rind of prismatic calcite (p) around intraclasts in lithofacies 8 (intraclast grainstone). Note the coarse, blocky calcite as last void-filling (b).

B. Same as (A) under cross-polarized light.

C. Thin-section photomicrograph (plane polarized light) of stalactitic calcite (s) beneath intraclasts and skeletal particles. Note the preferred downward growth of this cement and the presence of coarse, blocky calcite as last void-filling (b).

D. Same as (C) under cross-polarized light.
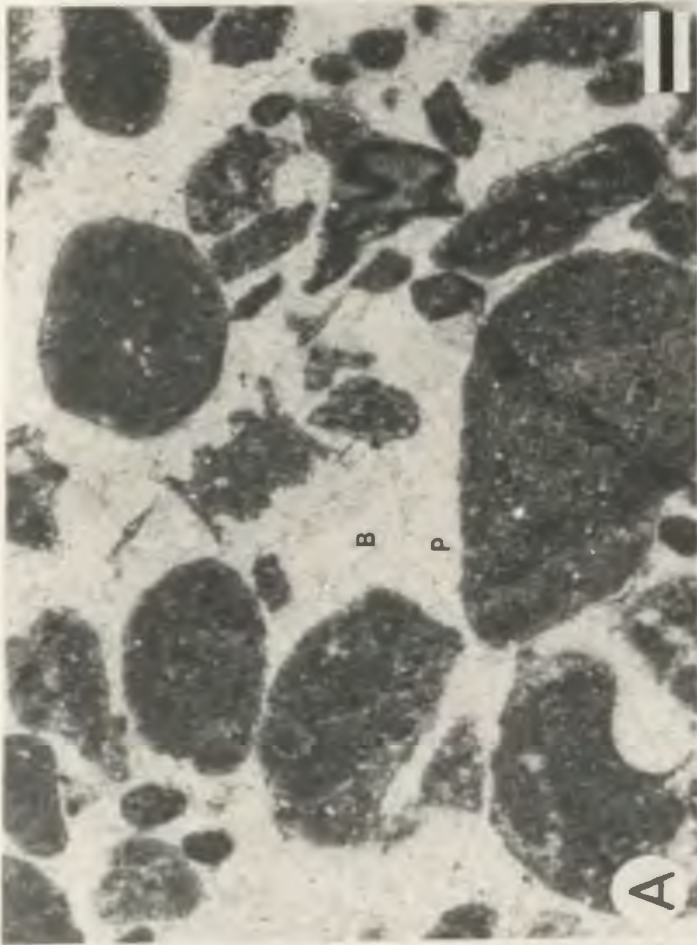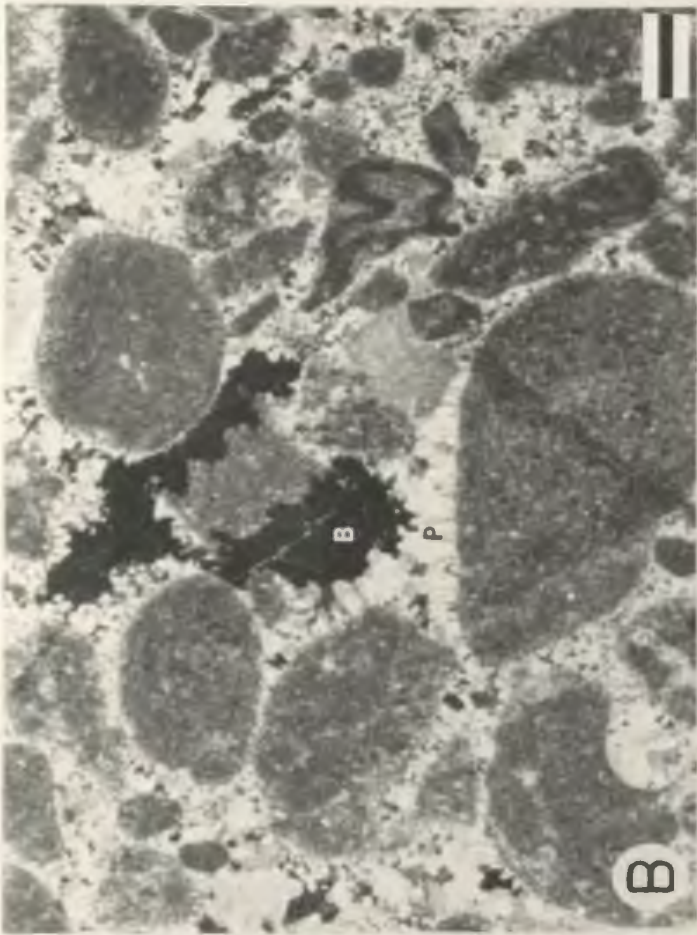
radiaxial fibrous calcite are absent. Individual crystals are iron-poor,
inclusion-poor, 100-500 μm long, and 30-80 μm wide. Crystals are in
optical continuity on trilobite and ostracod skeletons and exhibit a
distinctive sweeping extinction between crossed polars. In some cases,
prismatic calcite cements have an early, inclusion-rich phase which is
generally iron-poor and contains microdolomite inclusions.

Epitaxial calcite

This cement occurs always as epitaxial overgrowths on echinoderm
grains and are more common in all subtidal grainstone lithofacies (plate
4-12; B). These overgrowths have outgrown other cement types and only
prismatic calcite appears to have co-existed or competed with them on
non-echinoderm grains. The epitaxial calcite is usually iron-poor but an
outer iron-rich zone is sometimes present. In some grainstones
associated with beachrock, epitaxial overgrowths contain patchy
microdolomite inclusions giving a cloudy appearance to this cement.

Stalactitic calcite

Rare stalactitic calcite cement occurs only in fenestral mudstones
and oncolite/mollusk packstones and grainstones at the top of a
calcarenite cycle on Ile Saint-Charles SE. This cement is found in both
primary and secondary (biomoldic) pore systems as the first void-filling
cement and pre-dated blocky calcite (plate 8-5; C and D). The cement is
iron-poor, bladed to prismatic, and up to 2.0 mm long). Inclusions form
distinctive yellowish brown growth bands. It is also characterized by a
marked, pendulous fabric. Meniscus fabric are less common. This
preferred downward growth is commonly attributed to cementation in the

vadose zone as the waters dripped down from the undersides of the particles into the underlying pores (James and Choquette, 1984).

Blocky calcite

This cement is ubiquitous to all Mingan lithofacies and occurs as clear, coarsely crystalline mosaics of sparry calcite. Individual crystals range from 0.2 to 3 mm in size and have planar boundaries and straight extinction. It post-dates all other calcite cements (plates 8-4; B and 8-5; C and D), if present, and fills the remaining pore spaces (both primary and secondary pore systems). When earlier cements are absent, nucleation appears to have taken place at a limited number of sites on the pore walls and is well illustrated under cathodoluminescence (plate 8-7; D). Two distinct stages of blocky calcite are recognized in thin-section; an early iron-poor stage and a later iron-rich stage which may be absent. The earlier stage is sometimes buried by geopetal crystal debris. The later phase, in concert with ferroan dolomite cement, filled fractures that truncate other particles and cements.

Crystal debris

Crystal debris consists of angular, silt- to sand-sized particles that were deposited geopetally within both primary and secondary pores (plate 8-2, D). This debris is sometimes cross-laminated and characterized by horizontal to slightly inclined ($10°-20°$) upper surfaces, attesting to deposition by moving water. Iron-poor calcite cements (prismatic, blocky) predate or are contemporaneous with this debris, as indicated by the presence of crystal debris either overlying

or more commonly abutting these cements. Silt-sized debris, similar to the "vadose silts" described by Dunham (1969) from the Permian limestones of New Mexico, are well sorted and common in fenestrate and small secondary pores. In contrast, the sand-sized debris is more commonly found in fissures and larger secondary pores, poorly-sorted and may even display inverse grading. Under cathodoluminescence (plate 8-7; A and B), sand-sized debris exhibits discrete luminescence zones that are truncated at the debris margins. These zones are similar to those present in contemporaneous calcite cements. Again this background, crystal debris resulted clearly from the erosion of calcite cement by meteoric water (see discussion later) percolating through the pore system. It is also interesting to note that silt-sized debris has easily filtered into the pores forming an ubiquitous internal sediment, the sand-sized debris being mechanically trapped in larger pores and unable to move.

Summary

Synsedimentary cements are found only as rinds of fibrous calcite in bioherms and beachrocks. Fabric crystals of these fibrous cements suggest that they represent neomorphic replacement of a precursor fibrous carbonate. Radiaxial fibrous calcite is also regarded as the product of in situ neomorphic replacement of a metastable fibrous carbonate, possibly Mg calcite (Kendall and Tucker, 1973). Both fibrous cements precipitated under marine conditions but radiaxial fibrous calcite was clearly post-depositional occurring only in secondary pores beneath the intra-Mingan paleokarst. The style of fabric retention in

- 372 -

these fibrous cements, may be included with that of fossil skeletons retaining their microstructure (group 1).

In general, the post-sedimentary cements consist of inclusion-free, iron-poor calcite followed by iron-rich, blocky calcite as the last void-filling. The growth habits of iron-poor calcite cements are either prismatic, or epitaxial or blocky (early phase). These post-sedimentary cements were precipitated as calcite in a phreatic to deeper burial environments under increasingly reducing conditions.

PETROGRAPHY OF MINOR AUTHIGENIC MINERALS

Dolomite

Dolomite is limited in its distribution and abundance (less than 5%) in the Mingan Formation and occurs in four distinct crystal fabrics: 1) finely crystalline dolostones in silty dololaminites; 2) euhedral, sucrosic dolomites in laminated sandstones; 3) small, euhedral dolomites in more micritic lithofacies and 4) coarse, baroque dolomites in voids and fractures.

The finely crystalline dolostones in silty dololaminites (lithofacies 1) consist of a mosaic of rhombic, euhedral to subhedral crystals, averaging 30 um in size (plate 8-6; A). These crystals contain abundant inclusions and are iron-poor but internal iron-rich bands are present. When partially dolomitized, peloids are generally the preferred nucleation sites for these crystals. Fine-grained dolostones represent penecontemporaneous dolomitization of silty peloid limestones in the upper intertidal to supratidal environments. Evidence for this includes the well-preserved sedimentary fabrics (laminae, fenestrae, mudcracks)

PLATE 8-6

MINOR AUTHIGENIC MINERALS

Photomicrographs - Scale bar=1.0 mm

A. Thin-section photomicrograph (plane polarized light) of fine to
    medium-crystalline dolomite crystals in silty dololaminite. Note the
    fenestrate pores filled with blocky calcite.

B. Thin-section photomicrograph (plane polarized light) of euhedral
    dolomite crystals filling the interparticle pores in laminated
    sandstones (lithofacies 3). Note the presence of dedolomite and of
    blocky calcite as last void-filling stage. Inner part of dolomite
    crystals are completely dedolomitized and replaced by calcite.
    Close-up of plate 4-3; C.

C. Thin-section photomicrograph (cross-polarized light) showing three
    distinct cement phases in gastropod packstone: 1) radiaxial fibrous
    calcite (r) filling the intraskeletal pore (gastropod mold); 2)
    blocky calcite (b) and 3) coarse, saddle dolomite crystals (s) as
    last void-filling.

D. Thin-section photomicrograph (cross-polarized light) showing quartz
    overgrowths around quartz grains in lithofacies 4 (cross-bedded
    sandstones). Note that the detrital quartz grains (q), outlined by
    a dust line, are well rounded.
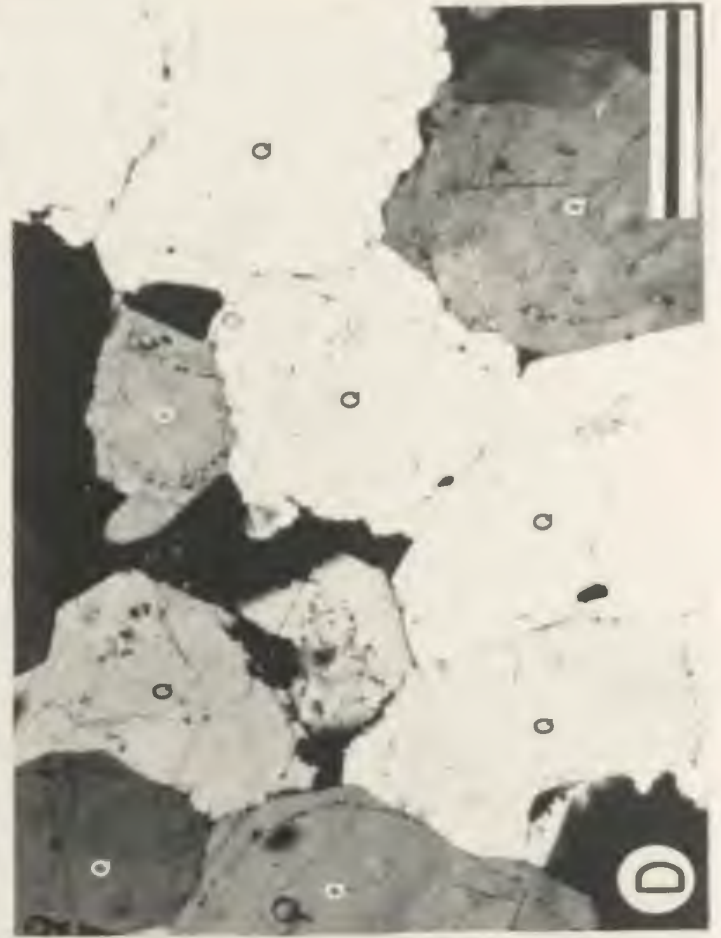
and their restricted stratigraphic occurrence. The former presence of evaporites (halite hoppers) suggests that Mg-rich surficial brines acted as the dolomitizing fluids.

The second type consists of sucrosic, euhedral dolomite crystals filling partially the interparticle pores (plates 4-3; D and 8-6; B) in laminated sandstones deposited in intertidal sand flats. These sandstones are found beneath the silty dololaminites in the upper part of the basal Corbeau Member. Individual crystals are 0.1 to 0.25 mm in size, and iron-poor with sometimes an iron-rich core. They display cloudy centers (inclusion-rich) surrounded by clear rims. Its stratigraphic position suggests that slow seepage of superficial, Mg-rich brines resulted in the formation of dolomite ce. nt and occurred to a depth of 2-3 m beneath the sediment surface. Dolomite cement is rare or absent in the coarser-grained sandstones at the base of the siliciclastic member.

The third type of dolomite is a broadly defined category and ubiquitous in distribution. It occurs (in order of importance) in burrow fills, fined-grained limestone matrices, cryptocrystalline grains (peloids, micritic intraclasts, oncoli coatings), and along stylolitic seams. These dolomites consist of small, scattered dolomite rhombs (50-100 μm in size) but may also form incipient mosaics with a crystal-supported fabric. Individual crystals are either iron-poor or iron-rich, inclusion-poor, and euhedral in shape.

Coarse, baroque (also called saddle dolomite by some workers) dolomite is present as the latest pore-filling cement in fractures and larger pore spaces (plate 8-6; C). In some coarser-grained sandstones, it may be intergrown with iron-rich, blocky calcite. The dolomite

consists of iron-rich, anhedral crystal mosaics. The crystals range from less than 50 um to up 500 um depanding on the pore sizes. They are also characterized by dark inclusions (possibly organic matter), curved crystal faces in rare open pores, and sweeping extinction under crossed polars.

Dedolomite

Dedolomite is commonly observed in all previously described dolomites with the exception of coarse, baroque dolomite. Dolomite rhombs are completely calcitized by iron-rich calcite (plate 8-6; B). Iron oxides, a common by-product of dedolomitization (Katz, 1971; Al-Hashimi and Hemingway, 1973) are absent. When incomplete, calcitized rhombs are present, relics indicate that the dolomite was originally iron-rich. Co-existing iron-poor dolomite rhombs remain unaffected. Dedolomite commonly occurs near fractures filled with iron-rich, blocky calcite. Furthermore, dedolomite affected the dolomite cement in the laminated sandstones where the iron-rich cores of dolomite rhombs are selectively replaced by iron-rich calcite. This calcite is usually in optical continuity with large, blotchy calcite crystals that fill the adjacent pore space.

Dedolomite in ancient carbonate sequences has often been interpreted as a near-surface diagenetic product and its occurrence in the subsurface may indicate the presence of an unconformity (Chilingar et al., 1979). Two mechanisms have been proposed to explain the process: 1) reaction of dolomite with a calcium sulfate solution derived from oxydation of pyrite (Shearman et al., 1961; Evamy, 1963) and 2) alteration of iron-rich dolomite by oxygenated meteoric water to produce

disseminated hematite and goethite within the calcite zone in dedolomite (Al-Hashimi and Hemingway, 1973, Frank, 1981). Although, recent studies suggest that the formation of dedolomite may also occur under a wide range of conditions, for instance, by the upward movement of hot, calcium-rich brines (Land and Prezbindowski, 1981; or during burial at higher temperatures (Budai et al., 1984).

Quartz and Feldspars

Quartz and feldspar overgrowths are present only in the coarse-grained, arkosic sandstones (plate 8-6; D) at the base of the siliciclastic Corbeau Member. Under cathodoluminescence, these sandstones are characterized by well-rounded, detrital quartz and feldspars and by the absence of fitted fabric or solution at grain contact. This indicates that only minor cement was derived from pressure solution. Indeed, common weathered feldspars (calcitized) in the sandstones suggest that dissolution of unstable feldspars alone has supplied the material necessary for the amount of authigenic quartz and feldspars observed. Diagenetic alteration of the feldspars during burial released ions that provided important intrastratal sources of ions (K, Al, Si) which are locally reprecipitated in authigenic minerals (Walker, 1984; Dutton and Land, 1985). The smectite to illite transformation, if complete, in the overlying shales may also be a source of silica for quartz overgrowths (Boles and Franks, 1979), however, that source might have been limited during early burial. A possible explanation for the absence of these authigenic minerals in the laminated sandstones is that the earlier dolomite cement had singularly reduced the available number of nucleation sites for precipitation.

CEMENT STRATIGRAPHY

Three distinct stages of calcite cement are present in the Mingan
Formation and can be differentiated by using a combination of staining
and cathodoluminescence. These stages include: A) synsedimentary,
iron-poor cements with blotchy luminescence; B) post-sedimentary,
iron-poor cements with strongly zoned luminescence and C)
post-sedimentary, iron-rich cements with uniform, dull to
non-luminescent properties. Complete cement sequences are rarely
observed because certain stages may be missing but the order of
succession is always present. The cement stratigraphy of rocks beneath
and above the intra-Mingan paleokarst unconformity is described in the
following section.

Pre-karst strata exhibit a variety of cement sequences associated
either with the basal siliciclastic unit (i.e. Corbeau Member) or the
overlying limestones (i.e. Perroquet and Fantome Members). In the
siliciclastics (fig. 8-1), the stage A is absent but sucrosic, euhedral
dolomites, contemporaneous with deposition, are present in the laminated
sandstones as the first pore-filling. These dolomites are dull to
non-luminescent. Stage B, characterized by iron-poor calcite cement, is
rare or absent. Quartz and feldspar overgrowths in the coarser-grained
sandstones, interpreted as pre-compaction in origin, clearly predate the
last stage of carbonate cementation. Stage C is ubiquitous in
distribution and consists of iron-rich, blocky calcite, locally
intergrown with baroque dolomite crystals. These iron-rich cements
always occur as the last pore-filling in the pre-karst siliciclastics.
They are sometimes the only pore-filling cement.

In contrast to the siliciclastics, pre-karst limestones (fig. 8-2)

Figure 8.1- Schematic diagram showing the cement microstratigraphy of siliciclastic lithofacies in the basal Corbeau Member. The most common cement is iron-rich, blocky calcite intergrown locally with saddle dolomite. This calcite cement is ubiquitous and occurs as the last pore-filling, but is predated by an early dolomite cement in the laminated sandstones and by quartz and feldspar overgrowths in the coarser-grained sandstones.

BASAL SILICICLASTICS

CALCITE CEMENT   OTHER CEMENTS

Blocky   Early Dolomite   Saddle Dolomite   Quartz & Feldspar
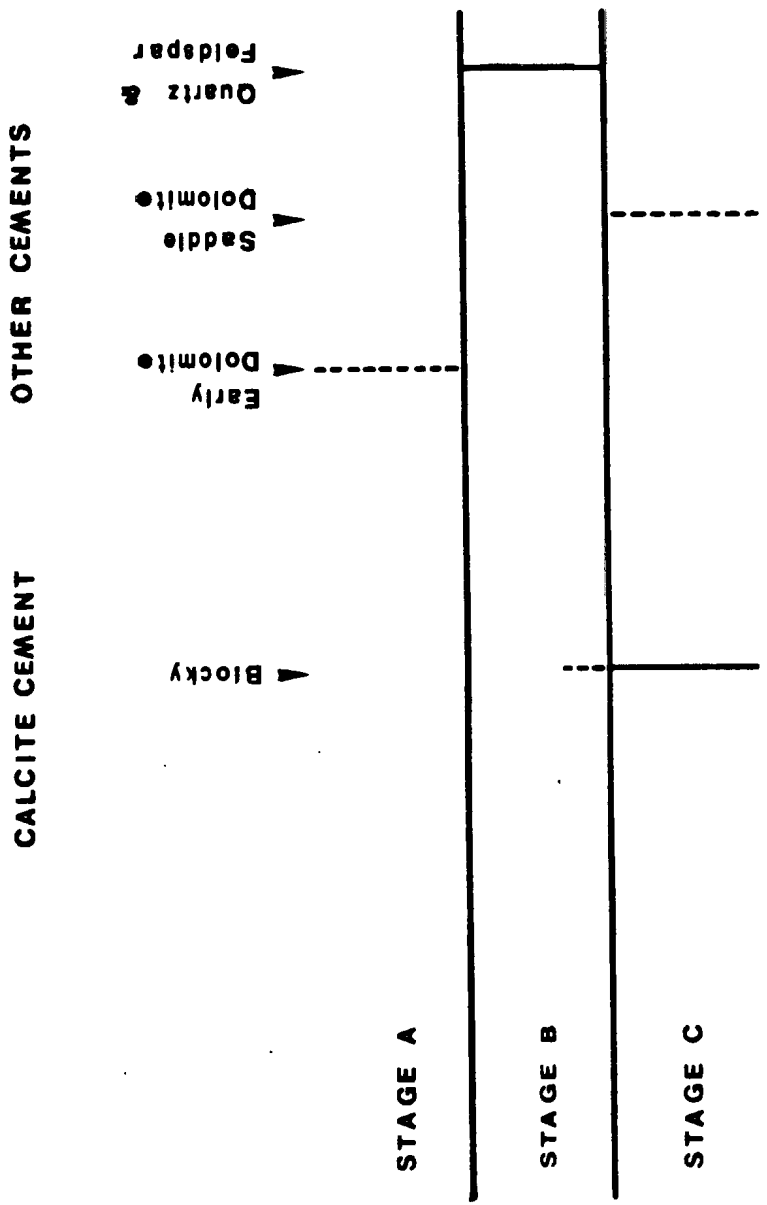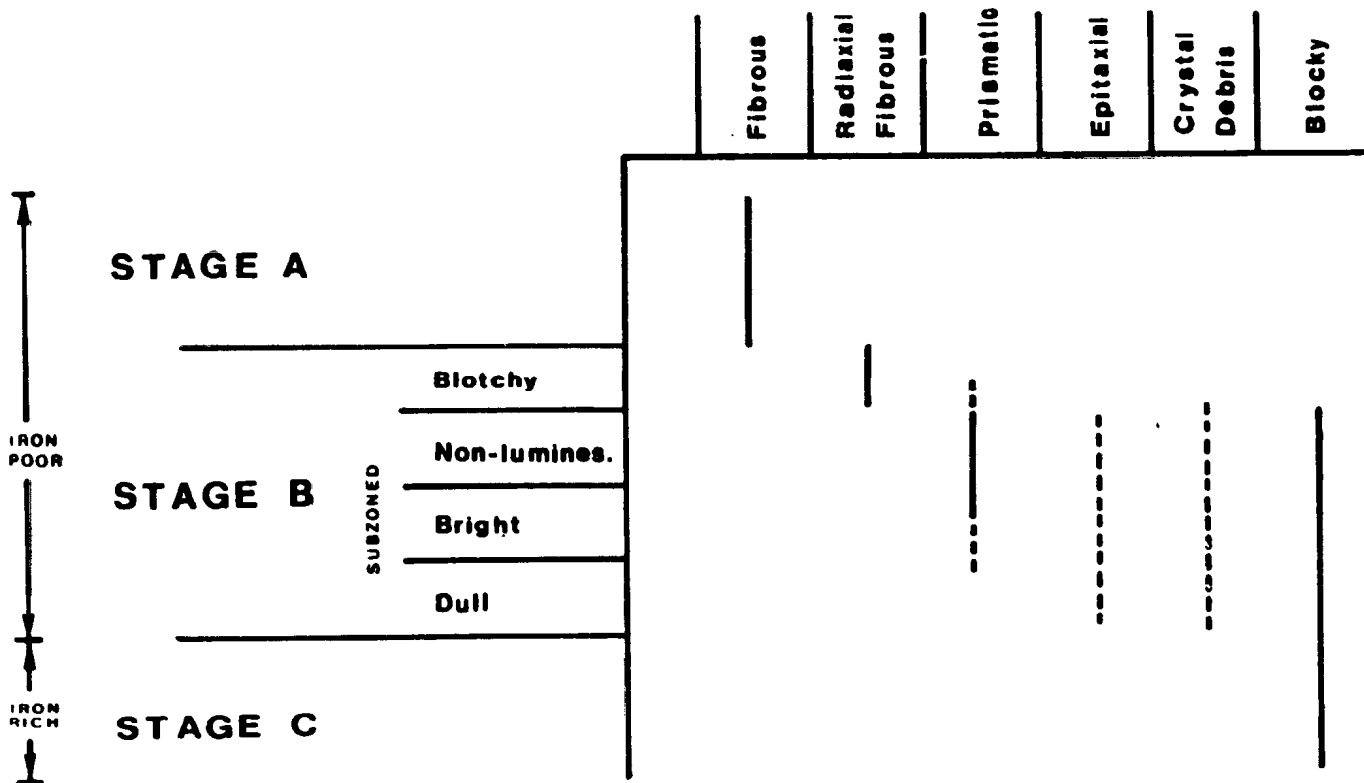
STAGE A

STAGE B

STAGE C

Figure 8.2- Schematic diagram illustrating the different stages and
growth habits of calcite cement in pre-karst limestones. Stages A
and B are iron-poor whereas calcite cement in stage C is iron-rich.
Stage B is further subdivided into four substages and includes an
early substage of inclusion-rich calcite cement followed by three
distinctive substages of inclusion-poor cement, each being
characterized by its luminescent pattern. Crystal debris was also
formed contemporaneously with other inclusion-poor calcite cements
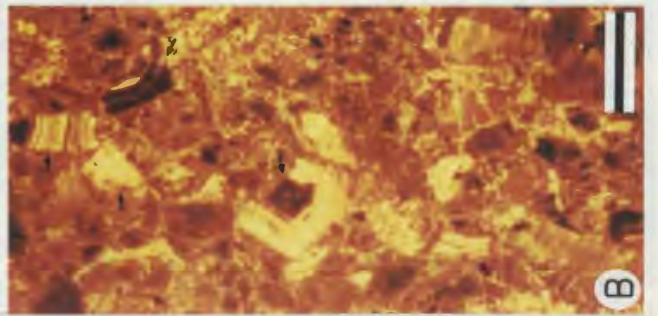(stage B).

PRE-KARST LIMESTONES

generally display a more complete cement sequence. Stage A is represented by isopachous layers of fibrous calcite filling some fenestrate pores. Stage B consists of two possible cement types or end-members depending on whether or not precipitation occurred in fissures and secondary solution pores or in primary pores. Radiaxial fibrous calcite is the most common cement in fissures and connected solution pores and occurs as isopachous linings. This cement is iron-poor but contains abundant microdolomite and has a blotchy luminescence (plate 8-7; A). It is also banded with up to three distinct zones of iron-poor, clear calcite that are brightly luminescent (plate 8-7; C). Geopetal, internal marine sediment predates and/or alternates with radiaxial fibrous calcite. In primary pores, calcite cements are commonly iron-poor and inclusion-poor and exhibit well-defined zones under cathodoluminescence which are from oldest to youngest: 1) a non-luminescent zone (black); 2) a bright zone (yellow) and 3) a dull zone (orange). These zones are, in turn, strongly zoned on a smaller scale (plate 8-7; A,D, and E). Cement habits (to be discussed later) range from prismatic to blocky (early, iron-poor phase). Crystal debris (silt to sand-sized) is common and abuts many luminescent subzones. This debris is clearly erosional in origin because well-developed luminescence subzones in larger debris are truncated at their margins (plate 8-7; B). It formed also contemporaneously with the iron-poor calcite cements as indicated by the presence of superimposed generations of crystal debris in a given pore, for instance debris with subzone 1 being found only in the lower part of the pore and that with subzones 2 and/or 3 being found at the top. Stage C, the final pore filling, consists of iron-rich, calcite (plate 8-7; D and E) and dolomite cements

PLATE 8-7

CATHODOLUMINESCENCE PETROGRAPHY

A. Thin-section photomicrograph of calcite cement filling a large secondary pore in fenestral mudstones (m). Calcite cement is of two types: 1) radiaxial fibrous calcite (r) with blotchy luminescence and 2) iron-poor, prismatic to bladed calcite (p) with three zones of luminescence (non-luminescent, luminescent, dull), all subzoned on a smaller scale. Note the absence of prismatic calcite, at the base of the pore, inhibited by concomitant internal sedimentation. Two generations of internal geopetal sediment are present and include: 1) marine carbonate mud (m) post-dating fibrous calcite but pre-dating prismatic calcite and 2) crystal debris (d), contemporaneous with prismatic calcite. Note the fining-upward nature of crystal debris with coarser debris at the bottom (detail in B). Scale bar is 1.5 mm.

B. Thin-section photomicrograph of crystal debris at the base of the pore. Note the luminescence subzones in larger debris truncated at their margins (arrow). Scale bar is 250 μm.

C. Thin-section photomicrograph of radiaxial fibrous calcite with two distinct bands of clear calcite with bright luminescence. Scale bar is 1.0 mm.

D. Thin-section photomicrograph of blocky calcite cement filling interparticle pores in pre-karst limestones (lithofacies 8: intraclast grainstone). Blocky calcite is of two types: 1) first phase of iron-poor calcite (1) with subzoned luminescence patterns and 2) second phase of iron-rich calcite (2) with dull luminescence. Note, on the pore wall, the limited number of nucleation sites in the first phase of cementation. Scale bar is 250 μm.

E. Thin-section photomicrograph of prismatic and blocky calcite cements filling interparticle pores in pre-karst limestones (lithofacies 8: intraclast grainstone). Calcite cements are: 1) iron-poor prismatic calcite with subzoned luminescence pattern and 2) iron-rich blocky calcite with dull luminescence. Note the large number of nucleation sites in prismatic calcite that were in early competition for the pore space during cemention. Scale bar is 250 μm.

F. Thin-section photomicrograph of epitaxial overgrowths on echinoderm grains (e) in post-karst limestones (lithofacies 12: skeletal-ooid grainstone). Epitaxial calcite (e) is iron-poor and exhibits subzoned luminescence patterns (1) and followed by iron-rich blocky calcite (2) with dull luminescence (2). Scale bar is 500 μm.

G. Thin-section photomicrograph (plane polarized light) of spar-filled bryozoan mold. Note the zooecia filled with lime mud. Scale bar is 250 μm.

H. Same area as (G), illustrating the subzoned luminescent nature of the bryozoan mold filled with iron-poor blocky calcite.
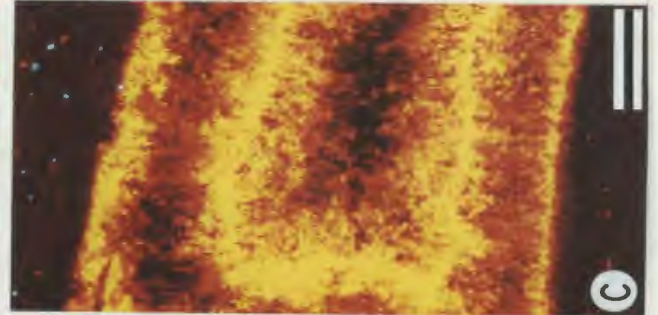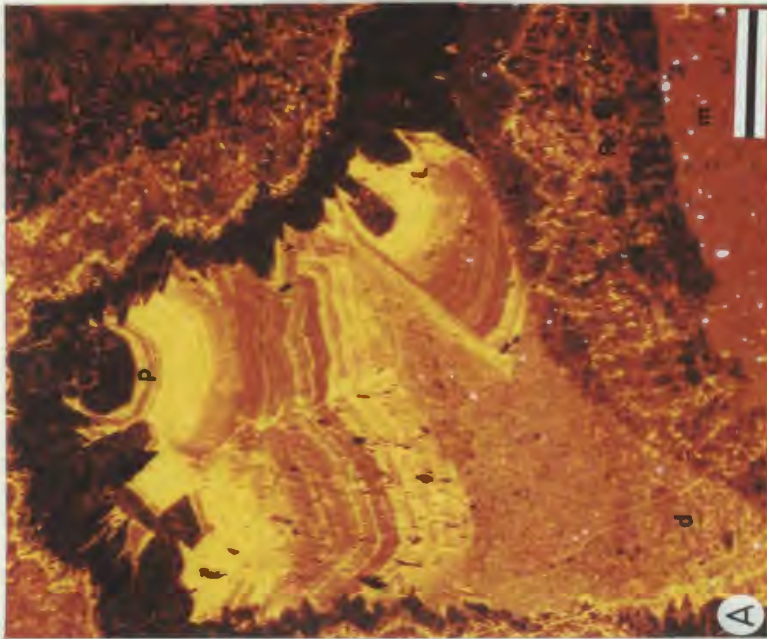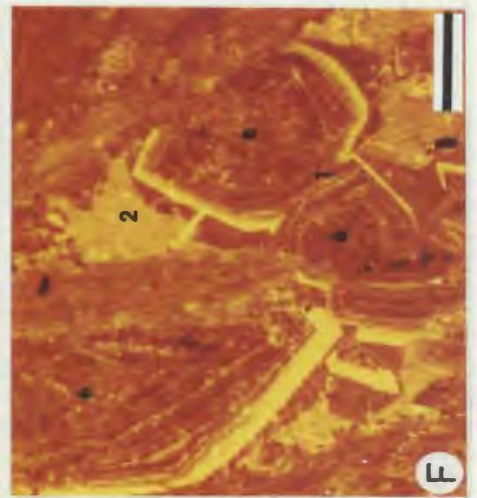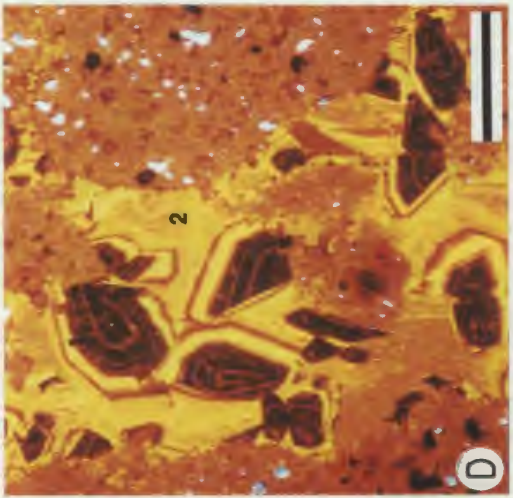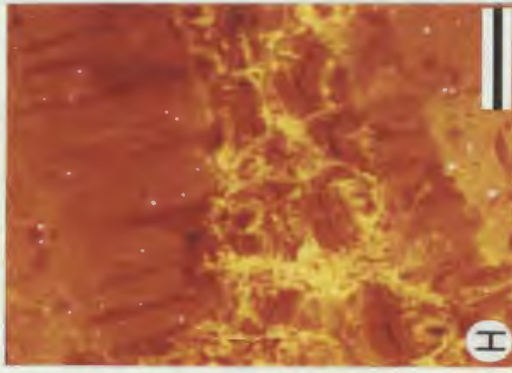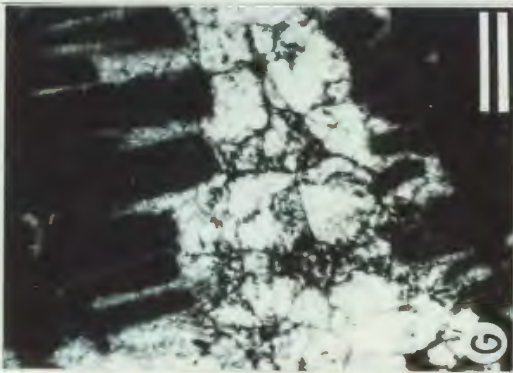
similar to those of the previously described siliciclastics. Baroque
(saddle) dolomite, however, is present only in large solution pores.
Stages A (0-5%) and C (10-30%) cements are volumetrically minor as
pore-fillings in comparison to those of stage B (70-90%).

The post-karst limestones (fig. 8-3), especially grainstones capping
calcarenite cycles, have a cement stratigraphy similar to that of the
pre-karst limestones but differences are also present. Stage A cements
are similar and occur in reef limestones (growth cavities, large
intraskeletal pores) and in beachrocks. The early phase of prismatic and
epitaxial calcite cement is sometimes inclusion-rich and has a blotchy
luminescence. Stage B cements are represented by co-existing prismatic
and epitaxial calcites. These cements are truncated by paleokarst
surfaces capping each calcarenite cycle. The three-fold luminescent
zonation is less pronounced but is still characterized by abundant
subzones (plate 8-7; F and G). Stage C cements are still iron-rich,
blocky calcite (plate 8-7; F) and baroque (saddle) dolomite. These
cements (mainly blocky calcite) are volumetrically important in areas
unaffected by the paleokarst surfaces.

DIAGENETIC EVOLUTION

Diagenesis of the Mingan Formation occurred in three general
environments: submarine, near-surface and deeper burial. The sequence of
diagenetic events is summarized in fig. 8-4.

Submarine diagenesis

The submarine environment here refers to the area at or slightly
below the sediment-sea water interface where diagenetic processes occur

Figure 8.3- Schematic diagram showing the different stages and growth
    habits of calcite cement in the post-karst limestones. Stages A and
    B are iron-poor whereas calcite cement in stage C is iron-rich.
    Stage B is further subdivided into three distinctive substages of
    inclusion-poor cement, each being characterized by its luminescent
    pattern.

POST-KARST LIMESTONES
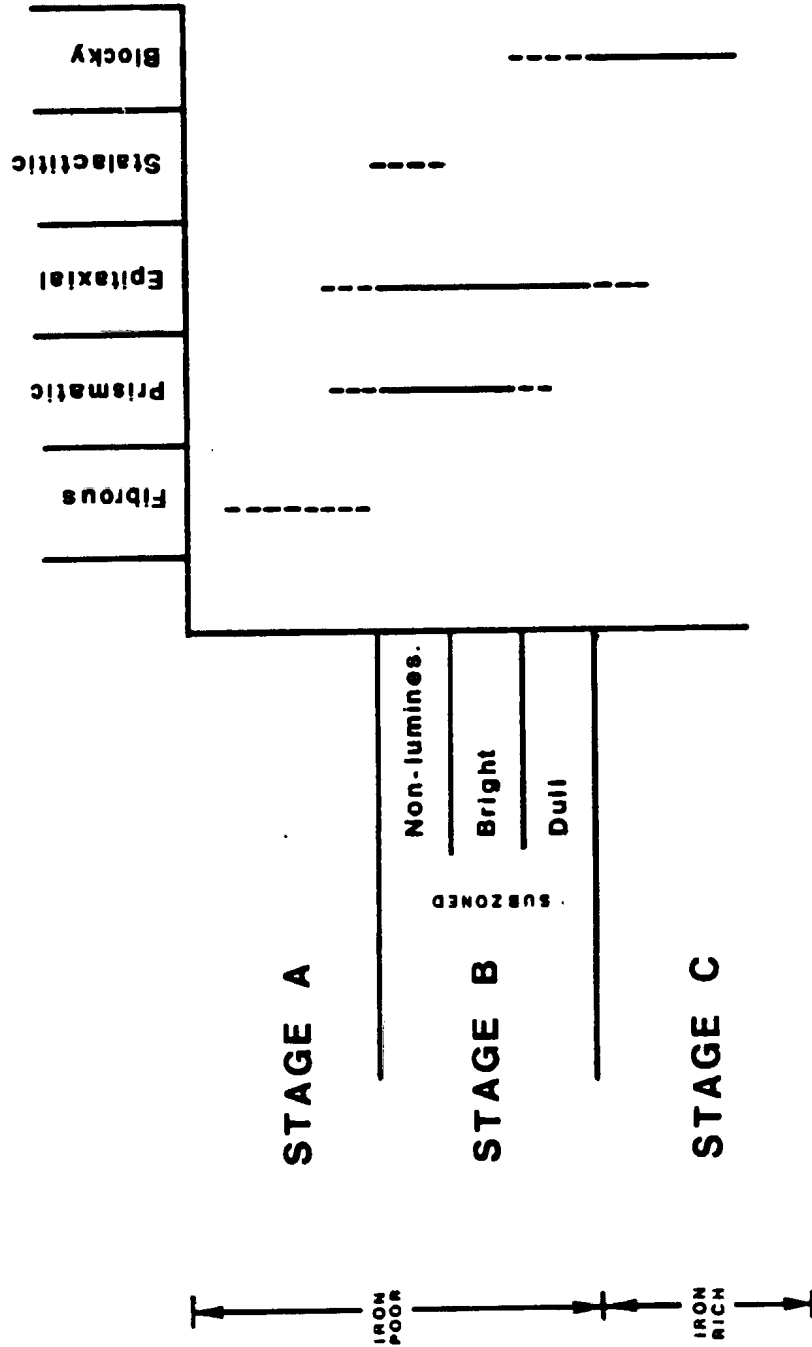
CALCITE CEMENTS

	Fibrous	Prismatic	Epitaxial	Stalactitic	Blocky

STAGE A — Non-lumines.

STAGE B — Bright / Dull — SUBZONED

STAGE C

IRON POOR ← → ← IRON RICH →

Figure 8.4- Paragenetic sequence of the diagenetic events that occurred after the final deposition of Mingan sediments which altered under progressive burial conditions. Legend:

1- Fibrous to bladed cement in reef limestones, beachrocks, and oolitic sands.

2- Micrite envelopes ubiquitous in distribution.

3- Supratidal dolomite in siliciclastic tidal flats.

4- Mineralogical stabilization of original aragonitic and calcitic components.

5- Fissuring in pre-karst limestones.

6- Marine internal sedimentation and cementation (radiaxial fibrous) in fissures and secondary pores in pre-karst limestones.

7- Shallow phreatic cementation (iron-poor cements) beneath pre-karst limestones or more locally beneath skeletal-ooid sands .

8- Erosion of phreatic cements and deposition of crystal debris.

9- Karst erosion associated with the intra-Mingan unconformity or contemporaneous with the sedimentation in calcarenite cycles.

10- Quartz and feldspar overgrowths in basal arkosic sandstones.

11- Matrix dolomite ubiquitous in distribution.

12- Deeper phreatic cement (iron-rich, blocky calcite) ubiquitous in distribution.

13- Saddle dolomite in larger primairy and secondary pores.

14 - Late stage fracturation.

15- Stylolites and solution seams ubiquitous in distribution.
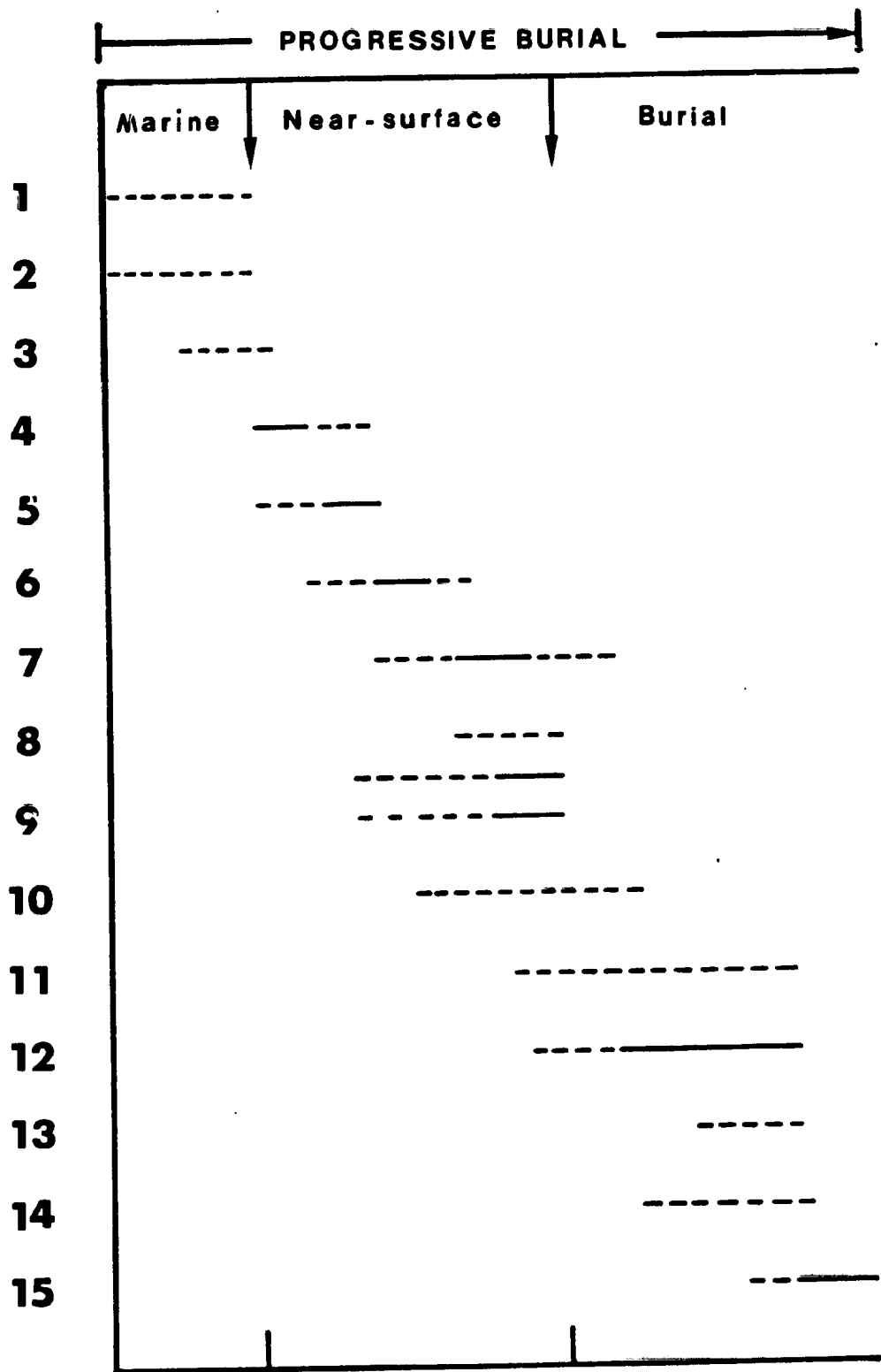
contemporaneously with sedimentation. The most common manifestations of submarine diagenesis are: 1) cements; 2) micrite envelopes and micritized particles and 3) supratidal dolomites. In the Mingan Formation, evidence of submarine cementation is limited to thin, isopachous fringes of both fibrous and prismatic (inclusion-rich) calcites. Both cements fill the primary pore systems of small reef mounds and sand shoals. Fibrous calcite cements with meniscus and gravitational fabrics also formed in beachrock. Distribution of these cements is similar to the occurrences of modern sea floor precipitates across shallow water platforms (James et al., 1976; Dravis, 1979; Moore, 1973, 1977). James and Choquette (1983) pointed out that the major prerequisites for early submarine cementation are an oxidizing environment, a stable substrate, and good water exchange. It is believed that synsedimentary, micritic cement was responsible for the early lithification on carbonate tidal flats and possibly of reefs. This can, however, only be inferred on the basis of indirect evidence and cannot be proven with any confidence.

Cementation also occurred during the micritization of carbonate grains, associated with the boring activities of algae and bacteria (Bathurst, 1966; Margolis and Rex, 1971; Alexandersson, 1972). In the Mingan Formation, micrite envelopes along with micritized grains are present in all calcarenitic lithofacies containing little micrite. Intense and prolonged micritization may have produced abundant peloids, however, these "diagenetic" grains are hardly distinguishable from other cryptocrystalline grains (fecal pellets, micritic intraclasts, cement aggregates).

Dolomite formed diagenetically on siliciclastic tidal flats by

- 392 -

seepage of Mg-rich surficial brines into the underlying supratidal and intertidal sediments (i.e. silty dololaminites). Finely crystalline dolomites replaced supratidal sediments inferred to be mainly peloidal limestones at the time of deposition. In contrast, the underlying intertidal sediments, composed of arkosic sands, were cemented by coarse dolomite rhombs. A similar example of subsurface primary (non-replacement) dolomitization in brines occurs today beneath a porous quartz sand sabka in the Persian Gulf (Shinn, 1973; DeGroot, 1973).

Near-surface diagenesis

This diagenetic environment is characterized by a variety of shallow processes. Fluids involved in the near-surface diagenesis were mostly meteoric water but marine waters appear to have recirculated through the primary and secondary pore system. Several lines of evidence support the interpretation that this diagenetic phase mainly occurred in a meteoric regime: 1) presence of subaerial exposure surfaces with either a regional (paleokarst unconformity) or a more local extent (calcarenite cycles); 2) selective biomoldic porosity; 3) truncation of submarine calcite cement (i.e. fibrous) along solution-enlarged pores; 4) rare microstalactitic calcite cements and 5) pervasive, spar calcite cements that are generally iron-poor, clear, and zoned under cathodoluminescence. Two distinct suites of diagenetic features, formed under near-surface conditions, are separated by the intra-Mingan paleokarst unconformity and now discussed separately.

In the pre-karst limestones, a general sequence of diagenetic events can be determined on the basis of cross-cutting relationships observed

in thin-section. This sequence includes: 1) neomorphism and both fabric and non-fabric selective dissolution; 2) fissuring; 3) precipitation of marine and meteoric calcite cement and 4) final karst erosion. During initial subaerial exposure, all particles composed of Mg calcite and aragonite are unstable in magnesium-deficient meteoric waters, and altered to calcite. This mineralogical transformation is well documented from Holocene and Pleistocene carbonate sequences (Friedman, 1964; Land, 1967; Matthews, 1974). First, dissolution of Mg calcite and precipitation of calcite occurred on a microscale, original crystal fabrics being preserved when observed under the light microscope (Oti and Muller, in press). This is followed shortly after by the inversion of aragonite to calcite. In general, the original crystal fabrics are completely destroyed, leaving a hole.

Aragonite alteration on a macroscale in the pre-karst limestones was important in the formation of moldic porosity which was mainly derived from the selective dissolution of mollusk shells. On the other hand, components with well-preserved fabrics (fossil, ooid, fibrous calcite cement) are now composed of iron-poor calcite, this suggests that they were either calcite originally or were altered to iron-poor calcite from some metastable precursor. In the latter case, alteration must have occurred in a near-surface environment where meteoric waters (usually vadose) are better oxygenated, and thus iron is not incorporated into the neomorphic calcite. Furthermore, the metastable precursor, if Mg-calcite, altered first before aragonite dissolution was finished (see discussion above). Non-fabric selective dissolution also occurred beneath the exposed surface, especially in mud-supported lithofacies and resulted in the enlargement of both primary (shelter, fenestral) and

co-existing secondary (moldic) pores. Little cementation appears to have
been formed during this phase of aragonite cementation. There are
several ways to explain the apparent absence of cementation: 1) not
enough $CaCO_3$ was available for cementation from the dissolution of
aragonite skeletons; 2) time was insufficient to have precipitation
which operates at a much more slower rate than the rate of Mg-calcite or
aragonite dissolution (Schmalz, 1967) and 3) carbonates were dissolved
and held in solution because fluids were always undersaturated with
respect to calcite. At about the same time, fissures and irregular
cracks, connected with the surface, formed in early lithified peritidal
deposits. These fissures may have increased the circulation of meteoric
waters into the subsurface as well as the extent of non-fabric selective
dissolution.

Cementation of the primary and secondary pore systems was influenced
by fluids ranging from marine to meteoric in origin. With renewed
submergence over the exposed surface, marine waters began to recirculate
through the pore system (corresponding to stage 2 in fig. 6-4). Calcite
cement with radiaxial fibrous fabrics, if primary, precipitated in
fissures and connected porous horizons where marine waters were
actively circulating. Internal marine sedimentation preceded or was
coincident with this cementation. The shoreline position, however,
varied with time and pore fluids periodically changed to a more meteoric
composition. This resulted in a banded fibrous cement with alternating
inclusion-rich and inclusion-free zones, the latter being iron-poor and
brightly luminescent and suggesting precipitation from near-surface
oxygenated waters. A permanent meteoric regime finally developed with a
further fall in sea level (corresponding to stage 3 in fig. 6-4).

Different calcite cement (mainly prismatic and blocky) formed in a
phreatic setting and was pervasive, filling most of the primary and
remaining secondary pores. These cements are iron-poor, clear, and
compositionally zoned with respect to Mn^2 and/or Fe^2 under
cathodoluminescence. Strongly zoned cements such as these probably
formed under continually fluctuating chemical conditions which are most
typical of meteoric waters (Harris et al, 1985; Walls and Burrowes,
1985). Silt to sand-sized debris from these cements forms common,
geopetal accumulations, indicating that water circulation was important
and physically eroded newly forming cements. Vadose cements with
meniscus and/or gravitational fabrics are absent. A source of $CaCO_3$
other than the already consumed aragonite to calcite is required for the
formation of this phreatic cement. This "external source" was most
likely dissolution and weathering of the subaerially exposed carbonates.
If calcite precipitation was prevented by inhibiting factors (e.g.
kinetics of crystal growth, flux of CO_2), groundwaters would easily have
become progressively oversaturated, a situation frequently observed
today in natural groundwaters (James and Choquette, 1984).
Oversaturation, combined with good circulation, in the groundwaters
probably reached a stage where calcite cements precipitated on a large
scale as the inhibiting factors were exceeded. Calcite cementation was
pervasive and finally reached a stage where the porosity and
permeability were significantly reduced, at a time when the limestones
were still subaerially exposed. The final episode of near-surface
diagenesis was probably one of surface weathering and karstification
rather than calcite precipitation. The absence of vadose cements may be
explained by this final, erosional episode which remodelled the upper

part of the exposed sequence.

The siliciclastics beneath the pre-karst limestones were apparently unaffected by near-surface processes. The shaly unit capping the siliciclastic unit probably acted as a impermeable layer or "seal" that inhibited downward movement of meteoric waters. Little calcite cement was precipitated even in the porous, coarser-grained sandstones. Small lenses of fossilifereous limestones in these sandstones are devoid of near-surface cements characterized by strong luminescent zoning. Instead they are characterized by a pervasive overpacking of grains (mainly pelmatozoans) which resulted from grain-to-grain pressure solution before the pores of the rock were filled by cement. Quartz and feldspar overgrowths in the coarse-grained sandstones are the only evidence of cementation prior to any significant burial. Their strong substrate selectivity argues for precipitation from mildly oversaturated waters. .

In the post-karst limestones, near-surface diagenesis affected most strongly the sediments directly beneath paleokarst surfaces associated with calcarenite cycles. Calcite cements here are mainly phreatic and petrographically similar to those in the pre-karst limestones. Sand shoal areas were progressively exposed and acted as local catchment surfaces for meteoric waters. Dissolution was fabric-selective as evidenced by molds of ooids and skeletal components, mainly mollusks and some bryozoans. The early non-luminescent phase of calcite cement (usually prismatic) is rarely seen in these molds. In some cases, internal sediments (crystal silt) partially filled biomoldic molds prior to filling by later phreatic calcite cements. This suggests that dissolution of the metastable precursor (aragonite ?) was coincident with or did not occur before the earliest phase of precipitation.

Furthermore, early calcite cements around the oomoldic pores are
sometimes disturbed by earliest post-depositional deformation and argue
against the formation of oomoldic porosity under deep burial conditions.
Vadose calcite cements are rare and found only in the upper part (30 cm)
of a few calcarenite cycles. As time proceeded, surface karstification
caused erosion and peneplanation over the subaerially exposed sand
shoals as evidenced by phreatic calcite cements truncated along
extensive planar surfaces capping each calcarenite cycle. Chemical
weathering and erosion at the surfaces of these sand shoals were
probably responsible for the limited occurrence of vadose precipitates
which most likely occurred in thin zones beneath the newly exposed
carbonate sediments at one point. The diagenetic environments in the
post-karst limestones are repeated through time, like the depositional
environments. Diagenetic patterns in the calcarenite cycles are similar,
to some extent, to those described recently by Heckel (1983) for
carbonate rocks in Pennsylvanian eustatic cycles of Kansas. Each Kansas
cycle (about 5 m thick) is capped by a nearshore shale unit and consists
of a lower transgressive and an upper regressive carbonate unit which
are separated by an offshore shale unit. Two distinct diagenetic trends
may be recognized in both Mingan and Kansas cycles: A) dissolution,
neomorphism, and cementation by meteoric water occurred before much
compaction took place and B) sediments that were more deeply buried and
compacted before cementation took place. Diagenetic features in trend A
developed with emergence that terminated in deposition of either a
Mingan or Kansas cycle. Sediments characterized by trend B escaped the
"aggressive" effects of meteoric diagenesis either because meteoric
water did not penetrate the offshore shale to affect the underlying

transgressive carbonates of the Kansas cycles or more simply because sediments were never subaerially exposed (Mingan cycles). The diagenetic patterns in both Mingan and Kansas cycles are, however, different and appear to be related to their own depositional history. For instance, diagenetic patterns in the Mingan cycles consists of lens-shaped units of diagenetic trend A (sand-shoal facies) within units of trend B (inter-shoal facies). In contrast, diagenetic patterns in the Kansas cycles are composed of laterally persistent units of alternating trends (i.e. A-B-A-B-A).

Deeper burial diagenesis

This diagenetic environment occurs beneath the phreatic aquifer and is unaffected by near-surface processes as carbonate sediments undergo progressive burial. This also corresponds to the deep crustal environment of Bathurst (1980) or mesogenetic environment of Choquette and Pray (1970). The transition from the near-surface environment, however, is generally gradual and difficult to identify. In the Mingan sequence, the important changes (only in carbonates) which occur during this phase include: last stage cementation, mechanical compaction and chemical compaction.

Calcite cements, precipitated during this phase, are generally iron-rich, blocky, and have more uniform, luminescent patterns (usually dull). A burial environment is suggested for these cements because they are the last pore-filling cement and occur both vertically and laterally throughout the sequence. They also fill fractures which truncate near-surface as well submarine calcite cements. Calcite cementation was closely accompanied by less common, baroque dolomite which is also iron-rich. Similar conclusions about the late diagenetic origin of

baroque dolomite have been reached by other workers (Choquette, 1971; Folk and Assereto, 1974; Radke and Mathis, 1980). Radke and Mathis (1980) suggested that the temperature of formation of baroque or saddle dolomite is high, within the range of 60 and 150 degrees Centigrade.

Mechanical compaction is minor and consists mainly of brittle grain deformation in coarser-grained calcarenites only where grains are fragile and/or where little early diagenetic cement has formed to weld these grain together. In mud-supported lithofacies, grain breakage is even less common but cannot be used to evaluate the importance of mechanical compaction. Experimental work has shown that modern carbonate muds and mud-supported carbonate sands can be rapidly compacted from original porosities of 70% to values of 30-40% with only minor breakage of the sedimentary particles (Shinn and Robbin, 1983).

Chemical compaction by pressure solution is widespread and includes: sutured grain contacts, solution seams, and stylolites. Sutured grain contacts are rare in the Mingan limestones with only a few exceptions as discussed earlier. One explanation for this may be that the sediments became lithified early, before much burial, in the saturated meteoric phreatic environment.

Solution seams are generally formed in fine-grained limestones which commonly exhibit lumpy or nodular bedding typical of many carbonate sequences (Garrison and Kennedy, 1977; Wanless 1979). In contrast, calcarenitic limestones are characterized by well-defined stylolites. These variations may be related to the original content of argillaceous material. Clay minerals encourage the effects of pressure solution by facilitating the diffusion of dissolved material away from points of stress (Weyl, 1959; Oldershaw and Scoffin, 1967).

Solution seams and stylolites cut all preexisting fabrics with the exception of some fractures filled by iron-rich calcite cement. This suggests that iron-rich calcite cementation and fracturing generally occurred before or was coincident with pressure solution. It is well established that pressure solution is an important source of $CaCO_3$ for deeper burial cements (Wong and Oldershaw, 1981). Stylolites may also provide a source for subsurface dolomitizing fluids (Wanless, 1979). This could explain the common occurrence of euhedral dolomite rhombs within and adjacent to stylolites in the mud matrix of some limestones.

The amount of overburden needed to produce significant pressure solution as shown by the Mingan limestones is poorly understood. Dunnington (1967) however, suggested that pressure solution became effective at depths of 600 to 900 m. On the other hand, the colour alteration index (CAI=1) of the Mingan conodonts shows that the amount of overburden was less than ca. 1200 m in the study area (Nowlan and Barnes, in press). So, burial depth may be bracketed between 600 and 1200 m.

DISCUSSION

Original mineralogy of grains and cements

There is a general consensus about diagenetic processes affecting a polyphase assemblage of carbonate minerals, like those found in modern carbonates, under meteoric conditions (Bathurst, 1975; James and Choquette, 1984): 1) no obvious textural change occurs when Mg calcite components change to calcite under light petrographic examination; 2) alteration of aragonite components change to calcite via either microscale or macroscale dissolution-precipitation mechanisms; 3) microscale aragonite alteration occurs when calcite precipitates

immediately after dissolution and original component structures are cross-cut by the boundaries of large calcite crystals and 4) macroscale aragonite alteration occurs when calcite precipitates at a later stage than dissolution, the resulting void being filled only later. From the preceding discussion, it is suggested that the Mingan components retaining their original fabric were calcitic, those particles which are now only spar-filled molds were aragonitic and those particles with relic microstructures truncated by coarse neomorphic spar were also aragonitic.

Components with well-preserved microfabrics (group 1) are of three types: 1) fossil skeletons (ostracods, trilobites, brachiopods, echinoderms, bryozoans and tabulate coral Eofletcheria); 2) ooids with radial cortex and 3) fibrous cements (radial, radiaxial) with abundant microdolomite inclusions. There is no direct evidence from this study whether these components were calcite or Mg calcite. The presence of microdolomite inclusions in some components (echinoderms and fibrous calcite), however, argues in favour of original Mg calcite (Lohmann and Meyers, 1977) .

Components with spar-filled molds (group 2) include mollusks, bryozoans and ooids associated with calcarenite cycles. These components, originally aragonite, have been dissolved and the molds eventually filled with calcite cement.

Components with relic microfabrics (group 3) are bryozoans, solenoporacean algae, and the tabulate coral Billingsaria. These components consist of a rather coarse calcite mosaic, similar to that observed in "calcitized" aragonite skeletons, in which the crystal boundaries truncate the relics of the original skeleton structure.

- 402 -

These observations are consistent with those made on similar components throughout the geological record. There are, however, fossil skeletons such as tabulate corals and bryozoans which may exhibit more than one style of fabric retention. The conclusions reached by this study are important because there is no consensus concerning the original mineralogy of these Paleozoic fossil skeletons. First, fabric retentions in the Mingan tabulate corals are of three styles: 1) those with preserved microstructure (Eofletcheria); 2) possibly those with spar-filled molds (Tetradium?) and 3) those with "calcitized" skeletons (Billingsaria). Second, these three different styles of fabric retention are also present in the Mingan bryozoans, each style, however, being selectively developed within the same bryozoan skeleton. From these petrographic evidence, it is suggested that the Middle Ordovician bryozoans and tabulate corals were in part calcitic and in part aragonitic. Furthermore, the suggestion that the Middle Ordovician bryozoans had a "mixed" original mineralogy is also supported by observations on the mineralogy of modern bryozoans which are mainly Mg calcite but some are aragonitic (Milliman, 1974). It is not clear whether the mineralogy of these Middle Ordovician fossil skeletons was controlled by intrinsic (ontogenic, phylogenic) or extrinsic (environmental) factors; further combined petrographic and taxonomic studies are need.

On the basis of these observations, it is evident that the full spectrum of carbonate minerals (aragonite, Mg calcite, calcite) in Middle Ordovician time was present both as organism skeletons or as direct marine precipitates (ooids, fibrous cement). Recent studies have shown that temporal changes in non-skeletal carbonate mineralogy

occurred throughout the Phanerozoic (Wilkinson, 1982; Sandberg, 1983). For instance, these studies suggested that the most important sea floor precipitates during the Ordovician were calcitic. It is also evident from this study that Ordovician seas could have, at least locally, precipitated aragonitic components (ooids); calcitic components being still predominant in volume.

Formation of geopetal crystal debris

It has been long recognized that calcitic internal sediment of silt grade, like that present in the Mingan limestones, is not ordinary geopetal sediment of micrite, biomicrite, or biopelsparite and is ubiquitous in carbonate rocks of all ages (Bathurst, 1975). Dunham (1969) concluded that this type of internal sediment ("vadose silts") must have been deposited in the vadose zone from percolating meteoric water. Their origin, however, is more equivocal but Dunham (1969) suggested that the crystal silts derived from the primary sediment by a combination of winnowing and selective dissolution processes.

The petrographic observations of geopetal crystal debris in the Mingan limestones may be summarized by the following characteristics: 1) mechanically deposited debris found in both primary and secondary vugs, indicating clearly a post-depositional origin; 2) more common in fenestral mudstones and fissures beneath the intra-Mingan paleokarst; 3) debris ranges from silt- to sand-sized crystals, larger particles being found only in larger pores and 4) cathodoluminescence confirms that the larger silt- and sand-sized particles are angular crystal debris derived from the erosion of iron-poor calcite cements (subzoned luminescence patterns) precipitated under phreatic, meteoric conditions.

- 404 -

On the basis of this petrographic evidence, it is suggested that most, if not all, crystal debris in the Mingan limestones formed by internal erosion of calcite cement as meteoric water percolated through the pore system. The sand-sized crystal debris was mechanically trapped in larger pores whereas the infiltration of smaller debris was more pervasive and as result itsr distribution was ubiquitous. These findings are quite important since crystal silts are commonly regarded as an indication of meteoric vadose environment and of subaerial exposure of the sediment (Dunham, 1969). Dunham (1969) assumed that only meteoric water in the vadose zone could be fast enough to carry crystal silt. On the other hand, it is also important to point out that the formation of crystal debris in the Mingan limestones was contemporaneous with the precipitation of phreatic cements as indicated by different superimposed generations of crystal debris with luminescence zoning similar to that present in the phreatic calcite cements. From the preceding discussion, it is suggested that crystal debris may also have formed under phreatic conditions if velocities of meteoric water circulating through the pore system were fast enough and/or carbonate rocks were porous enough.

SUMMARY

1) Diagenetic evolution of the Mingan limestones was the result of three distinct phases of diagenesis: marine, near-surface and deeper burial. The most single important phase affecting these rocks was near-surface diagenesis, especially in limestones beneath the intra-Mingan paleokarst or beneath paleokarst surfaces in calcarenite cycles. Major diagenetic processes during this phase included

dissolution and neomorphism of metastable carbonate components followed by an important stage of meteoric calcite (iron-poor) cementation.

2) On the basis of good petrographic evidence, components of the Mingan limestones were originally composed of a polymineralic carbonate assemblage including aragonite, Mg calcite, and calcite.

3) Middle Ordovician sea floor precipitates were mainly calcitic but aragonitic precipitates were also formed as indicated by the ooid cortex in Mingan calcarenite cycles which are now filled with calcite cement

4) Some important conclusions reached by this study about limestone diagenesis in general are the following:

      a) Paleozoic tabulate corals and bryozoans were both aragonitic and calcitic.

      b) vadose cementation may be absent in spite of evidence for subaerial exposure. The absence of vadose cement may be explained if the final episode of subaerial exposure which was one of weathering and karstification which eroded the upper part of exposed sequences. It is also possible that the vadose cementation, especially in calcarenite cycles, occurred in thin zones beneath newly exposed carbonate sediments, and as result vadose cements might be impossible to recognize.

      c) Crystal debris, similar to Dunham's vadose silts, may also form under phreatic conditions if velocities reached by meteoric water are sufficient. Crystal debris in the Mingan limestones resulted from the internal erosion of phreatic cements

d) Growth habits in calcite cements may be influenced by the
local variations of meteoric water circulating through the pore system.
On the basis of similar luminescent attributes, iron-poor prismatic and
blocky (only its early phase) calcite cements in the Mingan limestones
were contemporaneously precipitated in different but adjacent pore
spaces. A two end-member model may be envisaged where only scattered
calcite rhombs precipitated in areas receiving little flow of meteoric
water. In contrast, areas with higher meteoric water flow developed
rapidly an isopachous rind of calcite crystals around the pore spaces.

CHAPTER 9

SUMMARY AND CONCLUSIONS

The Mingan Islands, located along the Quebec North Shore of the Gulf
of St. Lawrence, display superb coastal exposures of Lower and Middle
Ordovician carbonates. These carbonates comprise dolostones of the
Romaine Formation and overlying limestones of the Mingan Formation.
Siliciclastics are found only at the base of both formations.

STRATIGRAPHY

1) The late Canadian to earliest Whiterockian Romaine Formation can
be subdivided into three formal members: 1) Sauvage Member, represented
by basal transgressive sandstones; 2) Sainte-Genevieve Member,
represented by subtidal carbonates (sucrosic dolostones) and 3) Grande
Ile Member, represented by cyclic peritidal carbonates (mainly finely
crystalline dolostones).

2) The Chazyan Mingan Formation can be subdivided into four formal
members: 1) Corbeau Member, represented by peritidal siliciclastics; 2)
Perroquet Member, represented by subtidal limestones beneath the
intra-Mingan paleokarst unconformity; 3) Fantome Member, represented by
peritidal limestones and 4) Grande Pointe Member, represented by
subtidal limestones overlying the Intra-Mingan paleokarst unconformity.

DEPOSITIONAL HISTORY

The depositional history of Ordovician strata in the Mingan Islands

can be separated into five distinct periods: 1) deposition of the
Romaine Formation; 2) development of the post-Romaine unconformity; 3)
deposition of the lower Mingan Formation; 4) development of the
intra-Mingan unconformity, and 5) deposition of the upper Mingan
Formation.

1) Deposition of the Romaine Formation took place on a segment
(called here the "St. Lawrence platform") of the Ordovician epeiric
shelf which rimmed North America, as the platform was undergoing slow
subsidence, and possibly during a time of global sea level rise. Eight
discrete lithofacies can be recognized and grouped into three
assemblages: a) basal transgressive sandstones overlying the Precambrian
basement, b) a middle assemblage of subtidal carbonates and c) an upper
assemblage of cyclic peritidal carbonates. A "classic" shallowing-upward
sequence, defined by these lithofacies assemblages, is displayed by the
Romaine Formation. Carbonate lithofacies represent sediments deposited
in sabkha-like tidal flats (dololaminites, laminated shales,
ripple-laminated sandstones, stromatolites), lagoons (burrowed
dolomicrite), patch reef complexes (thrombolite mounds), and deeper
shelf settings (burrow-mottled dolostones).

Carbonate lithofacies assemblages in the Romaine Formation can be
correlated over 500 km across the St. Lawrence platform with similar
contemporaneous units in western Newfoundland. Sedimentation styles on
the platform changed through time from subtidal to peritidal. Unlike
island-tidal flats in western Newfoundland, peritidal sedimentation
occurred on a broad tidal flat resulting in the deposition of laterally
continuous lithofacies, over 20 km.

Romaine sediments were pervasively dolomitized before the development of the post-Romaine unconformity was complete. Dolomitization was of two types: a) penecontemporaneous with deposition in sabkha-like environments resulting in finely-crystalline dolostones and b) in shallow mixing zones resulting in sucrosic dolostones.

2) The Whiterockian post-Romaine unconformity formed on exposed Romaine dolostones as the passive platform margin became convergent during the incipient Taconic orogeny and possibly during a time of global sea level lowering. A migrating peripheral bulge caused tilting of the platform and differential weathering of the exposed dolostones which eventually resulted in the formation of an extensive karst plain, covered by a blanket of residual eolian sand.

3) With progressive collapse of the shelf margin, marine transgression was diachronous across the platform, beginning during Chazyan time in the Mingan Islands. Three lithofacies assemblages can be recognized in the lower Mingan Formation: a) peritidal siliciclastics overlying the post-Romaine unconformity, b) subtidal limestones occurring only in the eastern Mingan Islands and c) an upper assemblage of peritidal limestones.

With Chazyan transgression, the sediment blanket overlying the post-Romaine paleokarst was reworked and the karst plain was locally exposed on the sea floor. These exposed dolomites were bored by marine endolithic organisms (Trypanites), and eventually covered with resedimented sands near the strandline. A siliciclastic tidal flat system, including algal marshes, intertidal mud and sand flats and tidal

channels, subsequently migrated over strandline sands.

Sedimentation changed abruptly from siliciclastic to carbonate with the deposition of peritidal and subtidal limestones. Bahamas-style tidal flats prograded eastward over adjacent lagoonal and open shelf sediments.

4) The Chazyan intra-Mingan unconformity formed on exposed peritidal limestones, possibly due to local tectonic movements. Weathering and karstification caused fissuring of the early lithified limestone and eventually developed a karst topography with substantial relief.

5) The deposition of upper Mingan limestones occurred with subsequent reinundation of the intra-Mingan unconformity. It resulted in an irregular coastline or series of islands which developed beachrock or rocky shorelines with intertidal notches. Subtidal sedimentation was locally controlled by karst erosion topography with sand shoals forming tidal deltas, 1-1' km wide, in the large depressions.

Three distinct calcarenite cycles can be recognized in these sand shoal deposits. Sand shoal sediments were periodically exposed due to minor sea level fluctuations. The amount of sea level fall, however, is clearly minor because inter-shoal areas, located in relatively deeper waters, were not affected by subaerial exposure. These inter-shoal areas became sites of more restricted deposition caused by poor water circulation behind exposed sand shoals.

MINGAN REEF LIMESTONES

1) Reef limestones are of three types: a) biostromes representing in

situ accumulations of potential reef building organisms, b) small bioherms representing isolated reefs that grew under quiet conditions and c) bioherm complexes representing patch reefs that grew under more turbulent conditions. Mingan reefs formed as small biogenic structures scattered on the outer part of an open shelf or ramp.

2) Major reef organisms are lithistid sponges, bryozoans, tabulate corals and solenoporacean algae. Various biotic assemblages, either dominated by a single taxon or with several taxa, can be recognized and include: a) sponge-bryozoan-coral assemblages in both biostromes and bioherm complexes, b) corals in bioherms, c) bryozoans in bioherms and d) solenoporacean algae-coral assemblages in bioherm complexes. These organisms, characterized by delicate branching and encrusting forms, performed as bafflers and binders rather than frame builders during reef growth.

3) Two stages of reef growth can be discerned in the reef cores of some Mingan bioherms; the first stage is a bafflestone unit forming the bulk of reef core and the second stage is a bindstone unit capping the reef core.

4) Synsedimentary marine sedimentation was insignificant and limited to thin, isopachous rinds of fibrous calcite in the growth cavities of some bioherms. More important in stabilizing these bioherns was the presence of cyanophyte mats and crusts which are now characterized by a relic vermiform fabric.

5) Mingan bioherms conform to the "basic pattern" observed in Early Paleozoic bioherms, being mound-shaped structures composed of abundant skeletons and rich in lime mud. In fact, they differ only in the primary biotic builders

6) Reef builders in the Mingan bioherms are in part inherited from older bioherms and in part newly evolved taxa supporting the view that a gradual change in the style of bioherms occurred throughout Early and Middle Ordovician time.

7) Stromatoporoids, an important builder in contemporaneous bioherms of the Chazy area in New York, are conspicuously absent in the Mingan bioherms.

PALEOKARST

Three different types of paleokarst surfaces can be recognized in the Mingan sequence: 1) an extensive karst plain developed on top of the dolostones of the Romaine Formation; 2) an irregular karst within limestones of the Mingan Formation and 3) local paleokarst surfaces associated with calcarenite cycles.

1) Dolines or sinkholes, up to 30 m in diameter, can be locally found as the first-order relief on the post-Romaine paleokarst. On a smaller scale, rundkarren and kamenitzas formed beneath a sediment blanket overlying exposed Romaine dolostones. .rmation of the post-Romaine paleokarst can be envisaged to have taken place in four stages: a) subaerial exposure of the Romaine dolostones, b) tectonic tilting and development of an irregular topography during the initial phase of subaerial exposure, c) progressive bevelling of the Romaine dolostones and formation of a karst plain and,d) reworking and redeposition of strandline sands of the sediment blanket overlying the post-Romaine paleokarst as sea level rose again.

2) On a regional scale, the intra-Mingan paleokarst formed irregular topographic features or landforms, The paleokarst in the eastern Mingan

Islands was characterized by two regional depressions, 6-10 km wide whereas the same surface in the western part was more irregular with closely-space depressions, usually less than 2-3 km apart. On a smaller scale, the paleokarst developed landforms such as ridges, pinnacles and depressions with up to 20 m of relief. Small sharp-crested karren developed on bare substrates and were superimposed on the larger scale features. With subsequent reinundation, the intra-Mingan paleokarst was locally sculpted by intertidal notches forming along rocky shorelines.

3) In contrast to the paleokarst unconformities, paleokarst surfaces, associated with calcarenite cycles, developed contemporaneously with sedimentation and only on sand shoal deposits in response to minor fluctuations in sea level. Various sharp-crested karren, including trittkarren, formed on the exposed sand shoals. The profile of these features, however, changed through time, eventually evolving into extensive peneplaned surfaces.

LIMESTONE DIAGENESIS

1) Components of the Mingan limestones were originally composed of a polymineralic carbonate assemblage including aragonite, Mg calcite and calcite. Fossil skeletons were mainly calcitic, with the exception of mollusks and solenoporacean algae. Furthermore, fossil skeletons with mixed mineralogy such as tabulate corals and bryozoans were composed of calcite and aragonite. Ooids are of two types; calcitic ooids with radial cortex occurring in peritidal sediments and aragonitic ooids occurring in sand shoal deposits. Marine cements were originally calcite and possibly fibrous Mg calcite.

2) Alteration of the Mingan limestones resulted from three distinct

phases of diagenesis: marine, near-surface and deeper burial. Near-surface diagenesis was the most intense beneath subaerial exposure surfaces either on a regional scale (intra-Mingan paleokarst), or on a local scale (calcarenite cycles). Dissolution and neomorphism of metastable carbonate components followed by an important phase of meteoric cementation were the most important processes that occurred during near-surface diagenesis.

3)Post-sedimentary cements precipitated as calcite in phreatic to deeper burial environments under increasingly reducing conditions. Cements are commonly iron-poor, with clear calcite followed by iron-rich calcite as the last void-filling cement. Growth habits (prismatic vs blocky) in iron-poor calcite cements may have been controlled by local variations of meteoric water circulating through the pore system.

4) Vadose cements are not present beneath paleokarst surfaces. They were either eroded by subsequent karstification or were precipitated in zones too thin to be easily recognized.

5) Crystal debris in the Mingan limestones resulted from the internal erosion of contemporaneous phreatic calcite cements and subsequently deposition as geopetal internal sediment. Crystal debris, similar to Dunham's vadose silt, may also form under phreatic conditions and should be used with caution as an indicator of vadose diagenesis.

BIBLIOGRAPHY

ADAMS, J.E., AND RHODES, M.L., 1960, Dolomitization by seepage refluxion: Amer. Assoc. Petroleum Geol. Bull., v. 44, p. 1912-1920.

AHR, W.M., 1973, The carbonate ramp: an alternative to the shelf model: Trans. Gulf Coast Assoc. Geol. Soc., v. 23, p. 221-225.

AITKEN, J.D., 1966, Middle Cambrian to Middle Ordovician cyclic sedimentation, southern Rocky Mountains of Alberta, Canada: Can. Petroleum Geol. Bull., v. 14, p. 405-411.

AITKEN, J.D., 1967, Classification and environmental significance of cryptalgai limestones and dolomites, with illustrations from the Cambrian and Ordovician of southwestern Alberta: Jour. Sed. Petrology, v. 37, p. 1163-1178.

AL-AASM, I.S., AND VEIZER, JAN, 1982, Chemical stabilization of low-Mg calcite: an example of brachiopods: Jour. Sed. Petrology, v. 52, p. 1051-1400.

ALBERSTADT, L.P., WALKER, K.R., AND ZURAWSKI, R.P., 1974, Patch reefs in the Carters Limestone (Middle Ordovician) in Tennessee and vertical zonation in Ordovician reefs: Geol. Soc. America Bull., v. 85, p. 1171-1182.

ALEXANDERSSON, T. 1972, Micritization of carbonate particles: process of precipitation and dissolution in modern shallow marine sediments: Bull. Geol. Insts. Univ. Uppsala, N.S., v. 3, p. 201-236.

AL-HASHIMI, W.S., AND HEMINGWAY, J.E., 1973, Recent dedolomitization and the origin of rusty crusts of Northumberland: Jour. Sed. Petrology, v. 43, p. 82-91.

ALLEN, J.R., 1982, Sedimentary structures: their character and physical basis: Elsevier, Amsterdam, p. 222-231.

ASHTON, MICHAEL, 1981, Carbonate tidal rhythmites from the Middle Jurassic of Britain: Sedimentology, v. 28, p. 689-698.

ASSERETO, R.L., AND KENDALL, C.G. St.C., 1977, Nature, origin and classification of peritidal tepee structures and related breccias: Sedimentology, v. 24, p. 153-210.

BACK, W., HANSHAW, B.B., PLUMMER, L.N., AND WEIDIE, A.E., 1979, Geochemical significance of groundwater discharge and carbonate solution of the formation of Caleta Xel Ha, Quintana Roo, Mexico: Water Resources Research, v. 15, p. 1531-1535.

BACK, W., HANSHAW, B.B., AND VAN DRIEL, J.N., 1984, Role of groundwater in shaping the eastern coastline of the Yucatan Peninsula, Mexico, in Lafleur, r.g., ed., Groundwater as a geomorphic agent: Allen and Unwin Inc., Winchester, p. 157-172.

BADIOZAMANI, K., 1973, The Dorag dolomitization model-application to the the Middle Ordovician of Wisconsin: Jour. Sed. Petrology, v. 43, p. 965-984.

BARNES, C.R., 1984, Early Ordovician eustatic events in Canada: in Bruton, D.L., ed., Aspects of the Ordovician System: Paleont. Contributions from the Univ. of Oslo 295, p. 51-64.

BARNES, C.R. NORFORD, B.S., AND SKEVINGTON, DAVID, 1981, The Ordovician System in Canada: Intern. Union Geol. Sciences, Publ. #8, 27 p.

BATHURST, R.G., 1959, The cavernous structures of some Mississippian stromatactis reefs in Lancashire, England: Jour. Geol., v. 67, p. 506-521.

BATHURST, R.G., 1966, Boring algae, micrite envelopes and lithification of molluscan biosparites: Geol. Jour., v. 5, p. 15-32.

BATHURST, R.G., 1975, Carbonate sediments and their diagenesis: Elsevier Scientific Publishing Co, Amsterdam, 658 p.

BATHURST, R.G., 1980, Deep crustal diagenesis in limestones: Rev. Invest. Geol., Dipucation Provincial, Univ. de Barcelona, v. 34, p. 89-100.

BATHURST, R.G., 1982, Genesis of stromatactis cavities between submarine crusts in Paleozoic carbonate mud buildups: Jour. Geol. Soc., v. 139, p. 165-181.

BELT, E.S., AND BUISSIERES, L., 1981, Upper Middle Ordovician submarine fans and associated facies, northeast of Quebec City: Can. Jour. Earth Sciences, v. 18, p. 981-994.

BERGERON, M., 1980, Etat d'avancement des travaux, rapport 2, projet "dolomie": Ministere de l'Energie et des Ressources (Quebec), GM 37343.

BERRY, W.B., 1960 Graptolite faunas of the Marathon Region, west Texas. Bureau of Economic Geology, Univ. of Texas, Publ. 6005. 179 p.

BEUF, S., BIJU-DEVAL, B., CHAPARAL, O., ROGNON, R., GARIEL, O., AND BENNECEF, A., 1971, Les gres du Paleozoique inferieur au Sahara: Technip, Paris, 464 p.

BILLINGS, E., 1865, Paleozoic fossils (vol. 1): Geological Survey of Canada (1865), 426 p.

BLATT, HARVEY, MIDDLETON, G.V., AND MURRAY R.C., 1980, Origin of sedimentary rocks, 2nd ed.,: Prentice-Hall, New Jersey, 782 p.

BOARDMAN, R.S., AND CHITAM, R., 1969, Skeletal growth, intracolony variation, and evolution in Bryozoa: Jour. Paleontology, v. 43, p. 205-233.

BOGLI, J., 1980, Karst hydrology and physical speleology: Springer-Verlag, Berlin-Heidelberg, 285 p.

BOLES, J.R., AND FRANKS, S.G., 1979, Clay diagenesis in Wilcox sandstones of southwest Texas: implications of smectite diagenesis on sandstone cementation: Jour. Sed. Petrology, v. 49, p. 55-70.

BOURQUE, P.A., AND GIGNAC, H, 1983, Sponge-constructed stromatatic mud mounds, Silurian of Gaspe Quebec: Jour. Sed. Petrology, v. 53, p. 521-532.

BOURQUE, P.A., MAMET, B., AND ROUX, A., 1981, Algues Siluriennes du Synclinorium de la Baie des Chaleurs, Quebec, Canada: Revue de Micropaleontologie, v. 24, p. 83-126.

BOVA, J.A., 1983, Peritidal cyclic and incipiently drowned platform sequences Lower Ordovician Chepultepec Formation, Virginia (unpublished M.S. thesis): Virginia Polytechnic Institute and State Univ., Blacksburg, Virginia.

BRAND, UWE, 1981, Mineralogy and chemistry of the Lower Pennsylvanian Kendrick fauna, eastern Kentucky: Chemical Geol., v. 32, p. 1-16.

BRAND, UWE, AND VEIZER, JAN, 1980, Chemical diagenesis of a multicomponent carbonate system – 1: Trace elements: Jour. Sed. Petrology, v. 50, p. 1219-1236.

BRAND, UWE, AND VEIZER, JAN, 1981, Chemical diagenesis of a multicomponent carbonate system – 2: Stable isotopes: Jour. Sed. Petrology, v. 51, p. 701-997.

BRENNER, R.L., 1980, Construction of process-response models for ancient epicontinental seaway depositional systems using partial analogs: Amer. Assoc. Petroleum Geologists Bull., v. 64, p. 1223-1244.

BRIDGES, P.H., 1982, The origin of cyclothems in the late Dinantian platform carbonates at Crich Derbyshire: Proc. Yorkshire Geol. Soc., v. 44, p.158-180.

BRIDGES, P.H., AND LEEDER, M.R., 1976, Sedimentary model for intertidal mudflat channels with examples from the Solway Firth, Scotland: Sedimentology,v. 23, p. 533-552.

BROADHEAD, T.W., AND WATERS, J.A., 1980, Echinoderms, notes for a short course: Univ. of Tennessee, Stud. Geol. 3, 235 p.

BROOD, K. , 1978, Bryozoans, in Huq, B.U., and Boersma, A., eds., Introduction to marine micropaleontology: Elsevier, New York, p. 189-201.

BUCHBINDER, B., MAGARITZ, M., AND BUCHBINDER, L.G., 1983, Turonian to
    Neogene paleokarst in Israel: Paleogeography, Paleoclimatology,
    Paleoecology, v. 43, p. 329-350.

BUDAI, J.M., LOHMANN, K.C., AND OWEN, R.M., 1984, Burial dedolomite in
    the Mississippian Madison Limestone, Wyoming and Utah thrust belt:
    Jour. Sed. Petrology, v. 54, p. 276-288.

BUSH, P., 1973, Some aspects of the diagenetic history of the sabkha in
    Abu Dhabi, Persian Gulf, in Purser, B.H., ed., The Persian Gulf –
    Holocene carbonate sedimentation and diagenesis in a shallow
    epicontinental sea: Springer-Verlag, Heidelberg, Berlin, p. 395-407.

BUXTON T.M., AND SIBLEY, D.F., 1981, Pressure solution features in a
    shallow buried limestone: Jour. Sed. Petrology, v. 51, p. 19-26.

CADOT, H.M., VAN SCHMUS, W.R., AND KAESLER, R.L., 1972, Magnesium in
    calcite of marine ostracoda: Geol. Soc. America, v. 83, p.
    3519-3522.

CHAVE, K.E., 1954, Aspects of the biogeochemistry of magnesium. 1.
    Calcareous marine organisms: Jour. Geol., v. 62, p. 266-283.

CHERNS, L., 1982, Paleokarst, tidal erosion surfaces and stromatolites
    in the Silurian Eke Formation of Gotland, Sweden: Sedimentology, v.
    29, p. 819-833.

CHILINGAR, G.V., ZENGER, D.H., BISSELL, H.J., AND WOLF, K.H., 1979,
    Dolomites and dolomitization, in Larsen, G., and Chilingar, G.V.,
    eds., Diagenesis in sediments, 2nd edition, Part A: Elsevier,
    Amsterdam, p. 423-436.

CHOQUETTE, P.W., 1971, Late ferroan dolomite cement, Mississippian
    carbonates, Illinois Basin, U.S.A., in Bricker, O.P., Carbonate
    cements: Johns Hopkins Univ. Studies in Geology 19, p. 339-346.

CHOQUETTE, P.W., AND PRAY, L.C., 1970, Geologic nomenclature and
    classification of porosity in sedimentary carbonates: Amer. Assoc.
    Petroleum Geol. Bull., v. 54, p. 207-250.

CHURCH, S.B., 1974, Lower Ordovician patch reefs in western Utah:
    Brigham Young Univ. Geol. Stud. 21, p.41-62.

CHURNET, H.G., AND MISRA, K.C., 1981, Genetic implications of the trace
    element distribution pattern in the Upper Knox carbonate rocks,
    Cooper Ridge District, East Tennessee: Sedimentary Geol., v. 30, p.
    173-194.

CHURNET, H.G., MISRA, K.C., AND WALKER, W.R., 1982, Deposition and
    dolomitization of Upper Knox carbonate sediments, Cooper Ridge
    District, east Tennessee: Geol. Soc. America Bull., v. 93, p. 73-86.

CLUFF, R.M., 1984, Carbonate sand shoals in the Middle Mississippian (Valmeyeran) Salem-St. Louis-Ste. Genevieve Limestones, Illinois Basin, in Harris, P.M., ed., Carbonate sands - a core workshop: Soc. Econ. Paleontologists Mineralogists, Core workshop 5, p. 94-135.

COHEN, C.R., 1982, Model for a passive to active continental margin transition: implications for hydrocarbon exploration: Amer. Assoc. Petroleum Geol, Bull., v. 66, p. 708-718.

COOPER, G.A., 1956, Chazyan and related brachiopods: Smithsonian Misc. Collections, v. 127, Pt. 1, 1024 p.

COPPER, PAUL, 1974, Structure and development of Early Paleozoic reefs: Proc. 2nd Int. Coral Reef Symposium, v. 6, p. 365-386.

CORBEL, JEAN, 1963, Marmite de geants et microformes karstiques. Norois ann., v. 10, #10, p. 121-132.

COWELL, D.W., 1976, Karst geomorphology of the Bruce Peninsula, Ontario (unpublished M.S. thesis), McMaster University.

CUFFEY, R.J., 1977, Bryozoan contributions to reefs and bioherms through geologic time, in Frost, S.H. et al, eds., Reefs and related carbonates - ecology and sedimentology: Amer. Assoc. Petroleum Geol., Studies Geol. 4, p. 181-194.

CUFFEY, R.J., FONDA, S.S., KOSICH, D.F., GEBELEIN, C.D., BLIEFNICK, D.M., AND SOROKA, L.G., 1977, Modern tidal-channel bryozoan reefs at Joulter Cays (Bahamas): Proc. 3th Int. Coral Reef Symposium, Univ. of Miami, p. 339-345.

DAVIES, G.R., 1970, Carbonate bank sedimentation eastern Shark Bay, western Australia, in Logan et al, eds., Carbonate sedimentation and environments, Shark Bay, western Australia: Amer. Assoc. Petroleum Geologists, Memoir 13, p. 85-168.

DAVIES, G.R., 1977, Former magnesian calcite and aragonite submarine cements in Upper Paleozoic reefs of the Canadian Artic: a summary: Geology, v. 5, p. 11-15.

DAVIS, R.A., 1975, Intertidal and associated deposits of the Prairie du Chien Group (Lower Ordovician) in the upper Mississippian Valley, in Ginsburg, R.N., ed., Tidal deposits: A casebook of recent examples and fossil counterparts: Springer-Verlag, New York, p. 67-73.

DEFFEYES, K.S., LUCIA, F.J., AND WEYL, P.K., 1965, Dolomitization of recent and Plio-Pleistocene sediments by marine evaporite waters on Bonaire, Netherlands Antilles, in Pray, L.C., and Murray, R.C., Dolomitization and limestone diagenesis, a symposium: Soc. Econ. Paleontologists Mineralogists, Spec. Pub. 13, p. 71-88.

DeGROOT, K., 1973, Geochemistry of tidal flat brines, S.E. Qatar, Persian Gulf, in Purser, B.H., ed., The Persian Gulf - Holocene carbonate sedimentation and diagenesis in a shallow epicontinental sea: Springer-Verlag, Heidelberg, Berlin, p. 377-394.

DEMICCO, R.V., 1983, Wavy and lenticular-bedded carbonate ribbon rocks
of the Upper Cambrian Conococheague Limestone, Central Appalachians:
Jour. Sed. Petrology, v. 53, p. 1121-1132.

DEPATIE, J., 1967, Geologie de la region du lac a l'Ours: Ministere de
l'Energie et des Ressources (Quebec), Rapport preliminaire #559, 13
p.

DESROCHERS, A., 1981, Etude sedimentologique de la Formation de La
Vieille dans la region de Clemville – Port-Daniel, Baie des Chaleurs
(unpublished M.S. thesis), Univ. Laval.

DESROCHERS, A., 1984, Lower and Middle Ordovician platform carbonates,
Mingan Islands, Quebec: Geol. Ass. Canada, Abstracts with program,
p. 37.

DESROCHERS, A., AND JAMES, 1985: Early Paleozoic surface and subsurface
paleokarst: Middle Ordovician carbonates, Mingan Islands, Quebec:
2nd SEPM Annual Midyear Meeting, Abstracts with program, p. 23.

DICKSON, J.A.,1966, Carbonate identification and genesis as revealed by
staining: Jour. Sed. Petrolology, v. 36, p. 491-505.

DONALDSON, J.A., AND RICKETTS, B.D., 1979, Beachrock in Proterozoic
dolostone of the Belcher Islands, Northwest Territories, Canada:
Jour. Sed. Petrology, v. 49, p. 1287-1294.

DONOVAN, D.T., AND JONES, 1979, Causes of worldwide changes in sea
level. Jour, Geol. Soc., v. 136, p. 187-192.

DOTT, R.H., AND BYERS, C.W., 1980, SEPM research conference on modern
shelf and ancient cratonic sedimentation – the orthoquartzite-
carbonate suite revisited: Jour. Sed. Petrology, v. 50, p. 329-346.

DRAVIS, J., 1979, Rapid and widespread generation of recent oolitic
hardgrounds on the high energy Bahamian platform, Eleuthera Bank,
Bahamas: Jour. Sed. Petrology, v. 49, p. 195-205.

DRIESE, S.G., BYERS, C.W., AND DOTT, R.H., Jr., 1981, Tidal deposition
in the basal Upper Cambrian Mt. Simon Formation in Wisconsin: Jour.
Sed. Petrology, v. 51, p. 367-381.

DUBOIS, J., LAUNAY, J., AND RECY, J., 1974, Uplift movements in New
Caledonia-Loyalty Islands area and their plate tectonics
interpretation: Tectonophysics, v. 26, p. 133-150.

DUBOIS, J., LAUNAY, J., AND RECY, J., 1975, Some new evidence on
lithospheric bulges close to island arcs: Tectonophysics, v. 26, p.
189-196.

DUNHAM, J.B., AND OLSON, E.S., 1980, Shallow subsurface dolomitization
of subtidally deposited carbonate sediments in the Hanson Creek
Formation (Ordovician-Silurian) of central Nevada, in Zenger, D.H.
et al, eds., Concepts and models of dolomitization: Soc. Econ.
Paleontologists Mineralogists, Spec. Pub. 28, p. 139-162.

DUNHAM, R.J., 1962, Classification of carbonate rocks according to depositional texture: Amer. Assoc. Petroleum Geologists, Memoir #1, p. 108-121.

DUNHAM, R.J., 1969, Early vadose silt in Townsend mound (reef), New Mexico, in Friedman, g.m., ed., Depositional environments in carbonate rocks; a symposium: Soc. Econ. Paleontologists Mineralogists, Spec. Pub. 14, p. 182-191.

DUNHAM, R.J., 1970, Stratigraphic reefs vs ecologic reefs: Amer. Assoc. Petroleum Geol. Bull., v. 54, p. 1931-1932.

DUNNINGTON, H.V., 1954, Stylolite development post-dates rock induration: Jour. Sed. Petrology, v. 24, p. 27-49.

DUTTON, S.P., AND LAND, L.S., 1985, Meteoric burial diagenesis of Pennsylvanian arkosic sandstones, southwestern Anadarko Basin, Texas: Amer. Assoc. Petroleum Geol. Bull., v. 69, p. 22-38.

EKDALE, A.A., BROMLEY, R.G., AND PEMBERTON, S.G., 1984, Ichnology: trace fossils in sedimentology and stratigraphy: Soc. Econ. Paleontologists and Mineralogists, Short Course 15, 317 p.

EMBRY, A.F., AND KLOVAN, J.E., 1971, A late Devonian reef tract on northeastern Banks Island, N.W.T.: Can Petroleum Geol. Bull., v. 19, p. 730-781.

EMERY, K.O., 1946, Marine solution basins: Jour. Geology, v. 54, p. 209-228.

ENOS, PAUL, 1977, Holocene sediment accumulations of the south Florida shelf margin, in Enos, Paul, and PERKINS, R.D., eds., Quaternary sedimentation in south Florida, Geol. Soc. America, Memoir 147, 198 p.

ENOS, PAUL, 1983, Shelf environment, in Scholle, P.A., Bebout, D.G., and Moore, C.H., Carbonate depositional environments: Amer. Assoc. Petroleum Geologists, Memoir 33, p. 267-298.

ENOS, PAUL, AND PERKINS, R.D., 1977, Quaternary sedimentation in south Florida, Geol. Soc. America, Memoir 147, 198 p.

ESTEBAN, M., AND KLAPPA, C.F., 1983, Subaerial exposure, in Scholle, P.A., Bebout, D.G., and Moore, C.H., eds., Carbonate depositional environments: Amer. Assoc. Petroleum Geologists, Memoir 33, p. 1-54.

EVAMY, B.D., 1963, The application of a chemical staining technique to a study of dedolomitization: Sedimentology, v. 2, p. 164-170.

FILION, D., AND PICKERILL, R.K., 1984, Systematic ichnology of the Middle Ordovician Trenton Group, St. Lawrence Lowland, eastern Canada: Maritime Sediments and Atlantic Geology, v. 20, p. 1-41.

FINKS, R.M., AND TOOMEY, D.F., 1969, The paleoecology of Chazyan (lower
   Middle Ordovician) reefs or mounds: New York State, 41st. Ann.
   Meeting, Plattsburg, p. 93-120.

FLOWER, R.H., 1957, Nautiloids of the Paleozoic, in Ladd, H.S., Treatise
   on marine ecology and paleoecology 2: Geol. Soc. America, Memoir 67,
   p. 829-852.

FLUGEL, H.W., 1976, Ein spongienmodell fur die Favositidae: Lethaia, v.
   9, p. 405-419.

FOERSTE, A.F., 1938, Cephalopoda, in Twenhofel, W.H., Geology of the
   Mingan Islands: Geol. Soc. America, Special Paper 11, p. 76-105

FOLK, R.L., 1968, Bimodal supermature sandstone: product of the desert
   floor: Intern. Geol. Congress, 23 rd, Prague, Proc., section 8, p.
   8-32.

FOLK, R.L., AND ASSERETO, R., 1974, Giant aragonite rays and baroque
   white dolomite in tepee-fillings, Triassic of Lombardy, Italy
   (abstr.): Amer. Assoc. Petroleum Geol, Abstracts with programs,
   Annual meeting, San Antonio, p. 34-35.

FOLK, R.L., AND LAND, L.S., 1975, Mg/Ca ratio and salinity: two controls
   over crystallization of dolomite: Amer. Assoc. Petroleum Geologists
   Bull., v. 59, p. 60-68.

FORTEY, R.A., 1979, Early Ordovician trilobites from the Catoche
   Formation (St. George Group), western Newfoundland: Geol. Survey of
   Canada, Bull. 321, p. 61-114.

FORTEY, R.A., 1980, The Ordovician of Spitbergen, and its relevance to
   the base of the Middle Ordovician in North America, in Wones, D.R.,
   ed., The Caledonides in the USA: Virginia Polytechnic Institute and
   State University, Dept. of Geol. Sciences, Memoir 2, p. 33-40.

FORTEY, R.A., 1984, Global earlier Ordovician transgressions and
   regressions and their biological implications: in Bruton, D.L., ed.,
   Aspects of the Ordovician System: Paleont. Contributions from the
   Univ. of Oslo 295, p. 37-50.

FRANK, J.R., 1981, Dedolomitization in the Taum Sauk Limestone (Upper
   Cambrian) southeast Missouri: Jour. Sed. Petrology, v. 51, p. 7-18.

FREY, R.W., AND PEMBERTON, S.G., 1984, Trace fossils facies models, in
   Walker, R.G.,ed., Facies models, 2nd ed.: Geol. Assoc. Canada,
   Reprint Ser. 1, p. 189-208.

FRIEDMAN, G.M., 1964, Early diagenesis and lithification in carbonate
   sediments: Jour. Sed. Petrology, v. 34, p. 777-813.

FRIEDMAN, G.M., 1965, Terminology of crystallization textures and
   fabrics in sedimentary rocks: Jour. Sed. Petrology, v. 35, p.
   643-655.

FROST, S.H., 1977, Ecologic controls of Caribbean and Mediterranean
Oligocene reef coral communities: Proc. 3th Int. Coral Reef
Symposium, Univ. of Miami, p. 367-375.

GAUTHIER-LAROUCHE, G., 1981, Origine et toponymie de l'archipel de
Mingan: Commission de toponymie du Quebec, Etudes et recherches
toponymiques 1, 165 p.

GARRET, P., 1970, Phanerozoic stromatolites: noncompetitive ecologic
restriction by grazing and burrowing animals: Science, v. 169, p.
171-173.

GARRET, P., 1977, Biological communities and their sedimentological
record, in Hardie, L.A., ed., Sedimentation on the modern carbonate
tidal flats of northwest Andros Island, Bahamas: Johns Hopkins
Univ., Studies Geol. 22, p. 124-158.

GARRET, P., SMITH, D.L., WILSON, A.O., AND PATRIQUIN, D. et al, 1971,
Physiography, ecology, and sediments of two Bermuda patch reefs:
Jour. Geology, v. 79, p. 647-668.

GARRISON, R.E., AND KENNEDY, W.J., 1977, Origin of solution seams and
flaser structure in Upper Cretaceous chalks of southern England:
Sed. Geology, v. 19, p. 107-137.

GINSBURG, R.N., 1953, Intertidal erosion on the Florida Keys: Marine
Sciences Bull., v. 3, p. 59-69.

GINSBURG, R.N., 1971, Landward movement of carbonate mud: new model for
regressive cycles in carbonates (abstract): Amer. Ass. Petroleum
Geologists, v. 55, p. 340.

GINSBURG, R.N., AND HARDIE, L.A., 1977, Layering: the origin and
environmental significance of lamination and thin bedding, in
Hardie, L.A., ed., Sedimentation on the modern carbonate tidal flats
of northwest Andros Island, Bahamas: Johns Hopkins Univ., Studies
Geol. 22, 202 p.

GINSBURG, R.N., AND SCHROEDER, J., 1973, Growth and submarine
fossilization of algal cup reefs, Bermuda: Sedimentology, v. 20, p.
575-614.

GOREAU, T.F., AND LAND, L.S., 1974, Fore-reef morphology and
depositional processes, North Jamaica, in Laporte, L.F., ed., Reefs
in time and space: Soc. Econ. Paleontologists Mineralogists, Spec.
Pub. 17, p. 77-89.

GRANT, R.E., 1972, The lophophore and feeding mechanisms of the
Productidina (Brachiopoda): Jour. Paleontology, v. 46, p. 213-248.

GREGG, J.M., AND SIBLEY, D.F., 1984, Epigenetic dolomitization and the
origin of xenotopic dolomite texture: Jour. Sed. Petrology, v. 54,
p. 908-931.

HALLEY, R.B., HARRIS, P.M., AND HINE, A.C., 1983, Bank margin
    environment, in Scholle, P.A., Bebout, D.G., and Moore, C.H., ed.,
    Carbonate depositional environments: Amer. Assoc. Petroleum
    Geologists, Memoir 33. p. 463-506.

HANSHAW, B.B., BACK, W.E., AND DEIKE, R.G., 1971, A geochemical
    hypothesis for dolomitization by groundwater: Econ. Geol., v. 66, p.
    710-724,

HARDIE, L.A., 1977, Sedimentation on the modern carbonate tidal flats of
    northwest Andros Island, Bahamas: Johns Hopkins Univ., Studies Geol.
    22, 202 p.

HARDIE, L.A., AND GARRET, P., 1977, General environmental setting, in
    Hardie, L.A., ed., Sedimentation on the modern carbonate tidal flats
    of northwest Andros Island, Bahamas: Johns Hopkins Univ., Studies
    Geol. 22, 12-49 p.

HARRIS, P.M., 1979, Facies anatomy and diagenesis of a Bahamian sand
    shoal: Sedimenta VII, Comparative Sedimentology Lab., Univ. of
    Miami, 163 p.

HARRIS, P.M., 1984, Cores from a modern carbonate sand body; The
    Joulters ooid shoal, Great Bahama Bank, in Harris, P.M., ed.,
    Carbonate sands - a core workshop: Soc. Econ. Paleontologists
    Mineralogists, Core workshop 5, p. 429-464.

HARRIS, P.M., KENDALL, C.G. St. C., AND LERCHE, IAN, 1985, Carbonate
    cementation - a brief review, in Schneidermann, N., and Harris,
    P.M., eds., Carbonate cements: Soc. Econ. Paleontologists
    Mineralogists, Spec. Pub. 35, p. 79-96.

HARTMAN, W.D., 1977, Sponges as reef builders and shapers, in Frost,
    S.H. et al, eds., Reefs and related carbonates - 'ecology and
    sedimentology: Amer. Assoc. Petroleum Geol., Studies Geol. 4, p.
    127-134.

HARTMAN, W.D., AND GOREAU, T.F., 1975, A Pacific tabulate sponge, living
    representative of a new order of sclerosponges: Postilla, v. 167, 21
    p.

HAYWICK, D.W., 1984, Dolomites and dolomitization of the Lower
    Ordovician St. George Group of western Newfoundland (unpublished
    M.S. thesis): Memorial University of Newfoundland.

HECKEL, P.H., 1983, Diagenetic models for carbonate rocks in
    midcontinent Pennsylvanian eustatic cyclothems: Jour. Sed.
    Petrology, v. 53, p. 733-780.

HINE, A.C., 1983, Relict sand bodies and bedforms of the northern
    Bahamas: evidence of extensive early Holocene sand transport, in
    Peryt, T.M., ed., Coated grains: Springer-Verlag, p. 116-131.

HINE, A.C., AND STEINMETZ, J.C., 1984, Cay Sal Bank, Bahamas – A partially drowned carbonate platform: Marine Geology, v. 59, p. 135-164.

HINE, A.C., WILBER, R.J., AND NEUMANN, A.C., 1981, Carbonate sand bodies along contrasting shallow-bank margins facing open seaways, northern Bahamas: Amer. Assoc. Petroleum Geologists Bull., v. 65, p. 261-290.

HISCOTT, R.N., 1985, Ophiolitic source rocks for Taconic-age flysch: trace element evidence: Geol. Soc. America Bull., v. 95, p. 1261-1267.

HISCOTT, R.N., JAMES, N.P., AND PEMBERTON, S.G., 1984, Sedimentology and ichnology of the Lower Cambrian Bradore Formation, coastal Labrador: fluvial to shallow-marine transgressive sequence: Can. Petroleum Geol. Bull., v. 32, p. 11-26.

HISCOTT, R.N., QUINLAN, G.M., AND STEVENS, R.K., 1983, Comment on "Analogous tectonic evolution of the Ordovician foredeeps, southern and central Appalachians": Geology, v. 10, p. 562-566.

HOFFMAN, PAUL, 1976, Stromatolite morphogenesis in Shark Bay, western Australia, in Walter, M.R., ed., Stromatolites: Elsevier, New York, 61-273.

HOFMANN, H.J., 1963, Ordovician Chazy Group in southern Quebec, Amer. Assoc. Petroleum Geologists Bull., v. 47, p. 270-301.

HOFMANN, H.J., 1969, Attributes of stromatolites: Geol. Survey of Canada, Paper 69-39, p. 1-58.

HOFMANN, H.J., 1972, Stratigraphy of the Montreal area: 24th Int. Geol. Congress, Guidebook, Excursion B-03,

HOFMANN, H.J., 1979, Chazy (Middle Ordovician) trace fossils in the Ottawa-St. Lawrence Lowlands: Geol. Survey Canada, Bull. 321, p. 27-59.

HOROWITZ, A.St., AND POTTER, P.E., 1971, Introductory petrography of fossils: Springer-Verlag, Berlin-Heidelberg-New York, 302 p.

INDEN, R.F, AND MOORE, C.H., 1983, Beach environment, in Scholle, P.A., Bebout, D.G., and Moore, C.H., eds., Carbonate depositional environments: Amer. Assoc. Petroleum Geologists, Memoir 33, p. 211-266.

JACOBI, R.D., 1981, Peripheral bulge – a causual mechanism for the Lower/Middle Ordovician unconformity along the western margin of the northern Appalachians: Earth and Planetary Science Letters, v. 56, p. 245-251.

JAMES, N.P., 1974, Diagenesis of scleractinian corals in the subaerial vadose environment: Jour. Paleontology, v. 48, p. 785-799.

JAMES, N.P., 1981, Megablocks of calcified algae in the Cow Head Group,
western Newfoundland: vestiges of a Cambro-Ordovician platform
margin: Geol. Soc. America Bull., v. 92, p. p. 799-811.

JAMES, N.P., 1983, Reef environment, in Scholle, P.A., Bebout, D.G., and
Moore, C.H., eds., Carbonate depositional environments: Amer. Assoc.
Petroleum Geologists, Memoir 33, p. 345-440.

JAMES, N.P., 1984a, Shallowing-upward sequences in carbonates, in
Walker, R.G., ed., Facies models, 2nd ed.: Geol. Assoc. Canada,
Reprint Ser. 1, p. 213-228.

JAMES, N.P., 1984b, Reefs, in Walker, R.G., ed., Facies models, 2nd ed.:
Geol. Assoc. Canada, Reprint Ser. 1, p. 229-244.

JAMES, N.P., AND KOBLUK, D.R., 1978, Lower Cambrian patch reefs and
associated sediments, southern Labrador, Canada: Sedimentology, v.
25, p. 1-32.

JAMES, N.P., AND STEVENS, R.K., 1982, Anatomy and evolution of a Lower
Paleozoic continental margin, western Newfoundland: 11th Int.
Congress on Sedimentology, Hamilton, Canada, Excursion 2B, 75 p.

JAMES, N.P., AND CHOQUETTE, P.W., 1983, Diagenesis 6 – The sea floor
diagenetic environment: Geoscience Canada, v. 10, p. 162-178.

JAMES, N.P., AND CHOQUETTE, P.W., 1984, Diagenesis 9 – Limestones – the
meteoric diagenetic environment: Geoscience Canada, v. 11, p.
161-194.

JAMES, N.P., AND KLAPPA, C.F., 1983, Petrogenesis of early Cambrian reef
limestones, Labrador, Canada: Jour. Sed. Petrology, v. 53, p.
1051-1097.

JAMES, N.P., GINSBURG, R.N., MARSZALEK, D.S., AND CHOQUETTE, P.W., 1976,
Facies and fabric specificity of early subsea cements in shallow
Belize (British Honduras) reefs: Jour. Sed. Petrology, v. 46, p.
523-544.

JENNINGS, J.N., 1971, Karst: M.I.T. Press, Cambridge, Massachusetts, 252
p.

JOHNSON, J.G., AND MURPHY, M.A., 1984, Time-rock model for
Siluro-Devonian continental shelf, western United States: Geol. Soc.
America, v. 95, p. 1349-1359.

JOHNSON, J.G., KLAPPER, G., AND SANDBERG, C.A., 1985, Devonian eustatic
fluctuations in Euramerica: Geol. Soc. America Bull., v. 96, p.
639-648.

JONES, B. AND DIXON, O.A., 1976, Storm deposits in the Read Bay
Formation (Upper Silurian) Somerset Island, Arctic Canada (An
application of Markov chain analysis): Jour. Sed. Petrology, v. 46,
p. 393-401.

KAPP, U.S., 1975, Paleoecology of Middle Ordovician stromatoporoid mounds in Vermont: Lethaia, v. 8, p. 195-207.

KATZ, A., 1968, Calcian dolomites and dedolomitization: Nature, v. 217, p. 439-440.

KAYE, C.A., 1959, Shoreline features and Quaternary shoreline changes Puerto Rico: U.S. Geol. Survey, Prof. Paper 317-B, p. 49-140.

KENDALL, A.C., 1985, Radiaxial fibrous calcite: a reappraisal, in Schneidermann, N., and Harris, P.M., eds., Carbonate cements: Soc. Econ. Paleontologists Mineralogists, Spec. Pub. 35, p. 59-78.

KENDALL, A.C., AND TUCKER, M.E., 1973, Radiaxial fibrous calcite: a replacement after acicular carbonate: Sedimentology, v. 20, p. 365-389.

KENDALL, C.g. St. C., AND SCHLAGER, W., 1981, Carbonates and relative changes in sea level: Marine Geology, v. 44, p. 181-21".

KEPPIE, J.D., 1985, Emplacement of Canadian Taconic allochthons: Geol. Soc. America, Abstracts with programs, v. 17, p. 23.

KERR, J.W., 1974, Geology of Bathurst Island Group and Byam Martin Island, Arctic Canada: Geol. Survey of Canada, Memoir 378.

KLAPPA, C.F., 1983, A process-response model for the formation of pedogenic calcretes, in Wilson, R.C., ed., Residual deposits: Geol. Soc., Spec. Pub. 11, p. 211-220.

KLAPPA, C.F., AND JAMES, N.P., 1980, Small lithistid sponge bioherms, early Middle Ordovician Table Head Group, western Newfoundland: Can. Petroleum Geol. Bull., v. 28, p. 435-451.

KLAPPA, C.F., OPALINSKI, P.R., AND JAMES, N.P., 1980, Middle Ordovician Table Head Group of western Newfoundland: a revised stratigraphy: Can. Jour. Earth Sciences, v. 17, p. 1007-1019.

KLEIN, G. de V., 1977, Clastic tidal facies: Continuing Education Publication Company, Champaign, Illinois, 149 p.

KOBLUK, D.R., 1981a, Cavity-dwelling biota in Middle Ordovician (Chazy) bryozoan mounds from Quebec: Can. Jour. Earth Sciences, v. 18, p. 42-54.

KOBLUK, D.R., 1981b, Middle Ordovician (Chazy Group) cavity-dwelling boring sponges: Can. Jour. Earth Sciences, v. 18, p. 1101-1108.

KOBLUK, D.R., 1984, Coastal paleokarst near the Ordovician-Silurian boundary, Manitoulin Island, Ontario: Can. Petroleum Geol. Bull., v. 32, p. 398-407.

KOBLUK, D.R., JAMES, N.P., AND PEMBERTON, S.G., 1978, Initial diversification of macroboring ichnofossils and exploitation of the macroboring niche in the Lower Paleozoic: Paleobiology, v. 4, p. 163-170.

KOBLUK, D.R., PEMBERTON, S.G., KAROLYI, M., AND RISK, M.J., 1977, The Silurian-Devonian disconformity in southern Ontario: Can. Petroleum Geol. Bull., v. 25, p. 1157-1186.

KREBS, W., 1971, Devonian reef limestones in the eastern Rhenish Schiefergebirge, in Muller, G., ed., Sedimentology of part of central Europe: 8th Int. Sed. Congress, Heldelberg, Guidebook, p. 45-81.

KREISA, R.D., 1981, Storm-generated sedimentary structures in subtidal marine facies with examples from the Middle and Upper Ordovician of southwestern Virginia: Jour. Sed. Petrology, v. 51, p. 823-848.

KYLE, J.R., 1983, Economic aspects of subaerial carbonates, in Scholle, P.A., Bebout, D.G., and Moore, C.H., Carbonate depositional environments: Amer. Assoc. Petroleum Geologists, Memoir 33, p. 73-92.

LAND, L.S., 1967, Diagenesis of skeletal carbonates: Jour. Sed. Petrology, v. 37, p. 914-930.

LAND, L.S., 1973, Holocene meteoric dolomitization of Pleistocene limestones, north Jamaica: Sedimentology, v. 20, p. 411-424.

LAND, L.S., 1976, Early dissolution of sponge spicules from reef sediments, North Jamaica: Jour. Sed. Petrology, v. 46, p. 967-969.

LAND, L.S., 1985, The origin of massive dolomite: Jour. Geol. Education, v. 33, p.112-125.

LAND, L.S., AND PREZBINDOWSKI, D.R., 1981, The origin and evolution of saline formation waters, lower Cretaceous carbonates, south-central Texas, U.S.A.: Jour, Hydrology, v. 54, p. 51-74.

LASH, G.G., 1982, Could Middle Ordovician carbonate shelf depositional patterns in the Appalachian orogen indicate collision along an irregular continental margin (abst.): Amer. Assoc. Petroleum Geol., v. 66, p. 1171.

LEUTLOFF, A.H., AND MEYERS, W.J., 1984, Regional distribution of microdolomite inclusions in Mississippian echinoderms from southwestern New Mexico: Jour. Sed. Petrology, v. 54, p. 432-446.

LEVI, C., 1973, Systematique de la classe des Demosponsgiaria (Demosponges), in Grasse, P.P., ed., Traite de Zoologie: Masson et Cie., Paris, v. I, p. 577-631.

LOGAN, B.W., 1974, Inventory of diagenesis in Holocene-Recent carbonate sediments, Shark Bay, western Australia: Amer. Assoc. Petroleum Geologists, Memoir 22, p. 195-249.

LOGAN, B.W., HOFFMAN, P., AND GEBELEIN, C.D., 1974, Algal mats, cryptalgal fabrics, and structures, Hamelin Pool, western Australia: Amm. Assoc. Petroleum Geologists, Mem. 22, p. 140-193.

LOGAN, B.W., REZAK, R., AND GINSBURG, R.N., 1964, Classification and environmental significance of algal stromatolites: Jour. Geol., v. 72, p. 68-83.

LOGAN, B.W., DAVIES, G.R., READ, J.F., AND CEBULSKI, D.E., 1970, Carbonate sedimentation and environments, Shark Bay, western Australia: Amm. Assoc. Petroleum Geologists, Mem. 13, 223 p.

LOGAN, B.W., HARDING, J.L., AHR, W.M., WILLIAMS, J.D., AND SNEAD, R.G., 1969, Carbonate sediments and reefs, Yucatan shelf, Mexico: Amer. Assoc. Petroleum Geol., Memoir 11, 196 p.

LOGAN, W.E., 1863, Report on the geology of Canada: Geological Survey of Canada, Rept. Prog. (1863), 983 p.

LOHMANN, K.C., AND MYERS, W.J., 1977, Microdolomite inclusions in cloudy prismatic calcites – a proposed criterion for former high-magnesium calcites: Jour. Sed. Petrology, v. 47, p. 1078-1088.

LONGLEY, W.M., 1950, Cote Nord du Saint-Laurent de Mingan a Aguanish: Ministere de l'Energie et des Ressources (Quebec), Rapport geologique #42, Partie 1, p. 1-35.

LONGMAN, M.W., 1980, Carbonate diagenetic textures from near-surface diagenetic environments: Amer. Assoc. Petroleum Geol. Bull., v. 63, p. 461-487.

LOREAU, J.P., AND PURSER, B.H., 1973, Distribution and ultrastructure of Holocene ooids in the Persian Gulf, in Purser, B.H., ed., The Persian Gulf – Holocene carbonate sedimentation and diagenesis in a shallow epicontinental sea: Springer-Verlag, Heidelberg, Berlin, p. 279-328.

LOUCKS R.G., AND ANDERSON J.H., 1980, Depositional facies and porosity development in Lower Ordovician Ellenburger Dolomite, Puckett Field, County, Texas, in Halley, R.B., and Loucks, R.G., eds., Carbonate reservoir rocks: Soc. Econ. Paleontologists Mineralogists, Core workshop 1, p. 1-31.

LOWENSTAM, H., 1963, Biologic problems relating to the composition and diagenesis of sediments, in Donnelly, T.W., ed., The earth sciences: Univ. of Chigago Press, p. 137-195.

LOWRY, W.D., AND TILLMAN, C.G., 1974, Tectonic rather than eustatic origin of the Middle Ordovician Knox (Beekmantown) unconformity of the central and southern Appalachians (abs.): Geol. Soc. America, Abstracts with programs, v. 6, p. 850.

LUDVIGSEN, ROLF, 1978, Middle Ordovician trilobite biofacies, southern
    Mackenzie Mountains, in Stelck, C.R., and Chatterton, B.D., eds.,
    Western and Arctic Canadian Biostratigraphy, Geol. Assoc. Canada,
    Special Paper 18, p. 1-37.

LUDVIGSEN, ROLF, 1979, A trilobite zonation of Middle Ordovician rocks,
    southwestern District of Mackenzie: Geol. Survey of Canada, Bull.
    312.

MACQUEEN, R.W., AND GHENT, E.D., 1970, Electron microprobe study of
    magnesium distribution in some Mississippian echinoderm limestones
    from western Canada: Can. Jour. Earth Sciences, v. 7, p. 1308-1317.

MALPAS, J., AND STEVENS, R.K., 1977, The origin and emplacement of the
    ophiolite suite with examples from western Newfoundland:
    Geotectonics, v. 11, p. 453-466.

MARESCH, W.V., 1974, Plate tectonics origin of the Caribbean mountain
    system of northern South America: discussion and proposal: Geol.
    Soc. America Bull., v. 85, p. 669-682.

MARGARITZ, M., GOLDENBERG, L., KAFRI, U., AND ARAD, A., 1980, Dolomite
    formation in the seawater-freshwater interface: Nature, v. 287, p.
    622-624.

MARGOLIS, S., AND REX, R.W., 1971, Endolithic algae and micrite envelope
    formation in Bahamian ooids are revealed by scanning electron
    microscopy: Geol. Soc. America Bull., v. 82, p. 843-852.

MASLYN, R.M., 1977, Fossil tower karst near Molas Lake, Colorado:
    Mountain Geol., v. 14, p. 17-25.

MATTHEWS, R.K., 1974, A process approach to diagenesis of reefs and reef
    associated limestones, in Laporte, L.F., ed., Reefs in time and
    space: Soc. Econ. Paleontologists Mineralogists, Spec. Pub. 18, p.
    234-256.

MAZZULLO, S.J., 1980, Calcite pseudospar replacive of marine acicular
    aragonite and implications for aragonite cement diagenesis: Jour.
    Sed. Petrology, v. 50, p. 409-423.

MAZZULLO, S.J., AND EHRLICH, R., 1983, Grain-shape variation in the St.
    Peter sandstone: a record of eolian and fluvial sedimentation of an
    early Paleozoic cratonic sheet sand: Jour. Sed. Petrology, v. 53, p.
    105-119.

MAZZULLO, S.J., AND FRIEDMAN, G.M. 1975, Conceptual model of tidally
    influenced deposition on margins of epeiric seas: Lower Ordovician
    (Canadian) of eastern New York and southwestern Vermont: Amer.
    Assoc. Petroleum Geolologists Bull., v. 59, p. 2123-2141.

MILLER J.A., 1975, Facies characteristics of Laguna Madre wind-tidal
    flats, in Ginsburg, R.N., ed., Tidal deposits: A casebook of recent
    examples and fossil counterparts: Springer-Verlag, New York, p.
    67-73.

MILLIMAN, J.D., 1974, Marine carbonates: Springer-Verlag, Berlin, 375 p.

MONTY, C.A., AND HARDIE, L.A., 1976, Geological significance of the freshwater blue-green algal calcareous marsh, in Walter, M.R., ed., Stromatolites: Elsevier, Development in Sedimentology 20, p. 447-478.

MOORE, C.H., 1973, Intertidal carbonate sedimentation, Grand Cayman, West Indies: Jour. Sed. Petrology, v. 43, p. 591-602.

MOORE, C.H., 1977, Beach rock origin: some geochemical, mineralogical, petrographic considerations: Geoscience and Man, 18, p. 155-163.

MOORE, P.D., AND BELLAMY, D.J., 1974: Peatlands, Springer-Verlag, New York, 221 p.

MORROW, D.W., 1978, The influence of the Mg/Ca ratio and salinity on dolomitization in evaporite basins: Can. Petroleum Geol. Bull., v. 26, p. 389-392.

MORROW, D.W., 1982, Diagenesis 2, Dolomite part 2: Geoscience Canada, v.9, p. 95-107.

MOWBRAY, T., 1983, The genesis of lateral accretion deposits in recent intertidal mudflat channels, Solway Firth, Scotland, Sedimentology, v. 30, p. 425-435.

MULTER, H.G., 1969, Field guide to some carbonate environments, Florida Keys and western Bahamas: Miami Geol. Soc., Miami.

MURRIS, R.J., 1980, Middle East: stratigraphic evolution and oil habitat: Amer. Assoc. Petroleum Geol., v. 64, p. 597-618.

MUSSMAN, W.J., 1982, The Middle Ordovician Knox unconformity, Virginia Appalachians: transition from passive to convergent margin (unpublished M.S. thesis): Virginia Polytechnic Institute and State Univ.

NARBONNE, G.M., AND DIXON, O.A., 1984, Upper Silurian lithistid sponge reefs on Somerset Island, Arctic Canada: Sedimentology, v. 31, p. 25-50.

NEUMANN, A.C., 1966, Observations on coastal erosion in Bermuda and measurements of the boring rate of the sponge Cliona lampa: Limnol. Oceanogr., v. 11, p. 92-108.

NOBLE, J.P., AND HOWELLS, 1974, Early marine lithification of nodular limestones in the Silurian of New-Brunswick: Sedimentology, v. 21, p. 597-609.

NORTH AMERICAN COMMISSION ON STRATIGRAPHIC NOMENCLATURE, 1983, North American stratigraphic code: Amer. Assoc. Petroleum Geologists, v. 67, p. 841-875.

NOWLAN, G.S., 1981, Stratigraphy and conodont faunas of the Lower and Middle Ordovician Romaine and Mingan Formations, Mingan Islands, Quebec (abs.): Maritime Sediments and Atlantic Geology, v. 17, p. 67.

OLDERSHAW, A.E., AND SCOFFIN, T.P., 1967, The source of ferroan and non-ferroan calcite cements in the Halkin and Wenlock limestones: Geol. Jour., v. 5, p. 309-320.

OTI, M., AND MULLER, G., in press, Textural and mineralogical changes in coralline algae during meteoric diagenesis: an experimental approach: Geologische Rundschau.

PALMER, T.J., AND FURSICH, F.T., 1981, Ecology of sponge reefs from the Middle Jurassic of Normandy: Paleontology, v. 24, p. 1-23.

PEMBERTON, S.G., KOBLUK, D.R., YEO, R.K., AND RISK, M.J., 1980, The boring Trypanites at the Silurian-Devonian disconformity in southern Ontario: Jour. Paleontology, v. 54, p. 1258-1266.

PERRODON, ALAIN, 1983, Geodynamique des bassins sedimentaires et systemes petroliers: Bull. Centres Rech. Explor.-Prod. Elf-Aquitaine, v. 7, p. 645-676.

PERYT, T.M., 1981, Phanerozoic oncoids - an overview: Facies, v. 4, p. 197-214.

PERYT, T.M., 1983, Oncoids: comment to recent development, in Peryt, T.M., Coated grains: Springer-Verlag, Berlin-Heidelberg, p. 273-275.

PICKERILL, R.K., AND HARLAND, T.L., 1984, Midddle Ordovician microborings of probable sponge origin from eastern Canada and eastern Norway: Jour. Paleontology, v. 58, p. 885-891.

PIERSON, B.J., 1980, Late Cenozoic facies succession and diagenesis on a Bahamian atoll (abstract): Intern. Assoc. Sedimentologists, 1st European Mtg., Bochum, p. 203-205.

PIERSON, B.J., 1982, Cyclic sedimentation, limestone diagenesis, and dolomitization in Upper Cenozoic carbonates of the southeastern Bahamas (unpublished Ph.D. thesis): University of Miami, Coral Gables, 295 p.

PITCHER, M., 1964, Evolution of Chazyan (Ordovician) reefs of eastern United States and Canada: Can. Petroleum Geol. Bull., v. 12, p. 632-691.

PITCHER, M., 1971, Middle Ordovician reef assemblages: Proc. N. Amer. Paleont. Convention, Chigago, Part J, p. 1341-1357.

PLUHAR, A., AND FORD, D.C., 1970, Dolomite karren of the Niagara Escarpment, Ontario, Canada: Zeitschrift fur Geomorphologie, v. 14 p. 392-410.

PLUMMER, L.N., 1975, Mixing of seawater with calcium carbonate groundwater, in Whitten, E.H., ed., Quantitative studies in the geological sciences: Geol. Soc. America, Memoir 142, p. 219-236.

PRATT, B.P., 1979, The St. George Group (Lower Ordovician), western Newfoundland: Sedimentology, Diagenesis and Cryptalgal Structures (unpub. M.S. thesis): Memorial Universdity of Newfoundland, 231 p.

PRATT, B.P., 1982a, Stromatolite decline - a reconsideration: Geology, v. 10, p. 512-516.

PRATT, B.R., 1982b, Stromatolitic framework of carbonate mud-mounds: Jour. Sed. Petrology, v. 52, p. 1203-1227.

PRATT, B.P., AND JAMES, N.P., 1982, Cryptalgal-metazoan bioherms of early Ordovician age in the St George Group, western Newfoundland: Sedimentology, v. 29, p. 543-569

PRATT, B.P. AND JAMES, N.P., in press, The St. George Group (Lower Ordovician) of western Newfoundland: tidal flat island model for carbonate sediments in shallow epeiric seas: Amer. Assoc. Petroleum Geologists Bull.

PURDY, E.G., 1974, Reef configurations: cause and effect, in Laporte, L.F., ed., Reefs in time and space: Soc. Econ. Paleontologists Mineralogists, Spec. Pub. 17, p. 9-76.

PURSER, B.H., 1969, Syn-sedimentary marine lithification of Middle Jurassic limestones in the Paris Basin: Sedimentology, v. 12, p. 205-230.

PURSER, B.H., 1972, Subdivision et interpretation des sequences carbonatees: Mem. B.R.G.M. 77, p. 679-698.

PURSER, B.H., 1973, The Persian Gulf - Holocene carbonate sedimentation and diagenesis in a shallow epicontinental sea: Springer-Verlag, Heidelberg, Berlin, 471 p.

PURSER, B.H., AND EVANS, E., 1973, Regional sedimentation along the Trucial Coast, SE Persian Gulf, in Purser, B.H., ed., The Persian Gulf - Holocene carbonate sedimentation and diagenesis in a shallow epicontinental sea: Springer-Verlag, Heidelberg, Berlin, p. 211-231.

PURI, H.S., 1964, Ostracods as ecological and paleoecological indicators: Pub. Sta. Zool. Napoli 33, 612 p.

PYE, R., 1983, Red residual soils, in Wilson, R.C., ed., Residual deposits: Geol. Soc., Spec. Pub. 11.

QUINLAN, G.M., AND BEAUMONT, C., 1984, Appalachian thrusting, lithopheric flexure, and the Paleozoic stratigraphy of the eastern interior of North America: Can. Jour. Earth Sciences, v. 21, p. 973-996.

RADKE, R.M., AND MATHIS, R.L., 1980, On the formation of saddle
   dolomite: Jour. Sed. Petrology, v. 50, p. 1149-1168.

RAMPINO, M.R. AND SANDERS, J.E., 1980, Holocene transgression in
   south-central Long Island, New York, Jour. Sed. Petrology, v. 50, p.
   1063-1080.

READ, J.F., 1980, Carbonate ramp-to-basin transitions and foreland basin
   evolution, Middle Ordovician, Virginia Appalachians: Amer. Assoc.
   Petroleum Geologists Bull., v. 64, p. 1575-1612.

READ, J.F., 1982, Geometry, facies, and development of Middle Ordovician
   carbonate buildups, Virginia Appalachians: Amer. Assoc. Petroleum
   Geol. Bull., v. 66, p. 189-209.

READ, J.F., AND GROVER, G.A., Jr., 1977, Scalloped and planar erosion
   surfaces, Middle Ordovician limestone, Virginia: analogues of
   Holocene exposed karst or tidal rock platforms: Jour. Sed.
   Petrology, v. 47, p. 956-972.

READ, J.F., et al, 1984, Models for generation of 5th order carbonate
   cycles (abs.): Geol. Soc. America, Abstracts with Programs, Reno,
   Ann. Mtg., p. 631.

REINECK, H.E., 1975, German North Sea tidal flats, in Ginsburg, R.N.,
   ed., Tidal deposits: A casebook of recent examples and fossil
   counterparts: Springer-Verlag, New York, p. 5-12.

REINSON,G.E., 1984, Barrier-island and associated strand-plain systems,
   in Walker, R.G., ed., Facies models, 2nd ed.: Geol. Assoc. Canada,
   Reprint Ser. 1, p. 119-140.

REVELLE, R., AND EMERY, K.O., 1957, Chemical erosion of beachrock and
   exposed reef rock: U.S. Geol. Survey, Prof. Paper 260T, p. 699-709.

RICHARDSON, J., 1856, Report of the year 1856: Geological Survey of
   Canada, Rept. Prog. 1853-56 (1857), p. 191-245.

RICHTER, D.K., 1983, Calcareous ooids: a synopsis, in Peryt, T.M.,
   Coated grains: Springer-Verlag, Berlin-Heidelberg, p. 71-99.

RICHTER, D.K., AND FUCHTBAUER, 1978, Ferroan calcite replacement
   indicates former magnesian calcite skeletons: Sedimentology, v. 25,
   p. 843-861.

RIDING, R., 1981, Composition, structure, and environmental setting of
   Silurian bioherms and biostromes in northern Europe, in Toomey,
   T.M., ed., European fossil reef models: Soc. Econ. Paleontologists
   Mineralogists, Spec. pub. 30, p. 41-85.

RIGBY, J.K., 1966, Evolution of Lower and Middle Ordovician sponge reefs
   in western Utah: Geol. Soc. America, Spec. Paper 87, 137 p.

RIGBY, J.K., 1971, Sponges and reef and related facies through time:
   Proc. N. Amer. Paleont. Convention, Chicago, Part J, p. 1374-1388.

RIGBY, J.K., 1983, Fossil Desmospongia, in Broadhead, T.W., ed., Sponges and spongiomorphs: Univ. of Tennessee, Dept. of Geol. Sciences, Stud. Geol. 7, p. 12-39.

RITTER, D.F., 1978, Process geomorphology: Wm. C. Brown, Dubuque, Iowa, p. 465-511.

RIVA, JOHN, 1969, Middle and Upper Ordovician graptolite faunas of the St. Lawrence Lowlands of Quebec and of Anticosti Island: Amer. Assoc. Petroleum Geologists, Memoir #12, p. 513-536.

RIVA, JOHN, 1974, A revision of some Ordovician graptolites of eastern North America: Paleontology, v. 17, p. 1-40.

RODGERS, JOHN, 1971, The Taconic orogeny: Geol. Soc. America Bull., v. 82, p. 1141-1177.

ROEHL, P.O., 1967, Stony Mountain (Ordovician) and Interlake (Silurian) facies analogs of recent low energy marine and subaerial carbonates, Bahamas: Amer. Assoc. Petroleum Geol. Bull., v. 51, p. 1979-2032.

ROLIFF, W.A., 1968, Oil and Gas Exploration, Anticosti Island, Quebec: Geol. Assoc. Canada, Proceeding, v. 19, p. 31-37.

ROSS, C.A., AND ROSS, J.R., 1985, Late Paleozoic depositional sequences are synchronous and worldwide: Geology, v. 13, p. 194-197.

ROSS, J.R., 1963a, Constellaria from the Chazyan (Ordovician), Isle de la Motte, Vermont: Jour. Paleon., v. 37, p. 51-56.

ROSS, J.R., 1963b, New Ordovician species of Chazyan trepostome and cryptostome bryozoa: Jour. Paleon., v. 37, p. 57-63.

ROSS, J.R., 1963C, Chazyan (Ordovician) leptotrypellid and atactotoechid bryozoa: Paleontology, v. 5, p. 727-739.

ROSS, J.R., 1963d, The bryozoan trepostome Batostoma in Chazyan (Ordovician) strata: Jour. Paleon., v. 37, p. 857-867.

ROSS, J.R., 1964, Morphology and phylogeny of early Ectoprocta (Bryozoa): Geol. Soc. America Bull., v. 75, p. 927-948.

ROSS, J.R., 1972, Paleoecology of Middle Ordovician ectoproct assemblages: 24th Intern. Geol. Congress Proc., v. 7, p. 96-102.

ROSS, J.R., 1981, Ordovician environmental heterogeneity and community organization, in Gray, J. et al, eds., Communities of the past: Hutchinson Ross Publishing Co., Stroudsburg, p.1-33.

ROSS, R.J., Jr., 1949, Stratigraphy and trilobite faunal zones of the Garden City Formation, northeastern Utah: Amer. Jour. Science, v. 247, p. 472-491.

ROSS, R.J., Jr., 1976, Ordovician sedimentation in the western United States, in Basset, M.G., ed., The Ordovician System: Proceedings of a Paleontological Symposium, Birmingham, 1974, Univ. of Wales Press and National Museum of Wales, 699 p.

ROSS, R.J. Jr. et al, 1982, The Ordovician System in the United States: Int. Union Geol. Sciences, Pub. 12, 73 p.

ROSS, R.J., Jr, JAANUSSON, V., AND FRIEDMAN, I, 1975, Lithology and origin of Middle Ordovician calcareous mudmound at Meikeljohn Peak, southern Nevada: U.S. Geol. Survey, Prof. Paper 871, 48 p.

ROWLEY, D.B., AND KIDD, W.S., 1981, Stratigraphic relationships and detrital composition of the Medial Ordovician flysch of western New England: implications for the tectonic evolution of the Taconic orogeny: Jour. Geol., v. 89, p. 199-218.

RUCKER, J.B., AND CARVER, R.E., 1969, A survey of the carbonate mineralogy of cheilostome bryozoa: Jour. Paleontology, v. 43, p. 791-799.

RUPPEL, S.C., AND WALKER, K.R., 1982, Sedimentology and distinction of carbonate buildups: Middle Ordovician, east Tennessee: Jour. Sed. Petrology, v. 52, p. 1055-1071.

RUPPEL, S.C., AND WALKER, K.R., 1984, Petrology and depositional history of a Middle Ordovician carbonate platform: Chickamauga Group, northeastern Tennessee: Geol. Soc. America Bull., v. 95, p. 568-583.

SANDBERG, P.A., 1975a, Bryozoan diagenesis: bearing on the nature of the original skeleton of rugose corals: Jour. Paleontology, v. 49, p. 587-606.

SANDBERG, P.A., 1975b, New interpretations of Great Salt Lake ooids and of ancient nonskeletal carbonate mineralogy: Sedimentology: v. 22, p. 497-537.

SANDBERG, P.A., 1983, An oscillating trend in Phanerozoic non-skeletal carbonate mineralogy: Nature, v. 305, p. 19-22.

SANDO, W.J., 1974, Ancient solution phenomena in the Madison limestone (Mississippian) of North-Central Wyoming: Jour. Research U.S. Geol. Survey, v. 2, p. 133-141.

SAVOY, L., HARRIS, A.G., AND REPETSKI, J.E., 1981, Paleogeographic implications of the Lower/Middle Ordovician boundary, northern Great Valley, eastern Pennsylvania to southeastern New York (abs.): Geol. Soc. America, Abstracts with programs, v. 13, p. 174.

SCHEINDER, J.H., 1976, Biological and inorganic factors in the destruction of limestone coasts: Contribution to sedimentology 6, 112 p.

SCHEINDER, J.H., 1977, Carbonate construction and decomposition by epilithic and endolithic micro-organisms in salt- and freshwater, in Flugel, E., ed., Fossil algae - Recent results and developments: Springer-Verlag, Berlin-Heidelberg, p. 248-260.

SCHLAGER, W., 1981, The paradox of drowned reefs and carbonate platforms: Geol. Soc. America Bull., v. 92., p. 197-211

SCHMALZ, R.F., 1967, Kinetics and diagenesis of carbonate sediments: Jour. Sed. Petrology, v. 37, p. 60-67.

SCHUCHERT, C. AND TWENHOFEL, W.H., 1910, Ordovic-Siluric section of the Mingan and Anticosti Islands: Geol. Soc. America Bull., v. 21, p. 686-693.

SCHWARTZ, M.L., 1967, The Bruun (sic) theory of sea-level rise as a cause of shore erosion: Jour. Geology, v. 75, p. 76-92.

SCOFFIN, T.P., 1971, The conditions of growth of the Wenlock reefs of Shropshire, England: Sedimentology, v. 17, p. 173-219.

SCOFFIN, T.P., 1972, Cavities in the reefs of the Wenlock limestones (mid-Silurian) of Shropshire, England: Geologischen Rundschau, v. 61, p. 565-578.

SEARLE, M.P., JAMES, N.P., CALON, T.J., AND SEWING, J.D., 1983, Sedimentological and structural evolution of the Arabian continental margin in the Musandam Mountains and Dibba zone, United Arab Emirates: Geol. Soc. America, v. 94, p. 1381-1400.

SEILACHER, A., 1967, Bathymetry of trace fossils: Marine Geol., v. 5, p. 413-428.

SHANMUGAM, G. AND LASH, G.G., 1982, Analogous tectonic evolution of the Ordovician foredeeps, southern and central Appalachians: Geology, v. 10, p. 562-566.

SHANMUGAM, G. AND LASH, G.G., 1983, Reply on "Analogous tectonic evolution of the Ordovician foredeeps, southern and central Appalachians": Geology, v. 10, p. 562-566.

SHANMUGAM, G., AND WALKER, K.R., 1978, Tectonic significance of distal turbidites in the Middle Ordovician Blockhouse and Lower Sevier Formations in east Tennessee, v. 278, p. 551-578.

SHANMUGAM, G., AND WALKER, K.R., 1980, Sedimentation, subsidence, and evolution of a foredeep basin in the Middle Ordovician, southern Appalachians: Amer. Jour. Science, v. 280, p. 479-496.

SHARMA, K.N. AND FRANCONI, A., 1975, Regions des Rivieres Magpie, Saint-Jean, Romaine: Ministere de l'Energie et des Ressources (Quebec), Rapport geologique #163, 73 p.

SHAW, F.C., 1968, Early Middle Ordovician Chazy trilobites of New York: New York State Museum Memoir 17, 163 p.

SHAW, F.C., 1980, Shallow-water lithofacies and trilobite lithofacies of the Mingan Formation (Ordovician), Eastern Quebec, Le Naturaliste Canadien, v. 107, p. 227-242.

SHEARMAN, D.J., KHOURI, J., TAHA, S., 1961, On the replacement of dolomite by calcite in some Mesozoic limestones from the French Jura: Geol. London Assoc. Proc., v. 71, p. 1-12.

SHINN, E. A.. 1968, Practical significance of birdeye structures in carbonate rocks: Jour. Sed. Petrology, v. 38, p. 215-223.

SHINN, E.A., 1983a, Birdseyes, fenestrae, shrinkage pores, and loferites: a reevaluation: Jour. Sed. Petrlogy, v. 53, p. 619-628.

SHINN, E.A., 1983b, Tidal flat, in Scholle, P.A., Bebout, D.G., and Moore, C.H., eds., Carbonate depositional environments: Amer. Assoc. Petroleum Geologists, Memoir 33, p. 171-211.

SHINN, E.A., AND ROBBIN, D.M., 1983, Mechanical and chemical compaction in fine-grained shallow-water limestones: Jour. Sed. Petrology, v. 53, p. 595-618.

SHINN, E.A., GINSBURG, R.N., AND LLOYD, R.M., 1965, Recent supratidal dolomite from Andros Island, Bahamas, in Pray, L. C., and Murray, R.C., eds., Dolomitization and limestone diagenesis-a symposium: Soc. Econ. Paleontologists Mineralogists Spec. Pub. 13, p. 112-123.

SHINN, E.A., LLOYD, R.M., AND GINSBURG, R.N., 1969, Anatomy of a modern carbonate tidal flat, Andros Island, Bahamas: Jour. Sed. Petrology, v. 39, p. 1202-1228.

SHINN, E.A., HALLEY, R.B., HUDSON, J.H., LIDZ, B.H., 1977, Limestone compaction: an enigma: Geology, v. 5, p. 21-24.

SIBLEY, D.F., 1980, Climatic control of dolomitization, Seroe Domi Formation (Pliocene), Bonaire, N.A.: Soc. Econ. Paleontologists Mineralogists, Spec. Pub. 28, p. 247-258.

SIMONE, LUCIA, 1981, Ooids: a review: Earth Sciences Review, v. 16, p. 319-355.

SLOSS, L.L., 1963, Sequences in the cratonic interior of North America: Geol. Soc. America Bull., v. 74, p. 93-113.

SMITH, D.L., 1972, Stratigraphy and carbonate petrology of the Mississippian Lodgepole Formation in central Montana (unpublished Ph. D. thesis): Univ. of Montana.

SOHN, I.G., 1985, Latest Mississippian (Namunian A) nonmarine ostracods from west Virginia and Virginia: Jour Paleontology, v. 59, p. 446-460.

SOMMERVILLE, I.D., 1979, A cyclicity in the early Brigantian (D2) Limestones east of the Clwydian Range, North Wales and its use in correlation: Geol. Jour., v. 14, p. 69-86.

SQUIRES, R.L., 1973, Burial environment, diagenesis, mineralogy and Mg and Sr contents of skeletal carbonates in the Buckhorn asphalt of Middle Pennsylvanian age, Arbuckle Mountains, Oklahoma (unpublished Ph. D.thesis): California Institute of Technology, Pasadena.

STEARN, C.W., 1983, Stromatoporoids: affinity with modern organisms, in Broadhead, T.W., ed., Sponges and spongiomorphs: Univ. of Tennessee, Dept. of Geol. Sciences, Stud. Geol. 7, p. 157-163.

STECKLER, M.S., AND WATTS, A.B., 1982, Subsidence history and tectonic evolution of Atlantic type continental margins, in Scrutton, R.A., ed., Dynamics of passive margin: Geodynamics Series, v. 6, p. 184-196.

STRINGFIELD, V.T., RAPP, J.R., AND ANDERS, R.B., 1979, Effects of karst and geologic structure on the circulation of water and permeability in carbonate aquifers: Jour. Hydrology, v. 43, p. 313-332.

SWEET, W.C., 1984, Graphic correlation of upper Middle and Upper Ordovician rocks, North American Mid-Continent Province, USA, in Bruton, D.L., ed., Aspects of the Ordovician System: Paleont. Contributions from the Univ. of Oslo 295, p. 23-36.

SWEET, W.C., ETHINGTON, R.L., AND BARNES, C.R., 1971, North American Middle and Upper Ordovician conodont faunas. Geol. Soc. America, Memoir 127, p. 163-193.

SWEETING, M.M., 1973, Karst landforms: Macmillan Publishing Co. Ltd., London, 362 p.

SWIFT, D.J., 1968, Shoreface erosion and transgressive stratigraphy: Jour. Geol., v. 76, p.444-456.

SWIFT, D.J., 1975, Barrier-island genesis: evidence from the Atlantic shelf, eastern U.S.A.: Sed. Geol., v. 14, p. 1-43.

SWIFT, D.J., 1976, Continental shelf sedimentation, in Stanley, D.J., and Swift, D.J., eds., Marine sediment transport and environment management: John Wiley and Sons, New York, p. 311-350.

THOMAS, W.A., 1977, Evolution of Appalachian-Ouachita salients and recesses from reentrants and promontories in the continental margin: Amer. Jour. Science, v. 277, p. 1233-1278.

THOMAS, W.A., 1983, Continental margins, orogenic belts, and intracratonic structures: Geology, v. 11, p. 270-272.

THOMPSON, A.M., 1975, Carbonate coastal environments in Ordovician shoaling-upward sequences, southern Appalachians, in Ginsburg, R.N., ed., Tidal deposits: A casebook of recent examples and fossil counterparts: Springer-Verlag, New York, p. 397-406.

THORSTEINSSON, R., AND KERR, J.W., 1968, Cornwallis Island and adjacent
smaller islands, Canadian Arctic Archipelago: Geol. Survey of
Canada, Paper 67-64.

THRAILKILL, J., 1968, Chemical and hydrologic factors in the excavation
of limestone caves: Geol. Soc. America Bull., v. 79, p. 19-46.

TOOMEY, D.F., 1970, An unhurried look at a Lower Ordovician mound
horizon, southern Franklin Mountains, west Texas, Jour. Sed.
Petrology, v. 40, p. 1318-1335.

TOOMEY, D.F., AND FINKS, R.M., 1969, Middle Ordovician (Chazyan) mounds,
southern Quebec: New York State Geol. Assoc., 41st. Ann. Meeting,
Plattsburg, p. 121-134.

TOOMEY, D.F., AND NITECKI, M.H., 1979, Organic buildups in Lower
Ordovician (Canadian) of Texas and Oklahoma: Fieldiana Geol. 2, 181
p.

TORUNSKI, H., 1979, Biological erosion and its significance for the
morphogenesis of limestone coasts and for nearshore sedimentation
North Adriatic): Senckenberg. Mar., v. 11, p. 193-265.

TUCKER, M.E., 1984, Calcitic, aragonitic and mixed calcitic-aragonitic
ooids from the mid-Proterozoic Belt Supergroup, Montana:
Sedimentology, v. 31, p. 627-644.

TURMEL, R., AND SWANSON, R., 1976, The development of Rodriguez Bank, a
Holocene mudbank in the Florida reef tract: Jour. Sed. Petrology, v.
46, p.497-519.

TWENHOFEL, W.H., 1926, Geology of the Mingan Islands, Quebec: Geol. Soc.
America Bull., v. 37, p. 535-550.

TWENHOFEL, W.H., 1931, Geology of the Mingan Islands, Quebec: Geol. Soc.
America Bull., v. 42, p. 575-588.

TWENHOFEL, W.H., 1938, Geology and paleontology of the Mingan Islands:
Geol. Soc. America Special Paper 11, 132 p.

VAIL, P.R., MITCHUM, R.M., AND THOMPSON, S., 1977, Seismic stratigraphy
and global sea level, in Payton, C., ed., Seismic stratigraphy -
Applications to hydrocarbon exploration: Amer. Assoc. Petroleum
Geologists, Memoir 26, p. 63-81.

VEEVERS, J.J., FALVEY, D.A., AND ROBINS, S., 1978, Timor Trough and
Australia: facies show topographic wave migrated 80 km during the
past 3 m.y.: Tectonophysics, v. 45, p. 217-227.

VON DER BORCH, C.C., 1979, Continent-island arc collision in the Banda
Arc: Tectonophysics, v. 54, p. 169-193.

WADDINGTON, G.W., 1950, Les depots de calcaires de la region de Mingan: Ministere de l'Energie et des Ressources (Quebec), Rapport Geologique #42, partie 2, p. 1-13.

WAGNER, C.W., AND TOGT, C. VAN DER, 1973, Holocene sediment types and their distribution in the southern Persian Gulf, in Purser, B.H., ed., The Persian Gulf - Holocene carbonate sedimentation and diagenesis in a shallow epicontinental sea: Springer-Verlag, Heidelberg, Berlin, p. 123-155.

WALCOTT, R.I., 1970, Isotasic response to loading of the crust in Canada: Can. Jour. Earth Sciences, v. 7, p. 2-13.

WALKEN, G.M., 1974, Paleokarstic surfaces in upper Visean (Carboniferous) limestones of the Derbyshire block, England: Jour. Sed. Petrology, v. 44, p. 1232-1247.

WALKEN, G.M., AND DAVIES, J., 1983, Polyphase erosion of subaerial omission surfaces in the late Dinantian of Anglesey, North Wales: Sedimentology, v. 30, p. 861-878.

WALKER, K.R., 1972, Trophic analysis: a method for studying the function of ancient communities: Jour. Paleontology, v. 46, p. 82-93.

WALKER, K.R., AND ALBERSTADT, L.P., 1975, Ecological succession as an aspect of structure in fossil communities: Paleobiology, v. 1, p. 238-257.

WALKER, K.R., AND BAMBACK, R.K., 1974, Feeding by benthic invertebrates: classification and terminology for paleoecological analysis: Lethaia, v. 7, p. 67-77.

WALKER, K.R., AND FERRIGNO, K.F., 1973, Major Middle Ordovician reef tract in east Tennessee: Amer. Jour. Science, v. 273 A, p. 294-325.

WALKER, R.G., 1984, Shelf and shallow marine sands, in Walker, R.G., ed., Facies models, 2nd ed.: Geol. Assoc. Canada, Reprint Ser. 1, p. 141-170.

WALKER, R.G., AND CANT, D.J., 1984, Sandy fluvial system, in Walker, R.G., ed., Facies models, 2nd ed.: Geol. Assoc. Canada, Reprint Ser. 1, p. 71-90.

WALKER, T.R., 1984, Diagenetic albitization of potassium feldspar in arkosic sandstones: Jour. Sed. Petrology, v. 54, p. 3-16.

WALLS, R.A., AND BURROWES, G., 1985, The role of cementation in the diagenetic history of Devonian reefs, in Schneidermann, N., and Harris, P.M., eds., Carbonate cements: Soc. Econ. Paleontologists Mineralogists, Spec. Pub. 35, p. 185-220.

WALLS, R.A., MOUNTJOY, E.W., AND FRITZ, P., 1979, Isotopic composition and diagenetic history of carbonate cements in Devonian Golden Spike reef, Alberta, Canada: Geol. Soc. America, v. 90, p. 963-982.

WANLESS, H.R., 1979, Limestone response to stress: pressure solution and dolomitization: Jour. Sed. Petrology, v. 49, p. 437-462.

WATTS, A.B., AND TALWANI, M., 1974, Gravity anomalies seaward of deep-sea trenches and their tectonic implications: Royal Astron. Soc. Geophys. Jour., v. 36, p. 57-90.

WEBBY, B.D., 1984, Ordovician reefs and climate: a review, in Bruton, D.L., ed., Aspects of the Ordovician System: Paleont. Contributions from the Univ. of Oslo 295, p. 89-100.

WEIMER, R.J., HOWARD, J.D., AND LINDSAY, D.R., 1982, Tidal flats, in Scholle, P. A., and Spearing, Darwin, eds., Sandstone depositional environments: Amer. Assoc. Petroleum Geologists, Memoir 31, p. 191-246.

WEYL, P.K., 1959, Pressure solution and the force of crystallization - a phenomenological theory: Jour. Geophys. Res., v. 64, p. 2001-2025.

WIEDENMEYER, F., 1980a, Diagenesis of sponge spicules, in Hartman, W.D. et al, eds., Living and fossil sponges: Sedimenta VIII, Comparative Sedimentolgy Lab., Univ. of Miami, p. 108-122.

WIEDENMEYER, F., 1980b, Shallow water sponges of the Bahamas, in Hartman, W.D. et al, eds., Living and fossil sponges: Sedimenta VIII, Comparative Sedimentolgy Lab., Univ. of Miami, p. 146-168.

WIGGINS, W.D., AND HARRIS, P.M., 1984, Cementation and porosity of shoaling sequences in the subsurface Pettit Limestone, Cretaceous of east Texas, in Harris, P.M., ed., Carbonate sands - a core workshop: Soc. Econ. Plaeontologists Mineralogists, Core workshop 5, p. 263-305.

WILKINSON, B.R., 1982, Cyclic cratonic carbonates and phanerozoic calcite seas: Jour. Geol. Education, v. 30, p. 189-203.

WILKINSON, B.R., BUCZYSKI, C., AND OWEN, R.M., 1984, Chemical control of carbonate phases: implications from Upper Pennsylvanian calcite-aragonite ooids of southeastern Kansas: Jour. Sed. Petrology, v. 54, p. 932-947.

WILKINSON, B.R., OWEN, R.M., AND CAROLL, A.R., 1985, Submarine hydrothermal weathering, global eustacy, and carbonate polymorphism in Phanerozoic marine oolites: Jour. Sed. Petrology, v. 55, p. 171-184.

WILLIAMS, H., 1978, Tectonic-lithofacies map of the Appalachian Orogen: Memorial University of Newfoundland, Map 1.

WILLIAMS, H., 1979, Appalachian orogen in Canada: Can. Jour. Earth Sciences, v. 16, p. 792-807.

WILLIAMS, H., AND STEVENS, R.K., 1974, The ancient continental margin of
    eastern North America, in Burk, C.A., and Drake, C.L., eds., The
    geology of continental margins: Springer-Verlag, New York, p.
    781-796.

WILSON, J.L., 1975, Carbonate facies in geologic history:
    Springer-Verlag, Berlin-Heidelberg-New York, 471 p.

WILSON, J.L. AND JORDAN, CLIF, 1983, Middle shelf environment, in
    Scholle, P.A., Bebout, D.G., and Moore, C.H., Carbonate depositional
    environments: Amer. Assoc. Petroleum Geologists, Memoir 33, p.
    297-344.

WONG, P.K., AND OLDERSHAW, A., 1981, Burial cementation in the Devonian,
    Kaybob reef complex, Alberta, Canada: Jour. Sed. Petrology, v. 51,
    p. 507-520.

WRAY, J.L., 1977, Calcareous algae: Elsevier, Amsterdam-Oxford-New York,
    Dev. Paleon. Stra. 4, 185 p.

WRIGHT, V.P., 1982, The recognition and interpretation of paleokarsts:
    two examples from the Lower Carboniferous of South Wales: Jour. Sed.
    Petrology, v. 52, p. 83-94.

WRIGHT, V.P., 1983, Morphogenesis of oncoids in the Lower Carboniferous
    Llanelly Formation of South Wales, in Peryt, T.M., ed., Coated
    grains: Springer-verlag, Berlin-Heidelberg, p. 426-434.

YOCHELSON, E.L., WHITE, J.S., AND GORDON, M., 1967, Aragonite and
    calcite in mollusks from the Pennsylvanian Kendrick shales (Jilson)
    in Kentucky: U.S. Geol. Survey, Prof. Paper 573-D, p.76-78.

RICHARDSON(1856)	IKENHOFEL(1938)	TOPOGRAPHIC MAP(1979) 1:50,000	GAUTHIER LAROUCHE (1981)
	Parroquet Island	Ile aux Perroquets	Ile aux Perroquets
		Ile de la Maison	Ile de la Maison
		Ile du Wreck	Ile du Wreck
Mingan Island	Mingan Island	Ile Nue de Mingan	Ile Nue de Mingan
		Le Havre	Le Havre
		L'Ilot	L'Ilot
Harbour Island	Harbour Island	Ile du Havre de Mingan	Ile du Havre de Mingan
	Inner Birch Island	Ile aux Bouleaux	Ile a Bouleaux de Terre
	Outer Birch Island	Petite Ile aux Bouleaux	Ile a Bouleaux du Large
	Large Island	Grande Ile	Grande Ile
	Moutange Island	Ile Moutange	Ile de la Grosse Romaine
	Montas Island	Ile Montas	Ile de la Petite Romaine
	Quarry Island	Ile a la Proie	Ile Quarry
Niapiscau Island	Niapiscau Island	Ile a Samuel	Ile Niapiskau
		Anse des Bonnes Femmes	Bonnes Femmes de Niapiskau
	Cairn Island	Ile du Fantome	Ile du Fantome
	Virgin Island	Ile a Firmin	Ile a Firmin
	Cormorant Island	Ile du Havre	Ile du Havre
		Pointe aux Morts	Pointe aux Morts
		Ile a Calculots	Ile a Calculots
		Ile aux Goelands	Ile aux Goelands
	Walrus Island	Petite Ile au Marteau	Petite Ile au Marteau
	Seal Island	Grosse Ile au Marteau	Grosse Ile au Marteau
	Clearwater Point	Grande Pointe	Grande Pointe
	Anchorite Point	Pointe Corageuse	Pointe Corageuse
	Adams Island	Ile de la Chasse Passe	Ile de la Chasse Passe
	St-Charles Island	Ile St-Charles	Ile Saint-Charles
	Trilobite Bay	Baie des Trilobites	Baie des Trilobites
	Betchewun Bay	Baie Puffin	Baie Puffin
		Le Sanctuaire	Ile a Calculot des Betchewans
		Ile aux Sauvages	Le Innu
	Hunting Island	Ile a la Chasse	Ile a la Chasse
	Indian Point	Pointe du Sauvage	Pointe du Sauvage
		Tete de la Perdrix	Tete de la Perdrix
		Ile de l'Ancre	Petite Ile Sainte-Genevieve
	Ste-Genevieve Island	Ile Ste-Genevieve	Ile Sainte-Genevieve
	Pillage Bay	Baie Nickerson	Baie Saint-Laurent
		Mont Ste-Genevieve	Mont Sainte-Genevieve

APPENDIX B - LITHOLOGICAL DESCRIPTIONS OF TYPE AND REFERENCES SECTIONS

		THICKNESS(m)	
UNIT	DESCRIPTION	UNIT	TOTAL

POINTE DU SAUVAGE & ILE SAINTE-GENEVIEVE W SECTIONS

Romaine Formation (Sauvage Member)

1	Cross-bedded arkosic sandstones (litho. A), gastr., brach., Skolithos.	2.0	2.0

Romaine Formation (Sainte-Genevieve Member)

2	Burrow-mottled dolostones (litho. G), medium- bedded unit, intraclast layers (10-20 cm)	3.2	3.2

Units 1 and 2 are exposed at Pointe du Sauvage.

3	Covered (Baie Saint-Laurent).	9.0	14.2
4	Burrow-mottled dolostone (litho. G), thin-bedded unit passing up section into massive thick beds, intraclast layers (5-20 cm) with cross-laminations. gastr., brach., ceph., grapt.	19.4	33.6
5	Thrombolite mounds (litho. H), massive thick-bedded unit.	10.0	43.6

Top of unit 6 is not exposed on Ile Sainte Genevieve but can be observed on Ile Innu where it is directly overlain by siliciclastics of the Mingan Formation.

GRANDE ILE NW SECTION

Romaine Formation (Grande Ile Member)

1	Burrowed dolomicrite (litho. E). chert nodules.	0.8	0.8
2	Stromatolite (litho. D), LLH forms.	0.6	1.4
3	Ripple-laminated dolomicrite (litho. C).	1.0	2.4
4	Burrowed dolomicrite (litho. E).	0.7	3.1

UNIT	DESCRIPTION	THICKNESS(m)	
		UNIT	TOTAL
5	Ripple-laminated dolomicrite (litho. C), siliceous, grading up into dololaminites (litho. B) at the top of the unit.	0.9	4.0
	Units 1-5 are exposed only at low tide on the wave-cut platform.		
6	Ooid dolostone (litho. F), massive unit.	0.8	4.8
7	Stromatolite (litho. D), LLH forms, intraclasts	0.8	5.6
8	Burrowed dolomicrite (litho. E) grading up into ripple-laminated dolomicrite (litho. C)	1.4	7.9
9	Ooid dolostone (litho. F), massive unit.	0.9	7.9
10	Stromatolite (litho. D), LLH forms, grading up into ripple-laminated dolomicrite (litho. C)	2.1	16.9
11	Ooid dolostone (litho. F), massive unit.	0.8	10.8
12	Stromatolite mound (litho. D) grading up into ripple-laminated dolomicrite (litho C).	2.6	13.4
	Bedding in units 10-12 is disturbed by sedimentary boudinage. Units better exposed on Grande Ile NE.		
13	Ooid dolostone (litho. F), massive unit.	1.0	14.4
14	Burrow-mottled dolostone (litho. G), massive thick-bedded unit.	4.2	18.6
15	Interbedded burrowed dolomicrite (litho. E), ripple-laminated dolomicrite (litho C) and shaly dololaminite (litho. B).	2.0	20.6
16	Burrowed dolomicrite (litho. E), brachiopod in dolostone beds (5-10 cm) with vuggy porosity and bituminous material.		
	Top of unit 16 is sharply overlain by siliciclastics of the Mingan Formation. Units 15 and 16 is exposed only at low tide on the wave-cut platform.		

UNIT	DESCRIPTION	THICKNESS(m)	
		UNIT	TOTAL

ILE DU HAVRE NE SECTION

Mingan Formation (Corbeau Member)

1	Shale with chert pebbles.	0.2	0.2

Base of unit 1 is sharp overlying dolomites of the
Romaine Formation.

2	Cross-bedded arkosic sandstones (litho. 4), thick sets, brach., <u>Diplocraterion</u>.	1.2	1.4
3	Laminated shales (litho. 2), transitional contact with unit 2.	3.8	5.2
4	Channellized arkosic sandstones in unit 3 (litho. 5), low-angle cross-stratification, shale clasts, irregular margin, inart. brach.	1.4	-
5	Laminated sandstones (litho. 3), flaser bedding, ripple laminations.	0.8	6.0

Unit 5 is sharply overlain by skeletal limestones of
the Grande Pointe Member. Silty dololaminite unit
capping the Corbeau Member is truncated by the intra-
Mingan unconformity but is well exposed on Ile du
Havre SW.

ILE AUX PERROQUETS SECTION

Mingan Formation (Perroquet Member)

1	Burrowed lime mudstone (litho. 10), massive unit.	0.4	0.4
2	Burrowed skeletal wackestone/packstones, thinly-bedded unit with shale interbeds, brach.	0.8	1.2
3	Burrowed lime mudstone/wackestone (litho. 10), massive unit.	0.4	1.6

APPENDIX B (continued)

		THICKNESS(m)	
UNIT	DESCRIPTION	UNIT	TOTAL

4	Burrowed skeletal wackestone/packstone (litho. 11), thin-bedded unit with wavy solution seams, oncolite lenses (3-5 cm thick).	2.4	4.0
5	Skeletal grainstone (litho. 12), cross-bedding, lenticular unit.	1.2	–
6	Idem to unit 4.	2.2	6.2

Units 1-6 are exposed on Ile aux Perroquets and Ile de la Maison but unit 5 is present only on Ile de la Maison.

| 7 | Covered. | 1.0 | 7.2 |
| 8 | Fenestral mudstones (litho. 7) of the Fantome Member exposed on Ile du Wreck. | 5.0 | 12.2 |

ILE DU FANTOME W SECTION

Mingan Formation (Fantome Member)

| 1 | Interbedded mudstone/skeletal wackestone (litho. 10) and intraclast grainstone (litho. 8), gastr. | 2.0 | 2.0 |

Basal contact of unit 1 is sharp and conformable and overlain by a silty dololaminite unit capping the Corbeau Member.

| 2 | Interbedded cryptalgalaminite (litho. 6) and fenestral mudstone (litho. 7), medium-bedded unit. | 2.2 | 4.2 |
| 3 | Fenestral mudstone (litho. 7), well-bedded unit (10-20 cm). | 10.6 | 14.8 |

Upper contact of unit 3 is the intra-Mingan unconformity and overlain by skeletal limestones of the Grande Pointe Member. Units 1-3 are locally truncated by the unconformity on Ile du Fantome W.

UNIT	DESCRIPTION	THICKNESS(m)	
		UNIT	TOTAL

GRANDE POINTE SECTION

Mingan Formation (Grande Pointe Member)

1	Brachiopod coquina (litho. 16), basal unit overlying siliciclastics of the Corbeau Member.	0.1	0.1
2	Interbedded nodular lime mudstone and shale (litho. 15).	0.4	0.5
3	Skeletal-ooid grainstone (litho. 12), cross-bedding, paleokarst surface at the top.	5.0	5.5
4	idem to unit 3.	3.7	9.2
	Units 3 and 4 interdigitate laterally with skeletal wackestone/packstone (litho. 11).		
5	Skeletal wackestone/packstone (litho 11) grading up into peloid grainstone (litho 12).	1.6	10.8
6	Skeletal wackestone/packstone (litho. 11), unevenly-bedded unit. Poor exposure.	8.8	19.4

	ROMAINE FORMATION	MINGAN FORMATION
ALGAE [5]		
Girvanella sp.		X
Ortonella sp.		X
Garwoodia sp.		X
Hedstroemia sp.		X
Parachaetetes sp.		X
Nuia sp.		X
SPONGES [8]		
Archaeoscyphia minganesis	X	
Archaeoscyphia sp.		X
Anthaspidella sp.		X
Calycocoelia sp.		X
Eospngia sp.		X
Hudsonospongia sp.		X
Lissocoelia sp.		X
Psarodictyon? sp.		X
Rhopolocoelia sp.		X
Zittelella sp.		X
Hindia sp.		X
STROMATOPOROIDS [10]		
Labechia sp.		X
TABULATE CORALS [1]		
Billingsaria parva		X
Eofletcheria incerta		X
Lichenaria sp. [5]		X
Tetradium? sp. [5]		X
BRYOZOANS [4]		
Ceramoporella sp.		X
Constellaria islendis		X
Batostoma chazyensis/campensis		X
Nicholsonella sp.		X
Nicholsonella sp. indet.		X
Lamottopora duncanae		X
Jordonopora heroensis		X
Stictopora fenestrata		X
Eopachydictya gregaria		X
Chazydictya chazyensis		X
Phylloporina sp.		X

Taxon		
BRACHIOPODS [3]		
Ancistrorhyncha? vacua		X
Camarella varians		X
Dactylogonia extensa		X
Glyptomena champlainensis minganensis		X
Glyptorthis sp.		X
Hesperorthis ignicula		X
Lingulella? huronensis minganensis		X
Mimella minganensis		X
M. piger		X
Onychoplecia longirostris		X
Petrocrania prona		X
Pomonotrema grandeava [11]	X	
Rostricellula orientalis		X
R. pristina		X
R. triangulata		X
Schizambon duplicimuratum		X
Syntrophia lateralis		X
ECHINODERMS [11]		
Bolboporites americanus		X
Palaeocystites pulcher		X
OSTRACODS [11]		
Ctenobolbina parroquetensis		X
Dilobella minganensis		X
Leperditia limatula		X
L. minganensis		X
Schmidtella crassimarginata		X
TRILOBITES [9]		
Amphilichas sp.		X
Bathyurus amplimarginatus [2]	X	
B. romainensis [2]	X	
B. sp.		X
Bumatus sp.		X
Calyptaulax sp.		X
Ceraurinella sp.		X
Cybeloides sp.		X
Dolichoharpes sp.		X
Eorobergia sp.		X
Failleana sp.		X
Glaphurina sp.		X
Hibbertia sp.		X
Illeanus sp.		X
Nanilleanus sp.		X
Kawina sp.		X
Petigurus cybele [2]	X	
Pliomerops sp.		X
Remopleurides sp.		X
Sphaerexochus sp.		X
Thaloeps sp.		X
Uromystrum sp.		X

GASTROPODS [11]

	Col 1	Col 2
Bucania minganensis		X
Conularia parroquetensis		X
Euconia amphitrite		X
E. ramseyi	X	
Fusispira calcifera	X	
Helicotoma perstriata	X	
Holopea vigneauensis		X
Lophospira? aspera		X
L. hermoine		X
L. perengulata		X
Maclurites magnus		X
M. romainensis	X	
Raphistoma striatum		X
Raphistomina laurentina	X	
R. pillagensis	X	
Troconema abruptum	X	
T. tricarinatum	X	
Tryblidium nycteis	X	

CEPHALOPODS [6]

	Col 1	Col 2
Barrendoceras minganensis		X
B. natator		X
Camaroceras deparcum	X	
C. indigator	X	
C. sp.	X	
Casinoceras magister	X	
Catoraphiceras sordidum	X	
Centrotarphyceras billingsi	X	
Deiroceras diffidens		X
Diestoceras maccoyi		X
D. sp.		X
Endoceras mingannese		X
Endoceras velox	X	
E. sp.		X
Eurystomites ferox		X
Minganoceras subturbinatum		X
Orthoceras? antenor		X
O.? cornuum		X
O. shumardi		X
Piloceras acinaces	X	X
Plectoceras jason		X
P. tyrans		
Protocycloceras? becki	X	
P. lamarki	X	
Schroederoceras? minganensis	X	
S. vagum	X	
Spyroceras maro		X
S. magnosiphonatum		X
S. minganense		X
S. twenhofeli		X
Tarphyceras? apollo	X	
T.? palinurus	X	
Trundoleoceras canadense	X	
T. coarctum	X	

ROMAINE FORMATION   DYNGAN FORMATION

FIGURE 10 STRATIGRAPHIC SECTION

2&3   4   5   7   8   9A   1
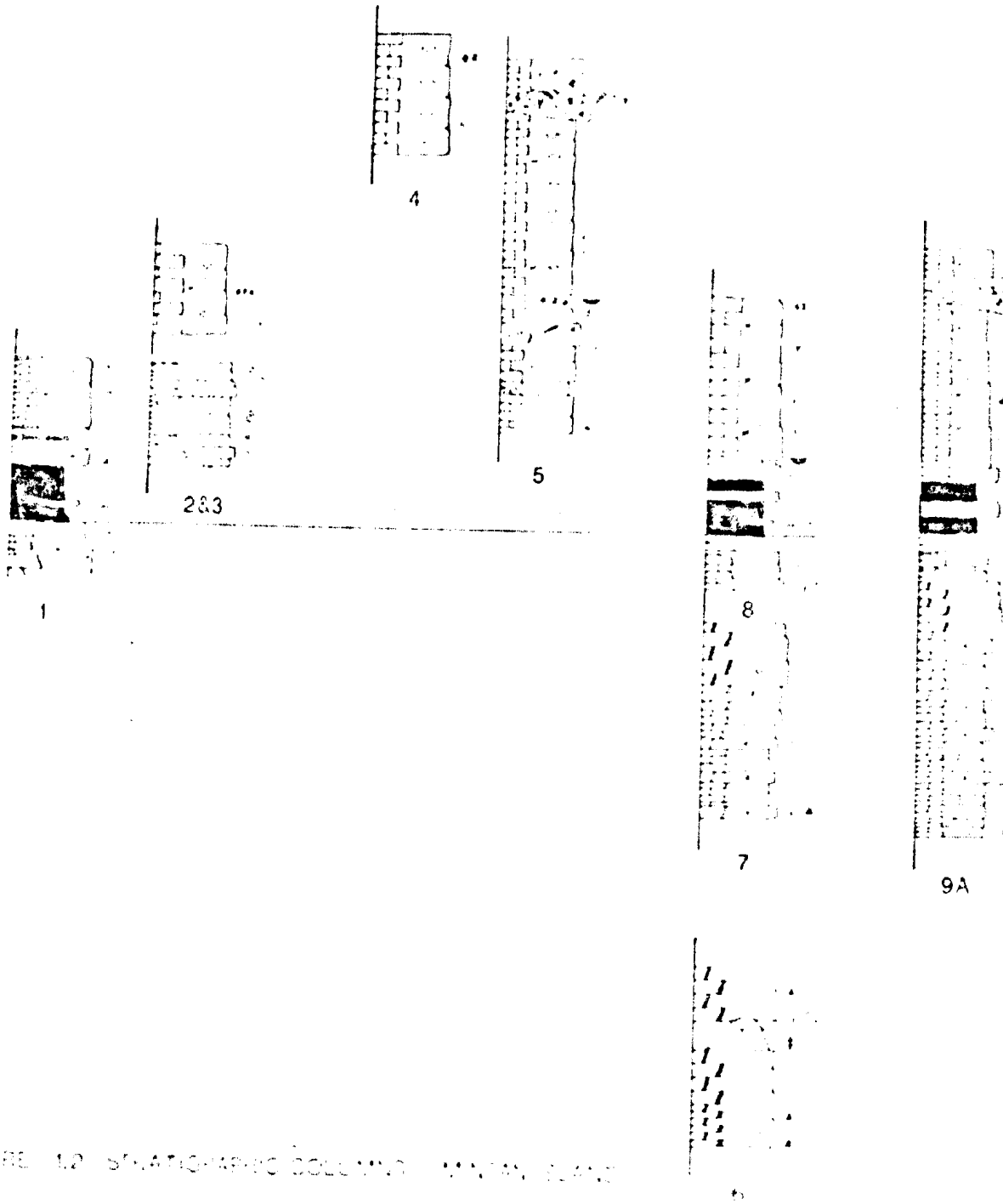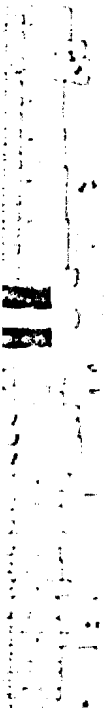
9A
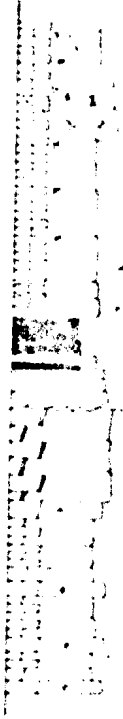
9B
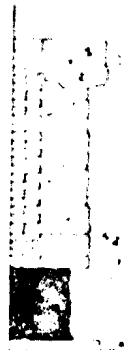
11A

11B

11C

11D

13A
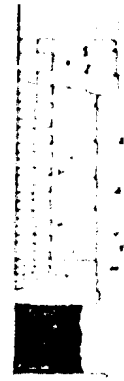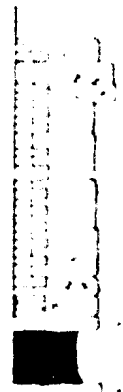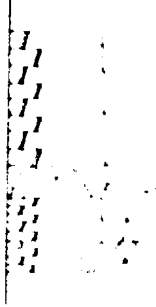
10
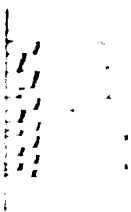
12
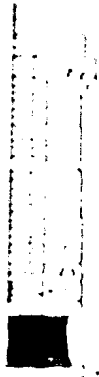
13A

13B

13C

13D

15A

15B

16

17A

12

14A

14B

17B

17C

17D

18

19

20

21A

21B

N

20

21A

21B

22A

22B

22C

23

21

LEGEN

25B

25D

27

25A

25C

28

29A

26

END

29B

30

33

29A

28

29B

30

31

32

33

ROMAINE FORMATION | MINGAN FORMATION

1

FIGURE 1.2